Mobile Information Systems

Connected Vehicles: Applications and Communication Challenges

Lead Guest Editor: Barbara M. Masini
Guest Editors: Gianluigi Ferrari, Cristiano Silva, and Ilaria Thibault

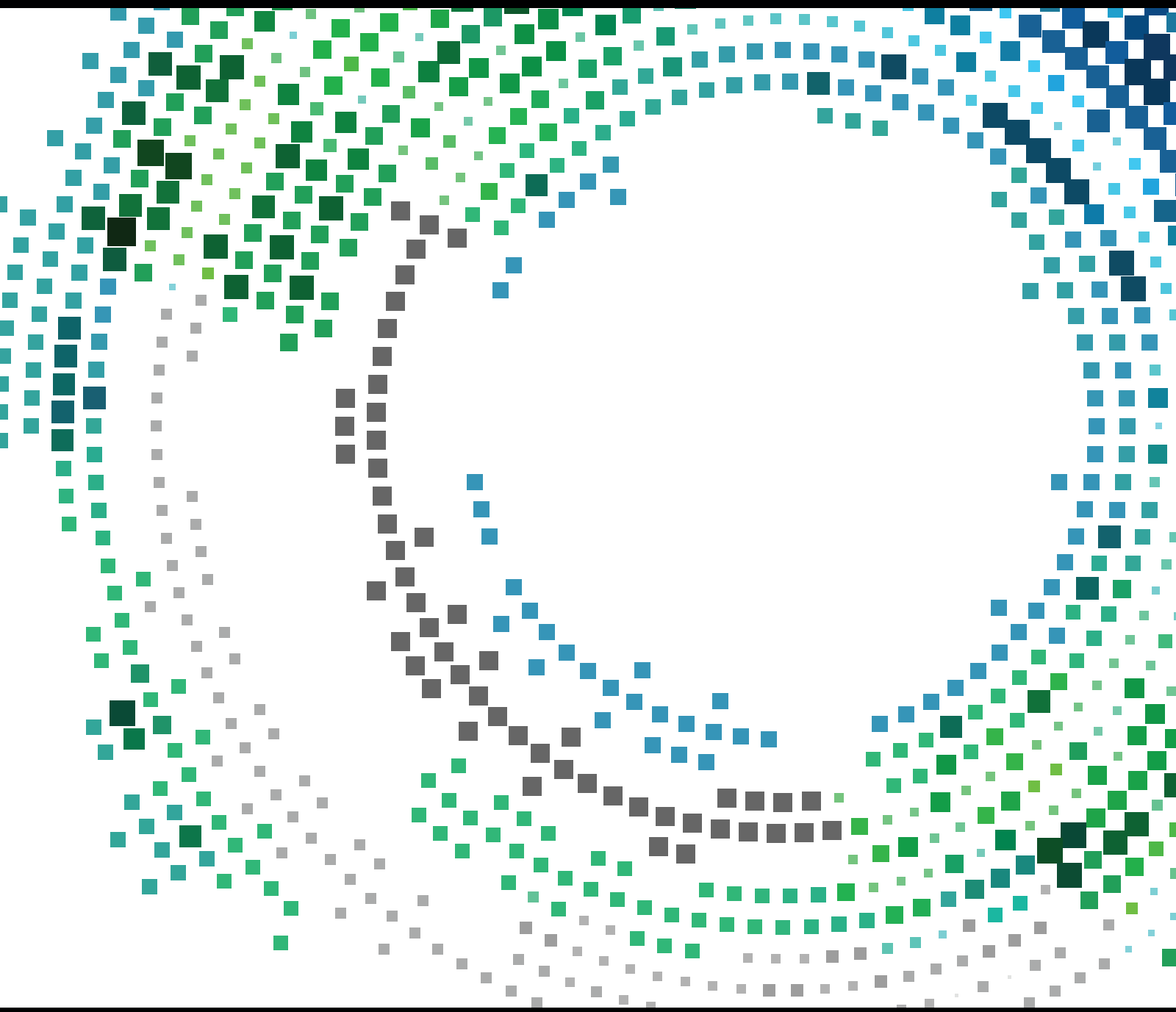

Connected Vehicles: Applications and Communication Challenges

Mobile Information Systems

Connected Vehicles: Applications and Communication Challenges

Lead Guest Editor: Barbara M. Masini
Guest Editors: Gianluigi Ferrari, Cristiano Silva, and Ilaria Thibault

Editorial Board

Contents

Hindawi
Mobile Information Systems
Volume 2017, Article ID 1082183, 2 pages
https://doi.org/10.1155/2017/1082183

Editorial

Connected Vehicles: Applications and Communication Challenges

Barbara M. Masini,[1] Gianluigi Ferrari,[2] Cristiano Silva,[3] and Ilaria Thibault[4]

[1]*National Research Council (CNR), Institute of Electronics, Computer and Telecommunication Engineering (IEIIT), Wireless Communication Group, Bologna, Italy*
[2]*Internet of Things (IoT) Lab, Department of Engineering and Architecture, University of Parma, Parma, Italy*
[3]*Department of Technology, Federal University of São João del-Rei (UFSJ), São João del-Rei, MG, Brazil*
[4]*Vodafone Group Research and Development, Newbury, UK*

Correspondence should be addressed to Barbara M. Masini; barbara.masini@ieiit.cnr.it

Received 13 July 2017; Accepted 13 July 2017; Published 28 August 2017

Connected vehicles are expected to be a pillar of a smart society and to revolutionize the way people move. The use of wireless communication technologies integrated on board (or in the driver's or passengers' pockets) is the key to connecting vehicles, infrastructures, and travellers. The widespread use of connected vehicles generates high volumes of transportation-related data, enabling plenty of new applications which, according to Cisco visual networking index, will give a boost to the second fastest growing industry segment (after connected healthcare), with a predicted 37% compound annual growth rate.

Connected vehicles will improve safety, traffic management, and urban and suburban mobility and will enhance the development of new services like accident prevention, Internet access, Internet backbone, ride-sharing, vehicular social networking, environment monitoring, infotainment, usage-based insurance, preemptive maintenance, and many more. This phenomenon is fostering an acceleration of standardization efforts to define new architectures and requirements for the various emerging vehicular applications scenarios. In addition to well established vehicular communication standards, that is, the IEEE WAVE/802.11p in US and the ETSI ITS G5 in Europe, different working groups within 3GPP have recently completed a set of cellular vehicle-to-anything (V2X) features as part of the LTE-Advanced suite of specifications, and studies on future 5G systems will take these concepts even further by evaluating how cellular communications together with emerging access technologies—such as visible light and mm-waves—can play a key role in enhancing the on-board intelligence of future vehicles.

This special issue focuses on connected vehicle-driven applications and aims at covering cutting-edge research advances in topics covering standardization, wireless communication technologies challenges, field trials, and tight interworking between on-board vehicle intelligence and wireless communication standards.

A general view on architectures and technologies for connecting vehicles is provided in the following survey by the Guest Editors themselves: "A Survey on Infrastructure-Based Vehicular Networks" by C. M. Silva et al. The paper presents an in-depth survey of more than ten years of research on infrastructures, wireless access technologies, and deployment. In fact, even if direct vehicle-to-vehicle communications will allow new challenging applications, the infrastructure still represents the key to let vehicular connectivity available and suitable also nowadays. The paper also identifies the limitations of present technologies and infrastructures and the challenges associated with such infrastructure-based vehicular communications, also highlighting potential solutions.

Wireless access technologies and ongoing standard solutions are investigated in the following two papers, related to IEEE 802.11p and LTE, respectively.

The paper "An Efficient Channel Access Scheme for Vehicular Ad Hoc Networks" by S. A. Hussain et al. focuses on IEEE 802.11p standard and proposes an efficient channel access scheme for vehicular networks under high vehicular traffic densities and high mobility. In the proposed scheme, the contention window of the random access protocol is dynamically varied according to the instants in correspondence to which vehicles are going to leave the road side unit (RSU) coverage area, giving higher service priority to vehicles leaving sooner the service area. The presented results show that this approach guarantees higher throughput with respect to the standard solution.

The paper "LTE Network Enhancement for Vehicular Safety Communication" by W. Kim and E.-K. Lee focuses on LTE for vehicular applications, as standardized by 3GPP. The authors investigate the feasibility of beacons delivery in terms of network overhead and end-to-end latency, finally proposing three potential solutions to reduce the overhead and the delay, still keeping the safety level high.

Channel modelling is addressed in the following two papers.

The paper "Empirical Study and Modeling of Vehicular Communications at Intersections in the 5 GHz Band" by S. A. Hadiwardoyo et al. presents an empirical study of vehicular communication effectiveness at intersections in the 5 GHz band real field trials at different types of intersections in the city of Valencia (Spain). The goal of this work is to determine the communication restrictions imposed by the different intersections themselves. On the basis of empirical results, the packet delivery probability is also modelled at different distances from the center of the intersection: this allows deriving the expected success ratio when delivering event-based messages.

The paper "Three-Dimensional Vehicle-to-Vehicle Channel Modeling with Multiple Moving Scatterers" by D. Du et al. proposes a generalized 3D channel model with no constraints on the position of local moving scatters. On the basis of this model, the corresponding space-time correlation functions, time correlation functions, and space correlation functions are then analytically investigated for MIMO vehicle-to-vehicle (V2V) links. The theoretical results of the space-Doppler power spectral density are compared with the available measured data showing good agreement and, thus, the applicability and generality of the proposed model.

Safety for pedestrian is considered as example application in the paper "High-Accuracy Tracking Using Ultrawideband Signals for Enhanced Safety of Cyclists" by D. Dardari et al. which focuses on the impact of vehicles on cyclists. After providing a statistical analysis of accidents involving cyclists, the authors present a new risk detection architecture providing high-accuracy localization and tracking of road users based on ultrawideband (UWB) technology. Experimental results show the possibility of achieving centimeter-level localization accuracy and good tracking capabilities, even in harsh propagation environments.

We hope that readers will enjoy the papers published in this special issue and will be inspired for further research work in the topic of connected vehicles.

Barbara M. Masini
Gianluigi Ferrari
Cristiano Silva
Ilaria Thibault

Hindawi
Mobile Information Systems
Volume 2017, Article ID 6123868, 28 pages
https://doi.org/10.1155/2017/6123868

Review Article

A Survey on Infrastructure-Based Vehicular Networks

Cristiano M. Silva,[1] Barbara M. Masini,[2] Gianluigi Ferrari,[3] and Ilaria Thibault[4]

[1]*Departamento de Tecnologia, Universidade Federal de São João del-Rei, São João del-Rei, MG, Brazil*
[2]*National Research Council, Institute of Electronics, Computer and Telecommunication Engineering (CNR-IEIIT), Bologna, Italy*
[3]*IoT Lab, Department of Information Engineering and DISS-Road Security Center, University of Parma, Parma, Italy*
[4]*Vodafone Group Research and Development, Newbury, UK*

Correspondence should be addressed to Cristiano M. Silva; cristiano@ufsj.edu.br

Received 23 December 2016; Revised 17 April 2017; Accepted 23 April 2017; Published 6 August 2017

Academic Editor: Dik Lun Lee

The infrastructure of vehicular networks plays a major role in realizing the full potential of vehicular communications. More and more vehicles are connected to the Internet and to each other, driving new technological transformations in a multidisciplinary way. Researchers in automotive/telecom industries and academia are joining their effort to provide their visions and solutions to increasingly complex transportation systems, also envisioning a myriad of applications to improve the driving experience and the mobility. These trends pose significant challenges to the communication systems: low latency, higher throughput, and increased reliability have to be granted by the wireless access technologies and by a suitable (possibly dedicated) infrastructure. This paper presents an in-depth survey of more than ten years of research on infrastructures, wireless access technologies and techniques, and deployment that make vehicular connectivity available. In addition, we identify the limitations of present technologies and infrastructures and the challenges associated with such infrastructure-based vehicular communications, also highlighting potential solutions.

1. Introduction

More and more vehicles are connected to the Internet through vehicle-to-anything (V2X) communication technologies, changing the automotive industry and the transportation system. By embedding computing devices into cars, roads, streets, and transit equipment (such as street signs, radars, traffic cameras, and others), we will be capable of digitalizing the transportation system [1], letting vehicles autonomously exchange data with other vehicles (V2V communications), with the network infrastructure (V2I communications), with the road infrastructure (V2R communications), with pedestrians (V2P communications), and so forth. Data collected by vehicles and pushed back from a remote control center will contribute to developing new services for vehicular users, automotive industries, and network providers. Connectivity is, then, the key issue for the provision of value-added services ranging from road safety, traffic management, and environment monitoring, up to autonomous driving. Connectivity will also enhance data collection and data exchange, driving new social and economic models which will impact the worldwide society and business.

As indicated by the European Transportation Policy [2], the use of Intelligent Transportation Systems is one of the key technologies for improving the safety, efficiency, and environmental friendliness of the transport industry. Intelligent Transportation Systems are grounded on sophisticated communication networks receiving data from several entities composing the traffic system. Data is processed and translated into useful information and recommendations to assist users of the transportation system and transit authorities. Such sophisticated communication network is commonly referred to as *vehicular network* [3–5]. Vehicular networks connect vehicles to provide a platform for the future deployment of large-scale and highly mobile applications. Applications are endless: driver assistance for faster, less congested, and safer roads; more efficient use of the transportation system; more efficient planning of routes and control of the traffic flow; more secure and greener traffic through digital driver

assistance; better planning and evolution of the system as a whole due to the availability of historical data, based on traffic and utilization trends detected via data mining techniques and autonomous driving.

The broad range of applications can be enabled by two main kinds of connectivity: infrastructure-based communications (hereafter V2I) and direct communications between vehicles (hereafter V2V). V2V communications are essentials for beaconing; coverage extensions; and very low latency applications. Focusing on V2I communications, vehicles may communicate to roadside units (RSUs) through short range communications or even to a remote control center by exploiting wide area networks. The infrastructure plays a coordination role by gathering global or local (potentially real time) information and then "suggesting" appropriate behaviors to drivers or managing specific services. These applications typically rely on an extended coverage, such as data collection at a remote infrastructure for traffic management, environmental monitoring, smart navigation, smart logistic, predictive vehicles maintenance, and pay as you drive.

Transit authorities may also deploy a dedicated infrastructure for vehicular communications. Such dedicated infrastructure is assumed to be reliable and trusted, enabling transit authorities to collect data from several sensors of the vehicle (airbag actioning, braking, videos, etc.), providing data for the real-time programming of smart traffic lights, traffic warnings, routing of emergency vehicles, road signing, and even autonomous driving in the near future. On the other hand, V2V communications are typically devoted to improve safety, providing low latency, fast network connectivity, and highly secure and high-speed communication typically used in platooning and collision avoidance systems [6–8].

Besides being needed for next-generation mobile applications, the use of a dedicated infrastructure for the vehicular communication also provides clear benefits in creating shortcuts in the graph of connections, restricting the ad hoc communication to small regions and position-based applications. At the end of 2016, Audi showed, for example, the first commercial V2I communication system in the United States: car-to-traffic-light chats to know how long the red light lasts. In the near future, such systems might help to save fuel and cut pollution or to provide infotainment and commercial information [9]. Whenever messages have to travel long distances, they can be tunneled, via the communication infrastructure, to the target region, improving network connectivity [10–15]. On the other hand, the deployment of a large-scale infrastructure is likely to demand huge investments. Hence, the research community has turned its attention to strategies for efficient deployment of a distributed communication infrastructure.

In this context, standardization entities are moving to develop reliable and secure wireless communications specifications to enable truly interoperable services worldwide. Allocation of dedicated spectrum for V2X communications both in US and in Europe has triggered standardization efforts in both regions to address a wide variety of V2X scenarios. As a result, two families of standards have been completed: the IEEE WAVE, with the 802.11p as the physical and lower-MAC layer standard, in 2010 in the US, and the first release of the ETSI intelligent transport systems (ITS), denoted as ETSI ITS-G5, in 2013 in Europe. In early 2014, different working groups within 3GPP have also started studying V2X as an additional feature for LTE-Advanced [16–18] and as a native feature for 5G. Other alternative solutions may be based on the rapidly spreading low-power wide area networks (LPWANs), which exploit sub-gigahertz unlicensed frequency bands and allow long-range radio links [19]. Owing to the long transmission range, sub-gigahertz technologies are attractive to support low data rate and long-lasting communications in vehicular networks.

This article is organized as follows. Section 2 briefly overviews the research in infrastructure-based vehicular networks from 2003 to 2016. Section 3 refers to vehicle-to-infrastructure (V2I) architectures. Section 4 refers to wireless access technologies and communication techniques. Section 5 discusses the deployment of infrastructure for vehicular networks. Section 6 concludes the article and points out to future challenges sketching potential solutions.

2. Overview of the Research in Infrastructure-Based Vehicular Networks

In the context of vehicular networks, infrastructure is a set of specialized communication devices supporting the network operation. Common properties include (but are not restricted to) network centrality, communication bandwidth, storage space, and high availability. Because vehicular network devices are initially envisioned to be located at roadsides, they are commonly referred to as RSUs and may provide a large number of functions, such as the following:

(i) Broadcast [20]
(ii) Channel allocation [21]
(iii) Caching [22]
(iv) Content download [23, 24]
(v) Data dissemination [25]
(vi) Data aggregation [26]
(vii) Data scheduling [27]
(viii) Gaming & streaming [28, 29]
(ix) Gateway [11, 22, 30]
(x) Hand-off [31–33]
(xi) Vehicles localization [34, 35]
(xii) QoS [36–39]
(xiii) Real-time support [40–42]
(xiv) Routing [14, 43, 44]
(xv) Security [45–48]
(xvi) Multihop comm [49].

Several technologies may be embedded in RSUs. Banerjee et al. [12] present an in-depth discussion and comparison of such technologies. Although most of the works consider stationary infrastructure, several papers [44, 50–55] propose

mobile architectures (public transportation buses, cabs, and ordinary vehicles). There are also proposals considering the use of low cost devices as an infrastructure [56], while other proposals consider the use of external communication devices (such as public Wi-Fi) [57].

The following basic groups can be envisioned to categorize the studies dealing with infrastructure-based vehicular networks.

(i) Architectures for infrastructure-based vehicular networks (Section 3): works are proposing new architectures, testbeds, proofs of concept, field trials and experimentations, and hardware studies.

(ii) Communication in infrastructure-based vehicular networks (Section 4): works are studying the vehicular communication in terms of protocols, data dissemination strategies, routing, connectivity, low level aspects of the communication, channel allocation, hand-off strategies, network throughput, quality of service, real-time messaging, and multihop data dissemination.

(iii) Security in infrastructure-based vehicular networks (Section 4.9): we present only a brief discussion of security in infrastructure-based vehicular networks (most of the strategies we could find target the ad hoc scenario).

(iv) Deployment of infrastructure for vehicular networks (Section 5): works are proposing strategies to physically locate the infrastructure, theoretical studies discussing metrics and strategies to evaluate deployments, and theoretical studies about requirements, features, or properties of network deployment.

In the early 2000s, most of the researches dealt with low level aspects of the communication. The high mobility of nodes, the constantly changing topology of vehicular networks, and the connectivity dependent on the location bring several interesting research challenges. The US Department of Transportation (USDOT) (US Department of Transportation, Research and Innovative Technology Administration, http://www.its.dot.gov/vii/) shows a clear focus on integrating vehicles for making the current transportation system more intelligent [58]. The research community is aware of the challenges imposed by vehicular communications. As we increase the number of participating vehicles in the network, the communication channel receives an increasing demand for multiple vehicles attempting to send and receive data simultaneously. The ASTM (American Society for Testing and Materials) and IEEE (Institute of Electrical and Electronics Engineers) adopt the Dedicated Short Range Communication (DSRC) (http://www.its.dot.gov/DSRC/) standard providing wireless communication capabilities for transportation applications within a 1,000 m range in highway speeds. DSRC provides seven channels in the spectrum between 5.850 and 5.925 GHz licensed for Intelligent Transportation Systems applications (Intelligent Transportation Systems Radio Service, ITS-RS) with channels designated for different applications, plus one channel reserved for V2V communications [4].

In the next few paragraphs, we overview the research conducted in infrastructure-based vehicular networks from 2003 to 2016.

In *2003-2004*, researchers focused on low level details (physical/MAC layers) of the vehicular communication. While [10] investigates the capacity of the wireless channel, the work [59] investigates channel access. Only few works start considering the impact of lower levels on applications, as, for example, in [60]. However, in these years, Intelligent Transportation Systems in general are considered; connected vehicles are included in the systems but with a lower and different attention.

In *2005-2006*, most of the researches are still on evaluating low level aspects of the communication, but the focus is not only on V2I communications, but also on V2V. The research community also visualizes the possibility of offering Internet access to vehicles. We notice works investigating novel architectures [11, 30], hand-off strategies [31–33], network throughput [61, 62], and multihop communication [63].

In *2007-2008*, the research community turns its attention to the validity of mobility models employed in vehicular simulations. They start to exploit the possible usage of the infrastructure for vehicular networks in terms of security and applications. The research community demonstrates interest in the potential use of public Wi-Fi access points to enhance the vehicular communication, and we notice the first works dealing with infrastructure deployment. We also find two surveys [3, 5] addressing vehicular ad hoc networks (VANETs). These works discuss vehicle-to-vehicle communication, the impact of decentralization, channel access, market issues, security, privacy, and validation of VANETs simulations. The infrastructure gains visibility as the research community realizes its importance to support the dissemination of data in vehicular networks [25, 64]. In order to reduce the deployment costs, some researchers focus on alternative less-expensive methods to achieve the benefits of a dedicated infrastructure, such as using publicly Wi-Fi [57] and the adoption of virtual infrastructure [50, 65] using vehicles.

The research community also realizes that bringing Internet access to drivers enables the development of a myriad of vehicular applications and traffic information systems. Examples of these envisioned applications are (i) Pothole Patrol [66] to monitor roads conditions; (ii) Waze Mobile App [67]; (iii) Peer on Wheels [68] to monitor traffic conditions; and (iv) RoadSpeak [69] to enable chatting between drivers. The performance of the network is deeply studied in works [58, 70–72], and the available communication hardware is evaluated in order to find out better solutions [12]. Testbeds are proposed in [73, 74] to evaluate practical aspects related to the vehicular communication, while requirements of privacy and security of the infrastructure are addressed in [47]. Moreover, Fiore and Härri [75] present an in-depth analysis of the topological properties of a vehicular network and found that simulation results are strongly affected by the mobility model, and they question the validity of studies conducted under unrealistic car mobility scenarios.

In *2009-2010*, over 40% of the works are addressing infrastructure deployment using heuristics [76–79], clusters [80], or proposing metrics [81]. A virtual infrastructure using

buses is presented in [51], while a secure infrastructure is proposed in [46]. When considering vehicle-to-infrastructure communication, we notice works addressing the scheduling [27], real-time communication [40, 41], delivery in sparse networks [42], analysis of connectivity [82–84], broadcast protocols [20], and cooperative georouting [43].

In *2011-2012*, we notice works addressing infrastructure deployment in terms of probabilistic models [85, 86], linear programming formulations [87–89], heuristics [90], genetic algorithms [91], and game-theory [92]. In terms of architecture, we notice analytic models for the selection of communicating devices [88, 93], proposals for light-weight infrastructures employing relay nodes [13], virtual infrastructures using the publish-subscribe paradigm [52], biologically inspired solutions [94], and reputation mechanisms [45]. In terms of communication, we notice works addressing routing [14, 44, 95], cooperative data dissemination [22], QoS controlled media access [36], multihop communication [49], content download [23], and data traffic [96, 97]. Mobility is addressed in [98–100].

In *2013-2014*, we notice works addressing high-level aspects of the infrastructure-based communication. Tonguz and Viriyasitavat [53] propose a self-organizing network using cars as RSUs. Luan et al. [56] propose the use of roadside buffers and cheap devices for store-and-forward messages to passing vehicles. Sommer et al. [54] study signal attenuation by buildings and propose the use of parked cars to help the signal propagation. When we consider communication, Harigovindan et al. [21] develop a mechanism for fair channel allocation, and Bruno and Nurchis [26] propose a mechanism to eliminate redundancy in data collected by vehicles in a distributed basis. A comparison among the impacts of different infrastructures on vehicular traffic performance is proposed in [101]: here, both cellular networks, broadcasting technologies, and V2V communications are analyzed and their performance is investigated when small and frequent traffic information fare was gathered from vehicles and retransmitted back to vehicles. The impacts of the number and position of RSUs are addressed, giving some answers to the deployment of new infrastructures on the roadside.

Deployment of infrastructure for vehicular networks is also addressed employing several techniques, such as genetic approaches [102], Voronoi diagrams [103], analytic models [104], randomized algorithms [105], content download [24], bipartite graphs [106], and intersection priority [107]. In [108], a cross-network information dissemination (which anticipates a topic discussed in the next time slot), denoted as "Cross-Network Effective Traffic Alert Dissemination" (X-NETAD), is proposed and experimentally validated: by leveraging the spontaneous formation of local Wi-Fi VANETs, with direct connections between neighboring vehicles, traffic alerts received from the cellular network are quickly disseminated.

In *2015-2016*, vehicular networks in general acquire still more importance [109]: this is, for example, demonstrated by the number of papers which contain the keywords *vehicular networks* of IEEEXplore database: 2,462 conference publications, 1,319 journals and magazines, and 336 early access articles, of which 126 conferences and 52 journals are related to vehicle-to-infrastructure communications. Attention is devoted to high precision positioning [110, 111] for quality of applications enhancements and cooperative transmission [112–114] to improve channel allocation and resource management in network infrastructure such as base stations and relays. Heterogeneous vehicular networks are also considered [115], where heterogeneity may be in wireless access technologies [116], vertical handovers [117], architectures, and autonomous driving [118]. Attention is also devoted to information acquisition [119] (also with crowd sensing [120, 121]) and to information dissemination [122–124]. The infrastructure is very often present for vehicular connectivity [125], but device-to-device (D2D) solutions gain an increasing importance [18, 126]. The possible adoption of LTE not only through the infrastructure of eNodeBs but also in direct mode enables new potential applications, also with low latency. Communication faces the issue of beaconing for vehicular awareness, addressing both the problem of channel load and adaptive beaconing. The scientific community focuses on safety applications [127] for different environments: platooning, lane changing, collision avoidance, and so forth. There are also some proposals focusing on planning [128–130] and managing [37–39, 131] vehicular networks.

3. Architectures of Infrastructure-Based Vehicular Networks

A general architecture is shown in Figure 1: vehicles are equipped with connected on-board units (OBUs) which can transmit data to other vehicles or to a remote control center exploiting different communication technologies and different infrastructures (cellular infrastructure, roadside infrastructures based on short range communications, and others). Important projects start to show relevant results, such as Fleetnet [132], Berkeley's California PATH (http://www.path.berkeley.edu/), and CarTel [133]. In particular, CarTel evaluates the V2I communication with city-wide trials in Boston and reports the upload bandwidth to vehicles using the unplanned open residential access. One of the main conclusions of CarTel is that the plethora of 802.11b access points spreading in cities can provide intermittent connectivity with high performance while available. Moreover, Wu et al. [30] state that infrastructure assessments are necessary to (i) evaluate communications architectures to identify those best suited for providing high bandwidth communications to travelers; (ii) examine design options and trade-offs; and (iii) quantitatively assess alternate approaches and evaluate their performance and reliability under realistic vehicle traffic conditions.

We identity the following categories of works addressing architectures for vehicular networks:

(i) Analytic Studies Addressing Specific Aspects of the Infrastructure

(ii) Benefits of Incorporating the Infrastructure in Vehicular Networks

(iii) Cooperative Architectures

(iv) Light and Smart Architectures

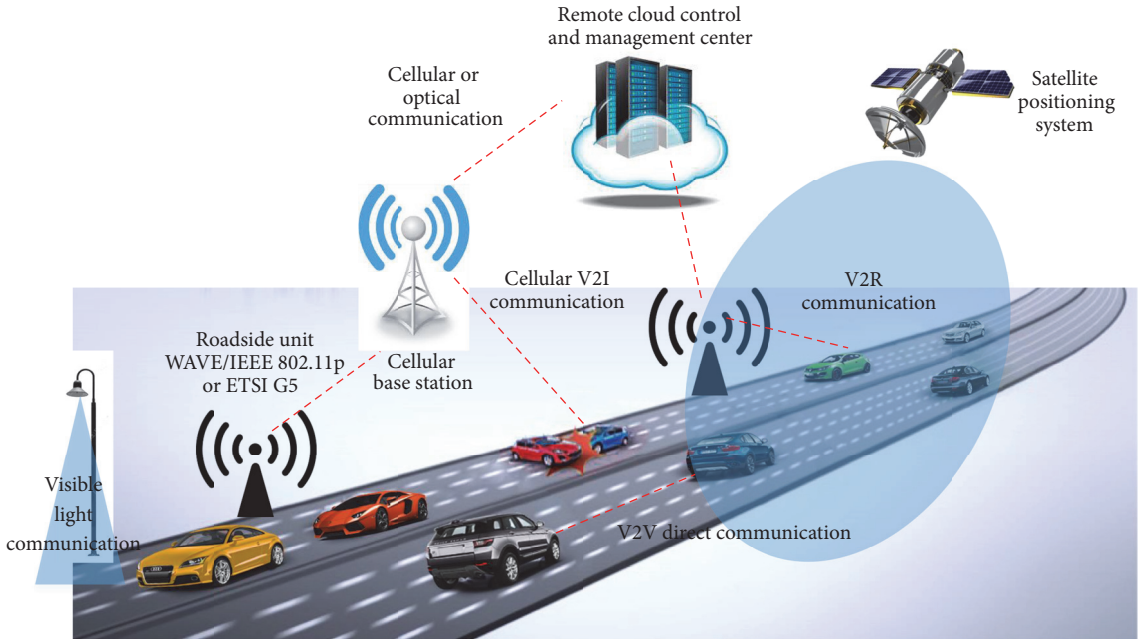

Figure 1: General architecture connecting vehicles. The figure shows several strategies for communication: (a) Visible Light Communication; (b) V2R Short Range Communication; (c) WAVE/IEEE 802.11p; (d) Cellular Communication; (e) Vehicle-to-Vehicle Communication; (f) Vehicle-to-RSU Communication; (g) Communication to Remote/Management Centers; (h) Positioning Systems.

(v) Architecture Employing Publicly Available Infrastructure

(vi) Testbeds and Real Deployments

(vii) Virtual Infrastructure

(viii) Hybrid Architectures.

In the remainder of this section, we overview the categories just outlined.

3.1. Analytic Studies Addressing Specific Aspects of the Infrastructure. Abdrabou and Zhuang [86] propose a framework based on the queuing theory that gives a delay bound for relaying messages to RSUs through V2V communication. Authors study the multihop packet delivery delay in a low-density vehicular network addressing a disrupted vehicle-to-infrastructure communication scenario where an end-to-end path is unlikely to exist between a vehicle and the nearest RSU.

3.2. Benefits of Incorporating the Infrastructure in Vehicular Networks. Kozat and Tassiulas [10] consider the transport capacity of an ad hoc network with a random flat topology under the presence of an infinite capacity infrastructure network. The main idea is to use the nodes as relays and the infrastructure as pathways to drive the message as fast as possible to the destination node. The results demonstrate a significant improvement achieved using the infrastructure support. Banerjee et al. [12] present a comprehensive comparison between different types of RSUs. Both analytical and simulation results reveal that both the relay and mesh nodes, as opposed to base stations, can be more cost-effective solutions even though a much larger number of such units are required to deliver the same level of performance as offered by the base stations. In addition, authors also suggest that adding a small infrastructure is vastly superior to a large number of mobile nodes with routing capabilities (multihop communications).

Reis et al. [13] study the effects of including RSUs as relay nodes to improve the communication in highway scenarios. Authors model the average time taken to propagate a packet to disconnected nodes when considering both scenarios of connected and disconnected RSUs. The trade-off between the required number of RSUs and the vehicular network performance in sparse scenarios is an important problem that needs careful study. The results show that significant improvements can be achieved with RSUs. For single-gap communications, the transmission delay can be reduced by 15% to 30%; for traversing multiple gaps, up to 25% reduction in the end-to-end delay with disconnected RSUs is achievable, and with connected RSUs, the decrease in delay can be of several orders of magnitude, depending on the desired area of interest. Authors conclude that sparse scenarios require a strong deployment of RSUs. In scenarios with multiple clusters, the connection between RSUs can greatly reduce the time to transmit information between vehicles. The use of RSUs to solve the disconnected network problem is still an important issue to tackle to be able to provide reliable communications for vehicular applications.

Gerla et al. [11] propose the vehicular grid, a large-scale ad hoc network with ubiquitous presence of the infrastructure. The vehicular grid must be entirely self-supporting for emergency operations (natural disaster, terrorist attack, etc.) and should also exploit the infrastructure during normal operations. The goal of the work is to bring Internet access

to drivers. Authors argue that the access is possible because every vehicle will be only a few hops away from the infrastructure (Wi-Fi, cellular, etc.). Authors show that routing propagation can be done across the urban environment. Additionally, Gerla and Kleinrock [134] perform a historical comparison of the evolution of the Internet to identify the possible paths to be followed by vehicular communication technologies. Authors argue that the type of assistance requested from the infrastructure will vary according to application. Ideal access points' installations for vehicles are traffic lights, light poles, overpasses, and other public structures. In particular, traffic lights are perfectly positioned to act as traffic routers since they form a traffic grid (i.e., they are placed where traffic is intense) and are equipped with power and directly maintained by local municipalities.

Mershad et al. [14] propose ROAMER (ROAdside Units as MEssage Routers in VANETs) to exploit RSUs to route packets between any source and destination in vehicular networks. The basic motivation behind using RSUs to route packets is that RSUs are stationary. It is much easier to send a packet to a fixed near target than to a remote moving object. ROAMER forwards packets to multiple neighbors to increase the chances of reaching destination without significantly increasing the overall traffic. Authors evaluate the RSU backbone routing performance via the ns-2 simulation platform and demonstrate the feasibility and efficiency of the scheme in terms of query delay, packet success delivery ratio, and total traffic.

3.3. Cooperative Architectures. Liang and Zhuang [22] propose roadside wireless local area networks (RS-WLANs) as a network infrastructure for data dissemination. More precisely, a two-level cooperative data dissemination approach is proposed. For the network level, the aim is to use available RS-WLANs to provide services to nomadic users. Packet level cooperation uses cooperative caching/transmission to improve the transmission rate: cooperative caching reduces the perception of limited bandwidth whereas cooperative transmission improves the packet transmission rate.

3.4. Light and Smart Architectures. Luan et al. [56] propose an infrastructure composed of roadside buffers, devices with limited buffer storage, and wireless connection to support the vehicular communication with the goal to reduce the costs of network deployment. In addition, Mishra et al. [52] propose the use of stationary info-stations and moving vehicles in a publish-subscribe model. Vehicles may act as publishers, subscribers, or brokers. Every major crossing of city is equipped with stationary info-stations that act as ultimate place holders for publications and subscriptions.

Palazzi et al. [28, 29] investigate an infrastructure for gaming over vehicular networks. They consider the problematic coexistence between TCP and UDP flows in the context of infrastructure-based vehicular networks. They observe that retransmissions of TCP are exacerbated in vehicular networks since the high mobility of vehicles generates continuous variations in the number and type of flows served by the infrastructure along the road. Thus, they propose the use of smart access points along roads, to be able to regulate heterogeneous transmission flows and make them coexist efficiently. Smart access points basically snoop transiting packets of various flows and computes the maximum data rate at which each elastic application will be able to transfer data without incurring in congestion losses. This data rate is computed and also included on the fly in transiting ACKs of TCP flows. They validate their strategy using the ns-2 simulator. Authors use a grid-like road network streaming the video Star Wars IV in high-quality MPEG4 format. Online gaming traffic is inspired by real traces of the popular Counter Strike action game, and it has (i) a server-to-client flow characterized by an interdeparting time of game updates of 200 bytes every 50 ms and (ii) a client-to-server flow of 42 bytes every 60 ms.

3.5. Architectures Employing Publicly Available Infrastructure. Marfia et al. [57] exploit the use of public Wi-Fi access points to provide vehicular communication. Authors map the public access points available in the city of Portland (US) and vehicles can opportunistically use the infrastructure to communicate with other vehicles in order to avoid long wireless ad hoc paths and to alleviate congestion in the wireless grid. Analytic and simulation models are used to optimize the communications and networking strategies. Authors conclude that the motion model has enormous impact on the results and that the presence of infrastructure largely improves the communication. When the community focuses on the shortness of contact time between vehicles and infrastructure, it becomes clear that scheduling algorithms should consider the data size and deadline or even employ broadcasting to serve a large number of requests. Zhang et al. [58] propose a scheduling scheme for RSUs to provide a balance between serving downloads and upload requests from fast-moving vehicles on highways. The infrastructure acts as routers to Internet access. Although the Internet connection proves to be of great value for drivers, the deployment and maintenance costs of the infrastructure are considered very high. Thus, the authors propose the deployment of cheap RSUs acting as buffers between vehicles.

3.6. Testbeds and Real Deployments. With the aim to create smarter roads by developing an infrastructure that is able to communicate with connected vehicles and with the aim to overcome geographical and standardization boundaries among different countries, Holland, Germany, and Austria developed the so-called Cooperative Intelligent Transport System (C-ITS) Corridor, which represents the first smart highway in Europe [135]. Two applications are implemented: roadworks warning and improved traffic management, both enabled by the cooperation of ETSI ITS-G5 and cellular networks. Roadworks warning aims to improve safety and is enabled by equipping roadworks safety trailers with a positioning/communication system. The roadworks safety trailer continuously transmits its position to a remote control center, where it is evaluated. If available, background information about the roadworks is added and sent back to the roadworks safety trailer. The trailer transmits a warning to approaching vehicles via ETSI ITS-G5. At the same time, the remote

control center can provide data to a Point of Access, where it is made available for third parties (the Point of Access is, for instance, the Mobility Data Marketplace (MDM) in Germany and the National Data Warehouse (NDW) in Netherlands).

The traffic management service, instead, aims at improving traffic management by highway operators: vehicles send messages to an ETSI ITS-G5 RSU, which then preprocesses the data and forwards it to the traffic control center via cellular network. These messages are standardized Cooperative Awareness Messages (CAM) and Decentralized Environmental Notification by Messages (DENM). CAM are sent continuously. They contain information about the current position of a vehicle, its speed, direction, and dimensions. DENM are sent event-driven when the vehicle detects ice, a traffic jam, or a broken-down vehicle, for example. The C-ITS Corridor represents the first real development given by a close cooperation between road operators and vehicle manufacturers (BMW, Daimler, Ford Deutschland, Adam Opel, and Volkswagen as well as the German Association of the Automotive Industry) [136].

In August 2012, the University of Michigan launched the Connected Vehicle Safety Pilot Model Deployment, the US's largest test of the potential of connected vehicles technologies. The project involved nearly 3,000 private cars, trucks, and buses equipped with OBUs to allow wireless communication with each other and with devices in the roadway infrastructure of northeast Ann Arbor. Communication was enabled by DSRC at 5.9 GHz [137]. The project is expanding to include up to 9,000 equipped vehicles, a back-haul communications network, and back-end data storage. Each OBU accumulates data at the rate of 10 times per second, allowing researchers to test connected vehicle operations for the applications of traffic efficiency, energy efficiency, and environmental benefits. Huge investments on connected vehicles are also done in Japan [138], where great attention on road safety and traffic management has been paid since 1998 [139] to deploy efficient roads and safer vehicles.

Wu et al. [140] propose a real testbed for evaluating communication between moving vehicles and infrastructure. Authors exploit the communication between vehicles and the infrastructure. Opportunistic forwarding (store-carry-forward) appears to be a viable approach for data dissemination using vehicle-to-vehicle communications for applications that can tolerate some data loss and delay. Studies show that V2V communication is feasible, although the propagation performance depends on factors such as the density of instrumented vehicles along the end-to-end path. Authors propose the infrastructure to reduce path vulnerability in critical areas or in a subset of vehicles equipped with cellular messaging systems. Field experiments were conducted using a laptop, 802.11b (IEEE 802.11 Wireless Local Area Networks Working Group; http://www.ieee802.org/11/) card with a 2.5 dB omnidirectional external antenna placed on the roof of the vehicle and a GPS receiver. They measured the wireless communication performance between a fixed roadside station and a moving vehicle. Most of the measurements show more than 500 m of effective communication range. They also measured communication performance between two vehicles traveling in opposite directions. Most test cases showed more than 200 m of effective communication range. Average time for effective communication is about 21 s. Authors conclude that vehicular communication is feasible.

Ormont et al. [74] mounted a testbed in the city of Madison, Wisconsin, to monitor Wi-Fi signals over the city. The main communication channel is the 3G cellular network. Clients were installed in two buses. Each city bus operates on multiple routes on a single day and is, therefore, able to traverse through significant parts of the city. Buses provide Internet access to passengers through 3G connection. A client is a laptop with a Wi-Fi interface running software that monitors and stores Wi-Fi networks found. Cellular interface provides continuous remote access to each testbed node to experimenters. A client node uses it to periodically upload measurement data to a back-end database system. Authors argue that such testbed can be used to draw coverage maps, analyze performance at specific locations, infer mobility patterns, and study relationships between performance and mobility.

Ruiz et al. [46] study the handover using WiMAX (IEEE 802.16; http://wirelessman.org/) and Wi-Fi applied to vehicular communication. They have mounted a testbed in the Campus of Espinardo, University of Murcia. Campus has a ring road that surrounds a huge enough building area. Any vehicle connected to the wireless network can freely move, using different access points that could be available throughout its path. These access points could belong to different domains and different wireless technologies like Wi-Fi, WiMAX, and Universal Mobile Telecommunication System (UMTS) (http://www.protocols.com/pbook/umts.htm). As a consequence of this, several types of handovers can be differentiated:

(i) Intradomain intratechnology handover

(ii) Intradomain intertechnology handover

(iii) Interdomain intratechnology handover

(iv) Interdomain intertechnology handover.

Authors use the Mobile Internet Protocol for IPv6 (MIPv6) (MIPL Mobile IPv6 Home Page; http://mobile-ipv6.org/) in order to make the vehicles change from service providers, but keeping the same IP address. They conclude that the deployment of wireless infrastructures must take into account the surrounding environment and the specific circumstances, using the advantages of the different wireless technologies available transparently to the end user.

The following demonstrations, trials, and projects prove how V2X communications based on cellular infrastructure can enable safety applications as well as improved comfort for the driver. 3GPP has in fact recently standardized a set of features that address vehicular communications both for direct (V2V) and for indirect (V2I, V2R) modes. More details on this technology are provided in Section 4.2.

Audi, Vodafone, and Huawei demonstrated vehicular safety applications on the world famous Circuit de Barcelona-Catalunya race track at the Mobile World Congress 2017. The applications were "see through" (connected cars can see a video feed from a vehicle in front of them in situations where it will help them to have visibility of other traffic, upcoming

entry roads, or other issues to negotiate); a traffic light warning (traffic light is about to change alerting the driver to slow down), pedestrian in the roadway warning; and emergency braking warning (other connected vehicles suddenly braking or changing lanes) [141].

In January 2017, Audi, Ericsson, Qualcomm, Swarco, and Kaiserslautern University announced the formation of Connected Vehicle to Everything of Tomorrow (ConVeX), that is, a consortium to carry out a V2X trial to evaluate range, reliability, and latency of LTE-based V2X communications. Additionally, the trial aimed at highlighting new use cases that help support traffic flow optimization and improve safety. ConVeX plans to use the results of the trial to inform regulators, provide important inputs to ongoing global standardization work, and shape a path for further development and future evolution of Cellular-V2X [142].

Ericsson, Orange, and PSA Group have also planned field trials to test advanced Cellular-V2X applications in France, starting in February 2017. The initial phase of testing focused on two use cases: "see through" between two connected vehicles on a road and "emergency vehicle approaching," aiming at notifying drivers when an emergency vehicle is nearby in real time. These two use cases rely on low latency and high throughput, given that two vehicles need to directly exchange a high-resolution video stream [143].

Vodafone, Bosch, and Huawei are currently working on a trial in the stretch of the A9 Nuremberg and Munich in Germany in the context of a project called Mobilfunk. During the trial, the consortium is demonstrating the viability of direct V2V communications and the ability to exhibit very low latency. In addition, the tests are intended to investigate how Cellular-V2X differs from the IEEE 802.11p [144].

Jaguar Land Rover, Vodafone, and other partners are currently involved in a project called Connected Intelligent Transport Environment (UKCITE) to create an environment for testing connected and autonomous vehicles. It involves equipping over 40 miles of urban roads, dual-carriageways, and motorways with various V2X technologies. The project establishes how this technology can improve journeys; reduce traffic congestion; and provide entertainment and safety services through better connectivity [145].

Audi, Deutsche Telekom, Huawei, and Toyota are conducting trials of Cellular-V2X technology on a section of the "digital A9 motorway testbed" near Ingolstadt, Germany. Audi AG and Toyota Motor Europe research cars and Deutsche Telekom infrastructure have been specially equipped with V2X hardware from Huawei to support the trial scenarios [146].

Continental, DT/T-Systems, Nokia, and Fraunhofer have demonstrated with a trial that vehicles on the motorway can share hazard information using Deutsche Telekom's LTE network. As extremely short transmission times are vital for this purpose, a section of the Deutsche Telekom network was equipped with innovative Mobile Edge Computing technology from Nokia Networks and upgraded with position-locating technology developed by Fraunhofer ESK. This combination permitted indirect signal transport times between two vehicles of less than 20 milliseconds [147].

3.7. Virtual Infrastructure. Jerbi et al. [50] observe that the need for an infrastructure can decrease the area of vehicular network applications. Therefore, the authors propose a self-organizing mechanism to emulate a geolocalized virtual infrastructure in order to avoid the costs of the deployment. To this purpose, vehicles currently populating the geographic region are used. The geolocalized virtual infrastructure mechanism consists in electing vehicles that will perpetuate information broadcasting within the intersection area. The geolocalized virtual infrastructure is composed of two phases: (i) select vehicles able to reach the broadcast area and (ii) only one among the selected vehicles is elected as the local broadcaster. The elected vehicle performs a local/single hop broadcast once it reaches the broadcast area. Authors conclude that the proposed geolocalized virtual infrastructure can (i) periodically disseminate the data within a given area; (ii) efficiently utilize the limited bandwidth; and (iii) ensure a high delivery ratio.

Luo et al. [51] propose MI-VANET (Mobile Infrastructure-based VANET), a two-tier architecture: buses constitute the mobile backbone for data delivery, while the low tier is composed of ordinary cars and passengers. Cars must register in buses in order to send/receive data. There is a score mechanism to choose the best bus. When the car is leaving the communication range of its registered bus, another bus will be chosen for registration. Authors use VanetMobiSim as a traffic simulator, and they assume that (i) vehicles are uniformly distributed over the road and (ii) buses represent 20% of the vehicles. Routing algorithm used on the high tier is called Mobile Infrastructure Routing. Each bus knows its location and has a digital street map including bus line information. MIRT is a location based reactive routing protocol that selects the optimal route and forwards the request hop-by-hop. Simulation results show that there is a 40–55% improvement in delivery ratio while the throughput is even doubled compared to greedy perimeter stateless routing (GPSR) for wireless networks (http://www.cs.cmu.edu/~./bkarp/gpsr/gpsr.html) in traditional vehicular networks.

Annese et al. [44] study the vehicle-to-infrastructure communication to provide UDP-based multimedia streams. The work considers continuous coverage by the infrastructure within the urban road topology and analyzes the vehicular communication as a mesh network [148]. Mesh networks are typically free-standing robust systems that can be conveniently integrated with the existing infrastructure and offer high bit rate services. Authors do not assume vehicles as end nodes (such as those proposed in [31–33, 73]), but as mesh nodes connecting the wireless medium and acting as routers. They argue that such new point of view is important because it allows the routing protocol to run on the mobile node itself, better adapting to the high-mobility profile of the node. The vehicle becomes a mobile hot spot that can act as a gateway towards the mesh infrastructure.

Because of the high investments required to deploy RSUs in large cities, Tonguz and Viriyasitavat [53] propose an alternative approach to roadside infrastructure by leveraging the use of existing DSRC-equipped vehicles to provide RSU's functionality. The approach employs a self-organizing

network paradigm and draws its inspiration from social biological colonies such as ants, bees, birds, and fishes. Such approach was formulated for the first time by Tonguz [94]. Vehicles acting as temporary RSUs must make brief stops during which they act as communication bridges for other vehicles in the network. Each vehicle runs the distributed gift-wrapping algorithm proposed by Viriyasitavat et al. [20]. Upon receiving a message, the vehicle determines whether it lies on the boundary of a coverage polygon. As a drawback, vehicles acting as temporary RSUs need to make brief stops (approximately 30 s) to reach the maximum number of uninformed vehicles. Authors argue that such increase in travel time is small when compared to increases due to accident-induced congestion. Finally, Sommer et al. [54] propose utilizing parked vehicles as relay nodes to address the disconnected network problem. Extensive simulations and real life experiments show that parked cars can increase cooperative awareness by over 40%.

3.8. Hybrid Architectures. Silva and Meira [55] propose integrating stationary RSUs and mobile RSUs into a single architecture. They argue that traffic presents fluctuations according to the type and time of day, weather conditions, events, road works, and accidents. An architecture composed just of stationary RSUs might not thus be able to properly support the network operation all the time. Similarly, an architecture composed just of mobile RSUs may lack part of the robustness provided by stationary RSUs. Furthermore, the traffic fluctuations are limited by the underlying road network, and road networks do not change as often as traffic does [149]. Therefore, it seems straightforward to assume that a set of RSUs will be stationary, while other RSUs will roam in order to meet the traffic changes.

Since major roads account for a higher transportation capacity, that is, they tend to be very popular routes, they are natural candidates for receiving the stationary RSUs. On the other hand, mobile RSUs may be assigned for handling secondary roads: during rush hours, the major roads get congested, and the drivers use secondary roads as an alternative route for escaping congestions, turning the secondary roads into a candidate for receiving temporary support from mobile-and-virtual RSUs, such as drones launched by the stationary RSUs. When considering the functionality, stationary RSUs act as a main backbone for data dissemination by covering the most important regions of an urban area (i.e., regions known as always presenting relevant traffic), while mobile RSUs provide a temporary support for the dissemination of traffic announcements. The results demonstrate that (i) the hybrid architecture improves the number of distinct vehicles experiencing V2I (vehicle-to-infra) contacts up to 45% and (ii) the feasibility of incorporating mobile RSUs within public transportation vehicles and drones, since the mobile RSUs must travel at speeds ranging from 5.2 km/h up to 11.3 km/h.

4. Communication in Infrastructure-Based Vehicular Networks

To address the requirements foreseen by future vehicular networks, different communication modes and technologies have to be adopted, so that the best radio access technology can be used depending on the applications requirements or on technology availability. Figure 1 represents different communication modes needed in a vehicular environment, such as wide area cellular, V2I, V2V, and V2R [3, 150, 151].

An overview of the key C-ITS and DSRC protocols from a standardization perspective is provided in [152] where the road to 5G is also sketched.

This section provides a summary of the currently available wireless communication standards for V2V, V2R, and V2I. The following subsections then present efforts in addressing communication in infrastructure-based vehicular networks.

4.1. IEEE WAVE and ETSI ITS-G5. In October 1999, the Federal Communications Commission (FCC) in US allocated 75 MHz of spectrum in the 5.9 GHz range (5825–5925 MHz) for Dedicated Short Range Communications (DSRC). This motivated the IEEE standardization body to specify a family of standards called Wireless Access in Vehicular Environments (WAVE) to deliver a communications framework to enable the services such as road safety applications, traffic management, and infotainment. The first trial version of WAVE standard was released in 2006. The IEEE WAVE standard specifies direct communication among vehicles as well as communication between vehicles and the infrastructure. The latter is enabled by deployment of roadside units (RSUs). The V2V mode addresses the need for safety applications which are latency sensitive and allows cars to send to each other periodic updates of their status (i.e., speed and position). Vehicles can communicate directly using the WAVE Short Message Protocols (WSMP). Each vehicle is then connected to the infrastructure through the V2I mode in order to exchange data and control information with the cloud. WAVE enables secure communication and physical access for low latency links, with speeds of up to 27 Mbps across a range of approximately 1000 m. The following standards are part of the IEEE WAVE family:

(i) IEEE 1609 series for architecture, security services for applications and management messages, networking service, multichannel operation, communication manager, over-the-air electronic payment data exchange protocol, and identifier allocations;

(ii) IEEE 1906.4 for MAC layer functions;

(iii) IEEE 802.11p for MAC sublayer management and physical layer.

In the context of DSRC, several research works have been carried out. Campolo et al. [153] present an analytical framework that models the service advertisement and access mechanisms in multichannel vehicular networks. The model accounts for dual-radio devices and computes the mean service discovery time and the service channel utilization. Bazzi et al. [150] demonstrate the impact of number and position of RSUs on the delivery rate of IEEE 802.11p also varying the routing algorithm.

In 2008, the European commission allocated 30 MHz within the 5.9 GHz band for C-ITS wireless communications.

Following this allocation, the European Telecommunications Standard Institute (ETSI) developed a set of standards for C-ITS, whose objectives are very similar to the ones that motivated the development of WAVE in the US and whose access layer uses a specific set of options of the IEEE 802.11p specifications. IEEE 802.11p in US and ITS-G5 Release 1 in Europe have been considered to date as the de facto standard technologies for vehicular communications at 5.9 GHz, but things are now changing since 3GPP has also standardized a set of communication features for vehicular scenarios, which we refer to as Cellular-V2X, as outlined in Section 4.2.

4.2. 3GPP Cellular-V2X. Cellular systems are nowadays widely recognized as drivers of innovation in a wide range of technical fields, and they today represent the most adopted solution to collect data from vehicles and retransmit them to the network through on-board units. This avoids having to build new set-ups or expensive installations at the roadside. Issues like authorization, authentication, and resource allocation are currently always handled by the wide area network.

Moreover, today 3GPP is playing a key role in specifying new features for supporting a wide range of vehicular modes of communications (V2V, V2I, and V2R). We refer to this set of features as Cellular-V2X technologies. Within the Technical Specification Group (TSG) Services and Architecture (SA), a basic set of requirements to support early Cellular-V2X applications has been specified in [154] following the studies reported in [16]. These requirements are sufficient for vehicles to directly and periodically exchange their own status information such as position, speed, and heading with neighboring vehicles, pedestrians, and road infrastructure nodes and also address the need to disseminate event-driven warning messages. These are the IEEE WAVE and ETSI C-ITS main focus safety use cases. To address these use cases, the TSG Radio Access Network (RAN) specified V2V communications within Release 14, which builds on the device-to-device (D2D) communications features specified in Release 12 (where the focus was mainly on public safety type of use cases). Within this framework, a new communication interface called Sidelink (or PC5 interface) was specified in Release 12 [155] as a direct link between devices. Improvements to this interface have been added to [155] within Release 14 to address the V2V use cases in the ITS 5.9 GHz band and more specifically

(i) to handle higher Doppler associated with relative speeds of up to 500 Kmph at 5.9 GHz;

(ii) to insert arrangements for scheduling assignment and data resources;

(iii) to introduce a sensing with semi-persistent transmission based mechanism for distributed scheduling.

Two high-level deployment configurations are currently defined: distributed scheduling and eNB scheduling. Both configurations use a dedicated carrier for the V2V link, which is the target ITS 5.9 GHz band, and in both cases GNSS is used for time synchronization. This initial work was completed in September 2016 (see [156], which was used to inform 3GPP and external stakeholders that the specification work for V2V using Sidelink is complete). TSG-RAN then worked on enhancing these specifications by adding support for congestion control; coexistence with other ITS technologies that might be using the 5.9 GHz band; and the V2I interface (work item described in [157]). This work was completed within Release 14, which was frozen in February 2017. This can be considered as the first release of Cellular-V2X technologies.

In [158], TSG-SA has then defined new service requirements to further enhance 3GPP support for Cellular-V2X in the following areas:

(i) nonsafety V2X services (e.g., connected vehicle, mobile high data rate entertainment, mobile hot spot, office, home, and dynamic digital map update);

(ii) safety-related V2X services (e.g., autonomous driving, car platooning, and priority handling between safety-related V2X services and other services);

(iii) support for V2X services in multiple 3GPP radio access technologies (e.g., LTE and 5G) and networks environments including aspects such as interoperability with non-3GPP V2X technologies (e.g., ITS-G5, IEEE 802.11p, and ITS-Connect).

In order to address the requirements envisioned by the new use cases, vehicles require new levels of connectivity and intelligence. All the services in the three outlined areas will be addressed by subsequent 3GPP releases, and the Cellular-V2X features will continue to seamlessly evolve release after release by addressing new and more stringent requirements on network capacity, coverage, reliability, and latency [159–162].

5G is currently in the process of being specified by 3GPP in Release 15. It is a phased approach, and the first 5G release will be finished by the end of 2017, with focus on enhanced mobile broadband. Subsequent releases will focus on different use cases that require lower latency and higher reliability. The 5G new air interface, which is called New Radio (NR) in 3GPP context, will ensure increased performance in terms of throughput, latency, reliability, connectivity, and mobility. The architecture of a 5G system aims to support the convergence of different applications onto a common network, by flexible usage and configuration of network functions. 5G will help to reach a better coverage through the integration of various access technologies and is envisioned to support higher mobility, for example, 500 km/h. 5G is also envisioned to improve network reliability, with a 10–5-packet loss rate for safety-critical services.

Table 1 represents a set of vehicular applications addressed by ETSI C-ITS Release 1 and 3GPP Release 14. As mentioned above, the main focus of these two standards is safety and traffic management. ETSI also specifies requirements for infotainment, which, in the context of 3GPP, are addressed by earlier releases. The table highlights requirements for type of connectivity, beacon periodicity (BP) for periodic exchange of status information, and end-to-end latency. (All the applications are enabled by beacons exchange among vehicles.

Table 1: Applications and requirements for ETSI and 3GPP.

Application	V2X	Message type	Beacon periodicity [Hz]	End-to-end latency [ms]
ETSI safety				
Emergency electronic brake lights	V2X	Periodic	10	100
Safety function out of normal condition warning	V2X	Periodic	1	100
Emergency vehicle warning	V2X	Periodic	10	100
Slow vehicle	V2X	Periodic	2	100
Motorcycle warning	V2X	Periodic	2	100
Vulnerable road user warning	V2X	Periodic	1	100
Wrong way driving warning	V2X	Event-driven	10	100
Stationary vehicle warning	V2X	Event-driven	10	100
Traffic condition warning	V2X	Event-driven	10	N/A
Signal violation warning	V2X	Event-driven	10	100
Roadwork warning	I2V	Periodic	2	100
Decentralized floating car data	V2X	Event-driven	1–10	N/A
Precrash sensing warning	V2X	Event-driven	10	50
Hazardous location notification	V2X	Event-driven	N/A	
ETSI traffic management				
Regulatory speed limit	I2V	Event-driven	1–10	500
Traffic light optimal speed advisory	I2V	Periodic	2	100
Traffic information and recommended itinerary	I2V	Periodic	1–10	500
Enhanced route guidance and navigation	I2V	Periodic/event-driven	1	500
Intersection management	I2V	Periodic	1	500
Cooperative flexible lane change	I2V/V2V	Periodic/event-driven	1	500
Limited access warning	I2V/V2V	Periodic/event-driven	1–10	500
Electronic toll collection	I2V/V2I	Periodic/event-driven	1	200
Cooperative adaptive cruise control	V2X	Periodic	2	100
Highway platooning	V2X	Periodic	2	100
ETSI infotainment				
Point of interest notification/automatic access	I2V/V2I	Periodic/event-driven	1	500
Local electronic commerce/instant messaging	I2V/V2I	Periodic/event-driven	1	500
Car rental/sharing assignment/reporting	I2V/V2I	Periodic/event-driven	1	500
Media downloading/map download and update	I2V/V2I	Periodic/event-driven	1	500
Ecological/economical drive	I2V/V2I	Periodic/event-driven	1	500
Personal data synchronization/vehicle relation management	I2V/V2I	Periodic/event-driven	1	500
SOS service/stolen vehicle alert	I2V/V2I	Periodic/event-driven	1	500
Remote diagnosis and just in time repair notification	I2V/V2I	Periodic/event-driven	1	500
Vehicle data collection for product life cycle management	I2V/V2I	Periodic/event-driven	1	500
Insurance and financial services	I2V/V2I	Periodic/event-driven	1	500
Fleet management/loading zone management	I2V/V2I	Periodic/event-driven	1	500
Vehicle software/data provisioning and update	I2V/V2I	Periodic/event-driven	1	500
Vehicle and RSU data calibration	I2V/V2I	Periodic/event-driven	1	500

Table 1: Continued.

Application	V2X	Message type	Beacon periodicity [Hz]	End-to-end latency [ms]
3GPP safety				
V2I emergency stop use case	V2I	Periodic	10	100
Queue warning	V2X	Periodic	N/A	100
Road safety services	V2I	Periodic/event-driven	10	100
Wrong way driving warning	Periodic/event-driven	N/A	N/A	
Precrash sensing warning	Event-driven	N/A	20	
V2X in areas outside network coverage	Event-driven	N/A	N/A	
V2X road safety service via infrastructure	Event-driven	N/A	N/A	
Curve speed warning	V2I	Periodic	1	1000
Warning to pedestrian against pedestrian collision	V2X	Periodic	N/A	N/A
3GPP traffic management				
Automated parking system	V2X	Event-driven	N/A	100

Beacons packets are typically short and contain basic information such as the vehicle identification, position, speed, and acceleration. Hence, by exchanging beacons, vehicles become aware of the environment: more frequent beacons mean more consciousness of each own neighbor but higher channel load and risk of collisions.) Please note that the mode infrastructure to vehicle (I2V) has been used to identify those use cases that require updates being broadcast by the network to the vehicles.

4.3. Visible Light Communications: The IEEE 802.15.7 Standard. The great development and deployment of LEDs lights have increased the interest in Visible Light Communications (VLC) technology and to a recent standardization activity, namely, the IEEE 802.15.7 standardization group, which explicitly considers vehicles and illuminated roadside devices (such as traffic lights or street lights) among the addressed applications [163]. The IEEE 802.15.7 specification defines three different PHY levels, with a number of possible modulations and coding schemes, that support data rate ranging from 11.67 kb/s to 96 Mb/s. Since the specifications suggest only using PHY I in outdoor applications, the maximum data rate for vehicular communications is however presently limited to a maximum of 266.6 kb/s. At the MAC layer four options are foreseen by IEEE 802.15.7: either beacon enabled slotted random access or nonbeacon enabled unslotted random access, both with or without carrier sensing multiple access with collision avoidance (CSMA/CA). In VVLNs, nonbeacon enabled unsolved random access without CSMA/CA seems the preferable solution in most cases. At the same time, carrier sensing allows higher throughput and the increasing complexity required for its implementation does not appear as a problem in the vehicular scenario. Table 2 summarizes the main characteristics of the wireless access technologies for vehicular networks.

The following subsections present efforts addressing communication in infrastructure-based vehicular networks. We identify the following major categories of works composing the communication efforts:

(i) Analytic Studies Addressing Specific Properties of Vehicle-to-Infrastructure Communication

(ii) Strategies for Data Dissemination in Infrastructure-Based Vehicular Networks

(iii) Protocols for Infrastructure-Based Vehicular Networks

(iv) Routing in Infrastructure-Based Vehicular Networks

(v) Managing Infrastructure-Based Vehicular Networks

(vi) Privacy and Security in Infrastructure-Based Vehicular Networks

4.4. Analytic Studies Addressing Specific Properties of Vehicle-to-Infrastructure Communication. Ng et al. [84] study the access probability considering an infrastructure wherein a number of base stations are uniformly deployed along a long road, while other vehicles or cars are distributed on the road according to a Poisson distribution. The authors formulate a mathematical model that relates the density of vehicles, coverage range, and distance between adjacent base stations to infer the access probability. No measures of delay are given, and opposite-lane message relaying is not considered.

Ng and Mao [83] analyze the probability of k-hops connectivity in infrastructured wireless networks, while Malandrino et al. [23] address content downloading in vehicular networks leveraging both infrastructure-to-vehicle and vehicle-to-vehicle communication. Authors formulate a max-flow problem that accounts for practical aspects, including channel contention and the data transfer paradigm. The goal of the paper is to answer the following question: "what is the maximum downloading performance theoretically achievable through DSRC-based I2V/V2V communication in

Table 2: Main characteristics of wireless access for vehicular networks.

	WAVE IEEE 802.11p	3GPP LTE-A	IEEE 802.15.7 (VLC)	5G
Frequency	5.9 GHz	400 MHz–3.5 GHz	380–800 THz	New bands between 700 MHz and 100 GHz
Data rate	27 Mb/s	3 Gb/s (downlink) 1.5 Gb/s (uplink)	11.67 kb/s–96 Mb/s	Up to 1000 times greater
Communication range	<1000 m	Ubiquitous	<100 m	Ubiquitous
Latency	<100 ms	<100 ms	<50 ms	<10 ms
Mobility speed	<300 km/h	<300 km/h	N/A	<500 km/h
V2I communication	Supported after deployment of RSUs	Supported	May use the available roads lights	Networks cooperation
V2V communication	Supported	Supported from Release 14 in 5.9 GHz	Supported	Networks cooperation
Deployment	Requiring RSUs set-up	May use the available eNodes B	May use the available LEDs	Upper layers cooperation and management

a given mobility scenario?" Authors conclude that a density-based RSUs deployment yields performance close to optimum and that multihop traffic delivery is beneficial, although the gain is negligible beyond two hops away from the RSU.

Zhang et al. [49] propose an analytical model to predict both the uplink and downlink connectivity probabilities. The uplink connectivity probability is defined as the probability that messages from vehicles can be received by the infrastructure through multihop paths. The downlink connectivity probability is defined as the probability that messages can be broadcast from RSUs to all vehicles through multihop paths. Abdrabou and Zhuang [82] propose an analytic framework that helps to approximately estimate the minimum number of RSUs required to cover a road segment with a probabilistic vehicle-to-infrastructure delay guarantee, given that intermittent multihop connectivity exists between vehicles and RSUs, and vehicles are sending bursty traffic. In [42], the authors present a study of the relation between packet delivery delay and RSU density for vehicular-to-infrastructure communication in sparse vehicular networks where vehicles moving in one direction send their packets to vehicles traveling in the opposite direction in order to deliver the packets to the nearest RSU.

Lochert et al. [25] discuss the initial moments of a vehicular network and they demonstrate that during the rollout phase some kind of support is needed. Otherwise, many envisioned applications are unlikely to work until a large fraction of vehicles participate in the network. Authors use stationary support units to improve the refreshing rate of the information dissemination in city scenarios.

4.5. Strategies for Data Dissemination in Infrastructure-Based Vehicular Networks. Data dissemination is at the basis of most services enabled by vehicular networks and its importance is demonstrated by the large number of papers in the literature addressing this issue. In [164], for example, twenty-three different kinds of dissemination schemes have been reviewed and a comparative analysis is provided highlighting the benefits and drawbacks associated with each scheme.

Liu and Lee [41] propose push-based broadcast data dissemination in heavy traffic: messages are periodically broadcast to passing vehicles. In light traffic scenarios, vehicles query on-demand traffic information. Authors derive a mathematical model that shows the effectiveness of their solution and they conclude that data dissemination in vehicular networks should be adaptable to dynamic traffic environments: dynamic channel and data allocation is a critical, but an effective mechanism in providing hybrid scheduling between push-based and on-demand services.

Bruno and Nurchis [26] assume vehicles equipped with cameras and the problem is how to deliver the images to remote data collectors. Authors propose a data collection algorithm capable of eliminating the redundancy of data transmitted by moving vehicles. In a real situation, several vehicles may report the same event. Thus, data redundancy mitigation is necessary to improve the network efficiency. The model is based on the Maximum Coverage Problem [165] followed by submodular optimization.

Data scheduling is also addressed in [27], where the authors propose a downlink scheduler to deliver high-quality video-on-demand services over infrastructure-based vehicular networks. The scheduler is deployed at RSUs to coordinate the transmission of packets according to (i) importance of packet to video quality; (ii) playback deadline; and (iii) real-time information of vehicles.

Zhang et al. [166] also devise a scheduling algorithm to coordinate the distribution of data files in vehicular networks. A collection of data files are stored at distributed locations and delivered to passing vehicles. According to the popularity of files, the proposed algorithm schedules the location of

files through the selective upload and download of RSUs to maximize the delivery ratio of files to vehicles.

4.6. Protocols for Infrastructure-Based Vehicular Networks. Hadaller et al. [61] propose MV-MAX (Multi-Vehicular Maximum), a protocol to increase the global data transfer. Authors observe that when a RSU is shared by more than one vehicle, the vehicle with the lowest transmission rate reduces the effective transmission rate of all other vehicles. Observing that every vehicle eventually receives good performance when it is near the RSU, authors propose a medium access protocol that opportunistically grants access to vehicles with maximum transmission rate. The overall system throughput is improved by a factor of four.

Korkmaz et al. [63] propose a cross-layer multihop data delivery protocol with fairness guarantees where vehicles do not communicate with RSUs individually, but through one leader. The goal is to reduce the network traffic and to use bandwidth more efficiently. The leader will collect all information from other nodes and share it with RSUs.

Korkmaz et al. [40] propose a new protocol that employs fixed gateways along the road which perform periodic admission control and scheduling decisions for the packet traffic in their service area. The most important contribution of the protocol is providing delay bounded throughput guarantees for soft real-time traffic, which is an important challenge especially for a mobile multihop network. After the demands of the soft real-time traffic are met, the protocol supports the best-effort traffic using remaining bandwidth.

Ramani and Savage [31] propose SyncScan to continuously track nearby base stations by synchronizing short listening periods at the client with periodic transmissions from each base station. Brik et al. [32] propose MultiScan so that nodes rely on using their (potentially idle) second wireless interface to opportunistically scan and preassociate with alternate access points and eventually seamlessly hand-off ongoing connections.

4.7. Routing in Infrastructure-Based Vehicular Networks. A careful review of the main routing algorithms revealed that most proposals are inspired by either greedy forwarding (GF) or distance vector (DV): the former exploits the actual position of each node to find the route with the minimum source-destination distance, while the second finds the route with the minimum number of hops between the source and the destination. Since GF always tries to get closer to the destination, it appears more suitable for delay tolerant and not fully connected networks. On the other hand, DV also supports real-time communications.

Borsetti and Gozalvez [43] propose an infrastructure-assisted routing approach designed to improve the end-to-end performance, range, and operation of multihop vehicular communications by exploiting the reliable interconnection of infrastructure units. The infrastructure is wired-connected and uses the position of each vehicle to route the data. Authors use SUMO traces and a grid streets layout. They conclude that to obtain the maximum benefits from the proposed infrastructure-assisted routing approach, optimal infrastructure deployment strategies must be further investigated.

In [123], the well-known Ad hoc On-demand Distance Vector (AODV) routing protocol is modified by replacing the flooding mechanism, used in its route discovery process, with the probabilistic forwarding technique given by Irresponsible Forwarding (IF) [167]. The performance of the new routing protocol, denoted as irresponsible AODV (iAODV), is analyzed in three characteristic scenarios (pedestrian, pedestrian-vehicular, and vehicular). The obtained results show that the iAODV protocol can outperform the AODV protocol by significantly reducing the overhead traffic during the route discovery phase. In particular, iAODV takes advantage of, rather than combating, high node spatial density and/or data traffic load.

A promising solution to the information dissemination in urban environments is the intersection-based geographic routing protocol. In [168], four issues (i.e., intermittent connectivity, traffic light at intersections, and three-dimensional and traffic accident city scenarios) which strongly affect the performance of geographic routing protocols are addressed and their impact on the performance of routing protocols is demonstrated, suggesting important guidelines for network designers.

4.8. Managing Infrastructure-Based Vehicular Networks. The ultimate goal of a vehicular network is to serve as a communication layer for vehicular applications. There are several envisioned vehicular applications: monitoring roads conditions [66], vehicles' performance [169], driver's behavior [170], routes optimization [171, 172], smart traffic lights [149, 173], traffic monitoring [68], collaborative driving [69], and accident detection [174, 175] offering a large spectrum of traffic information solutions demanding minimal (and possibly distinct) QoS guarantees that must couple the vehicular network.

Traditional strategies for measuring the network performance are based on the network latency and bandwidth. However, when we consider mobile nodes, the latency and bandwidth become location-dependent, since both measurements fluctuate according to the nodes' locations. Similarly, typical metrics adopted in managing cellular networks do not seem to fully qualify for vehicular networks. However, we are not supposed to experience large-scale vehicular networks until we learn how to manage such networks. Metrics are the basis for defining Service Level Agreements that will guide the operation of vehicular networks. They will also indicate when the network demands upgrade and where the upgrade is supposed to take place.

We have captured two works addressing the QoS for lower layers: Luan et al. [36] focus on the MAC layer for V2I communications where multiple fast-moving vehicles with different on-top applications and QoS requirements compete for the transmissions to the roadside infrastructure, while Harigovindan et al. [21] develop a mechanism for fair channel allocation.

From a complementary perspective, there are also works proposing strategies based on higher layers. Silva and Meira [37] propose the Delta Network as a strategy to reflect

the connectivity experienced by vehicles. Delta is based on two measurements: (i) connectivity duration and (ii) percentage of vehicles presenting such connectivity duration. For instance, if a given vehicular network provides 20% of all vehicles connected during 30% of the trip duration, such network is considered a $\Delta_{0.2}^{0.3}$ Network. The authors argue that the Delta Network can be used to (i) support the design of new vehicular networks; (ii) compare the performance of distinct vehicular networks; and (iii) evaluate the adherence between vehicular applications and the network.

When Delta measures the time duration that vehicles are connected (only) to RSUs, the metric turns into a strategy for evaluating the quality of service provided by a given deployment of RSUs. However, in case we use Delta to measure the time duration that vehicles are connected between themselves, the metric becomes a strategy to measure the quality of service provided by the ad hoc V2V communication. We can also use Delta as a deployment strategy by formulating an optimization problem stating "how many RSUs are required (and where must they be deployed) so that we can achieve a vehicular network allowing that ρ_2 percent of the vehicles are connected to RSUs during ρ_1 percent of the trip duration?" In other words, we intend to find out how many RSUs are required to achieve a $\Delta_{\rho_2}^{\rho_1}$ Network.

The time duration that vehicles are connected is an important measurement. However, we must also characterize the interconnection gap (the time duration that vehicles are not connected). This is the goal of the Gamma Network proposed in [38, 39]. Gamma is a strategy for planning the roadside infrastructure in order to achieve predefined levels of service in terms of the interconnection gap and the share of vehicles experiencing such interconnection gap. A given layout of RSUs is considered $\Gamma_D\left(\frac{\tau}{\rho}\right)$ whenever ρ percent of all vehicles are guaranteed to meet RSUs in intervals less than (or equal to) τ seconds over the entire trip.

4.9. Privacy and Security in Infrastructure-Based Vehicular Networks. Extensive researches are being carried on to provide security and privacy in vehicular networks so that the true identity of the drivers and sensitive information are not exposed. Hence, the security and privacy issues must be handled carefully so that the adversaries cannot misuse them [176].

Plobl and Federrath [47] propose a set of security requirements for the infrastructure of vehicular networks in terms of integrity, confidentiality, and availability. In order to protect the integrity, the security infrastructure has to provide mechanisms that prevent and detect the modification of messages. Furthermore, the authenticity and integrity of the message must be provable instantly without further information. Proof of integrity and origin of data are recommended to prevent misuse of the network combined with correct time and position information in all messages to protect against replay and position spoofing attacks.

In terms of confidentiality, the security infrastructure also has to provide mechanisms that support different levels of confidentiality, and all messages should be protected against eavesdropping. In terms of availability, the network must provide real-time processing of messages, possibly using data compression techniques to reduce network bandwidth consumption combined with actions to complicate denial-of-service attacks. Authors propose that, after a once-only initialization, the system employs asymmetric cryptography within a public key infrastructure for messages influencing road safety. All other messages are protected by a system employing symmetric cryptography.

Gómez Mármol and Martínez Pérez [45] propose TRIP (Trust and Reputation Infrastructure-based Proposal), a model used to decide whether to accept a traffic warning coming from another vehicle or not by assessing the trustworthiness of the issuer of such message. Authors extend the requirements of the vehicular infrastructure by proposing that the security infrastructure should also be able to make fast decisions to deal with the constantly changing topology and fast switching of neighbors; otherwise, the communication becomes very inefficient. Network should also be resilient to security and privacy threats such as malicious nodes trying to drive the reputation of a reliable node down. Finally, the security must also be independent of mobility patterns in order to accurately perform under every possible traffic scenario.

As another example, the actors of the European C-ITS Corridor [135], which involves three countries in the experiment, faced the issues of confidentiality and availability from the early stages of the trial: for the roadworks warning application specific data protection laws were not necessary, whereas for cooperative traffic management with the inclusion of vehicle data, privacy protection has been applied to grant anonymity still providing some security to verify the authenticity of messages.

Oliveira et al. [48] propose a Social Network for Vehicular Certification (SNVC) for the exchange of cryptographic material in daily relationships. The SNVC establishes trust degrees among users in the social network and a reputation mechanism allows tracking the reputation of users. The reputation mechanism can identify users that collaborate in the generation of reliable information at the cyber-physical Mobile Opportunistic Network.

5. Deployment of Infrastructure for Vehicular Networks

The deployment of infrastructure is one of the most critical decisions when designing vehicular networks. Deployment is the task of defining the exact location of RSUs within the road network. A misleading deployment incurs in waste of valuable resources and degradation of the network performance. So far, the deployment of infrastructure for vehicular networks is an open problem since it depends on the intrinsic mobility of the network nodes and also on the applications running on top of the vehicular network. Although the deployment of RSUs may resemble the deployment of base stations in cellular networks, there are several differences. While cellular networks use massive deployments, vehicular networks do not necessarily demand ubiquitous coverage. Instead, vehicles may engage in "infofueling" as they opportunistically drive through RSUs [177].

There are also important differences in terms of the mobility of nodes in vehicular networks and cellular networks. In cellular networks, the network designer starts a deployment plan by understanding how the population is distributed over the city. On the other hand, the vehicular networks designer must start by understanding the urban mobility. The reason is quite obvious: the most important clients of the network are moving vehicles. And vehicles may cover large distances in short periods of time. One of the most intuitive deployment strategies is to first cover the most dense location; that is, the location presenting the largest number of users is prioritized to receive the communication infrastructure. Such strategy is effective for cellular networks, but not for vehicular networks. Although placing RSUs at the densest locations seems reasonable, the assumption fails when we consider that those vehicles composing dense regions are originated from nearby and the dense region results of merging flows.

At first glance, it may seem reasonable to place works presenting deployment strategies in the same class as works presenting communication strategies. However, in this article we choose to keep them as separate classes, allowing us to present distinct discussions. Works assuming important premises in terms of the location of RSUs are considered to be part of the deployment class, while works addressing any aspect of the communication (routing, protocols, and data dissemination) without assuming premises regarding the location of RSUs are considered as pure communication works.

In fact, when we look at the evolution of works since early 2000s, we notice a clear distinction between works addressing communication aspects and works proposing deployment strategies. However, the gap between both classes is increasingly reduced over time. Basically, works originally addressing communication aspects incorporate more and more premises about the infrastructure supporting the operation of vehicular networks. With such premises becoming increasingly more assertive, it becomes hard to tell whether the work is addressing communication aspects or deployment aspects.

Since we performed this survey by reading each work individually in a time ascending order, such distinction is very clear in the early works, but it becomes fuzzy in more recent ones. Our perception indicates a tendency of works migrating from pure communication to deployment, which makes sense when we consider that the research community is moving towards infrastructure-based vehicular networks.

Deployment strategies are highly dependent on city dynamics and urban mobility. When we analyze real/realistic vehicular mobility traces (such as the Vehicular Mobility Trace of the City of Cologne (Germany) available at http://kolntrace.project.citi-lab.fr/), we notice flows of vehicles converging towards attraction (and very dense) areas. Furthermore, very dense regions do not appear as isolated islands, but they result from merging flows heading towards attraction areas.

Such issue indicates that very dense regions (in cities) tend to appear somehow interconnected, and vehicles traveling near very dense areas have high probability of joining the main flow. Thus, when we consider just the density of vehicles for placing the infrastructure, we may incur in redundant coverage by deploying RSUs covering the same flow several times, while vehicles traveling outside these very popular routes will not experience any vehicle-to-infrastructure contact.

In the remainder of this section, we overview selected works from the literature in order to present the evolution of this field. We identify the following classes of deployment strategies.

(i) Analytic Studies Addressing the Deployment of RSUs

(ii) Deployment Strategies Based on the V2I (Vehicle-to-Infrastructure) Contact Probability

(iii) Deployment Strategies for the Distribution of Content

(iv) Deployment Strategies Based on Clustering

(v) Deployment Strategies Based on Geometry

(vi) Deployment Strategies Based on Evolutionary Approaches

(vii) Linear Programming Models for Solving the Deployment of RSUs

(viii) Deployment Strategies Based on the Maximum Coverage Problem.

5.1. Analytic Studies Addressing the Deployment of RSU. The state of the art for vehicular communication deals with simulations, field trials, and analytic studies. Simulations are scalable, inexpensive, and *easy* to perform and provide a full understanding before the real implementation, but they cannot represent exactly the real environments and happenings. Field trials are real but expensive, difficult to perform, and sometimes not easy to be interpreted. Analytic studies allow addressing specific issues (such as the impact of latency, the delivery rate, and the impact of the density of vehicles on performance) before implementing simulations and trials, with the great advantage of highlighting which parameter and conditions affect the performance with more importance. In the following, some relevant analytic studies are proposed, each one dealing with a different aspect of V2I communication.

Nekoui et al. [72] propose the definition of an infrastructure for vehicular networks based on the conventional definition of transport capacity. Authors develop a mathematical model where the destination nodes are chosen at random by the source nodes, and they study the impact of the infrastructure in the capacity of the vehicular networks. Using an analytic model, they show that exploiting any number of infrastructure nodes beyond a certain amount enhances the achievable capacity. Although the authors propose to handle arbitrary topologies, they assume several simplifications in the mobility model.

Alpha Coverage provides worst case guarantees on the interconnection gap [76]. A deployment of RSUs is considered α-covered if any path of length α on the road network meets at least one RSU. The solution proposed by Alpha Coverage is very interesting, but it seems to make more sense

when the network designer intends a massive deployment. As a critical analysis, in some sense, Alpha Coverage assumes the underlying premise that all roads share the same relevance and characteristics (speed, relevance to the city, density of traffic, etc.). However, when we consider real scenarios, roads tend to be very different in terms of several factors.

Sou and Tonguz [85] investigate the allocation of RSUs along a highway. They analyze the performance of RSUs taking into account important issues such as the vehicle deceleration, channel congestion, different beacon frequencies, hidden node problem, and multilane traffic. The results indicate that on a 300 km highway, the rehealing delay is reduced by 70% whereas the average number of rehealing hops is reduced by 68.4% when we deploy 50 RSUs when compared to an operation with no RSUs. Authors conclude that the deployment of a small number of RSUs can achieve a substantial improvement in sparse vehicular networks.

Bazzi et al. [97] address cellular systems as the most feasible solution in the short term to collect information messages from vehicles to a remote control center. The paper proposes a mathematical model to evaluate the impact of the envisioned service on cellular systems capacity and coverage in simplified scenarios. Results show that the acquisition of small and frequent packets from vehicles is affected by interference more than other services, such as the voice service.

Furthermore, analytical results highlight that this service could not be feasible where cells are planned for high coverage with low capacity, such as in interurban scenarios. Note, however, that, in such a scenario, the reduced number of roads and the limited alternatives do not motivate the acquisition of measurements from all vehicles with such strict delay constraints. In any case, advanced strategies could be investigated, such as the fragmentation of packets into smaller parts that can be transferred with a higher processing gain but with an increased occupation of the resources in the time domain, the storing of data until better coverage is not reached, implying a higher average delivery delay, the use of vehicle-to-vehicle communication to quickly collect higher amounts of measurements in one vehicle, and justifying the use of unicast transmissions.

5.2. Deployment Strategies Based on the V2I Contact Probability. An important figure of merit in such a dynamic environment is the fraction of space and/or time of connectivity between the vehicle and the infrastructure, especially when the vehicle is out of coverage (of a cellular network eNodeB or of a RSU) and/or when the speed is high and the contact with a RSU is limited. The longer the contact opportunity, the easier the data transfer and the higher the quality of service.

The first work we could find in the literature is the one authored by Li et al. [178]. In this work, authors propose a deployment strategy similar to the base station placement in cellular systems. The goal is to minimize the power consumption and the average number of hops from access points to gateways under the assumption of full coverage by RSUs. Gateways connect access points to the Internet. Every vehicle is considered connected to access points. Vehicle speed, density, or movement patterns have not been considered. Scheme does not take into account the interference problem and the road topology.

Zheng et al. [81] present the evaluation of a deployment strategy through the contact opportunity, which measures the fraction of distance or time that vehicles are in contact with the infrastructure. The authors also propose a deployment algorithm intended to maximize the worst case contact opportunity under budget constraints. The solution is evaluated using computer simulations and a testbed in a university campus. They consider two baseline algorithms: Random Deployment and Max–Min Distance Sampling. The Max–Min Distance Sampling [179] starts at a randomly selected location and allocates RSUs iteratively maximizing the minimum graph distance in terms of shortest paths.

Lee and Kim [79] propose a greedy heuristic to place RSUs aiming to improve the vehicles connectivity while reducing disconnections. The heuristic counts the amount of reached vehicles by each intersection considering the transmission range of RSUs. Each intersection is considered a potential location for receiving RSUs. The locations are selected based on the number of vehicles, and the heuristic does not take into account the speed or density of vehicles in a given area.

Chi et al. [107] propose three optimal algorithms to allocate RSUs: greedy, dynamic, and hybrid algorithms. Authors assume (i) placing RSUs preferentially at important intersections; (ii) allocating RSUs until every intersection is covered; and (iii) distributing RSUs as even as possible. The relevance of each intersection is evaluated using traffic factors including vehicles' density, intersection popularity, and intersection particularity. The greedy algorithm simply deploys RSUs at intersections in descending order of the intersection priority. The dynamic algorithm concentrates on the even distribution of RSUs, while the hybrid algorithm combines the previous ones, while Xiong et al. [180] propose Roadgate to address the placement of RSUs guaranteeing a probability of contact between vehicles and the infrastructure.

Bazzi et al. [181] discuss the system design and address the cellular offloading issue in urban scenarios through the deployment of WAVE/IEEE 802.11p devices on vehicles and RSUs. The work shows the impact of the percentage of equipped vehicles, of the number of deployed RSUs, and of the adopted routing protocols on the amount of data delivered. Results, obtained through an integrated simulation platform taking both realistic vehicular environments and wireless network communication aspects into account, show that the deployment of few roadside units and the use of low complexity routing protocols lead to a significant reduction of cellular resource occupation, even approaching 100% with a high density of equipped vehicles. Hence, also the *content distribution* issue is, in part, addressed, as better explained in the following section.

5.3. Deployment Strategies for the Distribution of Content. There are also deployment strategies designed for the distribution of content. Data represent, in fact, a great richness and opportunity to develop new applications and service. Hence, the acquisition and distribution of data have acquired an

increasing importance in recent years, especially for applications dealing with traffic management, user profiling, and environment monitoring. Trullols-Cruces et al. [182] introduce a mixed-integer quadratic programming based optimum RSUs' deployment scheme to provide Internet access services for the maximum road traffic volumes with limited number of RSUs.

Additionally, Liu et al. [24] propose a deployment strategy for file downloading in vehicular networks. The V2I encounters are modeled as a time continuous homogeneous Markov chain. Filippini et al. [92] investigate the scenario where two network providers are competing for market shares using games theory. They consider the distribution of content along a road of length D. Each RSU is characterized by a coverage range R, which defines its service area, and by an application level goodput for the content delivery. The goodput depends on the wireless technology of the RSU. Both simultaneous and leader-follower deployments are evaluated.

Silva et al. [131] propose the Sigma Deployment for modeling the distribution of several contents in vehicular networks in the style of a Mobile Content Delivery Vehicular Network. Since a given content may be meaningful only to a given region of interest, they assume that each content type is related to a target region where it must be made available. Furthermore, given the wide range of envisioned vehicular applications, each content requires distinct performance levels from the network defined in terms of vehicle-to-infrastructure contact probability and vehicle-to-infrastructure contact duration. A given layout of RSUs is considered a $\Sigma \binom{R_c}{c} \binom{\rho_1}{\rho_2}$ Deployment whenever ρ_2 percent of vehicles traveling R_c are connected to RSUs able to provide the content c during at least ρ_1 percent of the trip duration along R_c (R_c is a subset of regions of the road network R, where the content c has to be available). The parameters ρ_1 and ρ_2 indicate performance guarantees for vehicles finding the content c inside the regions R_c of the road network. Finally, Lu et al. [104] investigate the capacity-cost trade-offs in terms of the wireless access infrastructure.

5.4. Deployment Strategies Based on Clustering. Kchiche and Kamoun [80] propose a greedy algorithm based on the centrality of group to select the best locations for the infrastructure. The algorithm aims to maximize the performance of the message distribution system by reducing the global delay and the communication overhead of messages. The authors demonstrate that both the centrality and equidistance of the infrastructure is important to improve the quality of the coverage.

5.5. Deployment Strategies Based on Geometry. Cheng et al. [102] propose a geometry-based coverage strategy to handle the deployment problem over urban scenarios using the shape and area of road segments. Patil and Gokhale [103] propose a Voronoi [183] diagram-based algorithm for the deployment of infrastructure using the packet delay and packet loss as criteria. The authors provide a collaborative mechanism for dynamic resources management in vehicular networks, allowing managing the network quality of service. The collaboration between vehicles and RSUs is enabled through a vehicle-to-infrastructure network. They use population census within SUMO's ActivGen API to generate traffic data mimicking the real world.

Liya et al. [105] propose a randomized algorithm that calculates an approximate distance for deploying RSUs by approaching the optimal distance step by step from the initial distance $d_0 = 2R_0$, where R_0 is the transmission range. The distance is sequentially increased to $d_0(1+\theta), d_0(1+\theta)^2, \ldots, d_0(1+\theta)^n$, until the network cannot meet connectivity. As a critical analysis, the idea presented in the work seems to be very promising for massive deployments, and we can possibly improve the efficiency of the strategy by using a better strategy for assigning the RSUs.

Sou [78] addresses the placement of RSUs in rural areas and roadways where the solutions must deal with the low density of vehicles and larger areas to be covered. The author proposes the deployment of RSUs equally distanced from each other along a roadway enabling some RSUs to enter the power-saving mode optimizing energy consumption.

5.6. Deployment Strategies Based on Evolutionary Approaches. The use of virus-evolutionary genetic algorithms can be useful for real-time route planning and traffic forecasting. Lochert et al. [65] study how the infrastructure should be used to improve the travel time of data over large distances. The authors present a multilayer aggregation scheme defining landmarks. Cars passing landmarks record the time travel, which is aggregated to infer the time travel between more distant landmarks. These aggregation steps are performed by the cars themselves in a completely decentralized basis. The minimal initial deployment of RSUs is handled by a genetic algorithm based on the travel time savings. Cavalcante et al. [91] apply genetic programming to solve the deployment of RSUs in vehicular networks. Such technique starts with an initial set of possible solutions combined across generations until some stop condition is reached. The authors model the problem as a Maximum Coverage and they impose a time limit.

In Intelligent Transportation Systems, a key role is played by efficient route planning services. Such systems still have the lack of a full support of real-time traffic monitoring and the consequent real-time update of the best route suggested. In [184], an architecture for the management of dynamic path planning is proposed and limitations of traditional search algorithms in these kinds of applications are discussed. A variant of the proposed approach is consequently presented, based on the adoption of genetic algorithm to improve the efficiency of real-time navigation. The genetic approach considers many solutions at a time, so it acquires knowledge and improves the set of candidate solutions during the search process, improving the efficiency of global search of traditional algorithms. Further improvements are also proposed through virus-enhanced variant: whereas typical genetic algorithms may not be able to solve large-scale problems within a practical amount of time, viruses give a direction to the search, improving thus search rate and quality of solutions and speeding the whole process up.

5.7. Linear Programming Models for Solving the Deployment of RSUs. Aslam et al. [87] use binary integer programming to solve the allocation of RSUs. They eliminate minor roads and model major roads as a grid. Authors present two different optimization methods for placement of a limited number of RSUs in an urban region: (a) analytical binary integer programming (BIP); (b) novel Balloon Expansion Heuristic (BEH). The BIP method utilizes branch and bound approach to find an optimal analytical solution whereas BEH method uses balloon expansion analogy to find an optimal or near optimal solution. Authors conclude that the BEH method is more versatile and performs better than BIP method in terms of the computational cost and scalability.

Wu et al. [89] focus on a highway scenario with multiple lanes, exits, and intersections along the road. Vehicles can communicate with the infrastructure or use multihop relay when out of the infrastructure's transmission range. Authors model the deployment of RSUs as an Integer Linear Program formulation considering both strategies of communication so that the aggregate throughput in the network is maximized. Authors also model the impact of wireless interference, vehicle population distribution, and vehicle speeds. The model is evaluated via ns-2 and VanetMobiSim (http://vanet.eurecom.fr/) simulations. Multihop relaying allows the vehicles to deliver packets forward to the RSUs ahead or backward, according to the smallest hop count. Authors demonstrate that the scheme overcomes uniformly distributed placement.

Liang et al. [88] study the deployment of the roadside infrastructure by formulating an optimization problem and solving it using Integer Linear Programming. The proposed optimization framework takes into account the effect of buildings on signal propagation, LAN lines, and road topology. The formulation assumes a grid-like road network.

Although using a grid-like road network may seem unrealistic, we can convert a complex road network into a grid-like structure by defining urban cells. We can partition the urban area into a set of $\psi \times \psi$ (same size) urban cells. The urban cells may have arbitrary sizes in order to meet the network designer needs. When we demand more/less accuracy, we simply increase/decrease the number of urban cells covering the road network.

Without loss of generality, we can assume that each urban cell is covered by deploying one single *logical* RSU. The logical RSU is the one able to entirely cover an urban cell. The concept of logical RSUs allows us to abstract from the exact location of RSUs inside urban cells, which seems to be more realistic since the exact physical deployment depends on taking into account several practical issues, such as the presence of energy supply, signal interference, presence of constructions blocking the signal, and others. The identification of such issues tends to demand in site inspection.

In other words, we split the deployment into two complementary subtasks. The intercell deployment is a high-level selection of the regions (each region is an urban cell) that must be covered by logical RSUs. When solving the intercell deployment, we are not concerned on the exact location of the RSUs within the road network. We simply partition the road network and select the better urban cells for receiving coverage. Although the size of the urban cell can be made arbitrarily small, a good compromise seems to be achieved when the dimensions of the urban cell reflect the transmission range of RSUs. We call this intercell deployment. However, when considering the intracell deployment, we intend to define the exact set of devices that will be used for covering the selected urban cell. For instance, the network designer may choose between using a high transmission range device and using a few low-range devices, according to the specifics of the urban cell.

5.8. Deployment Strategies Based on the Maximum Coverage Problem. Trullols et al. [77] study the deployment of RSUs in urban areas. Authors use a realistic data set and propose modeling the deployment as a Knapsack Problem (KP) and also as a Maximum Coverage Problem (MCP-g). The heuristic MCP-g models the deployment of RSUs as the traditional Maximum Coverage Problem [165]. In fact, it is an adaption of the greedy solution for the Maximum Coverage Problem. In order to solve the MCP-g, we need previous and full knowledge of the trajectories of all vehicles. It receives as input a collection of sets, each set representing an intersection. The sets are defined over a domain of elements where each element represents a vehicle. MCP-g also receives a number α of available RSUs. The goal is to select at most α of these sets such that the union of the selected sets has maximal cardinality (i.e., select those intersections that cover the maximum number of uncovered vehicles). Authors demonstrate that MCP-g achieves close-to-optimum results. In the same study, the authors propose the KP heuristic that does not assume knowledge of the vehicles trajectories. The performance of KP is poor when compared to MCP-g.

Cataldi and Harri [90] propose the allocation of RSUs considering the Maximum Coverage Problem over a benefit function. The covered area is not a circle, but a polygon-based representing measured heterogeneous any-directional communication conditions. Authors argue that the coverage area of an infrastructure node cannot be modeled as a circular shape because the intensity may not reflect the quality of the experienced connectivity. The benefit function is nonhomogeneous over the covered area and the experiments use the simulator iTETRIS (An Integrated Wireless and Traffic Platform for Real-Time Road Traffic Management Solutions, http://www.ict-itetris.eu). Authors conclude that there exists an upper bound on the number of RSUs that needs to be allocated to some region.

Xie et al. [185] address the placement of RSUs in a grid-like road network assuming knowledge of the source and sink of each vehicle. Based on historical data, authors propose a probabilistic model to infer the best locations for RSUs. The probabilistic model also relies on a feature of the wireless link indicating the probability that a vehicle will get the information when driving through some RSU. This work is an extension of the proposal presented by [77]. Additionally, Yan et al. [106] propose a class of algorithms named Tailor to select a minimum number of intersections to deploy the infrastructure using a two-step approach.

Assuming previous knowledge of vehicles trajectories is a common strategy in deployment studies. However, when we

Table 3: Comparison of deployment strategies.

Deployment	Summary
Analytic studies	Theoretical studies addressing specific issues allowing us to better understand the scenario before implementing simulations and trials. As a drawback, such formulations may not represent exactly the real environments and happenings
Deployment Strategies Based on the V2I Contact Probability	The V2I contact probability measures the expected number of contacts an average vehicle tends to experiment during a typical trip. As a drawback, the V2I contact probability is a generic measure that can help the deployment of simplistic applications. However, as we increase the complexity of vehicular applications, we demand a more complete set of measurements
Deployment Strategies for the Distribution of Content	Strategies for allocating RSUs in order to deliver large files, media, streaming, and gaming
Deployment Strategies Based on Clustering	The use of clustering strategies may help the network designer to understand the flow of vehicles and capture the most important zones in order to maximize the coverage with a given set of resources
Geometry-Based Deployment Strategies	Such strategies rely on geometric properties of the city in order to define the most promising locations for receiving RSUs. Such techniques are particularly promising when combined with Geographical Information Systems and Georeferenced Data, allowing full understanding of vehicular mobility. As a drawback, just a few authors have exploited such strategy, and, as far as we are concerned, any author has applied Geographical Information Systems for solving the deployment of RSUs
Deployment Strategies Based on Evolutionary Approaches	Evolutionary approaches involve the use of metaheuristics inspired by the process of natural selection commonly used to generate high-quality solutions to optimization and search problems by relying on bioinspired operators such as mutation, crossover, and selection
Linear Programming	Technique for the optimization of a linear objective function subject to linear equality and linear inequality constraints. As a drawback, solving realistic scenarios may be prohibitive given the required computational resources
Deployment Strategies based on the Maximum Coverage Problem (MCP)	In MCP, we have a collection of sets, each set holding specific elements. The same element can exist in multiple sets. The goal is to find the minimal collection of k whose cardinality is maximal. Given its intrinsic nature, MCP is frequently used as an abstraction for the deployment problem. As a drawback, MCP modeling tends to have application as simplistic applications such as the dissemination of traffic warnings. However, more complex applications demand more sophisticated strategies for planning the roadside infrastructure

intend to maximize the number of distinct vehicles contacting the infrastructure, we may rely just on the migration ratios of vehicles between distinct locations of the road network. Since the migration ratios of vehicles do not require identifying individual vehicles, strategies based on the migration ratios do not incur in privacy concerns, while reducing the computational overhead for solving the deployment. Silva et al. [186] propose the use of turning ratios at each intersection of the road network as a basic information to infer the mobility of vehicles. Using turning ratios, the authors define the Probabilistic Maximum Coverage Problem (PMCP) as a model that improves the allocation of RSUs when we lack previous knowledge of the vehicles trajectories.

In a posterior work, Silva et al. [128] show how to generalize the application of turning ratios to large cities using the concept of urban cells. They divide the city into a grid-like structure and use the migrations ratios between adjacent urban cells. The infrastructure is deployed in urban cells selected according to the PMCP. Additionally, Silva et al. [129] propose the Full Projection of the Flow (FPF model) based on a Markovian Model to place the RSUs without the need to identify vehicles. The FPF model achieves close-to-optimal coverage when we intend to maximize the number of distinct vehicles contacting the infrastructure without relying on the trajectories information.

5.9. Comparative. In Table 3, we summarize the deployment strategies in terms of technique being applied.

5.10. Summary of Tools and Features for Studying the Deployment of Infrastructure for Vehicular Networks. On the basis of the overview of this section, we summarized the most relevant characteristics of the proposed deployment strategies, distinguishing various perspectives.

5.10.1. Optimization Targets. Given a fixed number of available RSUs, deployment strategies may have several optimization targets, some of which are summarized below:

(i) Maximum number of vehicle-to-infrastructure contacts

(ii) Maximum capacity of the network

(iii) Minimizing the communication delay

(iv) Maximizing the connectivity of the network

(v) Maximizing data dissemination

(vi) Minimizing the energy consumption of the infrastructure

(vii) Minimizing the hop count of messages.

5.10.2. Deployment Scenarios. The main infrastructure deployment scenarios of interest are typically the following:

(i) Campus: often used in testbeds and realistic simulations

(ii) Highway: often used to represent sparse traffic

(iii) Random road networks: used in nonrealistic simulations

(iv) Rural: also used for sparse traffic

(v) Theoretical grid: easy to derive analytic expressions

(vi) Urban: often used in simulations.

From the perspective of location of RSUs, the scenarios can be further grouped into two main categories:

(i) Urban: majority of works consider that RSUs should be placed at intersections.

(ii) Highway/rural: studies about sparse traffic often rely on highways and rural areas. These efforts can be roughly characterized as equidistant and nonequidistant deployments.

5.10.3. Communication and Networking. Considering communication devices and network models, the works which appeared in the literature can be summarized as follows:

(i) Stationary RSUs

(ii) Publicly available Wi-Fi

(iii) Relays and meshes

(iv) Roadside buffers: devices used for storage and replication of messages

(v) Smart devices: devices offering some kind of feature to improve routing or data dissemination

(vi) Mobile RSUs (cars, buses, drones, and parked cars).

5.10.4. Vehicular Applications. The vehicular network deployment also depends on the data manipulated by the vehicular applications, which can be summarized as follows:

(i) File download: large files and streaming of video and music

(ii) Real-time data: interaction between drivers for gamming and voice

(iii) Traffic announcements: small self-contained messages.

5.10.5. Mobility Traces. The mobility traces used in the simulation of vehicular networks may be:

(i) real;

(ii) realistic;

(iii) synthetic (see the next subsection on mobility simulators);

(iv) generated using population census (via Sumo);

(v) unrealistic.

Examples of publicly available traces are the following:

(i) Geolife Trajectories (http://research.microsoft.com/en-us/downloads/b16d359d-d164-469e-9fd4-daa38f2b2e13/);

(ii) San Francisco Cabs (http://cabspotting.org/);

(iii) Cologne (http://kolntrace.project.citi-lab.fr/);

(iv) Zurich (http://www.lst.inf.ethz.ch/research/ad-hoc/car-traces/);

(v) Beijing Taxi Traces (http://research.microsoft.com/en-us/projects/tdrive);

(vi) Borlange (http://www.openstreetmap.org/traces?display_name=jetthe&tag=Borl%C3%A4nge);

(vii) Bologna (http://www.wcsg.ieiit.cnr.it/people/bazzi/bazzi_projects.html).

5.10.6. Mobility Simulators. The most used mobility simulators are as follows:

(i) Corsim (http://mctrans.ce.ufl.edu/featured/tsis/)

(ii) SUMO (http://sumo-sim.org/)

(iii) Transims (https://code.google.com/p/transims/)

(iv) The One (DTN simulator) (http://www.netlab.tkk.fi/tutkimus/dtn/theone/)

(v) VanetMobiSim (http://vanet.eurecom.fr/).

5.10.7. Network Simulators. The most used network simulators are as follows:

(i) Network Simulator 2 (http://www.isi.edu/nsnam/ns/)

(ii) Network Simulator 3 (http://www.nsnam.org/)

(iii) Omnet++ (http://www.omnetpp.org/)

(iv) Qualnet (http://web.scalable-networks.com/content/qualnet/)

(v) iTETRIS (An Integrated Wireless and Traffic Platform for Real-Time Road Traffic Management Solutions) (http://www.ict-itetris.eu).

6. Final Remarks and Future Directions

In this article, we overviewed several works addressing infrastructure-based architectures, communications, and deployments for connected vehicles. Our goal was to summarize solutions proposed in the literature and to present

an evolutionary picture of this research field. We organized the efforts into three categories: (i) deployment of infrastructures for vehicular networks; (ii) architectures for infrastructure-based vehicular networks; (iii) communication in infrastructure-based vehicular networks.

In a general sense, in the beginning of the 2000s, the works are concerned with identifying low level communication strategies allowing the vehicular communication. Most of the works deal with aspects of the vehicle-to-vehicle communication. Overtime, researchers become more interested in defining high-level aspects of the communication, such as providing Internet access to vehicles. The discussions on Intelligent Transportation Systems also drive the research towards the definition of novel applications.

The works start to make assumptions about a minimal infrastructure supporting the vehicular communication. Then, we have the first works proposing deployment strategies. Powered by more realistic mobility models and convinced of the need of a minimal infrastructure supporting the operation of vehicular networks, the research community gradually considers more assumptions about the placement of RSUs, and works that would originally deal only with communication or architectural aspects of the network, turn into deployment works.

In the years to come, the greatest challenge seems to be bringing Intelligent Transportation Systems into the streets. In order to achieve this, we demand the development of strategies for managing vehicular networks. Without them, governments will not be able to establish Service Level Agreements for network providers. The lack of strategies for managing vehicular networks also prevents network providers from planning future expansions of the network and computing the RoI (Return on Investments). Since Intelligent Transportation Systems are (typically) critical mission systems, and the decision-making is highly dependent on the data collected from the network, properly designing and managing the communication network is an essential step before deploying any vehicular application. Otherwise, there is reduced confidence on the availability and robustness of ITS systems.

Much more study is still to come. A thorough comprehension of the urban and rural mobility is certainly a crucial aspect for the development of ITS communication. An in-depth understanding of urban and rural mobility enables us to design, develop, evaluate, and validate more realistic ITS models in terms of algorithms, analytic formulations, optimization models, and probabilistic approaches. More sophisticated ITS models support the development of better strategies for planning and managing the communication in ITS. Furthermore, better ITS models combined with a better understanding of the role played by mobile networks may even allow new insights into the application of the Internet of Things, cloud-based services, and Software Defined Networks (SDNs), allowing the development of more sophisticated services and applications. The management aspects of Software Defined Networks, Internet of Things, and clouds are crucially important in the development and wide deployment of these networks. Their adoption in ITS systems is also vitally important for their wider applicability and real deployment.

To provide more efficient and effective vehicular applications, the communication network management should enable easy establishment along roads and in low-density areas. Where network coverage cannot be guaranteed, device-to-device (D2D) communication will be essential. 5G will represent a great technological breakthrough in this contest, by letting technologies and applications cooperate to achieve higher quality of service and experience. Furthermore, the use of social networking and crowd sourcing strategies may also represent a valuable source of management information for ITS. Handling large amounts of data from mobile devices in order to infer interesting knowledge and/or patterns may provide a turning point in terms of the ITS technology.

Conflicts of Interest

The authors declare that there are no conflicts of interest regarding the publication of this paper.

References

[1] D. F. Macedo, S. De Oliveira, F. A. Teixeira, A. L. L. Aquino, and R. A. Rabelo, "(CIA) 2-ITS: interconnecting mobile and ubiquitous devices for intelligent transportation systems," in *Proceedings of the 2012 IEEE International Conference on Pervasive Computing and Communications Workshops, PERCOM Workshops 2012*, pp. 447–450, March 2012.

[2] White Paper, European Transportation Policy for 2010: Time to Decide, Office for Official Publications of the European Communities, Luxembourg, 2001.

[3] H. Hartenstein and K. P. Laberteaux, "A tutorial survey on vehicular ad hoc networks," *IEEE Communications Magazine*, vol. 46, no. 6, pp. 164–171, 2008.

[4] S. Yousefi, M. S. Mousavi, and M. Fathy, "Vehicular Ad hoc Networks (VANETs): challenges and perspectives," in *Proceedings of the 6th International Conference on ITS Telecommunications (ITST '06)*, pp. 761–766, June 2006.

[5] J. Jakubiak and Y. Koucheryavy, "State of the art and research challenges for VANETs," in *Proceedings of the 5th IEEE Consumer Communications and Networking Conference (CCNC '08)*, pp. 912–916, Las Vegas, Nev, USA, January 2008.

[6] C. Bergnhem, S. Shladover, and E. Coelingh, "Overview of platooning systems," in *Proceedings of the 19th ITS World Congress*, Vienna, Austria, 2012.

[7] T. Taleb, A. Benslimane, and K. B. Letaief, "Toward an effective risk-conscious and collaborative vehicular collision avoidance system," *IEEE Transactions on Vehicular Technology*, vol. 59, no. 3, pp. 1474–1486, 2010.

[8] K. C. Dey, A. Rayamajhi, M. Chowdhury, P. Bhavsar, and J. Martin, "Vehicle-to-vehicle (V2V) and vehicle-to-infrastructure (V2I) communication in a heterogeneous wireless network - Performance evaluation," *Transportation Research Part C: Emerging Technologies*, vol. 68, pp. 168–184, 2016.

[9] Audi cars now talk to stoplights in vegas. IEEE Spectrum, 2016.

[10] U. C. Kozat and L. Tassiulas, "Throughput capacity of random ad hoc networks with infrastructure support," in *Proceedings of the 9th Annual International Conference on Mobile Computing And Networking*, pp. 55-56, San Diego, CA, USA, September 2003.

[11] M. Gerla, B. Zhou, Y.-Z. Lee, F. Soldo, U. Lee, and G. Marfia, "Vehicular grid communications: The role of the internet infrastructure," in *Proceedings of the 2nd Annual International Workshop on Wireless Internet, WICON '06*, August 2006.

[12] N. Banerjee, M. D. Corner, D. Towsley, and B. N. Levine, "Relays, base stations, and meshes," in *Proceedings of the 14th ACM international conference*, pp. 81–91, San Francisco, CA, USA, September 2008.

[13] A. B. Reis, S. Sargento, and O. K. Tonguz, "On the performance of sparse vehicular networks with road side units," in *Proceedings of the 2011 IEEE 73rd Vehicular Technology Conference, VTC2011-Spring*, pp. 1–5, May 2011.

[14] K. Mershad, H. Artail, and M. Gerla, "ROAMER: roadside Units as message routers in VANETs," *Ad Hoc Networks*, vol. 10, no. 3, pp. 479–496, 2012.

[15] Y. Wu, Y. Zhu, and B. Li, "Infrastructure-assisted routing in vehicular networks," in *Proceedings of the IEEE Conference on Computer Communications (INFOCOM '12)*, pp. 1485–1493, IEEE, Orlando, FL, USA, March 2012.

[16] 3GPP, Study on LTE support for Vehicle to Everything (V2X) services. TR22.885, 2016.

[17] 3GPP, Study on LTE-based V2X services, TR36.885, 2016.

[18] A. Bazzi, B. M. Masini, and A. Zanella, "Performance analysis of V2v beaconing using LTE in direct mode with full duplex radios," *IEEE Wireless Communications Letters*, vol. 40, no. 6, pp. 685–688, 2015.

[19] M. Centenaro, L. Vangelista, A. Zanella, and M. Zorzi, "Long-range communications in unlicensed bands: The rising stars in the IoT and smart city scenarios," *IEEE Wireless Communications*, vol. 230, no. 5, pp. 60–67, 2016.

[20] W. Viriyasitavat, F. Bai, and O. K. Tonguz, "UV-CAST: An urban vehicular broadcast protocol," in *Proceedings of the 2010 IEEE Vehicular Networking Conference, VNC 2010*, pp. 25–32, December 2010.

[21] V. P. Harigovindan, A. V. Babu, and L. Jacob, "Proportional fair resource allocation in vehicle-to-infrastructure networks for drive-thru Internet applications," *Computer Communications*, vol. 400, pp. 33–50, 2014.

[22] H. Liang and W. Zhuang, "Cooperative data dissemination via roadside WLANs," *IEEE Communications Magazine*, vol. 500, no. 4, pp. 68–74, 2012.

[23] F. Malandrino, C. Casetti, C.-F. Chiasserini, and M. Fiore, "Content downloading in vehicular networks: What really matters," in *Proceedings of the IEEE INFOCOM 2011*, pp. 426–430, April 2011.

[24] Y. Liu, J. Niu, J. Ma, and W. Wang, "File downloading oriented Roadside Units deployment for vehicular networks," *Journal of Systems Architecture*, vol. 590, no. 10, Part B, pp. 938–946, 2013.

[25] C. Lochert, B. Scheuermann, M. Caliskan, and M. Mauve, "The feasibility of information dissemination in vehicular ad-hoc networks," in *Proceedings of the 2007 Fourth Annual Conference on Wireless on Demand Network Systems and Services, WONS'07*, pp. 92–99, January 2007.

[26] R. Bruno and M. Nurchis, "Robust and efficient data collection schemes for vehicular multimedia sensor Networks," in *Proceedings of the 2013 IEEE 14th International Symposium on a World of Wireless, Mobile and Multimedia Networks, WoWMoM 2013*, June 2013.

[27] H.-H. Chen, S. Ou, K. Yang, and A. Galis, "A selective downlink scheduling algorithm to enhance quality of VOD services for WAVE networks," *Eurasip Journal on Wireless Communications and Networking*, vol. 2009, Article ID 478157, 2009.

[28] C. E. Palazzi, M. Roccetti, S. Ferretti, and S. Frizzoli, "How to let gamers play in infrastructure-based vehicular networks," in *Proceedings of the 2008 International Conference in Advances*, pp. 95–98, New York, NY, USA, December 2008.

[29] C. E. Palazzi, S. Ferretti, and M. Roccetti, "Smart Access Points on the road for online gaming in vehicular networks," *Entertainment Computing*, vol. 10, no. 1, pp. 17–26, 2009.

[30] H. Wu, R. Fujimoto, M. Hunter, and R. Guensler, "An architecture study of infrastructure-based vehicular networks," in *Proceedings of the 8th ACM international symposium*, pp. 36–39, Quebec, Canada, October 2005.

[31] I. Ramani and S. Savage, "SyncScan: practical fast handoff for 802.11 infrastructure networks," in *Proceedings of the Proceedings IEEE 24th Annual Joint Conference of the IEEE Computer and Communications Societies.*, pp. 675–684, Miami, FL, USA.

[32] V. Brik, A. Mishra, and S. Banerjee, "Eliminating handoff latencies in 802.11 WLANs using multiple radios," in *Proceedings of the 5th ACM SIGCOMM Conference*, p. 27, Berkeley, CA, USA, October 2005.

[33] Y. Amir, C. Danilov, M. Hilsdale, R. Musaloiu-Elefteri, and N. Rivera, "Fast handoff for seamless wireless mesh networks," in *Proceedings of the 4th international conference*, pp. 83–95, New York, NY, USA, June 2006.

[34] A. Boukerche, H. A. B. F. Oliveira, E. F. Nakamura, and A. A. F. Loureiro, "Vehicular Ad Hoc networks: a new challenge for localization-based systems," *Computer Communications*, vol. 310, no. 12, pp. 2838–2849, 2008.

[35] U. T. Rosi, C. S. Hyder, and T. Kim, "A Novel Approach for Infrastructure Deployment for VANET," in *Proceedings of the 2008 Second International Conference on Future Generation Communication and Networking (FGCN)*, pp. 234–238, Hainan, China, December 2008.

[36] T. H. Luan, X. Ling, and X. Shen, "Provisioning QoS controlled media access in vehicular to infrastructure communications," *Ad Hoc Networks*, vol. 100, no. 2, pp. 231–242, 2012.

[37] C. M. Silva and W. Meira, "Evaluating the performance of heterogeneous vehicular networks," in *Proceedings of the 82th IEEE Vehicular Technology Conference, VTC Fall 2015*, September 2015.

[38] C. M. Silva, D. L. Guidoni, F. S. Souza et al., "Using the inter-contact time for planning the communication infrastructure in vehicular networks," in *Proceedings of the 2016 IEEE 19th International Conference on Intelligent Transportation Systems (ITSC)*, pp. 2089–2094, Rio de Janeiro, Brazil, November 2016.

[39] C. M. Silva, D. L. Guidoni, F. S. Souza, C. G. Pitangui, J. F. Sarubbi, and A. Pitsillides, "Gamma Deployment: Designing the Communication Infrastructure in Vehicular Networks Assuring Guarantees on the V2I Inter-Contact Time," in *Proceedings of the 2016 IEEE 13th International Conference on Mobile Ad Hoc and Sensor Systems (MASS)*, pp. 263–271, Brasilia, Brazil, October 2016.

[40] G. Korkmaz, E. Ekici, and F. Özgüner, "Supporting real-time traffic in multihop vehicle-to-infrastructure networks," *Transportation Research Part C: Emerging Technologies*, vol. 180, no. 3, pp. 376–392, 2010.

[41] K. Liu and V. C. S. Lee, "RSU-based real-time data access in dynamic vehicular networks," in *Proceedings of the 13th International IEEE Conference on Intelligent Transportation Systems, ITSC 2010*, pp. 1051–1056, September 2010.

[42] A. Abdrabou, B. Liang, and W. Zhuang, "Delay analysis for a reliable message delivery in sparse vehicular ad hoc networks,"

in *Proceedings of the 53th IEEE Global Communications Conference, GLOBECOM 2010*, pp. 1–5, December 2010.

[43] D. Borsetti and J. Gozalvez, "Infrastructure-assisted geo-routing for cooperative vehicular networks," in *Proceedings of the 2010 IEEE Vehicular Networking Conference, VNC 2010*, pp. 255–262, December 2010.

[44] S. Annese, C. Casetti, C.-F. Chiasserini, N. Di Maio, A. Ghittino, and M. Reineri, "Seamless connectivity and routing in vehicular networks with infrastructure," *IEEE Journal on Selected Areas in Communications*, vol. 290, no. 3, pp. 501–514, 2011.

[45] F. Gómez Mármol and G. Martínez Pérez, "TRIP, a trust and reputation infrastructure-based proposal for vehicular ad hoc networks," *Journal of Network and Computer Applications*, vol. 350, no. 3, pp. 934–941, 2012.

[46] P. J. F. Ruiz, C. A. N. Guerra, and A. F. G. Skarmeta, "Deployment of a secure wireless infrastructure oriented to vehicular networks," in *Proceedings of the 24th IEEE International Conference on Advanced Information Networking and Applications, AINA2010*, pp. 1108–1114, April 2010.

[47] K. Plobl and H. Federrath, "A privacy aware and efficient security infrastructure for vehicular ad hoc networks," *Computer Standards Interfaces*, vol. 300, no. 6, pp. 390–397, 2008.

[48] T. R. Oliveira, C. M. Silva, D. F. Macedo, and J. M. Nogueira, "SNVC: Social networks for vehicular certification," *Computer Networks*, vol. 111, pp. 129–140, 2016.

[49] W. Zhang, Y. Chen, Y. Yang et al., "Multi-hop connectivity probability in infrastructure-based vehicular networks," *IEEE Journal on Selected Areas in Communications*, vol. 300, no. 4, pp. 740–747, 2012.

[50] M. Jerbi, S. M. Senouci, Y. G. Doudane, and A.-L. Beylot, "Geo-localized virtual infrastructure for urban vehicular networks," in *Proceedings of the 2008 8th International Conference on Intelligent Transport System Telecommunications, ITST 2008*, pp. 305–310, October 2008.

[51] J. Luo, X. Gu, T. Zhao, and W. Yan, "MI-VANET: A New Mobile Infrastructure Based VANET Architecture for Urban Environment," in *Proceedings of the 2010 IEEE Vehicular Technology Conference (VTC 2010-Fall)*, pp. 1–5, Ontario, Canada, September 2010.

[52] T. Mishra, D. Garg, and M. M. Gore, "A Publish/Subscribe Communication Infrastructure for VANET Applications," in *Proceedings of the 2011 IEEE Workshops of International Conference on Advanced Information Networking and Applications (WAINA)*, pp. 442–446, Biopolis, Singapore, March 2011.

[53] O. K. Tonguz and W. Viriyasitavat, "Cars as roadside units: A self-organizing network solution," *IEEE Communications Magazine*, vol. 51, no. 12, pp. 112–120, 2013.

[54] C. Sommer, D. Eckhoff, and F. Dressler, "IVC in cities: signal attenuation by buildings and how parked cars can improve the situation," *IEEE Transactions on Mobile Computing*, vol. 13, no. 8, pp. 1733–1745, 2014.

[55] C. M. Silva and W. Meira, "An architecture integrating stationary and mobile roadside units for providing communication on intelligent transportation systems," in *Proceedings of the 2016 IEEE/IFIP Network Operations and Management Symposium, NOMS 2016*, pp. 358–365, April 2016.

[56] T. H. Luan, L. X. Cai, J. Chen, X. S. Shen, and F. Bai, "Engineering a distributed infrastructure for large-scale cost-effective content dissemination over urban vehicular networks," *IEEE Transactions on Vehicular Technology*, vol. 63, no. 3, pp. 1419–1435, 2014.

[57] G. Marfia, G. Pau, E. De Sena, E. Giordano, and M. Gerla, "Evaluating vehicle network strategies for downtown Portland: Opportunistic infrastructure and the importance of realistic mobility models," in *Proceedings of the 5th International Conference on Mobile Systems, Applications and Services*, pp. 47–51, June 2007.

[58] Y. Zhang, J. Zhao, and G. Cao, "On scheduling vehicle-roadside data access," in *Proceedings of the 4th ACM International Workshop on Vehicular Ad Hoc Networks (VANET '07)*, pp. 9–18, New York, NY, USA, September 2007.

[59] V. Taliwal, D. Jiang, H. Mangold, C. Chen, and R. Sengupta, "Empirical determination of channel characteristics for DSRC vehicle-to-vehicle communication," in *Proceedings of the first ACM workshop*, p. 88, Philadelphia, PA, USA, October 2004.

[60] B. Masini, C. Fontana, and R. Verdone, "Provision of an emergency warning service through GPRS: performance evaluation," in *Proceedings of the 7th International IEEE Conference on Intelligent Transportation Systems*, pp. 1098–1102, Washington, DC, USA.

[61] D. Hadaller, S. Keshav, and T. Brecht, "MV-MAX," in *Proceedings of the 2006 SIGCOMM workshop*, pp. 269–276, Pisa, Italy, September 2006.

[62] B. Masini, L. Zuliani, and O. Andrisano, "On the Effectiveness of a GPRS based Intelligent Transportation System in a Realistic Scenario," in *Proceedings of the 2006 IEEE 63rd Vehicular Technology Conference*, pp. 2997–3001, Melbourne, Australia.

[63] G. Korkmaz, E. Ekici, and F. Özgüner, "A cross-layer multihop data delivery protocol with fairness guarantees for vehicular networks," *IEEE Transactions on Vehicular Technology*, vol. 550, no. 3, pp. 865–875, 2006.

[64] A. Bazzi, B. M. Masini, A. Conti, and O. Andrisano, "Infomobility provision through MBMS/UMTS in realistic scenarios," in *Proceedings of the 11th International IEEE Conference on Intelligent Transportation Systems, ITSC 2008*, pp. 25–30, December 2008.

[65] C. Lochert, B. Scheuermann, C. Wewetzer, A. Luebke, and M. Mauve, "Data aggregation and roadside unit placement for a vanet traffic information system," in *Proceedings of the 5th ACM International Workshop on VehiculAr Inter-NETworking (VANET '08)*, pp. 58–65, September 2008.

[66] J. Eriksson, L. Girod, B. Hull, R. Newton, S. Madden, and H. Balakrishnan, "The pothole patrol: using a mobile sensor network for road surface monitoring," in *Proceedings of the 6th International Conference on Mobile Systems, Applications, and Services (MobiSys '08)*, pp. 29–39, Breckenridge, Colo, USA, June 2008.

[67] Waze mobile app. 2008, http://www.waze.com.

[68] J. Rybicki, B. Scheuermann, W. Kiess, C. Lochert, P. Fallahi, and M. Mauve, "Challenge: peers on wheels–a road to new traffic information systems," in *Proceedings of the 13th Annual ACM International Conference on Mobile Computing and Networking (MobiCom '07)*, pp. 215–221, New York, NY, USA, 2007.

[69] S. Smaldone, L. Han, P. Shankar, and L. Iftode, "Roadspeak: Enabling voice chat on roadways using vehicular social networks," in *Proceedings of the 1st Workshop on Social Network Systems, SocialNets'08*, pp. 43–48, March 2008.

[70] M. Khabazian and M. K. Ali, "Generalized Performance Modeling of Vehicular Ad Hoc Networks (VANETs)," in *Proceedings of the 2007 IEEE Symposium on Computers and Communications*, pp. 51–56, Santiago, Portugal, July 2007.

[71] N. Wisitpongphan, F. Bai, P. Mudalige, and O. K. Tonguz, "On the routing problem in disconnected vehicular ad Hoc

networks," in *Proceedings of the IEEE INFOCOM 2007: 26th IEEE International Conference on Computer Communications*, pp. 2291–2295, May 2007.

[72] M. Nekoui, A. Eslami, and H. Pishro-Nik, "The capacity of vehicular ad hoc networks with infrastructure," in *Proceedings of the 6th Intl. Symposium on Modeling and Optimization in Mobile, Ad Hoc, and Wireless Networks, Wiopt 2008*, pp. 267–272, April 2008.

[73] A. Capone, M. Cesana, S. Napoli, and A. Pollastro, "MobiMESH: a Complete Solution for Wireless Mesh Networking," in *Proceedings of the 2007 IEEE Internatonal Conference on Mobile Adhoc and Sensor Systems*, pp. 1–3, Pisa, Italy, October 2007.

[74] J. Ormont, J. Walker, S. Banerjee, A. Sridharan, M. Seshadri, and S. Machiraju, "A city-wide vehicular infrastructure for wide-area wireless experimentation," in *Proceedings of the third ACM international workshop*, pp. 3–10, San Francisco, CA, USA, September 2008.

[75] M. Fiore and J. Härri, "The networking shape of vehicular mobility," in *Proceedings of the 9th ACM International Symposium on Mobile Ad Hoc Networking and Computing, MobiHoc '08*, pp. 261–272, New York, NY, USA, May 2008.

[76] Z. Zheng, P. Sinha, and S. Kumar, "Alpha coverage: bounding the interconnection gap for vehicular internet access," in *Proceedings of the IEEE INFOCOM*, pp. 2831–2835, IEEE, April 2009.

[77] O. Trullols, M. Fiore, C. Casetti, C. Chiasserini, and J. Barcelo Ordinas, "Planning roadside infrastructure for information dissemination in intelligent transportation systems," *Computer Communications*, vol. 330, no. 4, pp. 432–442, 2010.

[78] S. Sou, "A Power-Saving Model for Roadside Unit Deployment in Vehicular Networks," *IEEE Communications Letters*, vol. 140, no. 7, pp. 623–625, 2010.

[79] J. Lee and C. Kim, "A roadside unit placement scheme for vehicular telematics networks," in *Advances in Computer Science and Information Technology*, T. Kim and H. Adel, Eds., vol. 6059 of *Lecture Notes in Computer Science*, 2016.

[80] A. Kchiche and F. Kamoun, "Centrality-based Access-Points deployment for vehicular networks," in *Proceedings of the 2010 17th International Conference on Telecommunications, ICT 2010*, pp. 700–706, April 2010.

[81] Z. Zheng, Z. Lu, P. Sinha, and S. Kumar, "Maximizing the contact opportunity for vehicular internet access," in *Proceedings of the IEEE INFOCOM 2010*, pp. 1–9, March 2010.

[82] A. Abdrabou and W. Zhuang, "On a stochastic delay bound for disrupted vehicle-to-infrastructure communication with random traffic," in *Proceedings of the 2009 IEEE Global Telecommunications Conference, GLOBECOM 2009*, December 2009.

[83] S. C. Ng and G. Mao, "Analysis of k-hop connectivity probability in 2-D wireless networks with infrastructure support," in *Proceedings of the 53rd IEEE Global Communications Conference, GLOBECOM 2010*, December 2010.

[84] S. C. Ng, W. Zhang, Y. Yang, and G. Mao, "Analysis of access and connectivity probabilities in infrastructure-based vehicular relay networks," in *Proceedings of the IEEE Wireless Communications and Networking Conference 2010, WCNC 2010*, April 2010.

[85] S.-I. Sou and O. K. Tonguz, "Enhancing VANET connectivity through roadside units on highways," *IEEE Transactions on Vehicular Technology*, vol. 60, no. 8, pp. 3586–3602, 2011.

[86] A. Abdrabou and W. Zhuang, "Probabilistic delay control and road side unit placement for vehicular ad hoc networks with disrupted connectivity," *IEEE Journal on Selected Areas in Communications*, vol. 29, no. 1, pp. 129–139, 2011.

[87] B. Aslam, F. Amjad, and C. C. Zou, "Optimal roadside units placement in urban areas for vehicular networks," in *Proceedings of the 17th IEEE Symposium on Computers and Communication, ISCC 2012*, pp. 000423–000429, July 2012.

[88] Y. Liang, H. Liu, and D. Rajan, "Optimal placement and configuration of roadside units in vehicular networks," in *Proceedings of the IEEE 75th Vehicular Technology Conference, VTC Spring 2012*, June 2012.

[89] T. Wu, W. Liao, and C. Chang, "A Cost-Effective Strategy for Road-Side Unit Placement in Vehicular Networks," *IEEE Transactions on Communications*, vol. 600, no. 8, pp. 2295–2303, 2012.

[90] P. Cataldi and J. Harri, "User/operator utility-based infrastructure deployment strategies for vehicular networks," in *Proceedings of the IEEE 74th Vehicular Technology Conference, VTC Fall 2011*, pp. 1–5, September 2011.

[91] E. S. Cavalcante, A. L. L. Aquino, G. L. Pappa, and A. A. F. Loureiro, "Roadside unit deployment for information dissemination in a VANET: an evolutionary approach," in *Proceedings of the 14th Annual Conference Companion on Genetic and Evolutionary Computation (GECCO '12)*, pp. 27–34, ACM, Philadelphia, Pa, USA, July 2012.

[92] I. Filippini, F. Malandrino, G. Dán, M. Cesana, C. Casetti, and I. Marsh, "Non-cooperative RSU deployment in vehicular networks," in *Proceedings of the 2012 9th Annual Conference on Wireless On-Demand Network Systems and Services, WONS 2012*, pp. 79–82, January 2012.

[93] Z. Yu, J. Teng, X. Bai, D. Xuan, and W. Jia, "Connected coverage in wireless networks with directional antennas," in *Proceedings of the IEEE INFOCOM 2011*, pp. 2264–2272, April 2011.

[94] O. K. Tonguz, "Notice of violation of IEEE publication principles biologically inspired solutions to fundamental transportation problems," *IEEE Communications Magazine*, vol. 490, no. 11, pp. 106–115, 2011.

[95] S. Busanelli, G. Ferrari, V. A. Giorgio, and N. Iotti, "Information dissemination in urban vanets: single-hop or multihop?" *Chapter contribution in Roadside Networks for Vehicular Communications: Architectures, Applications and Test Fields*, pp. 237–263, 2012.

[96] T. Mangel and H. Hartenstein, "An analysis of data traffic in cellular networks caused by inter-vehicle communication at intersections," in *Proceedings of the 2011 IEEE Intelligent Vehicles Symposium, IV'11*, pp. 473–478, June 2011.

[97] A. Bazzi, B. M. Masini, and O. Andrisano, "On the frequent acquisition of small data through RACH in UMTS for its applications," *IEEE Transactions on Vehicular Technology*, vol. 600, no. 7, pp. 2914–2926, 2011.

[98] M. Koegel, W. Kiess, M. Kerper, and M. Mauve, "Compact vehicular trajectory encoding," in *Proceedings of the 2011 IEEE 73th Vehicular Technology Conference, VTC2011-Spring*, pp. 1–5, May 2011.

[99] S. Tayal and M. R. Triphath, "Vanet-challenges in selection of vehicular mobility model," in *Proceedings of the 2012 Second International Conference on Advanced Computing & Communication Technologies*, pp. 231–235, Washington, DC, USA, 2012.

[100] S. Busanelli, G. Ferrari, and V. A. Giorgio, "I2V highway and urban vehicular networks: a comparative analysis of the impact of mobility on broadcast data dissemination," *Journal of Communications*, vol. 60, no. 1, pp. 87–100, 2011.

[101] A. Bazzi, B. M. Masini, G. Pasolini, and O. Andrisano, "Smart navigation in intelligent transportation systems: Service performance and impact on wireless networks," *IARIAInternationalJournalonAdvancesinTelecommunications*, vol. 60, no. 7, pp. 57–70, 2013.

[102] H. Cheng, X. Fei, A. Boukerche, M. Abdelhamid, and M. Almulla, "A geometry-based coverage strategy over urban vanets," in *Proceedings of the 10th ACM Symposium on Performance Evaluation of Wireless Ad Hoc, Sensor, & Ubiquitous Networks PE-WASUN '13*, pp. 121–128, New York, NY, USA.

[103] P. Patil and A. Gokhale, "Voronoi-based placement of road-side units to improve dynamic resource management in Vehicular Ad Hoc Networks," in *Proceedings of the 2013 International Conference on Collaboration Technologies and Systems, CTS 2013*, pp. 389–396, May 2013.

[104] N. Lu, N. Zhang, N. Cheng, X. Shen, J. W. Mark, and F. Bai, "Vehicles meet infrastructure: toward capacity-cost tradeoffs for vehicular access networks," *IEEE Transactions on Intelligent Transportation Systems*, vol. 140, no. 3, pp. 1266–1277, 2013.

[105] X. Liya, H. Chuanhe, L. Peng, and Z. Junyu, "A randomized algorithm for roadside units placement in vehicular ad hoc network," in *Proceedings of the 9th IEEE International Conference on Mobile Ad-Hoc and Sensor Networks, MSN 2013*, pp. 193–197, December 2013.

[106] T. Yan, W. Zhang, G. Wang, and Y. Zhang, "Access points planning in Urban area for data dissemination to drivers," *IEEE Transactions on Vehicular Technology*, vol. 630, no. 1, pp. 390–402, 2014.

[107] J. Chi, Y. Jo, H. Park, and S. Park, "Intersection-priority based optimal RSU allocation for VANET," in *Proceedings of the 5th International Conference on Ubiquitous and Future Networks, ICUFN 2013*, pp. 350–355, July 2013.

[108] S. Busanelli, F. Rebecchi, M. Picone, N. Iotti, and G. Ferrari, "Cross-network information dissemination in vehicular ad hoc networks (VANETs): Experimental results from a smartphone-based testbed," *Future Internet*, vol. 50, no. 3, pp. 398–428, 2013.

[109] O. Kaiwartya, A. H. Abdullah, Y. Cao et al., "Internet of Vehicles: Motivation, Layered Architecture, Network Model, Challenges and Future Aspects," *IEEE Access*, vol. 4, no. 99, pp. 5356–5373, 2016.

[110] A. Fascista, G. Ciccarese, A. Coluccia, and G. Ricci, "A Localization Algorithm Based on V2I Communications and AOA Estimation," *IEEE Signal Processing Letters*, vol. 24, no. 1, pp. 126–130, 2017.

[111] B. W. Kim and S. Jung, "Vehicle Positioning Scheme Using V2V and V2I Visible Light Communications," in *Proceedings of the 2016 IEEE 83th Vehicular Technology Conference (VTC Spring)*, pp. 1–5, Nanjing, China, May 2016.

[112] E. Okamoto, K. Kunitomo, H. Akita, and T. Kyo, "A Cooperative V2I Uplink Transmission Scheme Utilizing V2V Network Coding," in *Proceedings of the 2016 IEEE 83th Vehicular Technology Conference (VTC Spring)*, pp. 1–5, Nanjing, China, May 2016.

[113] Afdhal and Elizar, "Enhanced route guidance and navigation for emergency vehicle using V2I-based cooperative communication," in *Proceedings of the 17th International Electronics Symposium, IES 2015*, pp. 145–150, September 2015.

[114] A. Ghosh, V. V. Paranthaman, G. Mapp, O. Gemikonakli, and J. Loo, "Enabling seamless V2I communications: Toward developing cooperative automotive applications in VANET systems," *IEEE Communications Magazine*, vol. 530, no. 12, pp. 80–86, 2015.

[115] K. Zheng, Q. Zheng, P. Chatzimisios, W. Xiang, and Y. Zhou, "Heterogeneous vehicular networking: a survey on architecture, challenges, and solutions," *IEEE Communications Surveys and Tutorials*, vol. 170, no. 4, pp. 2377–2396, 2015.

[116] A. Bazzi, B. M. Masini, A. Zanella, and A. Calisti, "Visible light communications in vehicular networks for cellular offloading," in *Proceedings of the IEEE International Conference on Communication Workshop, ICCW 2015*, pp. 1416–1421, June 2015.

[117] J. M. Marquez-Barja, H. Ahmadi, S. M. Tornell et al., "Breaking the vehicular wireless communications barriers: Vertical handover techniques for heterogeneous networks," *IEEE Transactions on Vehicular Technology*, vol. 640, no. 12, pp. 5878–5890, 2015.

[118] K. Zheng, Q. Zheng, H. Yang, L. Zhao, L. Hou, and P. Chatzimisios, "Reliable and efficient autonomous driving: the need for heterogeneous vehicular networks," *IEEE Communications Magazine*, vol. 530, no. 12, pp. 72–79, 2015.

[119] J. A. Sanguesa, F. Naranjo, V. Torres-Sanz, M. Fogue, P. Garrido, and F. J. Martinez, "On the study of vehicle density in intelligent transportation systems," *Mobile Information Systems*, vol. 2016, Article ID 8320756, 13 pages, 2016.

[120] B. M. Masini, "Vehicular networking for mobile crowd sensing," *Ad Hoc Networks*, vol. 36, pp. 407-408, 2016.

[121] A. Gorrieri, M. Martalò, S. Busanelli, and G. Ferrari, "Clustering and sensing with decentralized detection in vehicular ad hoc networks," *Ad Hoc Networks*, vol. 36, pp. 450–464, 2016.

[122] C.-C. Lo, K.-M. Chao, H.-Y. Kung, C.-H. Chen, and M. Chang, "Information Management and Applications of Intelligent Transportation System," *Mathematical Problems in Engineering*, vol. 2015, Article ID 613940, 2015.

[123] A. Gorrieri and G. Ferrari, "Irresponsible AODV routing," *Vehicular Communications*, vol. 20, no. 1, pp. 47–57, 2015.

[124] J. A. Sanguesa, M. Fogue, P. Garrido, F. J. Martinez, J.-C. Cano, and C. T. Calafate, "A survey and comparative study of broadcast warning message dissemination schemes for VANETs," *Mobile Information Systems*, vol. 2016, Article ID 8714142, 18 pages, 2016.

[125] M. Picone, M. Amoretti, G. Ferrari, and F. Zanichelli, "D4V: A peer-to-peer architecture for data dissemination in smartphone-based vehicular applications," *PeerJ*, vol. 2015, no. 1, article e15, 2015.

[126] A. Bazzi, A. Zanella, and B. M. Masini, "A distributed virtual traffic light algorithm exploiting short range V2V communications," *Ad Hoc Networks*, vol. 49, pp. 42–57, 2016.

[127] Z. Liu, M. Wu, K. Zhu, and L. Zhang, "SenSafe: A smartphone-based traffic safety framework by sensing vehicle and pedestrian behaviors," *Mobile Information Systems*, vol. 2016, Article ID 7967249, 2016.

[128] C. M. Silva, A. L.L. Aquino, and W. Meira, "Deployment of road-side units based on partial mobility information," *Computer Communications*, vol. 600, pp. 28–39, 2015.

[129] C. M. Silva, J. F. Sarubbi, and W. Meira, "Planning the communication infrastructure for vehicular networks without tracking vehicles," in *Proceedings of the 2015 IEEE 11th International Conference on Wireless and Mobile Computing, Networking and Communications (WiMob)*, pp. 882–887, Abu Dhabi, United Arab Emirates, October 2015.

[130] C. M. Silva and W. Meira, "Design of roadside communication infrastructure with QoS guarantees," in *Proceedings of the 2015 20th IEEE Symposium on Computers and Communication (ISCC)*, pp. 439–444, Larnaca, Cyprus, July 2015.

[131] C. M. Silva, F. A. Silva, J. F. Sarubbi, T. R. Oliveira, W. Meira, and J. M. Nogueira, "Designing mobile content delivery networks for the internet of vehicles," *Vehicular Communications*, vol. 8, pp. 45–55, 2017.

[132] W. J. Franz, R. Eberhardt, and T. Luckenbach, "Fleetnet-internet on the road," in *Proceedings of the 8th World Congresson Intelligent Transport Systems*, 2001.

[133] V. Bychkovsky, K. Chen, M. Goraczko et al., "The cartel mobile sensor computing system," in *Proceedings of the 4th international conference on Embedded networked sensor systems, SenSys*, pp. 383-384, ACM.

[134] M. Gerla and L. Kleinrock, "Vehicular networks and the future of the mobile internet," *Computer Networks*, vol. 550, no. 2, pp. 457–469, 2011.

[135] P. E. Ross, Europe's smart highway, http://spectrum.ieee.org/transportation/advanced-cars/europes-smart-highway-will-shepherd-cars-from-rotterdam-to-vienna.

[136] Cooperative its corridor joint deployment, https://www.bmvi.de/SharedDocs/EN/Anlagen/VerkehrUndMobilitaet/Strasse/cooperative-its-corridor.pdf?__blob=publicationFile.

[137] University of Michigan, connected Ann Arbor experiment web site, http://www.mtc.umich.edu/deployments/connected-ann-arbor.

[138] Tu-automotive japan 2016, http://www.tu-auto.com/japan/.

[139] Getting around in japan: The status and challenges of its, https://www.fhwa.dot.gov/publications/publicroads/99marapr/japan.cfm.

[140] H. Wu, M. Palekar, R. Fujimoto et al., "An empirical stud y of short range communications for vehicles," in *Proceedings of the 2nd ACM International Workshop on Vehicular Ad Hoc Networks (VANET '05)*, pp. 83-84, ACM, 2005.

[141] Vodafone demonstrates connected car over LTE at MWC, https://www.telecompaper.com/background/vodafone-demonstrates-connected-car-over-lte-at-mwc–1186851.

[142] Consortium of automotive and telecom companies host 3GPP Cellular-V2X technology field trial in Germany, http://sites.ieee.org/connected-vehicles/2017/01/03/consortium-automotive-telecom-companies-host-3gpp-cellular-v2x-technology-field-trial-germany/.

[143] Towards 5G initiative welcomes Qualcomm, shows Fast results, https://www.ericsson.com/news/170224-towards-5 g-initiative-welcomes-qualcomm_244010065_c.

[144] Vodafone, Bosch, Huawei test LTE-V2X in Germany, https://www.telecompaper.com/news/vodafone-bosch-huawei-test-lte-v2x-in-germany–1184329.

[145] UK CITE UK Connected Intelligent Transport Environment, https://www.ukcite.co.uk/.

[146] Deutsche Telekom trials LTE-V on the Ingolstadt autobahn test bed, http://www.telecomtv.com/articles/automotive/deutsche-telekom-trials-lte-v-on-the-ingolstadt-autobahn-test-bed-13772/.

[147] Deutsche Telekom, Fraunhofer, Nokia and Continental run LTE V2X trials on Autobahn test bed, http://telematicswire.net/deutsche-telekom-fraunhofer-nokia-and-continental-run-lte-v2x-trials-on-autobahn-test-bed/.

[148] I. F. Akyildiz, X. Wang, and W. Wang, "Wireless mesh networks: a survey," *Computer Networks*, vol. 470, no. 4, pp. 445–487, 2005.

[149] C. M. Silva, A. L. L. Aquino, and Meira W. Jr., "Smart traffic light for low traffic conditions," *Mobile Networks and Applications*, pp. 1–9, 2015.

[150] A. Bazzi, B. M. Masini, A. Zanella, and G. Pasolini, "IEEE 802.11p for cellular offloading in vehicular sensor networks," *Computer Communications*, vol. 60, pp. 97–108, 2015.

[151] S. Al-Sultan, M. M. Al-Doori, A. H. Al-Bayatti, and H. Zedan, "A comprehensive survey on vehicular Ad Hoc network," *Journal of Network and Computer Applications*, vol. 37, no. 1, pp. 380–392, 2014.

[152] A. Festag, "Standards for vehicular communicationfrom ieee 802.11p to 5 g," *eiElektrotechnik und Informationstechnik*, vol. 1320, no. 7, pp. 409–416, 2015.

[153] C. Campolo, A. Molinaro, A. Vinel, N. Lyamin, and M. Jonsson, "Service discovery and access in vehicle-to-roadside multi-channel VANETs," in *Proceedings of the IEEE International Conference on Communication Workshop, ICCW 2015*, pp. 2477–2482, June 2015.

[154] 3GPP. Service requirements for V2X services. TS 22.185, 2016.

[155] 3GPP. Evolved Universal Terrestrial Radio Access (E-UTRA); Physical channels and modulation. TS 36.211, 2016.

[156] 3GPP. Liaison statement from 3GPP RAN on LTE-based Vehicle-to-Vehicle communications. RP 161919, 2016.

[157] 3GPP. LTE-based V2X services. RP 161874, 2016.

[158] 3GPP. Study on enhancement of 3GPP support for 5G V2X services. TR 22.886, 2016.

[159] H. Cao, S. Gangakhedkar, A. R. Ali, M. Gharba, and J. Eichinger, "A 5G V2X testbed for cooperative automated driving," in *Proceedings of the 2016 IEEE Vehicular Networking Conference (VNC)*, pp. 1–4, Columbus, OH, USA, December 2016.

[160] H. Droste, G. Zimmermann, M. Stamatelatos et al., "The METIS 5G architecture: a summary of METIS work on 5G architectures," in *Proceedings of the 81th IEEE Vehicular Technology Conference (VTC '15)*, pp. 1–5, May 2015.

[161] J. Gozalvez, "Tentative 3GPP Timeline for 5G [Mobile Radio]," *IEEE Vehicular Technology Magazine*, vol. 100, no. 3, pp. 12–18, 2015.

[162] A. Nordrum, "Autonomous driving experts weigh 5G cellular network against dedicated short range communications," *IEEE Spectrum, Cars That Think*, May 2016.

[163] "IEEE standard for local and metropolitan area networks-part 15.7: short-range wireless optical communication using visible light," in *IEEE Std*, pp. 1–309, IEEE, 2011.

[164] J. A. Sanguesa, M. Fogue, P. Garrido, F. J. Martinez, J.-C. Cano, and C. T. Calafate, "A survey and comparative study of broadcast warning message dissemination schemes for VANETs," *Mobile Information Systems*, vol. 2016, Article ID 8714142, 18 pages, 2016.

[165] T. H. Cormen, C. E. Leiserson, R. Rivest, and C. Stein, *Introduction to algorithmen*, MIT press, 2001.

[166] Y. Zhang, J. Zhao, and G. Cao, "Service scheduling of vehicle-roadside data access," *Mobile Networks and Applications*, vol. 150, no. 1, pp. 83–96, 2010.

[167] S. Panichpapiboon and G. Ferrari, "Irresponsible forwarding," in *Proceedings of the 2008 8th International Conference on ITS Telecommunications (ITST)*, pp. 311–316, Phuket, Thailand, October 2008.

[168] M. Wang, Y. Zhang, C. Li, X. Wang, and L. Zhu, "A survey on intersection-based routing protocols in city scenario of VANETs," in *Proceedings of the 2014 International Conference on Connected Vehicles and Expo (ICCVE)*, pp. 821–826, Vienna, Austria, November 2014.

[169] D. A. Johnson and M. M. Trivedi, "Driving style recognition using a smartphone as a sensor platform," in *Proceedings of the 14th IEEE International Intelligent Transportation Systems Conference (ITSC '11)*, pp. 1609–1615, Washington, DC, USA, October 2011.

[170] R. Araújo, Â. Igreja, R. De Castro, and R. E. Araújo, "Driving coach: a smartphone application to evaluate driving efficient patterns," in *Proceedings of the 2012 IEEE Intelligent Vehicles Symposium, IV 2012*, pp. 1005–1010, IEEE, Alcala de Henares, Spain, June 2012.

[171] M. F. Faraj, J. F. M. Sarubbi, C. M. Silva, M. F. Porto, and N. T. R. Nunes, "A real geographical application for the School Bus Routing Problem," in *Proceedings of the 2014 17th IEEE International Conference on Intelligent Transportation Systems, ITSC 2014*, pp. 2762–2767, IEEE, Qingdao, China, October 2014.

[172] C. M. Silva, J. F. M. Sarubbi, D. F. Silva, M. F. Porto, and N. T. R. Nunes, "A Mixed Load Solution for the Rural School Bus Routing Problem," in *Proceedings of the 18th IEEE International Conference on Intelligent Transportation Systems, ITSC 2015*, pp. 1940–1945, IEEE, Las Palmas, Spain, September 2015.

[173] E. Koukoumidis, L.-S. Peh, and M. R. Martonosi, "SignalGuru: leveraging mobile phones for collaborative traffic signal schedule advisory," in *Proceedings of the 9th International Conference on Mobile Systems, Applications, and Services*, pp. 127–140, ACM, July 2011.

[174] J. Zaldivar, C. T. Calafate, J. C. Cano, and P. Manzoni, "Providing accident detection in vehicular networks through OBD-II devices and android-based smartphones," in *Proceedings of the 36th Annual IEEE Conference on Local Computer Networks (LCN '11)*, pp. 813–819, IEEE, Bonn, Germany, October 2011.

[175] C. Thompson, J. White, B. Dougherty, A. Albright, and D. C. Schmidt, "Using smartphones to detect car accidents and provide situational awareness to emergency responders," *Lecture Notes of the Institute for Computer Sciences, Social-Informatics and Telecommunications Engineering*, vol. 48, pp. 29–42, 2010.

[176] M. S. Al-Kahtani, "Survey on security attacks in vehicular ad hoc networks (VANETs)," in *Proceedings of the 6th International Conference on Signal Processing and Communication Systems (ICSPCS '12)*, pp. 1–9, Queensland, Australia, December 2012.

[177] R. H. Frenkiel, B. R. Badrinath, J. Borràs, and R. D. Yates, "Infostations challenge: Balancing cost and ubiquity in delivering wireless data," *IEEE Personal Communications*, vol. 70, no. 2, pp. 66–71, 2000.

[178] P. Li, X. Huang, Y. Fang, and P. Lin, "Optimal placement of gateways in vehicular networks," *IEEE Transactions on Vehicular Technology*, vol. 560, no. 6, pp. 3421–3430, 2007.

[179] S. Teng, "Mutually Repellant Sampling," in *Minimax and Applications*, vol. 4 of *Nonconvex Optimization and Its Applications*, pp. 129–140, Springer, Boston, Mass, USA, 1995.

[180] Y. Xiong, J. Ma, W. Wang, and D. Tu, "RoadGate: mobility-centric roadside units deployment for vehicular networks," *International Journal of Distributed Sensor Networks*, vol. 2013, Article ID 690974, 10 pages, 2013.

[181] A. Bazzi, B. M. Masini, A. Zanella, and G. Pasolini, "IEEE 802.11p for cellular offloading in vehicular sensor networks," *Computer Communications*, vol. 600, pp. 97–108, 2015.

[182] O. Trullols-Cruces, M. Fiore, and J. M. Barcelo-Ordinas, "Cooperative download in vehicular environments," *IEEE Transactions on Mobile Computing*, vol. 110, no. 4, pp. 663–678, 2012.

[183] F. Aurenhammer, "Voronoi diagrams—a survey of a fundamental geometric data structure," *ACM Comput. Surv*, vol. 230, no. 3, pp. 345–405, September 1991.

[184] C. De Castro, G. Leonardi, B. M. Masini, and P. Toppan, "An integrated architecture for infomobility services—advantages of genetic algorithms in real-time route planning," in *Proceedings of the International Conference on Evolutionary Computation (ICEC)*, Oct 2010.

[185] B. Xie, G. Xia, Y. Chen, and M. Xu, "Roadside Infrastructure Placement for Information Dissemination in Urban ITS Based on a Probabilistic Model," in *Network and Parallel Computing*, vol. 8147 of *Lecture Notes in Computer Science*, pp. 322–331, Springer, Berlin, Heidelberg, 2013.

[186] C. M. Silva, A. L. L. Aquino, and W. Meira Jr., "Design of roadside infrastructure for information dissemination in vehicular networks," in *Proceedings of the IEEE/IFIP Network Operations and Management Symposium: Management in a Software Defined World, NOMS 2014*, pp. 1–8, May 2014.

Hindawi
Mobile Information Systems
Volume 2017, Article ID 7231417, 14 pages
https://doi.org/10.1155/2017/7231417

Research Article

Three-Dimensional Vehicle-to-Vehicle Channel Modeling with Multiple Moving Scatterers

Derong Du, Xiaoping Zeng, Xin Jian, Lijuan Miao, and Haobo Wang

College of Communication Engineering, Chongqing University, Chongqing 400044, China

Correspondence should be addressed to Xin Jian; jianxin_zg@163.com

Received 30 November 2016; Revised 9 April 2017; Accepted 3 May 2017; Published 10 July 2017

Academic Editor: Barbara M. Masini

Connected vehicles have received much attention in recent years due to their significant societal benefit and commercial value. However, a suitable channel model for vehicle-to-vehicle (V2V) communications is difficult to build due to the dynamic communication environment. In this paper, a three-dimensional (3D) geometrical propagation model that includes line-of-sight (LoS), single bounced (SB), and multiple bounced (MB) rays is proposed. Each of multiple scatterers in the model is moving with a random velocity in a random direction. Based on the geometrical propagation model, a generalized 3D reference model for narrowband multiple-input-multiple-output (MIMO) V2V multipath fading channels is developed. The corresponding space-time correlation functions (ST-CFs), time correlation functions (T-CFs), and space correlation functions (S-CFs) are analytically investigated and numerically simulated in terms of various factors. Several notable ST-CFs for V2V and fixed-to-mobile (F2M) communications become the special cases of ST-CFs of the proposed model by adjusting the corresponding channel parameters. Finally, the theoretical results of the space-Doppler power spectral density (SD-PSD) are compared with the available measured data. The close agreements between the theoretical and measured SD-PSD curves confirm the utility and generality of the proposed model.

1. Introduction

Connected vehicles have the potential to improve the safety and efficiency of the automobile transportation [1], and they are expected to be a pillar of a smart society and to revolutionize the way people move. Different from the conventional fixed-to-mobile (F2M) cellular systems, vehicle-to-vehicle (V2V) is a kind of the mobile-to-mobile (M2M) communication which allows both the transmitter and receiver to be in motion [2]. Suitable channel models and channel characterizations are absolutely essential for successful design of V2V systems, where the quality of wireless links between vehicles can vary greatly and rapidly from one environment to another as one or both ends move [3].

Many M2M channel models have been proposed in various ways, some of which are summarized in [4], and these models have important reference values in modeling the V2V channel. The models in M2M communication environment can be traced back from two-dimensional (2D) [5–7] and three-dimensional (3D) [8–11] fixed scattering models to 2D [12–17] and 3D [18–20] moving scattering models. The M2M channel models with the assumption of stationary scatterers have been proposed in [5–11]. However, moving scatterers are unavoidable in M2M communications. Moving foliage, walking pedestrians, and passing vehicles are only a few examples of scatterers in motion, which can be observed in most of the real-world radio propagation environments [14, 21]. The impact of moving scatterers on channel characteristics has been studied in [22–25] for 2D F2M cellular and fixed-to-fixed (F2F) communications with line-of-sight (LoS) and single bounced (SB) rays.

Recently, modeling of M2M/V2V channels in the presence of moving scatterers has been discussed in [12–20]. A nonstationary multiple-input-multiple-output (MIMO) V2V channel model based on the geometrical street model was derived, and the impact of fixed and moving clusters of scatterers on the channel statistics was studied in [12, 15]. A single-input-single-output (SISO) V2V channel model was derived assuming a typical propagation scenario in which the local scatterers without specific constraints of positions

moved with random velocities in random directions in [13, 14]. The impact of mobile and stationary scattering clusters on the Doppler spectrum was investigated for wideband V2V communication channels in an urban canyon oncoming environment in [16, 17]. All previously reported models in [12–17] are 2D propagation models in which the rays are LoS, SB, or double bounced (DB). However, this 2D assumption does not seem to be appropriate for many communication scenarios, for example, urban V2V communications in which the transmitter and receiver antenna arrays are often located in close proximity to or lower than the surrounding scatterers.

A 3D geometrical propagation model that included both stationary and moving scatterers around the transmitter and receiver was proposed in [18], and this work was extended to wideband channels in [19]. The models in [18, 19] took into account that the rays in V2V channels could be both SB and DB; however, they imposed some constraints on the position of the local scatterers and assumed that the transmitter, receiver, and scatterers were in motion with constant velocities in 2D space. Therefore, the models in [18, 19] cannot fully capture the 3D spatial information. A preliminary investigation of the impact of multiple moving scatterers on the Doppler spectrum in 3D V2V communication scenarios was presented in [20]. However, the work of [20] did not investigate and take into account the space-time correlation functions (ST-CFs), scatterer velocity distributions, angle distributions, and so on.

It is unavoidable in V2V communications that the rays from the transmitter to receiver are multiple bounced (MB) by moving scatterers, especially in environments with high-density scatterers, for example, urban area. However, to the best of the authors' knowledge, the model and statistical properties of 3D V2V or M2M channels in the presence of multiple moving scatterers have been investigated rarely so far. This paper strives to alleviate the current lack of analytical studies by investigating the model and statistical properties of a narrowband 3D MIMO V2V channel in which the local multiple scatterers are moving with random velocities in random directions. The proposed reference model constructs the channel impulse response as a combination of LoS and MB components, and SB is considered as a special case of MB. Different from the assumption of all non-LoS (NLoS) path gains having the same size in [13, 14] and meanwhile compared with models in [18, 19], SB, DB, and other MB rays have more flexible and precise power weights in the proposed model. From the reference model, the corresponding ST-CFs, time correlation functions (T-CFs), and space correlation functions (S-CFs) are analytically investigated and numerically simulated in terms of various factors such as the maximum bounces, scattering forms, scatterer velocity distributions, and spacing between adjacent antenna elements. Finally, the theoretical space-Doppler power spectral density (SD-PSD) results with SD-PSDs in [18] and measured data in [26, 27] are compared. The close agreements between the analytically and empirically obtained SD-PSDs confirm the utility and generality of the proposed model and show the importance of including multiple moving scatterers in propagation models. The contributions and novelties of this paper are summarized as follows.

(i) We propose a generalized geometrical model and a generalized reference model that include LoS, SB, and MB rays between the transmitter and receiver for 3D narrowband MIMO V2V communications. The proposed model can be adapted to a wide variety of scenarios, for example, F2F, F2M, and M2M with certain bounces by adjusting model parameters.

(ii) To the best of the authors' knowledge, the impact of rays' different maximum bounces caused by the multiple moving scatterers on the ST-CFs and T-CFs is deeply investigated for the first time in V2V or M2M communication environments.

(iii) The ST-CFs obtained from the proposed reference model are relatively generalized and can be reduced to several existing ST-CFs and T-CFs, for example, those in [13, 14, 23, 28, 29].

The remainder of the paper is organized as follows. Section 2 describes the geometrical propagation model and presents a 3D reference model for narrowband MIMO V2V channels in the presence of multiple moving scatterers. Section 3 derives the channel ST-CFs, T-CFs, S-CFs, and SD-PSDs for different parametric sets. Numerical results and comparison between the theoretical results and measured data are provided in Section 4. Finally, Section 5 provides some concluding remarks.

2. 3D Geometrical Propagation Model and Reference Model

2.1. Geometrical Propagation Model. This paper considers the MIMO V2V communication links between transmitter T_X and receiver R_X, as shown in Figure 1. The radio propagation environment is characterized by 3D multiple moving scattering with either LoS or NLoS conditions between T_X and R_X. The MB waves emitted from the qth antenna element of T_X at an angle of departure (AOD) reach the pth antenna element of R_X at an angle of arrival (AOA) after being multiple scattered by the local moving scatterers.

For ease of reference, in this geometrical propagation model, the main parameters are summarized in Table 1, and the main assumptions are summarized as follows:

(i) The received signal power consists of LoS, SB, and MB scattering components with the corresponding power weights.

(ii) Both T_X and R_X are equipped with uniform linear arrays consisting of omnidirectional antenna elements.

(iii) T_X and R_X move with constant velocities in 3D space described by the fixed azimuth angles and elevation angles.

(iv) Each of the local scatterers on the links between T_X and R_X for the multiple bounces is in motion with a random velocity in a random direction in 3D space.

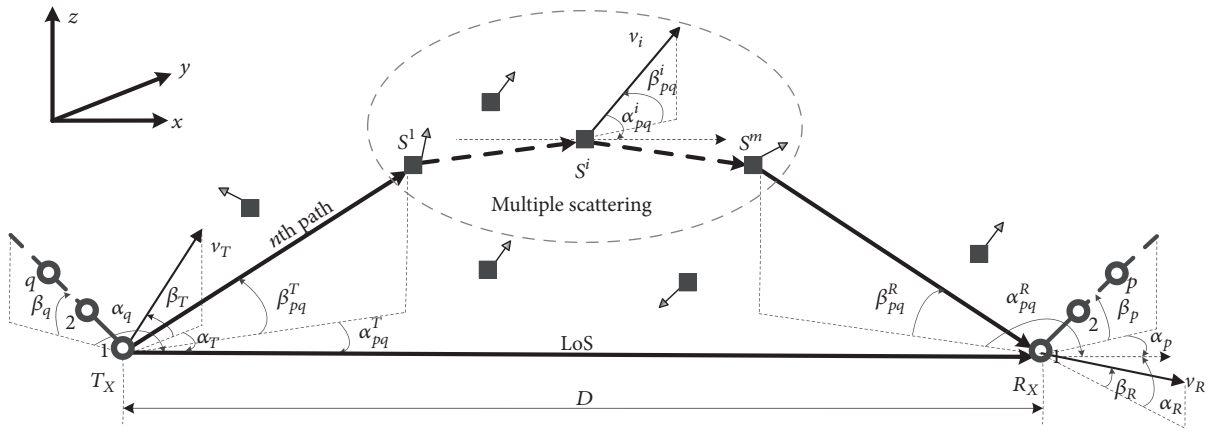

Figure 1: Geometrical propagation model with LoS and MB rays for the 3D MIMO V2V communication scenario. Empty circles represent the antenna elements, and solid squares represent the moving scatterers.

Table 1: Definition of the parameters used in the geometrical model.

Parameters	Definition	Attributes
S^i	The ith moving scatterer for the multiple bounces	Symbol
D	The distance between T_X and R_X	Deterministic
q, p	The antenna element identifier of T_X and R_X, respectively	Deterministic
Q, P	The number of antenna elements of T_X and R_X, respectively	Deterministic
d_T, d_R	The spacing between two adjacent antenna elements of T_X and R_X, respectively	Deterministic
α_q, β_q	The azimuth angle and elevation angle of T_X's antenna array, respectively	Deterministic
α_p, β_p	The azimuth angle and elevation angle of R_X's antenna array, respectively	Deterministic
α^T_{pq}, β^T_{pq}	The azimuth angle and elevation angle of AOD, respectively	Statistical
α^R_{pq}, β^R_{pq}	The azimuth angle and elevation angle of AOA, respectively	Statistical
v_T, v_R	The velocities of T_X and R_X, respectively	Deterministic
v^i_{pq}	The velocity of S^i	Statistical
α_T, β_T	The azimuth angle and elevation angle of v_T, respectively	Deterministic
α_R, β_R	The azimuth angle and elevation angle of v_R, respectively	Deterministic
α^i_{pq}, β^i_{pq}	The azimuth angle and elevation angle of v^i_{pq}, respectively	Statistical

(v) The geometrical propagation model does not impose specific constraints on the position of the local moving scatterers like [13, 14]. Owing to high path loss, we neglect the energy contribution of remote scatterers.

2.2. Reference Model. We can observe from Figure 1 that the complex faded envelope of the link between the qth antenna element of T_X and the pth antenna element of R_X can be written as a superposition of LoS and MB components; that is,

$$h_{pq}(t) = h^{\mathrm{LoS}}_{pq}(t) + h^{\mathrm{MB}}_{pq}(t), \tag{1}$$

$$h^{\mathrm{LoS}}_{pq}(t) = \rho_{pq} \cdot \exp\left\{j\left[2\pi f_{pq,\rho} t + 2\pi\left(f^q_{pq,\rho} + f^p_{pq,\rho}\right) + \theta_{pq,\rho}\right]\right\}, \tag{2}$$

$$h^{\mathrm{MB}}_{pq}(t) = \sum_{m=1}^{M} \sqrt{p_m} h^m_{pq}(t), \tag{3}$$

$$h^m_{pq}(t) = \lim_{N_m \to \infty} \sum_{n_m=1}^{N_m} c_{pq,n_m} \cdot \exp\left\{j\left[2\pi f_{pq,n_m} t + 2\pi\left(f^q_{pq,n} + f^p_{pq,n}\right) + \theta_{pq,n_m}\right]\right\}, \tag{4}$$

where ρ_{pq}, $f_{pq,\rho}$, $\theta_{pq,\rho}$, $f^q_{pq,\rho}$, and $f^p_{pq,\rho}$ denote the path gain, Doppler shift, phase shift, frequency shift for qth antenna element of T_X, and frequency shift for pth antenna element of R_X of $h^{\mathrm{LoS}}_{pq}(t)$, respectively; m denotes the amount of bounces, M is the maximum of m, p_m and N_m denote the power weight and path number of $h^m_{pq}(t)$, respectively; c_{pq,n_m}, f_{pq,n_m}, θ_{pq,n_m}, $f^q_{pq,n}$, and $f^p_{pq,n}$ denote the path gain, Doppler shift, phase shift, frequency shift for qth antenna element of T_X, and frequency shift for pth antenna element of R_X of the n_mth path in $h^m_{pq}(t)$. The LoS component $h^{\mathrm{LoS}}_{pq}(t)$ can be described by a complex sinusoid, and (2) is an extension of the (3.17) in [30]. $h^m_{pq}(t)$ denotes the NLoS component with m bounced

(mB) rays, and it is an extension of the (3.12) in [30]. Note that MB component $h_{pq}^{\mathrm{MB}}(t)$ of the channel impulse response consists of M clusters of rays reflected $m \in \{1, 2, 3, \ldots, M\}$ times from moving scatterers.

The channel gains (ρ_{pq}, c_{pq,n_m}), Doppler shifts and frequency shifts ($f_{pq,\rho}, f_{pq,\rho}^q, f_{pq,\rho}^p, f_{pq,n_m}, f_{pq,n}^q, f_{pq,n}^p$), and phases ($\theta_{pq,\rho}$, θ_{pq,n_m}) in this model can be calculated as follows.

2.2.1. Channel Gains. The central limit theorem states that $h_{pq}^m(t)$ equals a complex valued Gaussian random process with zero mean and variance $2\sigma_m^2 = \mathrm{Var}\{h_{pq}^m(t)\} = \lim_{N_m \to \infty} \sum_{n_m}^{N_m} E[c_{pq,n_m}^2]$. p_m in (3) denotes the power weight of the mth clusters of rays, and $\sum_{m=1}^{M} p_m = 1$. The channel gain of $h_{pq}(t)$ is normalized, i.e., $2\sum_{m=1}^{M} p_m\sigma_m^2 + \rho_{pq}^2 = 1$, and the Rice factor can be denoted as $K = \rho_{pq}^2/2\sum_{m=1}^{M} p_m\sigma_m^2$. These parameters have to be either set during simulations or estimated from measurements.

2.2.2. Doppler Shifts and Frequency Shifts. The frequency shifts $f_{pq,\rho}^q$, $f_{pq,\rho}^p$, $f_{pq,n}^q$, and $f_{pq,n}^p$ depend on the difference of the propagation distance (TPD) changes between $h_{pq}(t)$ and $h_{11}(t)$. On the other hand, the Doppler shifts $f_{pq,\rho}$ and f_{pq,n_m} depend on the geometrical relation between directions of movement of T_X, R_X, and multiple moving scatterers and the directions of AOD and AOA. For $\max(d_T, d_R) \ll D$, both the AOD and AOA of LoS rays are approximately equal to zero. Appendix A shows that $f_{pq,\rho}^q$, $f_{pq,\rho}^p$, $f_{pq,n}^q$, $f_{pq,n}^p$, and $f_{pq,\rho}$ are, respectively,

$$f_{pq,\rho}^q = \frac{(q-1)\, d_T f_0}{c} \cos\alpha_q \cos\beta_q, \tag{5}$$

$$f_{pq,\rho}^p = \frac{(p-1)\, d_R f_0}{c} \cos\alpha_p \cos\beta_p, \tag{6}$$

$$f_{pq,n}^q = \frac{(q-1)\, d_T f_0}{c} \left[\cos\left(\alpha_q - \alpha_{pq}^T\right)\cos\beta_q \cos\beta_{pq}^T + \sin\beta_q \sin\beta_{pq}^T\right], \tag{7}$$

$$f_{pq,n}^p = \frac{(p-1)\, d_R f_0}{c} \left[\cos\left(\alpha_p - \alpha_{pq}^R\right)\cos\beta_p \cos\beta_{pq}^R + \sin\beta_p \sin\beta_{pq}^R\right], \tag{8}$$

$$f_{pq,\rho} = \frac{f_0}{c}\left(v_T \cos\alpha_T \cos\beta_T + v_R \cos\alpha_R \cos\beta_R\right), \tag{9}$$

where f_0 is the carrier frequency and c denotes the speed of light.

$$f_{pq,n_m} = f_{pq}^T + f_{pq}^R + f_{pq,n_m}^{\mathrm{AOD}} + f_{pq,n_m}^{\mathrm{AOA}}, \tag{10}$$

where f_{pq}^T and f_{pq}^R are caused by the movement of T_X and R_X, respectively. $f_{pq,n_m}^{\mathrm{AOD}}$ and $f_{pq,n_m}^{\mathrm{AOA}}$ are caused by the movement of m scatterers relative to the directions of AOD and AOA, respectively. Using the similar mathematical manipulations in Appendix A, the respective components in (10) are

$$\begin{aligned} f_{pq}^T &= \frac{v_T f_0}{c}\left[\cos\left(\alpha_T - \alpha_{pq}^T\right)\cos\beta_T \cos\beta_{pq}^T + \sin\beta_T \sin\beta_{pq}^T\right], \\ f_{pq}^R &= \frac{v_R f_0}{c}\left[\cos\left(\alpha_R - \alpha_{pq}^R\right)\cos\beta_R \cos\beta_{pq}^R + \sin\beta_R \sin\beta_{pq}^R\right]. \end{aligned} \tag{11}$$

According to [31], the maximum Doppler shift for MB link over m moving scatterers with velocities $v_i \ll c$ is

$$f_m^{\max} = \frac{f_0}{c}\left(v_1 + 2\sum_{i=2}^{m-1} v_i + v_m\right). \tag{12}$$

Therefore, the remainder components of f_{pq,n_m} are [20]

$$\begin{aligned} f_{pq,n_m}^{\mathrm{AOD}} &\approx \frac{f_0}{c}\left(v_{pq}^1 P_{pq}^{\mathrm{AOD},1} + 2\sum_{i=2}^{m-1} v_{pq}^i P_{pq}^{\mathrm{AOD},i} + v_{pq}^m P_{pq}^{\mathrm{AOD},m}\right), \\ f_{pq,n_m}^{\mathrm{AOA}} &\approx \frac{f_0}{c}\left(v_{pq}^1 P_{pq}^{\mathrm{AOA},1} + 2\sum_{i=2}^{m-1} v_{pq}^i P_{pq}^{\mathrm{AOA},i} + v_{pq}^m P_{pq}^{\mathrm{AOA},m}\right), \end{aligned} \tag{13}$$

where $P_{pq}^{\mathrm{AOD},i}$ and $P_{pq}^{\mathrm{AOA},i}$ ($i = 1, 2, 3, \ldots, m$) are

$$\begin{aligned} P_{pq}^{\mathrm{AOD},i} &= \cos\left(\alpha_{pq}^i - \alpha_{pq}^T\right)\cos\beta_{pq}^i \cos\beta_{pq}^T + \sin\beta_{pq}^i \sin\beta_{pq}^T, \\ P_{pq}^{\mathrm{AOA},i} &= \cos\left(\alpha_{pq}^i - \alpha_{pq}^R\right)\cos\beta_{pq}^i \cos\beta_{pq}^R + \sin\beta_{pq}^i \sin\beta_{pq}^R. \end{aligned} \tag{14}$$

Note that if $\beta_T = \beta_R = \beta_{pq}^T = \beta_{pq}^R = \beta_{pq}^i = 0$ and $m = 1$, (10) equals (7) in [13] and (5) in [14] regardless of the plus or minus signs. The differences among these plus or minus signs are caused by the different forms of angles' expression.

2.2.3. Phases. The phase shift $\theta_{pq,\rho}$ can be assumed to be constant [30]. The phase shift θ_{pq,n_m} consists of the phase change caused by the interaction of the transmitted signal with the scatterers and the phase change caused by the TPD between the first and the last scatterers. Without loss of generality, we can assume that the phases θ_{pq,n_m} ($m = 1, 2, 3, \ldots, M$) are independent random variables. Here, it is assumed that they are uniformly distributed on the interval $[0, 2\pi)$ and independent of any other random variable.

3. Space-Time Correlation Function and Space-Doppler Power Spectral Density

Using the reference model described in Section 2, we can now derive the key temporal and spatial characteristics of MIMO V2V narrowband multipath fading channels with the local multiple moving scatters.

3.1. Space-Time Correlation Function. The normalized ST-CF between two complex faded envelopes $h_{pq}(t)$ and $h_{\overline{p}\overline{q}}(t)$ is defined as

$$R_{\overline{p}\overline{q},pq}(d_T, d_R, \tau) = E\left[h_{\overline{p}\overline{q}}(t)^* h_{pq}(t+\tau)\right], \quad (15)$$

where $(\bullet)^*$ denotes the complex conjugate operation, $E(\bullet)$ is the statistical expectation operator, $p, \overline{p} \in \{1, 2, 3, \ldots, P\}$, and $q, \overline{q} \in \{1, 2, 3, \ldots, Q\}$. The normalized T-CF can be obtained, if $p = \overline{p}$ and $q = \overline{q}$ in (15). The normalized space correlation function (S-CF) can be obtained by setting τ to zero in (15).

Since $h^1_{pq}(t), h^2_{pq}(t), \ldots, h^M_{pq}(t)$, and $h^{\mathrm{LoS}}_{pq}(t)$ are independent of each other, (15) can be simplified to

$$\begin{aligned} R_{\overline{p}\overline{q},pq}(d_T, d_R, \tau) &= R^{\mathrm{MB}}_{\overline{p}\overline{q},pq}(d_T, d_R, \tau) \\ &\quad + R^{\mathrm{LoS}}_{\overline{p}\overline{q},pq}(d_T, d_R, \tau) \\ &= \sum_{m=1}^{M} p_m R^m_{\overline{p}\overline{q},pq}(d_T, d_R, \tau) \\ &\quad + R^{\mathrm{LoS}}_{\overline{p}\overline{q},pq}(d_T, d_R, \tau), \end{aligned} \quad (16)$$

where $R^m_{\overline{p}\overline{q},pq}(d_T, d_R, \tau)$ and $R^{\mathrm{LoS}}_{\overline{p}\overline{q},pq}(d_T, d_R, \tau)$ denote the normalized ST-CFs of the mB and LoS components, respectively, and they are defined as

$$R^m_{\overline{p}\overline{q},pq}(d_T, d_R, \tau) = E\left[h^m_{\overline{p}\overline{q}}(t)^* h^m_{pq}(t+\tau)\right], \quad (17)$$

$$R^{\mathrm{LoS}}_{\overline{p}\overline{q},pq}(d_T, d_R, \tau) = E\left[h^{\mathrm{LoS}}_{\overline{p}\overline{q}}(t)^* h^{\mathrm{LoS}}_{pq}(t+\tau)\right]. \quad (18)$$

3.1.1. ST-CF of LoS Component. By substituting (2) into (18), the expression for the ST-CF of the LoS component can be written as

$$\begin{aligned} &R^{\mathrm{LoS}}_{\overline{p}\overline{q},pq}(d_T, d_R, \tau) \\ &\quad = \rho_{pq}\rho_{\overline{p}\overline{q}} E\left\{\exp\left\{j\left[2\pi t\left(f_{pq,\rho} - f_{\overline{p}\overline{q},\rho}\right) + 2\pi f_{pq,\rho}\tau\right.\right.\right. \\ &\quad\quad + 2\pi\left(f^q_{pq,\rho} + f^p_{pq,\rho} - f^{\overline{q}}_{\overline{p}\overline{q},\rho} - f^{\overline{p}}_{\overline{p}\overline{q},\rho}\right) + \theta_{pq,\rho} \\ &\quad\quad \left.\left.\left. - \theta_{\overline{p}\overline{q},\rho}\right]\right\}\right\}. \end{aligned} \quad (19)$$

For $\max(d_T, d_R) \ll D$, we assume $\rho_{pq} = \rho_{\overline{p}\overline{q}}$ and $\theta_{pq,\rho} = \theta_{\overline{p}\overline{q},\rho}$. Then, (19) can be written as

$$\begin{aligned} R^{\mathrm{LoS}}_{\overline{p}\overline{q},pq}(d_T, d_R, \tau) &= \rho^2_{pq} E\left\{\exp\left[j2\pi\left(f_{pq,\rho}\tau + \Delta f_\rho\right)\right]\right\} \\ &= \rho^2_{pq}\exp\left[j2\pi\left(f_{pq,\rho}\tau + \Delta f_\rho\right)\right], \end{aligned} \quad (20)$$

where Δf_ρ is defined as

$$\Delta f_\rho = f^q_{pq,\rho} + f^p_{pq,\rho} - f^{\overline{q}}_{\overline{p}\overline{q},\rho} - f^{\overline{p}}_{\overline{p}\overline{q},\rho}. \quad (21)$$

By substituting (5) and (6) into (21), Δf_ρ can be written as

$$\begin{aligned} \Delta f_\rho = \frac{f_0}{c}\left[\left(q - \overline{q}\right) d_T \cos\alpha_q \cos\beta_q \right. \\ \left. + \left(p - \overline{p}\right) d_R \cos\alpha_p \cos\beta_p\right]. \end{aligned} \quad (22)$$

3.1.2. ST-CF of mB Component. By substituting (4) into (17), the expression for the ST-CF of the mB component can be written as

$$\begin{aligned} &R^m_{\overline{p}\overline{q},pq}(d_T, d_R, \tau) \\ &\quad = \lim_{N_n\to\infty}\lim_{N_m\to\infty}\sum_{n_n=1}^{N_n} c_{\overline{p}\overline{q},n_n}\sum_{n_m=1}^{N_m} c_{pq,n_m} \\ &\quad\quad \times E\left\{\exp\left\{j\left[2\pi\left(f_{pq,n_m} - f_{\overline{p}\overline{q},n_n}\right)t + 2\pi f_{pq,n_m}\tau + 2\pi\left(f^q_{pq,n} + f^p_{pq,n} - f^{\overline{q}}_{\overline{p}\overline{q},n} - f^{\overline{p}}_{\overline{p}\overline{q},n}\right) + \theta_{pq,n_m} - \theta_{\overline{p}\overline{q},n_n}\right]\right\}\right\}. \end{aligned} \quad (23)$$

Under the assumption that θ_{pq,n_m} and $\theta_{\overline{p}\overline{q},n_n}$ are uniformly distributed on the interval $[0, 2\pi)$ and independent of each other, $E\{\exp[j(\theta_{pq,n_m} - \theta_{\overline{p}\overline{q},n_n})]\}$ equals 1. It is assumed that all the path gains of the mB component have the same size; that is,

$$c_{\overline{p}\overline{q},n_n} = c_{pq,n_m} = \sigma_m\sqrt{\frac{2}{N_m}}. \quad (24)$$

Then, (23) can be written as

$$\begin{aligned} &R^m_{\overline{p}\overline{q},pq}(d_T, d_R, \tau) \\ &\quad = 2\sigma^2_m \lim_{N_m\to\infty}\sum_{n_m=1}^{N_m} E\left\{\exp\left[j2\pi\left(f_{pq,n_m}\tau + \Delta f_{n_m}\right)\right]\right\}, \end{aligned} \quad (25)$$

where Δf_{n_m} is defined as

$$\Delta f_{n_m} = f^{q}_{pq,n} + f^{p}_{pq,n} - f^{\overline{q}}_{\overline{pq},n} - f^{\overline{p}}_{\overline{pq},n}. \tag{26}$$

It is assumed that AOD and AOA of $h^{m}_{pq}(t)$ and $h^{m}_{\overline{pq}}(t)$ are independent and identically distributed (i.i.d.). By substituting (7) and (8) into (26), Δf_{n_m} can be written as

$$\begin{aligned}\Delta f_{n_m} = \frac{f_0}{c}\{&(q - \overline{q})\, d_T \left[\cos\left(\alpha_q - \alpha^T_{pq}\right)\cos\beta_q \cos\beta^T_{pq} + \sin\beta_q \sin\beta^T_{pq}\right] \\ &+ (p - \overline{p})\, d_R \left[\cos\left(\alpha_p - \alpha^R_{pq}\right)\cos\beta_p \cos\beta^R_{pq} + \sin\beta_p \sin\beta^R_{pq}\right]\}.\end{aligned} \tag{27}$$

Since the number of local scatterers in the reference model is infinite, the parameters α^T_{pq}, β^T_{pq}, α^R_{pq}, β^R_{pq}, α^i_{pq}, and β^i_{pq} can be seen as continuous random variables with corresponding probability density functions (PDFs). Then, the ST-CF of the mB component (25) can be written as

$$\begin{aligned}R^{m}_{\overline{pq},pq}(d_T, d_R, \tau) = {} & 2\sigma^2_m \\ & \times \int\cdots\int\int\cdots\int\int\cdots\int\int\int\int\int \exp\left[j2\pi\left(f_{pq,n_m}\tau + \Delta f_{n_m}\right)\right] \\ & \times \prod_{i=1}^{m} p\left(\nu^i_{pq}\right) \prod_{i=1}^{m} p\left(\alpha^i_{pq}, \beta^i_{pq}\right) \\ & \cdot p\left(\alpha^T_{pq}, \beta^T_{pq}, \alpha^R_{pq}, \beta^R_{pq}\right) d\nu^1_{pq}\cdots d\nu^m_{pq} d\alpha^1_{pq}\cdots d\alpha^m_{pq} d\beta^1_{pq}\cdots d\beta^m_{pq} d\alpha^T_{pq} d\beta^T_{pq} d\alpha^R_{pq} d\beta^R_{pq}.\end{aligned} \tag{28}$$

Now, the complete expression of (16) can be obtained by substituting (20) and (28) into (16). $p(\alpha^T_{pq}, \beta^T_{pq}, \alpha^R_{pq}, \beta^R_{pq})$ describes the joint distribution of AOD and AOA, and it can be optionally used to present some propagation channel models. As a result, the ST-CF in (28) can provide a suitable platform to study the statistical properties of some different channel models, such as the random scattering model [13, 14], Jakes model [28], one-ring model [23], and two-ring model [29] as described in Section 3.1.3. Therefore, the ST-CF in (28) is a generalized and parametric expression. However, due to the complex nature of $p(\alpha^T_{pq}, \beta^T_{pq}, \alpha^R_{pq}, \beta^R_{pq})$, it is assumed that AOD and AOA are independent [13, 14, 32, 33], and azimuth angles and elevation angles in (28) are also independent [18, 19, 32]. The parameters in (28) such as the velocities of the multiple moving scatterers and random angles can be calculated as follows.

(i) Scatterer Velocity Distributions. The Gaussian, Laplace, exponential, and uniform distributions can be used to describe the velocity of moving scatterers [13]. In fact, the scatterer velocity ν^i_{pq} is always positive or equal to zero. We use the uniform distribution in (29) and half-Gaussian distribution in (30) to describe the velocity of multiple moving scatterers.

$$p\left(\nu^i_{pq}\right) = \frac{1}{\nu^i_{\max}}, \quad 0 \le \nu^i_{pq} \le \nu^i_{\max}, \tag{29}$$

where $\nu^i_{\max}$ is the maximum of ν^i_{pq}.

$$p\left(\nu^i_{pq}\right) = \frac{\sqrt{2}}{\sqrt{\pi}\sigma_{pq,i}} \exp\left[-\frac{{\nu^i_{pq}}^2}{2\sigma^2_{pq,i}}\right], \quad \nu^i_{pq} \ge 0, \tag{30}$$

where $\sigma_{pq,i}$ is the standard deviation of ν^i_{pq}.

(ii) Angle Distributions. To characterize the statistical angles in Table 1, we use the uniform distribution in (31) in the isotropic scattering environment and use the von Mises distribution in (32) and the cosine distribution in (33) in the nonisotropic scattering environment. In addition, the interval of azimuth angles α^T_{pq}, α^R_{pq}, and α^i_{pq} is $(-\pi, \pi]$, and the interval of elevation angles β^T_{pq}, β^R_{pq}, and β^i_{pq} is $(-\pi/2, \pi/2]$.

$$p(\gamma) = \frac{1}{\gamma_2 - \gamma_1}, \quad \gamma_1 \le \gamma \le \gamma_2, \tag{31}$$

$$p(\alpha) = \frac{\exp\left[k\cos\left(\alpha - \overline{\alpha}\right)\right]}{2\pi I_0(k)}, \quad \alpha_1 \le \alpha \le \alpha_1 + 2\pi, \tag{32}$$

where $I_0(\bullet)$ is the zeroth-order modified Bessel function of the first kind, $\overline{\alpha}$ is the mean angle, and k controls the spread of angles around the mean. The von Mises distribution PDF with $\overline{\alpha} = 0$ is used to describe the azimuth angles.

$$p(\beta) = \frac{\pi}{4\left|\beta_m\right|}\cos\left(\frac{\pi}{2}\frac{\beta}{\beta_m}\right), \quad -\beta_m \le \beta \le \beta_m, \tag{33}$$

where β_m is the maximum of β. The cosine distribution PDF is used to describe the elevation angles.

3.1.3. Special Cases of mB's ST-CF. If $\beta_T = \beta_R = \beta^T_{pq} = \beta^R_{pq} = \beta^i_{pq} = 0$, that is, the scattering environment is 2D,

some different special cases can be derived from the general expression of the mB's ST-CF in (28).

In the 2D scattering environment, (28) can be written as (B.2) in Appendix B. If $p = \overline{p}$, $q = \overline{q}$, and $m = 1$, (B.2) equals (11) in [13] and (6) in [14] regardless of the plus or minus signs under the assumption that the angles α^T and α^R are independent of each other in [13, 14]. In isotropic scattering environments, some other special cases with closed-form expressions can be derived as follows.

Appendix B shows that an approximate ST-CF of (B.2) can be written as

$$\begin{aligned} R^m_{\overline{pq},pq}(d_T, d_R, \tau) &= 2\sigma_m^2 J_0\left\{k_0\left[v_T\tau + (q-\overline{q})\, d_T\right]\right\} \\ &\times J_0\left\{k_0\left[v_R\tau + (p-\overline{p})\, d_R\right]\right\} \int \cdots \int J_0\left(2k_0 v^1_{pq}\tau\right) \\ &\times J_0\left(2k_0 v^m_{pq}\tau\right) \prod_{i=2}^{m-1} J_0\left(4k_0 v^i_{pq}\tau\right) \\ &\cdot \prod_{i=1}^{m} p\left(v^i_{pq}\right) dv^1_{pq} \cdots dv^m_{pq}, \end{aligned} \tag{34}$$

where $J_0(\bullet)$ denotes the zeroth-order Bessel function of the first kind and $k_0 = 2\pi f_0/c$ is the wave number.

Note that if m approaches to the infinity, (34) can be written as

$$\begin{aligned} &\lim_{m\to\infty} R^m_{\overline{pq},pq}(d_T, d_R, \tau) \\ &= \begin{cases} 2\sigma_m^2 J_0\left[(q-\overline{q})\, k_0 d_T\right] J_0\left[(p-\overline{p})\, k_0 d_R\right], & \tau = 0, \\ 0 & \tau > 0. \end{cases} \end{aligned} \tag{35}$$

In the NLoS communication environment with very high-density scatterers, (35) implies that the ST-CF approaches to zero at the nonzero time difference τ and has nothing to do with velocities of scatterers, T_X and R_X. The large-scale antenna arrays are very suitable to be used in this environment because the antenna element spacing can be reduced to a smaller value.

If v^i_{pq} is constant, (34) can be presented as the following closed-form expression:

$$\begin{aligned} &R^m_{\overline{pq},pq}(d_T, d_R, \tau) \\ &= 2\sigma_m^2 J_0\left\{k_0\left[v_T\tau + (q-\overline{q})\, d_T\right]\right\} \\ &\quad \times J_0\left\{k_0\left[v_R\tau + (p-\overline{p})\, d_R\right]\right\} J_0\left(2k_0 v^1_{pq}\tau\right) \\ &\quad \times J_0\left(2k_0 v^m_{pq}\tau\right) \prod_{i=2}^{m-1} J_0\left(4k_0 v^i_{pq}\tau\right). \end{aligned} \tag{36}$$

The T-CF of the classical F2M scenario with fixed scatterers is obtained, if $v_T = v^i_{pq} = 0$ $(i = 1, 2, 3, \ldots, m)$, $q = \overline{q}$, and $p = \overline{p}$ in (36). In this case, the ST-CF in (36) is $2\sigma_m^2 J_0(k_0 v_R \tau)$, which is known as the Jakes model [28]. If $v_T = 0, m = 1$, $q = \overline{q}$, and $p = \overline{p}$, the ST-CF in (36) results in $2\sigma_m^2 J_0(k_0 v^1_{pq}\tau) J_0(k_0 v_R \tau)$, which equals the T-CF of F2M single-ring channel model in the presence of moving scatterers reported in (11) of [23]. If $v^i_{pq} = 0$ $(i = 1, 2, 3, \ldots, m)$, $q = \overline{q}$, and $p = \overline{p}$, the ST-CF in (36) results in $2\sigma_m^2 J_0(k_0 v_T \tau) J_0(k_0 v_R \tau)$, which equals the T-CFs of the classical M2M two-ring channel model in the presence of fixed scatterers reported in (46) of [29]. If $v^i_{pq} = \tau = 0$ $(i = 1, 2, 3, \ldots, m)$, $q = p = 2$, and $\overline{q} = \overline{p} = 1$, the ST-CF in (36) results in $2\sigma_m^2 J_0(k_0 d_T) J_0(k_0 d_R)$, which equals the S-CF in (46) of [29].

The velocities of moving scatterers such as moving foliage, walking pedestrians, and passing vehicles generally are random variables. If v^i_{pq} is described by the uniform distribution in (29), (34) can be presented as the following closed-form expression:

$$\begin{aligned} R^m_{\overline{pq},pq}(d_T, d_R, \tau) &= \frac{\sigma_m^2}{2^{m-1}} J_0\left\{k_0\left[v_T\tau + (q-\overline{q})\, d_T\right]\right\} \\ &\times J_0\left\{k_0\left[v_R\tau + (p-\overline{p})\, d_R\right]\right\} \left[2J_0\left(2k_0 v^1_{\max}\tau\right)\right. \\ &+ \pi J_1\left(2k_0 v^1_{\max}\tau\right) H_0\left(2k_0 v^1_{\max}\tau\right) - \pi J_0\left(2k_0 v^1_{\max}\tau\right) \\ &\times \left. H_1\left(2k_0 v^1_{\max}\tau\right)\right] \left[2J_0\left(2k_0 v^m_{\max}\tau\right)\right. \\ &+ \left. \pi J_1\left(2k_0 v^m_{\max}\tau\right) H_0\left(2k_0 v^m_{\max}\tau\right) - \pi J_0\left(2k_0 v^m_{\max}\tau\right)\right] \\ &\cdot H_1\left(2k_0 v^m_{\max}\tau\right)] \times \prod_{i=2}^{m-1} \left[2J_0\left(4k_0 v^i_{\max}\tau\right)\right. \\ &+ \pi J_1\left(4k_0 v^i_{\max}\tau\right) \times H_0\left(4k_0 v^i_{\max}\tau\right) \\ &- \left. \pi J_0\left(4k_0 v^i_{\max}\tau\right) H_1\left(4k_0 v^i_{\max}\tau\right)\right], \end{aligned} \tag{37}$$

where $J_1(\bullet)$ denotes the first-order Bessel function of the first kind, $H_0(\bullet)$ denotes the zeroth-order Struve function, and $H_1(\bullet)$ denotes the first-order Struve function.

If v^i_{pq} is described by the half-Gaussian distribution in (30), (34) can be presented as the following closed-form expression:

$$\begin{aligned} R^m_{\overline{pq},pq}(d_T, d_R, \tau) &= 2\sigma_m^2 J_0\left\{k_0\left[v_T\tau + (q-\overline{q})\, d_T\right]\right\} \\ &\times J_0\left\{k_0\left[v_R\tau + (p-\overline{p})\, d_R\right]\right\} I_0\left(k_0^2\sigma^2_{pq,1}\tau^2\right) \\ &\times I_0\left(k_0^2\sigma^2_{pq,m}\tau^2\right) \exp\left(-k_0^2\sigma^2_{pq,1}\tau^2\right) \\ &\cdot \exp\left(-k_0^2\sigma^2_{pq,m}\tau^2\right) \\ &\times \prod_{i=2}^{m-1} I_0\left(4k_0^2\sigma^2_{pq,i}\tau^2\right) \exp\left(-4k_0^2\sigma^2_{pq,i}\tau^2\right). \end{aligned} \tag{38}$$

3.2. Space-Doppler Power Spectral Density. The SD-PSD can be obtained by taking the Fourier transform of the ST-CF in (16) with respect to time difference τ. From (16), it follows that

Table 2: Parameters used in the numerical simulation.

Parameters	Figures 2, 3, and 6	Figures 4, 5, and 7	Figures 8 and 9	Figure 10	Figure 11
f_0 (GHz)	2.435	2.435	2.435	29.5	2.435
K	2	2	2	2.4	2.41
k	5.4	5.4	3	—	3
q, p	2, 2	1, 1	2, 2	1, 1	1, 1
$\overline{q}, \overline{p}$	1, 1	1, 1	1, 1	1, 1	1, 1
d_T, d_R (λ)	1/2, 1/2	0, 0	variable	0, 0	0, 0
α_q, β_q (rad)	$\pi/2, \pi/6$	$\pi/2, \pi/6$	$\pi/2, \pi/6$	$\pi/2, \pi/6$	0, 0
α_p, β_p (rad)	$\pi/2, \pi/6$	$\pi/2, \pi/6$	$\pi/2, \pi/6$	$\pi/2, \pi/6$	0, 0
v_T, v_R (m/s)	25, 25	25, 25	25, 25	0, 0	12, 12
α_T, β_T (rad)	$\pi/2, 0$	$\pi/2, 0$	$\pi/2, 0$	0, 0	$\pi/2, 0$
α_R, β_R (rad)	$\pi/2, 0$	$\pi/2, 0$	$\pi/2, 0$	0, 0	$\pi/2, 0$

the SD-PSD is a summation of the SD-PSDs of the MB and LoS components; that is,

$$S_{\overline{pq},pq}(d_T, d_R, \omega) = \mathcal{F}_\tau \left\{ R_{\overline{pq},pq}(d_T, d_R, \tau) \right\} = \sum_{m=1}^{M} p_m S^m_{\overline{pq},pq}(d_T, d_R, \omega) + S^{\text{LoS}}_{\overline{pq},pq}(d_T, d_R, \omega). \quad (39)$$

The SD-PSD of the LoS component can be written as

$$S^{\text{LoS}}_{\overline{pq},pq}(d_T, d_R, \omega) = 2\pi\rho^2_{pq} \exp\left(j2\pi\Delta f_\rho\right) \delta\left(\omega - 2\pi f_{pq,\rho}\right), \quad (40)$$

where $\delta(\bullet)$ is the Dirac delta function.

Since the ST-CF of the mB component is the multiple integral as (28), the closed-form expression of SD-PSD cannot be derived. In Section 4.2, we show the SD-PSD of the 3D V2V channel in the presence of multiple moving scatterers by means of numerical integrations.

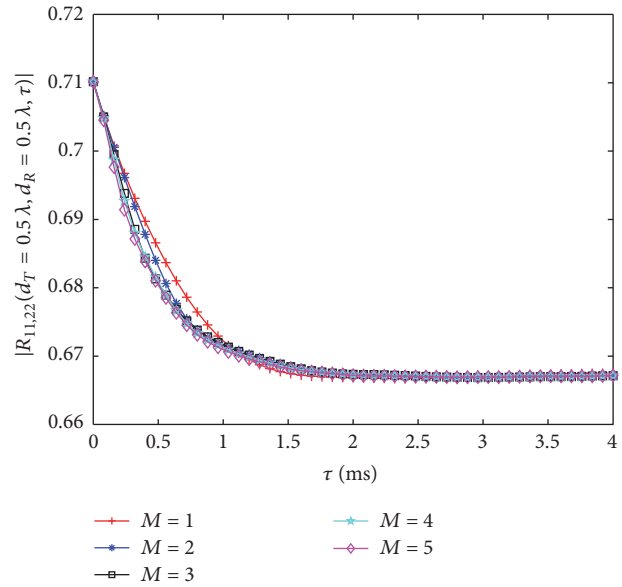

Figure 2: ST-CFs in (16) in the isotropic scattering scenario for different maximum bounces.

4. Numerical Results and Validation

This section demonstrates the normalized correlation functions and validates the Doppler power spectral density (D-PSD) described in Section 3 through the MATLAB numerical simulations. Unless indicated otherwise, the values of the numerical simulation parameters are summarized in Table 2.

4.1. Numerical Results. In this section, the numerical curves of ST-CFs, T-CFs, and S-CFs influenced by some important contributory factors are presented. As in the typical urban environments, the power weight of the mth cluster of rays has been set to $p_1 = p_2 = 1/2$ for $M = 2$, $p_1 = p_2 = p_3 = 1/3$ for $M = 3$, $p_1 = p_2 = 1/3$, $p_3 = p_4 = 1/6$ for $M = 4$, $p_1 = 1/3$, $p_2 = 1/4$, $p_3 = p_4 = 1/6$, and $p_5 = 1/12$ for $M = 5$.

4.1.1. ST-CFs and T-CFs for Different Scattering Scenarios and Bounces. Figures 2–5 demonstrate the ST-CFs and T-CFs for the different maximum bounces M in the 3D isotropic and nonisotropic scattering scenarios. The scatterer velocity is uniformly distributed with an average speed of 25 m/s that may be the velocity of passing vehicles. The other parameters used to obtain curves in Figures 2–5 are summarized in (Table 2, Cols. 2 and 3). As shown in Figures 2 and 4, the larger M is, the faster the ST-CFs and T-CFs decrease in the isotropic scattering scenario. However, the descent rates of ST-CFs and T-CFs increase slowly when M is larger than 3. The similar conclusions can be obtained from Figures 3 and 5; however, the ST-CF curves in Figure 3 have oscillations which may be caused by the nonisotropic scattering. However, this conclusion differs from [27] which showed that the triple- or higher-order bounced rays had statistical properties very similar to those of the double-bounced rays and could be approximated as double-bounced rays. The discrepancy may be caused by the different communication environments considered by us and [27]. Specifically, channel-sounding experimental campaign in [27] was conducted along surface

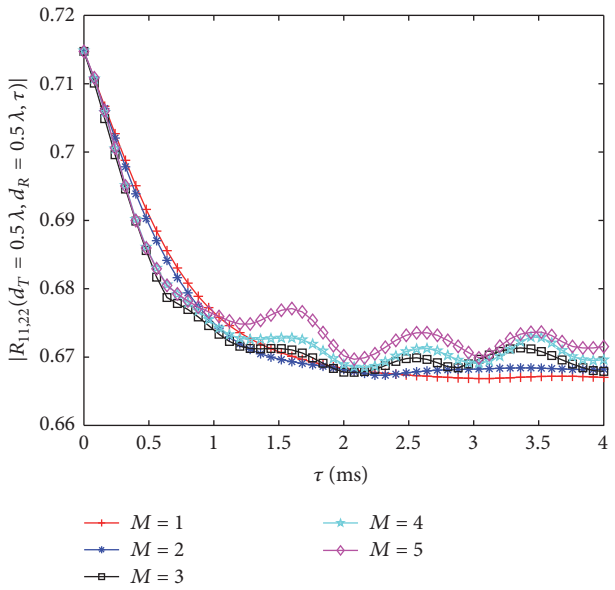

Figure 3: ST-CFs in (16) in the nonisotropic scattering scenario for different maximum bounces.

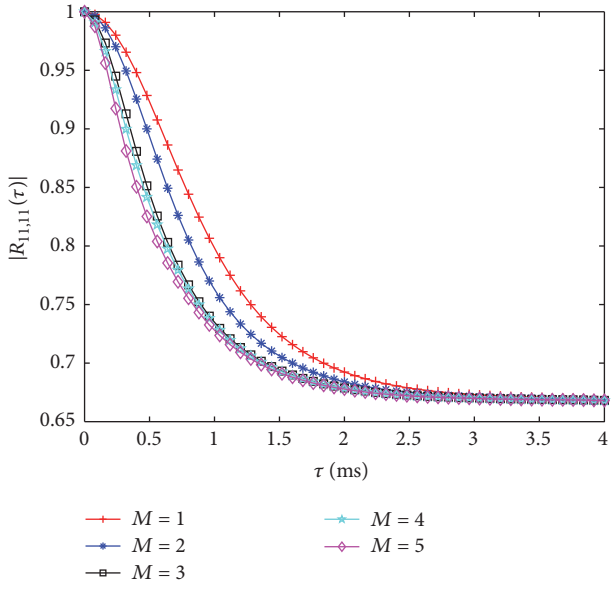

Figure 4: T-CFs in (16) with $p = \overline{p}$ and $q = \overline{q}$ in the isotropic scattering scenario for different maximum bounces.

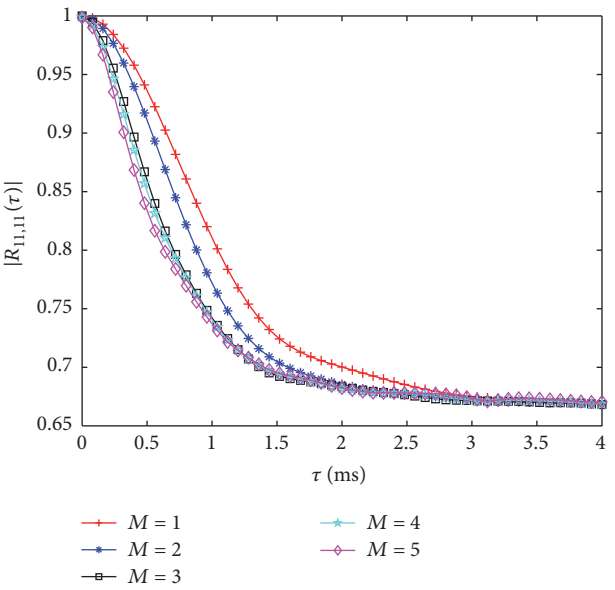

Figure 5: T-CFs in (16) with $p = \overline{p}$ and $q = \overline{q}$ in the nonisotropic scattering scenario for different maximum bounces.

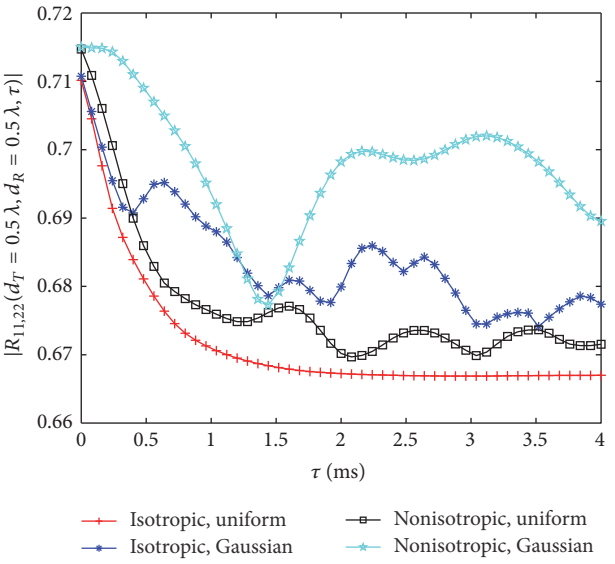

Figure 6: ST-CFs in (16) in the isotropic and nonisotropic scattering scenarios with $M = 5$ for different scatterer velocity distributions.

streets around the Georgia Tech campus and on the Interstate highways in the Midtown Atlanta metropolitan area which may have lower dense scatterers than our communication environments. The ST-CF curves in Figure 3 converge relatively slower for the larger M that means there are more local scatterers in motion with random velocities and random directions. As can be observed in Figures 4 and 5, the T-CFs in both figures are very similar that indicates that the scattering forms have no significant effect on the T-CFs of the 3D V2V channel in the presence of multiple moving scatterers. Furthermore, in Figures 2–5, it can be observed that a tendency to a limit value curve of ST-CFs and T-CFs can be inferred if M approaches infinity, and the similar inference also can be obtained in (35) for the 2D scattering environment.

4.1.2. ST-CFs and T-CFs for Different Scattering Scenarios and Scatterer Velocity Distributions. Figures 6 and 7 demonstrate the ST-CFs and T-CFs for the different scatterer velocity distributions in the 3D isotropic and nonisotropic scattering scenarios. We use two uniform distributions in the isotropic scattering environment and use the von Mises distribution and the cosine distribution in the nonisotropic scattering environment to describe all the statistical azimuth and elevation angles in Table 1, respectively. The average speed of the uniform and half-Gaussian distributions is 25 m/s,

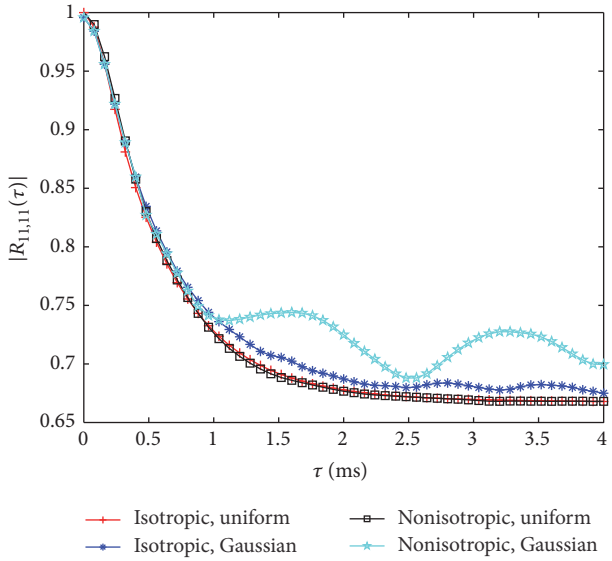

FIGURE 7: T-CFs in (16) with $p = \overline{p}$ and $q = \overline{q}$ in the isotropic and nonisotropic scattering scenarios with $M = 5$ for different scatterer velocity distributions.

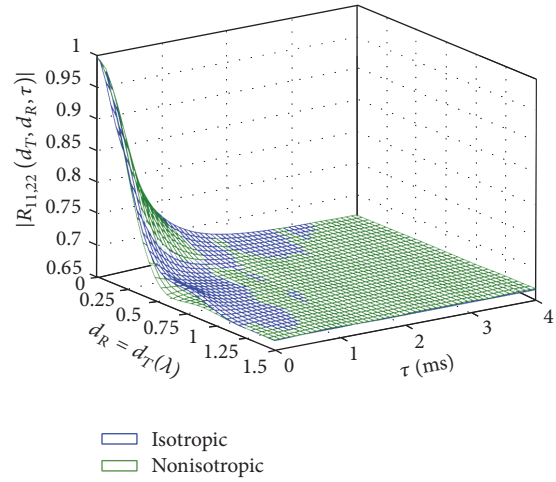

FIGURE 8: 3D ST-CFs in (16) in the isotropic and nonisotropic scattering scenarios with $M = 5$. λ is the carrier wavelength.

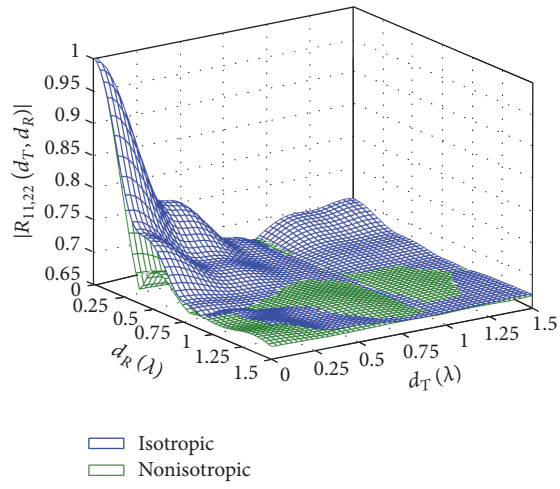

FIGURE 9: 3D S-CFs in (16) with $\tau = 0$ in the isotropic and nonisotropic scattering scenarios. λ is the carrier wavelength.

and the standard deviation of the half-Gaussian distribution is 31 m/s. The other parameters used to obtain curves in Figures 6 and 7 are summarized in (Table 2, Cols. 2 and 3). As shown in Figure 6, the ST-CF for the uniform distributed velocity of scatterers in the isotropic scattering environment decreases fastest, and both the nonisotropic scattering and the half-Gaussian distribution can result in swift oscillations of the fading curves. The comparison results indicate that the scatterer velocity distributions have more significant effect than the scattering forms on the ST-CFs of the 3D V2V channel in the presence of multiple moving scatterers. Figure 7 indicates that, not like scattering forms, the scatterer velocity distributions have significant effect on the T-CFs. Generally, the realistic propagation environment is nonisotropic scattering, and the scatterer velocity can be modeled by the half-Gaussian or uniform distribution. Therefore, the results of Figures 6 and 7 may be helpful in analysis of the system performance and modeling a specific propagation channel for V2V communications.

4.1.3. ST-CFs and S-CFs for Different Scattering Scenarios and Spacing between Adjacent Antenna Elements. Figures 8 and 9 demonstrate the 3D ST-CFs and S-CFs for the different spacing between adjacent antenna elements of T_X and R_X in isotropic and nonisotropic scattering scenarios. The set of the scatterer velocity in Figure 8 is the same as Figures 2–5, and the other parameters used to obtain curves in Figures 8 and 9 are summarized in (Table 2, Col. 4). Figures 8 and 9 show that spacing between adjacent antenna elements has significant effect on the 3D ST-CFs and S-CFs. Furthermore, the 3D ST-CFs in isotropic and nonisotropic scattering scenarios decrease to the bottom when $d_R = d_T$ tends to 1.2λ and 0.7λ, respectively. In addition, the 3D S-CF in nonisotropic scattering scenarios is explicitly less than that in isotropic scattering scenarios for most spacing between adjacent antenna elements as shown in Figure 9. Therefore, the large-scale antenna arrays employing the spatial multiplexing are more suitable to be used in the nonisotropic scattering scenarios owing to the high antenna space utilization. The spacing between adjacent antenna elements of antenna arrays is suggested to be more than λ in the V2V communications, especially in the environments with low-density scatterers.

4.2. Comparison with Measurements. The parametric nature of the proposed channel model makes it adaptable to a variety of propagation environments. D-PSD is one of the most important and unique channel characteristics for V2V communication channels. To illustrate the validity of the proposed model, we compare the modeled SD-PSDs of the 3D V2V channel with multiple moving scatterers with the measured F2F D-PSD in [26], the theoretical V2V SD-PSD in [18], and the measured V2V SD-PSD in [27].

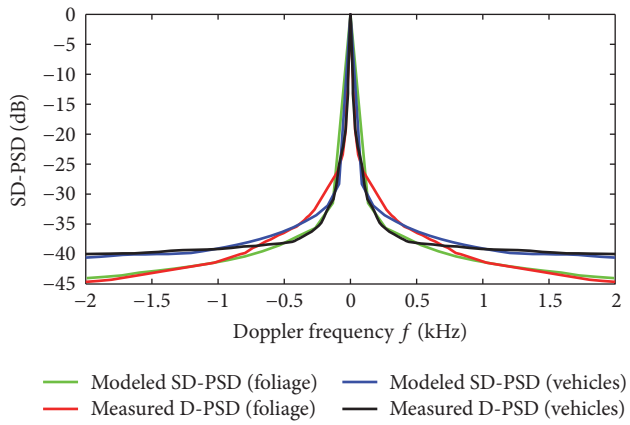

FIGURE 10: Comparison between the modeled SD-PSDs with $M = 5$ and the measured D-PSDs of Figure 4 in [26].

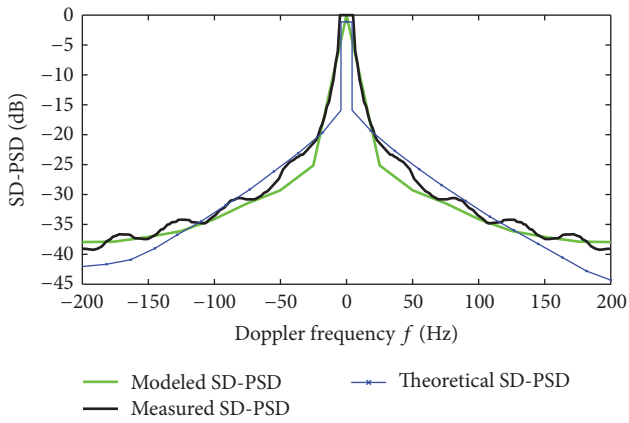

FIGURE 11: Comparison among the modeled SD-PSD with $M = 5$, the theoretical SD-PSD of Figure 8 in [18], and the measured SD-PSD of Figure 11 in [27].

Figure 10 shows the comparison between the modeled SD-PSDs obtained from the Fourier transform of the ST-CF presented in (16) in the isotropic scattering scenario and the measured D-PSDs of Figure 4 in [26]. The outdoor measurement experiments in [26] have shown that, at millimeter wavelengths, fading caused by foliage movement and the motion of nearby vehicles is a significantly deleterious effect in systems with static subscribers. Figure 4 in [26] shows the D-PSD generated by foliage movements and the D-PSD caused by passing vehicles, both in a fixed wireless channel at a carrier frequency of 29.5 GHz. We have used the half-Gaussian distribution with an average speed of 0.4 m/s and the standard deviation of 0.5 m/s to model the velocity of moving foliage scatterers, while the uniform distribution with an average speed of 6 m/s has been used to model the velocity of passing vehicles scatterers. The power weight of the mth cluster of rays scattered by the moving foliage or passing vehicles has been set to $p_1 = 9/16$, $p_2 = 5/16$, $p_3 = 1/16$, and $p_4 = p_5 = 1/32$. The other parameters used to obtain the modeled SD-PSD curves in Figure 10 are summarized in (Table 2, Col. 5). As can be observed in Figure 10, 40 dB fading bandwidths for the effect of the foliage and vehicles movements are 500 Hz and 1 kHz approximately, respectively. Fade depth due to foliage is less than the variation due to passing vehicles. Close agreements between the modeled and measured results are shown in Figure 10. These close matches can be seen not only for relatively slow moving scatterers but also for relatively fast moving scatterers as well.

Figure 11 shows the comparison among the modeled SD-PSD obtained from the Fourier transform of the ST-CF presented in (16) in the nonisotropic scattering scenario, the theoretical SD-PSD of Figure 8 in [18], and the measured SD-PSD of Figure 11 in [27]. The theoretical SD-PSD reproduced here is based on the two-cylinder model with moving and stationary scatterers for $d_R = d_T = 0$. The channel measurements in [27] for the measured SD-PSD were collected at 2.435 GHz in the urban street surface environment, and the spacing between two adjacent antenna elements of T_X and R_X was set to zero. We have used the half-Gaussian distribution with average speeds of 2.394 m/s, 0.798 m/s, and 0.4 m/s and the standard deviation of 3 m/s, 1 m/s, and 0.5 m/s to model the velocity of the first, the second, and the remaining moving scatterers on the communication links, respectively. The power weight of the mth cluster of rays has been set to $p_1 = 8/15$, $p_2 = 1/3$, $p_3 = 1/15$, $p_4 = 1/30$, and $p_5 = 1/30$ for $M = 5$. The other parameters used to obtain the modeled SD-PSD curve in Figure 11 are summarized in (Table 2, Col. 6). We note that, different from the measured SD-PSDs in [26], the measured SD-PSD curve in [27] has oscillations. The oscillating pattern in measurements for the case $d_R = d_T = 0$ may appear because it is not a true SISO scenario where only one transmit and one receive antenna are active [27]. As can be observed in Figure 11, the modeled SD-PSD matches better with measured SD-PSD than the theoretical SD-PSD in [18]. This may be because of the introduction of the multiple bounced rays into the propagation model or the constraints on the position of local scatterers in the two-cylinder model proposed in [18].

Figure 12 demonstrates the CDFs of the relative deviations between modeled/theoretical SD-PSDs and corresponding measured values in Figures 10 and 11. The mean relative deviation of the modeled SD-PSDs for foliage in Figure 10, modeled SD-PSDs for vehicles in Figure 10, modeled SD-PSDs in Figure 11, and theoretical SD-PSDs in Figure 11 is 2.56%, 2.16%, 3.9%, and 8.32%, respectively. As shown in Figure 12, more than 80% of the relative deviations of modeled SD-PSDs in Figures 10 and 11 are less than 5%, and the relative deviations of theoretical SD-PSDs in Figure 11 are explicitly larger than those of modeled SD-PSDs. In addition, from Figures 10 and 11, we note that the modeled SD-PSD matches better with measured SD-PSDs at the lower and higher Doppler frequencies than the middle Doppler frequencies. This may be because T_X and R_X were not strictly fixed, and not all the scatterers were in motion in measurements. The approximate calculation of the frequency shift in (A.4) and Doppler shift in (10) may be another factor which causes the mismatch at the middle Doppler frequencies, and more investigations concerning the accuracy of the proposed model will be addressed in future works.

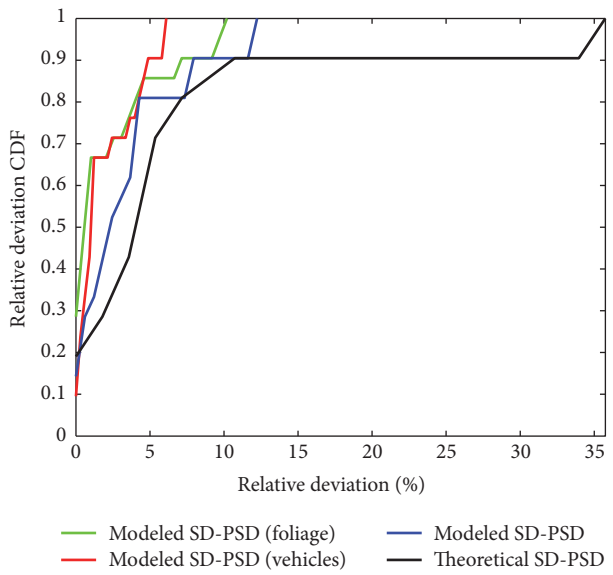

FIGURE 12: The relative deviation cumulative distribution functions (CDFs) of the modeled and theoretical SD-PSDs in Figures 10 and 11.

However, as shown in Figures 10–12, the acceptable matches confirm the utility and generality of the proposed model and show the need for including multiple moving scatterers in propagation model.

5. Conclusion

Without specific constraints on the position of the local moving scatterers, a 3D geometrical V2V propagation model that includes LoS, single bounced, and multiple bounced links between the transmitter and receiver was proposed. Based on the geometrical propagation model, a 3D reference model for narrowband MIMO V2V multipath fading channels was developed. From the reference model, the corresponding mathematical expressions and numerical results of ST-CFs, T-CFs, S-CFs, and SD-PSDs were studied for different parametric sets. It has been shown that the maximum bounces, scattering forms, scatterer velocity distributions, and spacing between adjacent antenna elements have significant effect on the ST-CFs, and only the maximum bounces and scatterer velocity distributions have significant effect on the T-CFs. Finally, the modeled SD-PSD results were compared with the measured data and the other literature's theoretical result. The close agreements between the analytically and empirically obtained channel statistics confirmed the utility and generality of the proposed model.

Appendix

A. Derivation Process of Frequency Shifts

The derivation process of $f_{pq,n}^{q}$ in (7) is presented in this section, and $f_{pq,\rho}^{p}$, $f_{pq,n}^{q}$, $f_{pq,n}^{p}$, and $f_{pq,\rho}$ can be calculated similarly.

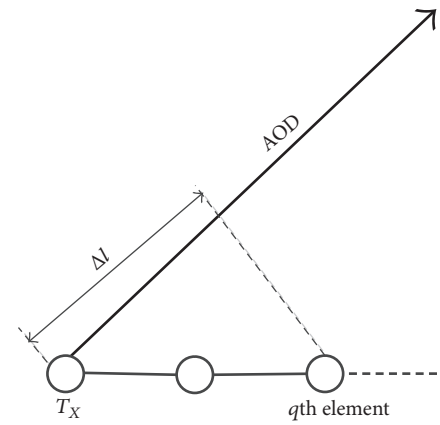

FIGURE 13: Projection from the coordinate vector of qth antenna element to the AOD direction.

According to Figure 1, the coordinate vectors of qth antenna element and the AOD direction can be written as, respectively,

$$\vec{L}_q = (q-1)\, d_T \left(\cos\beta_q \cos\alpha_q, \cos\beta_q \sin\alpha_q, \sin\beta_q\right), \tag{A.1}$$

$$\vec{L}_{\mathrm{AOD}} = \left(\cos\beta_{pq}^{T} \cos\alpha_{pq}^{T}, \cos\beta_{pq}^{T} \sin\alpha_{pq}^{T}, \sin\beta_{pq}^{T}\right). \tag{A.2}$$

Therefore, the projection Δl in Figure 13 is

$$\Delta l = \frac{\vec{L}_q \cdot \vec{L}_{\mathrm{AOD}}}{\left|\vec{L}_{\mathrm{AOD}}\right|} = (q-1)\, d_T \left[\cos\left(\alpha_q - \alpha_{pq}^{T}\right)\cos\beta_q \cos\beta_{pq}^{T} + \sin\beta_q \sin\beta_{pq}^{T}\right]. \tag{A.3}$$

Because we mainly consider the difference of the frequency shifts caused by the TPD changes to calculate ST-CFs, the TPD change of $h_{11}(t)$ is assumed to be zero. Eventually, $f_{pq,n}^{q}$ can be calculated as

$$f_{pq,n}^{q} \approx \frac{\Delta l f_0}{c} = \frac{(q-1)\, d_T f_0}{c}\left[\cos\left(\alpha_q - \alpha_{pq}^{T}\right)\cos\beta_q \cos\beta_{pq}^{T} + \sin\beta_q \sin\beta_{pq}^{T}\right]. \tag{A.4}$$

B. Derivation Process of Approximate ST-CFs

In the 2D scattering environment, the simplified and approximate expressions of (28) can be derived in this section. If $\beta_T = \beta_R = \beta_{pq}^{T} = \beta_{pq}^{R} = \beta_{pq}^{i} = 0$, (27) and (10) can be written as

$$\Delta f_{n_m} = \frac{f_0}{c}\left[(q-\overline{q})\, d_T \cos\left(\alpha_q - \alpha_{pq}^{T}\right) + (p-\overline{p})\, d_R \cos\left(\alpha_p - \alpha_{pq}^{R}\right)\right],$$

$$f_{pq,n_m} = \frac{f_0}{c}\left[\nu_T \cos\left(\alpha_T - \alpha_{pq}^T\right) + \nu_R \cos\left(\alpha_R - \alpha_{pq}^R\right) + \nu_{pq}^1 \cos\left(\alpha_{pq}^1 - \alpha_{pq}^T\right) + 2\sum_{i=2}^{m-1} \nu_{pq}^i \cos\left(\alpha_{pq}^i - \alpha_{pq}^T\right) + \nu_{pq}^m \cos\left(\alpha_{pq}^m - \alpha_{pq}^T\right) + \nu_{pq}^1 \cos\left(\alpha_{pq}^1 - \alpha_{pq}^R\right) + 2\sum_{i=2}^{m-1} \nu_{pq}^i \cos\left(\alpha_{pq}^i - \alpha_{pq}^R\right) + \nu_{pq}^m \cos\left(\alpha_{pq}^m - \alpha_{pq}^R\right)\right]. \tag{B.1}$$

If $\alpha_T = \alpha_q$ and $\alpha_R = \alpha_p$, that is, the antenna array and its velocity have the same directions, (28) can be simplified as by substituting (B.1) into (28)

$$\begin{aligned} &R_{\overline{pq},pq}^m (d_T, d_R, \tau) \\ &= 2\sigma_m^2 \int \cdots \int\int \cdots \int\int\int \exp\left\{jk_0\left[\left[\nu_T\tau + (q-\overline{q})\, d_T\right]\right.\right. \\ &\times \cos\left(\alpha_T - \alpha_{pq}^T\right) + \left[\nu_R\tau + (p-\overline{p})\, d_R\right] \cos\left(\alpha_R - \alpha_{pq}^R\right) \\ &+2\nu_{pq}^1 \tau \cos\left(\frac{\alpha_{pq}^T - \alpha_{pq}^R}{2}\right) \cos\left(\alpha_{pq}^1 - \frac{\alpha_{pq}^T + \alpha_{pq}^R}{2}\right) \\ &+4\tau \cos\left(\frac{\alpha_{pq}^T - \alpha_{pq}^R}{2}\right) \sum_{i=2}^{m-1} \nu_{pq}^i \cos\left(\alpha_{pq}^i - \frac{\alpha_{pq}^T + \alpha_{pq}^R}{2}\right) \\ &\left.\left.+2\nu_{pq}^m \tau \cos\left(\frac{\alpha_{pq}^T - \alpha_{pq}^R}{2}\right) \cos\left(\alpha_{pq}^m - \frac{\alpha_{pq}^T + \alpha_{pq}^R}{2}\right)\right]\right\} \prod_{i=1}^m p\left(\nu_{pq}^i\right) \\ &\cdot \prod_{i=1}^m p\left(\alpha_{pq}^i\right) p\left(\alpha_{pq}^T\right) p\left(\alpha_{pq}^R\right) d\nu_{pq}^1 \cdots d\nu_{pq}^m d\alpha_{pq}^1 \cdots d\alpha_{pq}^m d\alpha_{pq}^T d\alpha_{pq}^R, \end{aligned} \tag{B.2}$$

where $k_0 = 2\pi f_0/c$ is the wave number.

In isotropic scattering environment, we use the uniform distribution in (31) to describe all the random azimuth angles. In this case, (B.2) can be written as

$$\begin{aligned} &R_{\overline{pq},pq}^m (d_T, d_R, \tau) \\ &= \frac{\sigma_m^2}{2\pi^2} \int \cdots \int\int\int \exp\left\{jk_0\left[\nu_T\tau + (q-\overline{q})\, d_T\right] \cos\left(\alpha_T - \alpha_{pq}^T\right)\right. \\ &\left.+jk_0\left[\nu_R\tau + (p-\overline{p})\, d_R\right] \cos\left(\alpha_R - \alpha_{pq}^R\right)\right\} \\ &\times J_0\left[2k_0\nu_{pq}^1\tau \cos\left(\frac{\alpha_{pq}^T - \alpha_{pq}^R}{2}\right)\right] \\ &\times J_0\left[2k_0\nu_{pq}^m\tau \cos\left(\frac{\alpha_{pq}^T - \alpha_{pq}^R}{2}\right)\right] \\ &\times \prod_{i=2}^{m-1} J_0\left[4k_0\nu_{pq}^i\tau \cos\left(\frac{\alpha_{pq}^T - \alpha_{pq}^R}{2}\right)\right] \\ &\cdot \prod_{i=1}^m p\left(\nu_{pq}^i\right) d\nu_{pq}^1 \cdots d\nu_{pq}^m d\alpha_{pq}^T d\alpha_{pq}^R, \end{aligned} \tag{B.3}$$

where $J_0(\bullet)$ denotes the zeroth-order Bessel function of the first kind.

The AOD α_{pq}^T and AOA α_{pq}^R are uniformly and independently distributed, so $\alpha_{pq}^T - \alpha_{pq}^R$ can be equal to zero in average. As a consequence, the term $\cos[(\alpha_{pq}^T - \alpha_{pq}^R)/2]$ in (B.3) can be approximated by one [13, 14], and an approximate ST-CF can be written as from (B.3)

$$\begin{aligned} &R_{\overline{pq},pq}^m (d_T, d_R, \tau) \\ &= \frac{\sigma_m^2}{2\pi^2} \int \cdots \int\int\int \exp\left\{jk_0\left[\nu_T\tau + (q-\overline{q})\, d_T\right]\right. \\ &\cdot \cos\left(\alpha_T - \alpha_{pq}^T\right) \\ &\left.+jk_0\left[\nu_R\tau + (p-\overline{p})\, d_R\right]\right. \\ &\left.\cdot \cos\left(\alpha_R - \alpha_{pq}^R\right)\right\} J_0\left(2k_0\nu_{pq}^1\tau\right) \\ &\times J_0\left(2k_0\nu_{pq}^m\tau\right) \prod_{i=2}^{m-1} J_0\left(4k_0\nu_{pq}^i\tau\right) \\ &\cdot \prod_{i=1}^m p\left(\nu_{pq}^i\right) d\nu_{pq}^1 \cdots d\nu_{pq}^m d\alpha_{pq}^T d\alpha_{pq}^R. \end{aligned} \tag{B.4}$$

Eventually, the approximate ST-CF in (34) can be derived from (B.4) according to the definition of $J_0(\bullet)$.

Conflicts of Interest

The authors declare that they have no conflicts of interest.

Acknowledgments

This work was funded by the National Natural Science Foundation of China (no. 91438104, no. 61501065, no. 61571069, and no. 61601067), the Fundamental Research Funds for the Central Universities (no. 106112016CDJX160001), and the Chongqing Research Program of Basic Research and Frontier Technology (no. CSTC2016JCYJA0021).

References

[1] A. Bazzi, B. M. Masini, A. Zanella, and I. Thibault, "Beaconing from connected vehicles: IEEE 802.11p vs. LTE-V2V," in *Proceedings of 2016 IEEE 27th Annual International Symposium on Personal, Indoor, and Mobile Radio Communications (PIMRC)*, pp. 1–6, Valencia, Spain, September 2016.

[2] V. M. Rodrigo-Peñarrocha, J. Reig, L. Rubio, and et al., "Analysis of small- scale fading distributions in vehicle-to-vehicle communications," *Mobile Information Systems*, vol. 2016, Article ID 9584815, 7 pages, 2016.

[3] A. Bazzi, B. M. Masini, A. Zanella, and G. Pasolini, "IEEE 802.11p for cellular offloading in vehicular sensor networks," *Computer Communications*, vol. 60, pp. 97–108, 2015.

[4] X. Cheng, *MIMO channel modelling and simulation for cellular and mobile-to-mobile communication systems[Phd thesis]*, Heriot-Watt University, 2009.

[5] N. Avazov and M. Pätzold, "A geometric street scattering channel model for car-to-car communication systems," in *Proceedings of 4th Annual International Conference on Advanced*

Technologies for Communications, ATC2011, pp. 224–230, vnm, August 2011.

[6] X. Zhao, X. Liang, S. Li, and K. Haneda, "Mobile-to-Mobile Wideband MIMO Channel Realization by Using a Two-Ring Geometry-Based Stochastic Scattering Model," *Wireless Personal Communications*, vol. 84, no. 4, pp. 2445–2465, 2015.

[7] M. Walter, D. Shutin, and U.-C. Fiebig, "Delay-dependent doppler probability density functions for vehicle-to-vehicle scatter channels," *IEEE Transactions on Antennas and Propagation*, vol. 62, no. 4, pp. 2238–2249, 2014.

[8] P. T. Samarasinghe, T. A. Lamahewa, T. D. Abhayapala, and R. A. Kennedy, "3D mobile-to-mobile wireless channel model," in *Proceedings of 2010 Australian Communications Theory Workshop, AusCTW 2010*, pp. 30–34, aus, February 2010.

[9] M. Riaz, S. J. Nawaz, and N. M. Khan, "3D ellipsoidal model for mobile-to-mobile radio propagation environments," *Wireless Personal Communications*, vol. 72, no. 4, pp. 2465–2479, 2013.

[10] J. Chen and T. G. Pratt, "Three-dimensional geometry-based stochastic modeling and performance of 4×4 space-polarization mobile-to-mobile wideband MIMO channels," in *Proceedings of 2013 IEEE Global Communications Conference, GLOBECOM 2013*, pp. 3936–3941, usa, December 2013.

[11] Y. Bi, J. Zhang, M. Zeng, M. Liu, and X. Xu, "A Novel 3D Nonstationary Channel Model Based on the von Mises-Fisher Scattering Distribution," *Mobile Information Systems*, vol. 2016, Article ID 2161460, 2016.

[12] A. Chelli and M. Patzöld, "The impact of fixed and moving scatterers on the statistics of MIMO vehicle-to-vehicle channels," in *Proceedings of VTC Spring 2009 - IEEE 69th Vehicular Technology Conference*, esp, April 2009.

[13] A. Borhani and M. Pätzold, "Modeling of vehicle-to-vehicle channels in the presence of moving scatterers," in *Proceedings of 2012 IEEE Vehicular Technology Conference (VTC Fall)*, pp. 1–5, Quebec City, QC, Canada, September 2012.

[14] A. Borhani and M. Patzold, "Correlation and spectral properties of vehicle-to-vehicle channels in the presence of moving scatterers," *IEEE Transactions on Vehicular Technology*, vol. 62, no. 9, pp. 4228–4239, 2013.

[15] A. Chelli and M. Pätzold, "A non-stationary MIMO vehicle-to-vehicle channel model derived from the geometrical street model," in *Proceedings of the IEEE 74th Vehicular Technology Conference (VTC Fall '11)*, pp. 1–6, IEEE, San Francisco, Calif, USA, September 2011.

[16] M. D. Soltani, M. Alimadadi, Y. Seyedi, and H. Amindavar, "Modeling of doppler spectrum in V2V urban canyon oncoming environment," in *Proceedings of 2014 7th International Symposium on Telecommunications, IST 2014*, pp. 1155–1160, irn, September 2014.

[17] M. D. Soltani, M. Alimadadi, and A. Mohammadi, "Modeling of mobile scatterer clusters for doppler spectrum in wideband vehicle-to-vehicle communication channels," *IEEE Communications Letters*, vol. 18, no. 4, pp. 628–631, 2014.

[18] A. G. Zajić, "Impact of moving scatterers on vehicle-to-vehicle narrow-band channel characteristics," *IEEE Transactions on Vehicular Technology*, vol. 63, no. 7, pp. 3094–3106, 2014.

[19] A. G. Zajić, "Modeling impact of moving scatterers on doppler spectrum in wideband vehicle-to-vehicle channels," in *Proceedings of Proc. Eur. Conf. Antennas Propag*, p. 1, Lisbon, May 2015.

[20] J. Zhang, X. Yin, and X. Cheng, "Theoretical analysis and measurements: Doppler spectra of vehicular communication channels," in *Proceedings of 2012 12th International Conference on ITS Telecommunications, ITST 2012*, pp. 98–102, twn, November 2012.

[21] M. Picone, S. Busanelli, M. Amoretti, F. Zanichelli, and G. Ferrari, *Advanced Technologies for Intelligent Transportation Systems*, Springer, 2015.

[22] V. H. Pham, M. H. Taieb, J. Y. Chouinard, S. Roy, and H. T. Huynh, "On the double Doppler effect generated by scatterer motion," *REV Journal on Electronics and Communications*, vol. 1, pp. 30–37, 2011.

[23] S. Roy, H. T. Huynh, and P. Fortier, "Compound Doppler spread effects of subscriber motion and scatterer motion," *AEU - International Journal of Electronics and Communications*, vol. 57, no. 4, pp. 237–246, 2003.

[24] J. B. Andersen, J. O. Nielsen, G. F. Pedersen, G. Bauch, and G. Dietl, "Doppler spectrum from moving scatterers in a random environment," *IEEE Transactions on Wireless Communications*, vol. 8, no. 6, pp. 3270–3277, 2009.

[25] H. S. Rad, S. Gazor, and P. Shariatpanahi, "Non-fixed scatterers and their effects on MIMO multicarrier fading communication channels," in *Proceedings of 50th Annual IEEE Global Telecommunications Conference, GLOBECOM 2007*, pp. 3765–3769, usa, November 2007.

[26] N. Naz and D. Falconer, "Temporal variations characterization for fixed wireless at 29.5 GHz," in *Proceedings of 2000 IEEE 51st Vehicular Technology Conference. Proceedings. VTC2000-Springer*, pp. 2178–2182, Tokyo, Japan, 2000.

[27] A. G. Zajić, G. L. Stüber, T. G. Pratt, and S. T. Nguyen, "Wideband MIMO mobile-to-mobile channels: Geometry-based statistical modeling with experimental verification," *IEEE Transactions on Vehicular Technology*, vol. 58, no. 2, pp. 517–534, 2009.

[28] W. C. Jakes, *Microwave Mobile Communications*, Wiley-IEEE Press, Piscataway, NJ, USA, 1994.

[29] M. Pätzold, B. O. Hogstad, and N. Youssef, "Modeling, analysis, and simulation of MIMO mobile-to-mobile fading channels," *IEEE Transactions on Wireless Communications*, vol. 7, no. 2, pp. 510–520, 2008.

[30] M. Pätzold, *Mobile Radio Channels*, Wiley, Chichester, UK, 2nd edition, 2011.

[31] R. Wang and D. Cox, "Double mobility mitigates fading in ad hoc wireless networks," in *Proceedings of IEEE Antennas and Propagation Society International Symposium*, pp. 306–309, San Antonio, TX, USA.

[32] G. Bakhshi, K. Shahtalebi, and H. S. Rad, "A novel full-three-dimensional MIMO mobile-to-mobile channel reference model," in *Proceedings of 3rd International Conference on Signal Processing and Communication Systems, ICSPCS'2009*, usa, September 2009.

[33] W. Zhou, X. Wang, X. Wang, and W. Chen, "A modified two-erose- ring model for mimo mobile-to-mobile fading channels," in *Proceedings of 7th International Conference on Wireless Communications, Networking and Mobile Computing, WiCOM 2011*, 5, 1 pages, Wuhan, China, September 2011.

Hindawi
Mobile Information Systems
Volume 2017, Article ID 8246050, 10 pages
https://doi.org/10.1155/2017/8246050

Research Article

An Efficient Channel Access Scheme for Vehicular Ad Hoc Networks

Syed Asad Hussain,[1] Muddesar Iqbal,[2] Atif Saeed,[1,3] Imran Raza,[1] Hassan Raza,[4] Amjad Ali,[1] Ali Kashif Bashir,[5] and Adeel Baig[6,7]

[1]*Department of Computer Science, COMSATS Institute of Information Technology, Lahore, Pakistan*
[2]*Department of Computer Science and Informatics, London South Bank University, London, UK*
[3]*Department of Computing, Lancaster University, Lancaster, UK*
[4]*Department of Engineering Mathematics and Internetworking, Dalhousie University, Halifax, NS, Canada*
[5]*Department of Science and Technology, University of the Faroe Islands, Faroe Islands, Denmark*
[6]*School of Electrical Engineering & Computer Science (SEECS), National University of Sciences & Technology (NUST), Islamabad, Pakistan*
[7]*College of Computer and Information Systems (CCIS), Al Yamamah University, Riyadh, Saudi Arabia*

Correspondence should be addressed to Amjad Ali; amjad.ali@ciitlahore.edu.pk

Received 7 December 2016; Revised 24 March 2017; Accepted 18 May 2017; Published 13 June 2017

Academic Editor: Gianluigi Ferrari

Vehicular Ad Hoc Networks (VANETs) are getting more popularity due to the potential Intelligent Transport Systems (ITS) technology. It provides many efficient network services such as safety warnings (collision warning), entertainment (video and voice), maps based guidance, and emergency information. VANETs most commonly use Road Side Units (RSUs) and Vehicle-to-Vehicle (V2V) referred to as Vehicle-to-Infrastructure (V2I) mode for data accessing. IEEE 802.11p standard which was originally designed for Wireless Local Area Networks (WLANs) is modified to address such type of communication. However, IEEE 802.11p uses Distributed Coordination Function (DCF) for communication between wireless nodes. Therefore, it does not perform well for high mobility networks such as VANETs. Moreover, in RSU mode timely provision of data/services under high density of vehicles is challenging. In this paper, we propose a RSU-based efficient channel access scheme for VANETs under high traffic and mobility. In the proposed scheme, the contention window is dynamically varied according to the times (deadlines) the vehicles are going to leave the RSU range. The vehicles with shorter time deadlines are served first and vice versa. Simulation is performed by using the Network Simulator (NS-3) v. 3.6. The simulation results show that the proposed scheme performs better in terms of throughput, backoff rate, RSU response time, and fairness.

1. Introduction

The significant improvements in the Intelligent Transportation System (ITS) have led the key advancements in the conventional IEEE 802.11p standard. In order to support the ITS services and applications (i.e., traffic management, traveler information, and public safety messages which are further divided into two classes; (i) periodic (beacon) safety messages and (ii) event driven messages) over Vehicular Ad Hoc Networks (VANETs), the Wireless Access in the Vehicular Environment (WAVE) standard has specified the required changes in the conventional IEEE 802.11p standard [1–3]. In dense and high traffic load scenarios the WAVE prioritizes the messages by which its delay increases significantly; however, its throughput decreases considerably. The Federal Communications Commission (FCC) has allocated 5.9 GHz and 5.8 GHz bands in the USA and South Korea, respectively, for vehicular communication. Moreover, Dedicated Short Range Communications (DSRC) scheme is also proposed to allocate the spectrum for vehicular communications. This scheme

allocates spectrum between the vehicles and the roadside infrastructure or among the high speed vehicles within a range of up to 1 km.

In VANETs, vehicles can communicate with each other through roadside infrastructure known as Road Side Unit (RSU) as well as directly. Direct communication between vehicles is called Vehicle-to-Vehicle (V2V) communication. However, the conventional IEEE 802.11p standard does not provide satisfactory operating environment for VANETs under high traffic load and high mobility. Whereas, high traffic density and high mobility cause more frequent network topology changes as well as fluctuations in traffic density. This happens because the IEEE 802.11p shares basic characteristics of Distributed Coordination Function (DCF) of IEEE 802.11 and IEEE 802.11e (EDCF) [3–9] such as carrier sensing procedures and service priority levels, respectively. If a vehicle has high speed it is a likely chance that it will not be able to access the RSU for channel allocation while others can [10].

This paper presents an efficient channel allocation scheme which dynamically adapts the contention window (CW) for the vehicle according to the deadline. The deadline of each vehicle is calculated based on its speed. In the proposed scheme the CW for high speed vehicle and vehicle with emergency data is varied slowly which consequently gives quick access to the channel and vice versa. Simulation results present the comparative evaluation of the proposed scheme with conventional scheme and schemes proposed in [10, 11]. The proposed scheme performs better in terms of throughput, backoff rate, and RSU response time and fairness.

The rest of the paper is organized as follows. In Section 2, the related work is presented. Section 3 consists of motivations and main contribution; it also discusses the proposed RSU-based scheme for efficient channel access under high traffic load and mobility. Section 4 presents the performance analysis. Finally, Section 5 concludes the paper.

2. Related Work

We present a review of the work related to channel access for VANETs under high traffic density and high mobility conditions. The authors in [10] introduce clustering approach for periodic broadcasting of vehicle's information such as its one-hop neighbors and its average speed. Each cluster is maintained by a cluster head. The cluster head broadcasts messages to vehicles within its cluster. Due to high mobility of cluster heads routes/hops can be broken and established frequently resulting in overall low network performance. This scheme categorizes vehicles based on their speed deviation from average speed of neighboring vehicles. The vehicles adjust their CWs according to the three fixed contention window ranges and not based on the time they leave the range of the RSU.

The scheme proposed in [12] investigates the performance of IEEE 802.11p by proposing two approaches of adaptive backoff window sizes. One is centralized and other one is distributed. In the centralized scheme the base station knows the number of concurrent transmitting vehicles and uses this information to calculate the optimal window size. The number of transmitting vehicles information is broadcasted periodically by the base station. Once such a broadcast is received by a vehicle, it will calculate the optimal transmission probability. However, in distributed approach each vehicle only uses its local channel information to select the backoff time. Each vehicle increases its backoff window size when the number of vehicles increases and vice versa. The vehicle in solicitation-based IEEE 802.11p MAC protocol [13] solicits data frames in an opportunistic style by requesting transmissions of the frames from a WAVE Mode Basic Service Set (WBSS) provider by a WAVE-poll frame. This counters fast channel variation conditions due to speed variability of vehicles.

Suthaputehakun and Ganz in [14] deploy conventional IEEE 802.11e with EDCF mechanism for priority assignment in intervehicle communication. High priority messages are repetitively transmitted to increase the probability of transmission as compared to lower priority ones. This results in more collisions and congestion in the network. The scheme proposed in [15] does not use CW based access mechanism; rather it uses the concept of super-frame consisting of collision-free and collision based phases. The vehicles are polled by the RSU according to their deadlines. Contention Free Period (CFP) is assigned 80% fixed length of the super-frame. However, Balon and Guo in [16] have considered the number of frames received by each vehicle to estimate the reception rate of that vehicle. Each vehicle knows local state of the network by maintaining a table carrying entries for neighboring vehicle. The entries include a MAC address, the last sequence number, a weighted reception rate, and a time stamp. CW is adapted according to the local reception rate of the vehicle. As the number of vehicles increases, maintenance of tables gets time consuming and complex for highly varying and fast road traffic. Furthermore, the paper does not explain how much CW is altered and how its threshold value is determined for comparison.

In [17], transmission power and CW for vehicles is dynamically adapted based on the vehicle density and instantaneous packet collision rate, respectively. In order to determine the estimated collision rate and adapt CW accordingly, the proposed scheme deploys the conventional IEEE 802.11 approach as well as using the concept of local reception rate suggested by Balon and Guo in [16]. The proposed scheme has almost the same issues as the scheme proposed in [16]. Additionally, the algorithm compares the estimated collision rate with a threshold value to relate CW but does not discuss how this threshold value is calculated. The scheme proposed in [18] considers the priority of packets consisting of static and dynamic fields. The static priority field is defined according to the sender application and contents of the message. This factor consists of five priority levels adopted by car-to-car (C2C) Communication Consortium. Dynamic factors such as speed of the vehicle, message utility, and message validity are used to schedule messages. Message utility calculates the transmission zone covered by a vehicle; that is, the smaller the zone, the higher the priority to send the message. The message validity factor takes into account serving deadline of messages; the message whose deadline is earliest is served first.

In [19], authors calculate network traffic density to adjust the size of the CW. The proposed scheme estimates

the channel conditions using packet transmission status. It maintains channel states in a vector to update the CW in order to improve throughput of a network. In [20], a performance analysis of IEEE 802.11p is presented under the exchange of small status messages known as beacons. Vehicles use these beacon messages for establishing cooperative awareness. The cooperative awareness is used by different applications increasing road safety and efficiency of ITS. The proposed scheme targets real-time vehicle control by enhancing the efficiency of IEEE 802.11p broadcasts. The size of CW is adaptive based on traffic density improving delay and reception probability. Authors present a self-adaptive CW based scheme in [21] to improve the efficiency of VANETs. The proposed scheme uses persistence factor (PF) for dynamic adjustment of CW size. Moreover, based on total local reception rate of past few seconds, a vehicle can adapt the CW dynamically. To ensure more deterministic dynamic range [1, CW(i)], the proposed MAC protocol implements Sliding Contention Window (SCW) adaptive to changing network conditions, bound by the predefined range. The messages are prioritized according to their urgency for timely propagation. The integration of contention based MAC and IEEE 802.11e Enhance Distributed Channel Access (EDCA) increases the communication reliability.

Early Deadline First (EDF) concept is also introduced by EL Korbi and Azouz Saidane in [11]; the authors develop a Markov chain-based analysis modeling the backoff process of the EDF policy. Moreover, the authors implement this scheme in MANETs to evaluate EDF policy over IEEE 802.11 in a multihop environment by considering two routing protocols: (1) proactive Destination Sequenced Distance Vector (DSDV) and (2) the reactive Ad Hoc On-Demand Distance Vector (AODV). However, the proposed scheme is developed for static environments. In [22], Dang et al. implement MAC protocols increasing efficiency and reliability of VANETs. Both the control and service channel intervals are proposed to carry safety messages to ensure the security of broadcast messages. It is also proposed to use control channel for the transmission of service packets to improve the service throughput. Table 1 provides the comparison of the existing schemes in terms of EDF, adjustment of CW, throughput, and number of backoffs.

3. A RSU-Based Efficient Channel Access Scheme for VANETs under High Traffic and Mobility

In the section, first we present our motivation and main contributions and then we discuss the RSU-based proposed scheme.

3.1. Motivation and Contributions. Our work is motivated by the observation that the existing schemes do not consider the fast changing topology of VANETs. Some of the schemes discussed in Section 2 are static in their nature; they either have deployed the conventional IEEE 802.11 or IEEE 802.11e EDCF mechanisms for channel access rendering the vehicles around RSU without timely provision of services or are reactive in their operations such as the calculation of the parameters (tables, collision rate) to adapt the CW size which is slow and complex process, which defeats the whole concept of real-time services for highly mobile vehicular traffic. Some of the mechanisms use conventional concepts of Mobile Ad Hoc Networks (MANETs) such as cluster head for cluster formation. Due to dynamic nature of vehicles in VANETs, routes/hops are frequently broken and established which results in overall degradation of network performance. Our proposed scheme follows the IEEE 802.11p standard which is particularly designed for WLANs and modifies it to support VANETs. In the proposed scheme, priority is assigned to each vehicle based on its deadline. Furthermore, we determine the priority of each vehicle dynamically by changing its CW size according to its deadline. The CWs for high speed vehicle having low Early Deadline First (EDF) are assigned small CW which adapts slowly as compared to the low speed vehicle having high EDF.

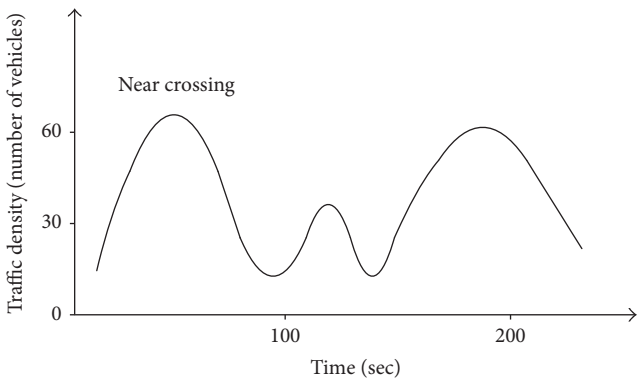

Figure 1: Traffic pattern near road crossing.

3.2. RSU-Based Proposed Scheme. The proposed scheme deals with the following parameters:

(1) speed of the vehicle,

(2) direction of the vehicle with respect to the RSU,

(3) emergency services.

The first two parameters are used to calculate the EDF value against each vehicle whereas the third parameter is used for tie breaking such as if multiple vehicles have the same value of EDF, then the vehicle having emergency service will be served first. However, the vehicle with small or low value of EDF is considered as high priority vehicle and the vehicle with high value of EDF is considered as low priority vehicle. The traffic density of vehicles generally follows the curve as shown in Figure 1. As it is clearly seen from the figure, traffic density is high near road crossings. Therefore, the vehicle's prioritization is highly required at this point. The working of the proposed scheme is as follows:

(1) The RSU selects the vehicle, which is moving towards it within its range.

(2) Time stamp of EDF is calculated for each vehicle, which is in the range of RSU. However, the EDF of

Table 1: Comparison of existing schemes.

Scheme	Applied on VANET	EDF	Adjustment of CW	Fast topology	Throughput calculated/not calculated	Backoffs calculated/not calculated
Alasmary and Zhuang Scheme [10]	Yes	No	Adjust CW sizes according to the three fixed CW ranges based on their speed and not based on the time they leave the range of the RSU	Yes	Average compared to proposed scheme	Average compared to proposed scheme
Wang et al. [12]	Yes	No	No	No	Not calculated	Not calculated
Choi et al. [13]	Yes	No	No	Yes	Not calculated	Not calculated
Suthaputehakun and Ganz [14]	Yes	No	It defines min and max CW size	No	Not calculated	Not calculated
Bohm and Jonsson [15]	Yes	No	No	No	Not calculated	Not calculated
Balon and Guo [16]	Yes	No	Local reception rate of the nodes	No	Not calculated	Not calculated
Rawat et al. [17]	Yes	No	It adapts the CW size considering the packet collision rate	No	Not calculated	Not calculated
Bouassida and Shawky [18]	Yes	Yes	No	No	Not calculated	Not calculated
Balador et al. [19]	Yes	No	Based on the network traffic density	No	Not calculated	Not calculated
Reinders et al. [20]	Yes	No	It adjusts the CW size based on traffic density	No	Not calculated	Not calculated

Table 1: Continued.

Scheme	Applied on VANET	EDF	Adjustment of CW	Fast topology	Throughput calculated/not calculated	Backoffs calculated/not calculated
Raut and Jeyakumar [21]	Yes	No	By sliding window with dynamic persistence factor (PF)	No	Not calculated	Not calculated
EL Korbi and Azouz Saidane Scheme [11]	No	Markov chain-based model	No	No	Not calculated	Not calculated
Dang et al. [22]	Yes	No	No	No	Scheme is evaluated for improving throughput	Not calculated
Proposed Scheme	Yes	Priority based scheme	This scheme assigns priority to vehicles based on their deadline in which they leave the range of RSU; the priorities are determined on real-time basis by changing CW size according to the deadlines in which the vehicles are going to leave the RSU range	Yes	Good as compared to EL Korbi and Azouz Saidane Scheme [11]	Good as compared to EL Korbi and Azouz Saidane Scheme [11]

a vehicle is calculated from its speed and geographic position as given below:

$$\text{EDF} = \frac{\text{Distance from RSU}}{\text{Speed of the Vehicle}}. \quad (1)$$

Each vehicle is assumed to know the service deadline of its request. This is reasonable because a GPS enabled vehicle can estimate the departure time based on its speed and geographic location. The high speed vehicle has high priority while it has low EDF. Therefore, it should be served first. Figure 2 shows traffic scheduling by RSUs.

(3) After a vehicle establishes connectivity with the RSU, its geographic location and radio range of RSU are calculated through beacon messages. The vehicle can estimate its departure time, which is its service deadline with the help of its driving speed and position information. Moreover, the vehicles are grouped according to their EDF.

(4) Vehicles with lowest values of EDF shall be served first because they will cross the RSU range first. The CW for such vehicles should adapt slowly as compared to other vehicles with high values of EDF. The CWs for high EDF vehicles change quickly (doubled). The vehicles with low EDF values are considered as high priority and vice versa for high EDF value vehicles. In conventional IEEE 802.11 and EDCF standards [3–9], whenever there is a collision the CW is always doubled to reduce number of collisions and it is set to minimum CW whenever there is a successful packet transmission irrespective of the conditions. Figure 3 shows the channel access mechanism of the proposed scheme. Moreover, Table 2 demonstrates the selected parameters for channel access in the proposed scheme.

(5) If multiple vehicles have the same value of EDF, then the one with single hop emergency message or small size data will be served first.

(6) If multiple vehicles with the same value of EDF are crossing the RSU, then they may generate a broadcast storm which causes packet collisions. This situation is mitigated through Master-Slave scheme [10]. A cluster is created based on the transmission radius of the very first vehicle in the first lane when vehicles stop at a crossing point. The cluster will comprise two types of vehicles: one is master and the rest are slaves. The master vehicle is the one having maximum signal strength that can cover the maximum transmission radius in the cluster and this aspect is decided by the RSU. In a cluster, only the master vehicle broadcasts messages to slave vehicles. If the slave vehicles in the cluster want to send specific messages, they send them to master vehicle for onwards transmission to other slave vehicles in a cluster or outside the cluster if necessary.

(7) If the RSU is not able to serve the fast moving vehicles due to their high speeds then it transfers the request to the next RSU depending on the direction of the vehicle. This may avoid dropping of the requests and system can manage to handle the high speed vehicles requests in the same way as mobile network does.

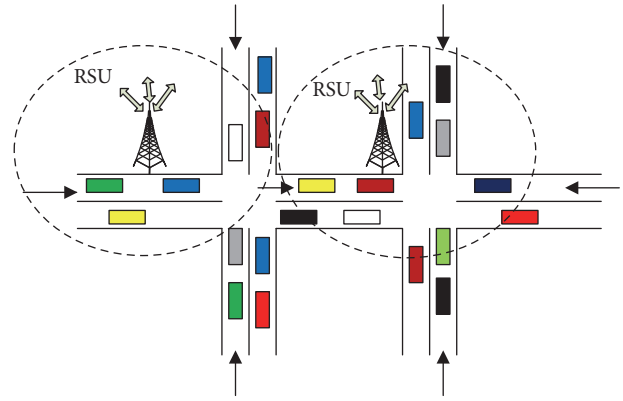

Figure 2: Traffic Scheduling by RSUs.

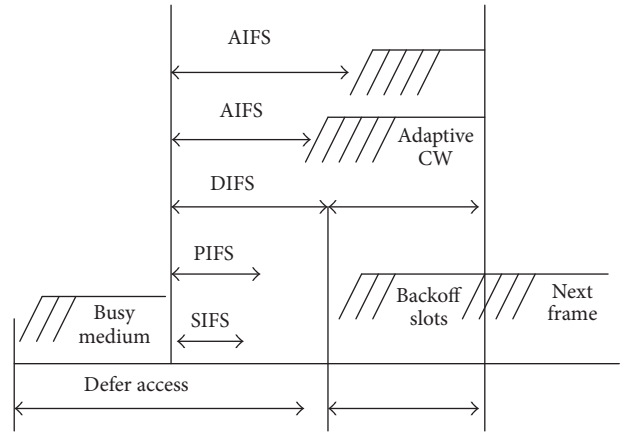

Figure 3: Channel access mechanism of the proposed scheme.

Algorithms 1 and 2 calculate the EDFs of the vehicles moving towards the RSU and new contention window, respectively. Algorithm 1 calculates the EDFs of moving vehicles as follows:

(1) For vehicle with least EDF (high priority), previous CW is increased linearly with the min limit of 3 and max limit of 7.

(2) For vehicles with EDF greater than least EDF (medium priority), a factor of 2 is added to the previous CW with the min limit of 7 and max limit of 15.

(3) For vehicle with EDF greater than medium priority (low priority), a factor of 2 is multiplied with the previous CW in min limit of 15 and max limit of 1023.

Algorithm 2 dynamically adapts the CWs of the vehicle which is present in the range of the RSU according to its EDF. It selects the vehicle as follows:

Table 2: Parameter used for channel access in proposed scheme.

Priority	EDF	CW change	CW min	CW max	AIFS
High	Low	Slow	3	7	SIFS + 2 ∗ Slot-time
Medium	Medium	Medium	7	15	SIFS + 2 ∗ Slot-time
Lowest	High	Fast	15	1023	SIFS + 7 ∗ Slot-time

Input: Vdc = Vehicle current distance, dp = Previous Distance, Rr = RSU Range
Output: Calculation of EDF
initialization;
begin
  while *Vehicle not crossingRSU* **do**
    read current distance of Vehicle
    if $Vdc < dp$ && $Vdc == Rr$ **then**
    $\text{EDF} = \frac{\text{Distance from RSU}}{\text{Speed of the Vehicle}}$;
    else
    go back to the beginning of then section;
  end
end

Algorithm 1: Calculation of EDF.

Input: VEDF = Vehicle EDF
VLEDF = Vehicle Least EDF
VMEDF = Vehicle Medium EDF
PCW = Previous CW.
Output: Calculation of New Contention Window
initialization;
begin
  if $VEDF < PCW$ **then**
    $PCW \uparrow R(3-7)$
  end
  if $VEDF \geq VLEDF$ **then**
    $2 + R(7-15)$
  else
    $2 * R(7-15)$
  end
end

Algorithm 2: Calculation of new contention window.

(1) if the current distance of the vehicle is less than its previous distance and the vehicle is in the range of the RSU,

(2) if current distance is greater than its previous distance and the vehicle is not within the range of the RSU.

4. Performance Analysis

We present and discuss our simulation parameters and performance analysis of the proposed scheme with respect to conventional scheme and schemes proposed in [10, 11]. Simulations are performed to evaluate the impact of mobility on IEEE 802.11p by using Network Simulator (NS-3) v. 3.6 [23].

Table 3: Simulation parameters.

Parameters	Values
Network area	500 ∗ 500 m
Propagation model	Two-ray ground
Number of vehicles	10, 30, 40, 63
Speed	8 km/h to 100 km/h
Simulation time	200 sec
Traffic type	CBR
Radio range	500 m
MAC layer	IEEE 802.11p
Packet size	512 bytes
Traffic load	Packet sent every 1 ms
Traffic lights	1
Number of Lanes	3 in each direction
SIFS time	25 microseconds

Moreover, we use Simulation of Urban MObility (SUMO) as mobility simulator [24]. It is an open source microscopic, multimodal traffic simulation package which includes net import and demand modeling component. The simulation environment implements a 3-lane highway scenario. Each lane has a length of 3 km and a width of 10 m. The speed of vehicles is variable from 8 km/h to 100 km/h, whereas each vehicle is using the IEEE 802.11p MAC protocol. Simulation time is set to 200 s for all the simulations results and the transmission range of each vehicle is set to 500 m. The packet length is set to be 512 bytes. The number of vehicles contending for the channel may vary from 10 to 63. The time slot parameter of IEEE 802.11p is set to be 10 sec, and SIFS time is 25 sec. Table 3 presents the simulation parameters.

Figure 4 shows the throughput analysis of the proposed scheme, the conventional scheme, and the schemes proposed in [10, 11]. It is clear from the figure that the throughput decreases as the number of vehicles increases. This is due to the reason that when the RSU serves more vehicles, the contention for channel increases, leading to more packet losses which consequently decreases the throughput. Hence, the proposed scheme performs better than the other schemes even with more number of vehicles.

Figure 5 presents the simulations analysis in terms of backoff rate. The number of backoffs increases as the number of vehicles increases. However, the proposed schemes in [10, 11] do not adapt CW according to the priority of vehicles. Therefore, they cause more backoffs compared to the proposed scheme.

Figure 6 presents performance comparison of RSU response times for 10, 30, 40, and 63 vehicles. It is clear from

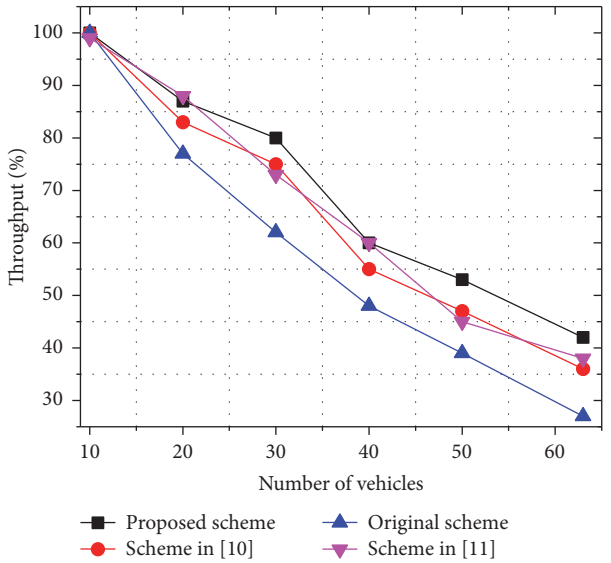

Figure 4: Throughput of vehicles in the range of the RSU.

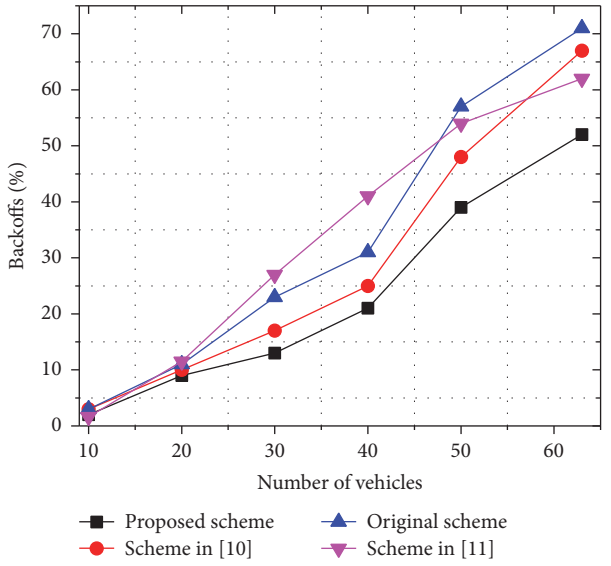

Figure 5: Backoff rate.

the figure that the response time of RSU in the proposed scheme is less compared to the conventional scheme as well as the schemes proposed in [10, 11] under the high traffic load scenarios. This is because the proposed scheme assigns priority to the high speed vehicles (less EDF) by assigning smallest CW and slowly varies it, whereas the schemes proposed in [10, 11] assign priority to the vehicles based on the deviation from the average speed of the neighbors. It means that vehicles with extremely high deviation (low and high speeds) from the average speed are assigned high priority compared to the vehicles with average speed which in this case varies between 50 km/h and 60 km/h. This is the reason of a sharp rise of response time at these average values. In our proposed scheme, we assign priorities to the vehicles on the basis of deviation d which is calculated as follows:

$$d = [V_i - V], \tag{2}$$

where V is the average speed and V_i is actual speed of a vehicle.

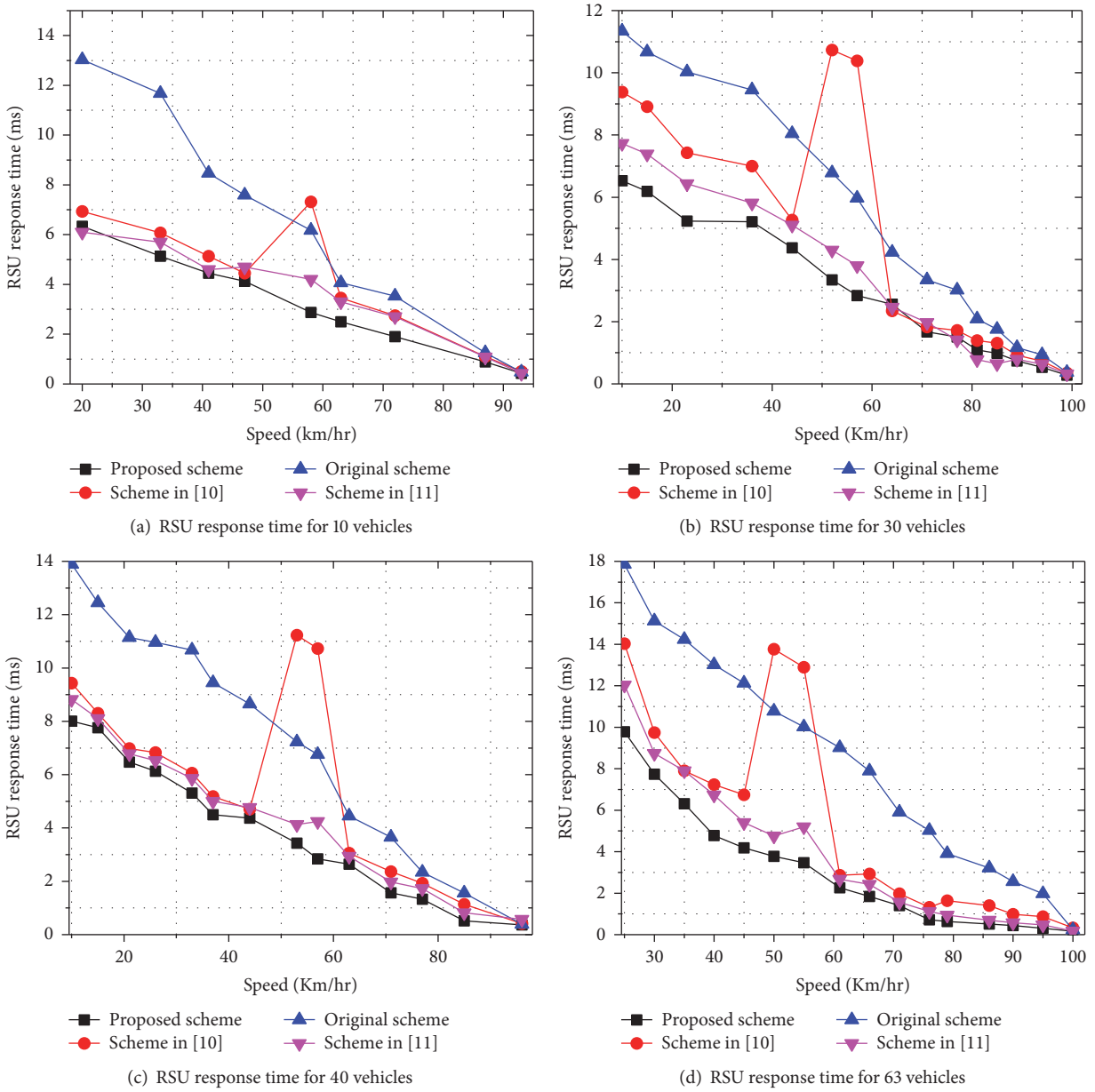

Figure 6: RSU response time for 10, 30, 40, and 63 vehicles.

Figure 7 shows the values of Jains fairness index plotted against the number of vehicles. Jains fairness index is calculated as follows:

$$f(x_1, x_2, x_3, \ldots, x_n) = \frac{\left(\sum_{i=1}^{n} x_i\right)^2}{n \sum_{i=1}^{n} \left(x_i\right)^2}, \quad (3)$$

where n represents the number of vehicles and x_i denotes the throughput for the ith connection. The result ranges from $1/n$ (worst case) to 1 (best case) and it is maximum when all the users receive the same allocation. Simulation shows poor Jain fairness index at low number of vehicles. This is because some vehicles have less connectivity than the others, whereas, the frequent fragmentation of the network is one of the major reasons for less connectivity of vehicles. Fairness index increases with the number of vehicles increasing or with more high traffic density.

5. Conclusion

In this paper we propose a RSU-based efficient channel access scheme for VANETs under high traffic and mobility conditions. It dynamically adapts the contention window of each vehicle based on its deadline of departure from the range of RSU. The contention window for higher priority packets is varied slowly and vice versa for lower priority ones. Simulations are performed to evaluate the mobility impact on the standard IEEE 802.11p. Our simulation results demonstrate

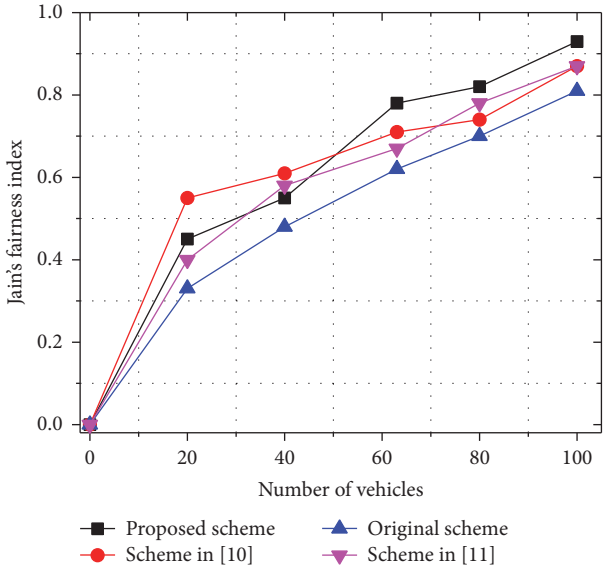

FIGURE 7: Jain's fairness index.

that the proposed scheme performs better than the conventional scheme and schemes proposed in [10, 11] in terms of throughput, backoff rate, RSU response time, and fairness.

Conflicts of Interest

The authors declare that there are no conflicts of interest regarding the publication of this paper.

References

[1] J.-M. Chung, M. Kim, Y.-S. Park, M. Choi, S. Lee, and H. S. Oh, "Time coordinated V2I communications and handover for WAVE networks," *IEEE Journal on Selected Areas in Communications*, vol. 29, no. 3, pp. 545–558, 2011.

[2] G. Karagiannis, O. Altintas, E. Ekici et al., "Vehicular networking: a survey and tutorial on requirements, architectures, challenges, standards and solutions," *IEEE Communications Surveys and Tutorials*, vol. 13, no. 4, pp. 584–616, 2011.

[3] B. P. Crow, I. Widjaja, J. G. Kim, and P. T. Sakai, "IEEE 802.11 wireless local area networks," *IEEE Communications Magazine*, vol. 35, no. 9, pp. 116–126, 1997.

[4] Y. Xiao, "IEEE 802.11 E: QoS provisioning at the MAC layer," *IEEE Wireless Communications*, vol. 11, no. 3, pp. 72–79, 2004.

[5] G. Bianchi, "Performance analysis of the IEEE 802.11 distributed coordination function," *IEEE Journal on Selected Areas in Communications*, vol. 18, no. 3, pp. 535–547, 2000.

[6] G. Bianchi, I. Tinnirello, and L. Scalia, "Understanding 802.11e contention-based prioritization mechanisms and their coexistence with legacy 802.11 stations," *IEEE Network*, vol. 19, no. 4, pp. 28–34, 2005.

[7] I. Inan, F. Keceli, and E. Ayanoglu, "Analysis of the 802.11e enhanced distributed channel access function," *IEEE Transactions on Communications*, vol. 57, no. 6, pp. 1753–1764, 2009.

[8] S. Mangold, S. Choi, G. R. Hiertz, O. Klein, and B. Walke, "Analysis of IEEE 802.11 e for QoS Support in Wireless LANs," *IEEE Wireless Communications*, vol. 10, no. 6, pp. 40–51, 2003.

[9] J. W. Robinson and T. S. Randhawa, "Saturation throughput analysis of IEEE 802.11e Enhanced distributed coordination function," *IEEE Journal on Selected Areas in Communications*, vol. 22, no. 5, pp. 917–928, 2004.

[10] W. Alasmary and W. Zhuang, "The Mobility Impact in IEEE 802.11p Infrastructureless Vehicular Networks," in *Proceedings of the 2010 IEEE Vehicular Technology Conference (VTC 2010-Fall)*, pp. 1–5, Ottawa, ON, Canada, September 2010.

[11] I. El Korbi and L. Azouz Saidane, "Performance evaluation of the Earliest Deadline First policy over ad hoc networks," *International Journal of Ad Hoc and Ubiquitous Computing*, vol. 10, no. 3, pp. 175–195, 2012.

[12] Y. Wang, A. Ahmed, B. Krishnamachari, and K. Psounis, "IEEE 802.11p performance evaluation and protocol enhancement," in *Proceedings of the IEEE International Conference on Vehicular Electronics and Safety (ICVES '08)*, pp. 317–322, IEEE, Columbus, Ohio, USA, September 2008.

[13] N. Choi, S. Choi, Y. Seok, T. Kwon, and Y. Choi, "A solicitation-based IEEE 802.11p MAC protocol for roadside to vehicular networks," in *Proceedings of the 2007 Mobile Networking for Vehicular Environments, MOVE*, pp. 91–96, May 2007.

[14] C. Suthaputehakun and A. Ganz, "Priority based inter-vehicle communication in vehicular ad-hoc networks using IEEE 802.11e," in *Proceedings of the 2007 IEEE 65th Vehicular Technology Conference (VTC '07)*, pp. 2595–2599, April 2007.

[15] A. Bohm and M. Jonsson, "Supporting real-time data traffic in safety-critical vehicle-to-infrastructure communication," in *Proceedings of the 2008 33rd IEEE Conference on Local Computer Networks (LCN '08)*, pp. 614–621, Montreal, QB, Canada, October 2008.

[16] N. Balon and J. Guo, "Increasing broadcast reliability in vehicular ad hoc networks," in *Proceedings of the VANET—Third ACM International Workshop on Vehicular Ad Hoc Networks*, pp. 104-105, Angeles, Calif, USA, September 2006.

[17] D. B. Rawat, D. C. Popescu, G. Yan, and S. Olariu, "Enhancing VANET performance by joint adaptation of transmission power and contention window size," *IEEE Transactions on Parallel and Distributed Systems*, vol. 22, no. 9, pp. 1528–1535, 2011.

[18] M. S. Bouassida and M. Shawky, "A cooperative congestion control approach within VANETs: formal verification and performance evaluation," *Eurasip Journal on Wireless Communications and Networking*, vol. 2010, Article ID 712525, 2010.

[19] A. Balador, C. T. Calafate, J. Cano, and P. Manzoni, "Congestion control for vehicular environments by adjusting IEEE 802.11 contention window size," in *Algorithms and Architectures for Parallel Processing*, vol. 8286 of *Lecture Notes in Computer Science*, pp. 259–266, Springer International Publishing, 2013.

[20] R. Reinders, M. Van Eenennaam, G. Karagiannis, and G. Heijenk, "Contention window analysis for beaconing in VANETs," in *Proceedings of the 7th International Wireless Communications and Mobile Computing Conference (IWCMC '11)*, pp. 1481–1487, July 2011.

[21] T. V. Raut and A. Jeyakumar, "Self-adaptive Cw size by sliding window with dynamic persistence factor," *Int. J. of Recent Trends in Engineering Technology*, vol. 11, no. 1, 2014.

[22] D. N. M. Dang, C. S. Hong, S. Lee, and E.-N. Huh, "An efficient and reliable MAC in VANETs," *IEEE Communications Letters*, vol. 18, no. 4, pp. 616–619, 2014.

[23] "Network Simulator(NS-3)," http://www.nsnam.org.

[24] M. Behrisch, L. Bieker, J. Erdmann, and D. Krajzewicz, "SUMO simulation of urban mobility: an overview," in *Proceedings of third International Conference on Advances in System Simulation (SIMUL '11)*, pp. 452–3969, 2011.

Hindawi
Mobile Information Systems
Volume 2017, Article ID 2861827, 15 pages
https://doi.org/10.1155/2017/2861827

Research Article

Empirical Study and Modeling of Vehicular Communications at Intersections in the 5 GHz Band

Seilendria A. Hadiwardoyo, Andrés Tomás, Enrique Hernández-Orallo, Carlos T. Calafate, Juan-Carlos Cano, and Pietro Manzoni

Department of Computer Engineering (DISCA), Universitat Politècnica de València, Camino de Vera, s/n, 46022 Valencia, Spain

Correspondence should be addressed to Seilendria A. Hadiwardoyo; seiha@upv.es

Received 22 December 2016; Accepted 13 March 2017; Published 23 March 2017

Academic Editor: Ilaria Thibault

Event warnings are critical in the context of ITS, being dependent on reliable and low-delay delivery of messages to nearby vehicles. One of the main challenges to address in this context is intersection management. Since buildings will severely hinder signals in the 5 GHz band, it becomes necessary to transmit at the exact moment a vehicle is at the center of an intersection to maximize delivery chances. However, GPS inaccuracy, among other problems, complicates the achievement of this goal. In this paper we study this problem by first analyzing different intersection types, studying the vehicular communications performance in each type of intersection through real scenario experiments. Obtained results show that intersection-related communications depend on the distances to the intersection and line-of-sight (LOS) conditions. Also, depending on the physical characteristics of intersections, the presented blockages introduce different degrees of hampering to message delivery. Based on the modeling of the different intersection types, we then study the expected success ratio when notifying events at intersections. In general, we find that effective propagation of messages at intersections is possible, even in urban canyons and despite GPS errors, as long as rooftop antennas are used to compensate for poor communication conditions.

1. Introduction

Intelligent Transportation System (ITS) is a basic element in future Smart Cities by addressing traffic-related issues. In particular, it is the combination of advanced Information and Communication Technology (ICT) systems and a better transportation infrastructure that paves the way for providing novel services in ITS environments [1]. ITS aims at making traffic more efficient, convenient, and safe [2], addressing noble goals like helping emergency services or changing the way we drive to reduce accidents, fuel consumption, and contaminant emissions. This will eventually minimize transportation problems such as congested roads, will promote road safety, and will in general help at making cities more sustainable [3].

A remarkable issue in ITS is its capability of providing safety applications. In fact, ITS solutions can conveniently provide warning notifications in emergency situations. For example, notifications about dangerous traffic conditions or about emergency breaking can be beneficial in providing a safer traffic flow for the drivers in a city [4]. According to [5], improving traffic safety is currently the second highest strategy priority in ITS and the first priority for future ITS solutions. Thus, we find that safety issues in the context of ITS are indeed essential.

As part of the ITS concept, communications between vehicles play an important role in distributing relevant information. This kind of communication can be enabled through vehicle-to-vehicle (V2V) communications which, combined with the ad hoc networking paradigm, gives rise to Vehicle Ad hoc Networks (VANETs) [4]. For more critical applications in the context of ITS, like real-time safety information, the diffusion of messages should be reliable and time-bounded [6]. Another consideration to bear in mind in the critical safety application domain is the delay of the messaging itself. The performance of distributing the message through V2V is expected to have a low transmission delay, though with a limited reliability. So, vehicles that belong to a certain V2V network facing a particular emergency situation should be alarmed as soon as possible. Otherwise, if the delay is too

high, the relevance of the message would be reduced, and it would probably expire [7].

Still in the same context, to have such critical communications, message dissemination should be as effective as possible. In the literature, several dissemination schemes were proposed in order to maximize the effectiveness of message dissemination. An example of a work that proposes reducing the warning message notification time while avoiding the broadcast storm problem was presented in [8]. However, it should be kept in mind that the dissemination process is affected by key factors such as the density of vehicles and the roadmap; in [9] authors address this challenge by proposing a system that adapts to high-density vehicular environments by considering the critical handling of intersections. Taking as reference the survey on this topic by Sanguesa et al. [10], we find that most of the cited schemes rely on GPS information and many of them on intersection-awareness to maximize event dissemination. Thus, the accuracy of the geolocation system becomes critical in the safety dissemination process, especially in urban scenarios to allow determining whether a vehicle is near or even in the middle of the intersection.

In this paper, we perform an empirical study of vehicular communication effectiveness at intersections in the 5 GHz band. To this purpose, we select different types of intersections available in the city of Valencia (Spain) and then perform actual field tests using vehicles to determine the communication restrictions imposed by the different intersections. In addition, based on the empirical results obtained, we model the packet delivery probabilities at different distances to the center of each particular intersection to determine the expected success ratio when delivering event-based messages and to allow integrating the results here presented in simulation platforms.

The paper is organized as follows: in the next section, we provide an overview of the main related works regarding intersection-dependent communications in V2V environments. In Section 3 we describe the methodology adopted for our work, detailing the different software and hardware elements involved. Then, in Section 4, we provide details about the different intersections chosen for our experiments. Experimental results are then presented and discussed in Section 5, followed by modeling of these results in Section 6. The models derived and then used to study the event notification effectiveness at intersections are presented in Section 8. Finally, in Section 9 we conclude this paper and refer to future works.

2. Related Works

In the literature, we can find several works in the scope of safety applications using V2V. A VANET-based emergency vehicle warning system was proposed in [24]. The system was tested in traffic environments including emergency vehicles and traffic lights. The system warns when an emergency vehicle is approaching. Another work, called Intersection Collision Warning, studies warning message dissemination using smartphones with built-in GPS; in particular, it uses the WiFi networks in smartphones to retrieve safety-related information like location, moving direction, and velocity [25]. Other works, like [26], proposed a safety-related Android application to inform nearby vehicles when administrative vehicles, like ambulances, police cars, and fire brigades, are approaching.

Focusing on the issue of signal obstruction, several works have studied its impact on the packet delivery ratio in VANET environments. The work by Böhm et al. [11] investigated the impact of the loss of line-of-sight (LOS) in terms of V2V communication impact, finding that limited LOS between vehicles transmitting and receiving the packets can still enable communications. The researchers in [12] additionally found that obstructing vehicles blocking the LOS significantly attenuate the signal; they also studied the packet delivery ratio under different scenarios, including parking lot areas or urban scenarios under both LOS and non-LOS. Sommer et al. [13] have modeled the IEEE 802.11p/DSRC radio shadowing in urban environments. Their model can estimate the signal attenuation of the wireless radio transmission with buildings as obstacles. The same researchers experimented the two-ray path loss model in both real and simulated environments [14]. In a later work [15], they proposed alternative solutions for signal shadowing caused by neighboring vehicles and buildings based on dynamic beaconing and tested their approach in a simulated environment. Other interesting related works include the deployment of RSUs (Road Side Units) in the vehicular environment [16, 17], studying how urban scenarios with buildings and vegetation affect V2I (Vehicle to Infrastructure) communications.

Regarding the issue of intersection management in the scope of the VANET message transmission process, there have been different proposals in recent years, especially at the network layer. In particular, these protocols used intersection locations as a factor to include within the packet routing strategy. The work by Chou et al. [27] proposed an intersection-based routing protocol that accounts for both the direction of packet transfers and the vehicle moving direction. Through simulation, the research investigated the effect of the number of vehicles on the delivery probability. Geographical conditions can also be taken as an approach for routing messages. In particular, the work by Saleet et al. [28] considers road layouts with intersections for routing. Later, Acarman et al. [29] showed how message routing can also be done by selecting intersections as points of relay using commercial navigation map data and having the connectivity information of road IDs. Similarly, other research works like [30] take advantage of intersections for forwarding messages. It focuses on a large scale urban VANET where the vehicles at intersections are used as virtual gateways that will gather the packets that must be forwarded to all passing vehicles [30].

Focusing instead on the different types of intersection, these can be characterized by the degree of obstruction: whether it is blocked by a building, blocked by plants, or blocked by cars themselves. The work by Schumacher et al. [18] finds that, in an urban scenario where there are buildings blocking the line-of-sight, communications are possible for distances ranging from 85 m to 115 m. By using the 5.9 GHz V2V communications under non-line-of-sight, their results showed that not only do buildings affect the communication but also the width of the street representing

the largest street intersection has also a significant impact on the delivery probability. Another research work [19] investigated the effects of vegetation on the performance of V2V communications at intersections. Tests were based on the 5.9 GHz communication band under non-line-of-sight conditions in a rural environment having different types of vegetation for the different seasons; results showed that the packet delivery ratio clearly depended on the type of vegetation and season. When transmitting a message between vehicles, a third vehicle located at the intersection would also affect communications, and the effect of cochannel interference will have an impact under both line-of-sight (open space) and non-line-of-sight (with buildings as obstructions) conditions. The work in [20] addressed this issue through measurements in the 5.9 GHz band. Experiments showed that a single vehicle would interfere and decrease the delivery ratio, no matter if the vehicle is placed near the receiver, near the sender, or between the sender and the receiver.

Finally, Table 1 summarizes the aforementioned related works for the sake of clarity. We categorized previous works taking relevant experiment characteristics into consideration, like the environment details and the performance metrics used.

In this work, our aim is to study transmission effectiveness on different types of intersections and at different distances. Referring again to Table 1, our work differs from other related works in terms of the frequency band and the performance metrics used, as well as the variety of intersections tested. Also, we present heat maps to characterize transmission effectiveness by showing the locations of the sender when having packets successfully delivered in each scenario. Based on our findings, we develop channel models that are applicable to different simulation environments. In addition, by using our models, we then perform an analytic study of the expected success ratio when attempting to deliver event-related messages at intersections for different degrees of positioning accuracy.

3. Methodology

In this section, we describe the methodology of the experiments performed. The goal is to measure the packet delivery ratio depending on the distance to the center of the intersection for different types of intersections and antenna locations. The expected results in different types of intersection will then be modeled. Later, in Section 7, we will also discuss the applicability of the obtained model and discuss its applicability in comparison with other path loss models.

3.1. General Overview. Our experimental work requires the utilization of appropriate hardware/software to measure the packet delivery ratio and also of a proper data analysis methodology, to process the gathered data after experiments are completed.

Two devices are used in the experiments. The first one is the *GRCBox* [23], which is our on-board unit providing fully functional V2V communications. This GRCBox is equipped with an antenna that will allow VANET communications in the 5.8 GHz band. The transmitting antennas have a 5 dBi gain and 200 mW transmission power. Packet transmission tests using this device will consider two alternative positions for the antenna. In one case we will put the antenna inside the vehicle, specifically on the dashboard. The other alternative considered will be putting the antenna on the rooftop of the vehicle. These variations will allow us to achieve new findings regarding the effect of antenna locations, expecting that having the antenna on the rooftop will provide a better transmission quality than having it on the dashboard.

Another device used in this experiment is an Android mobile phone. Taking into account the trends of using smartphones for vehicular communications and ITS-related researches, deploying an Android mobile phone can be an alternative solution to exploiting the cost of high-end ITS equipment for research purposes [31–33]. The Android phone is equipped with a custom application (the *Android tool*). This Android tool will allow performing controlled experiments in real environments by generating messages resembling those associated with the European (ETSI) standard, particularly the Decentralized Environmental Notification Messages (DENM) [34].

For the experiment itself, which includes real moving vehicles, at least two vehicles are needed: one acting as data sender and the other one acting as a data receiver. Regarding the positioning of the vehicles, the one acting as a data receiver will be static and stopped a few meters away from the center of the intersection, representing a vehicle stop at a semaphore or *stop* sign. The other vehicle, acting as a data sender, will be moving along a different street, crossing a common intersection.

Once the sender is moving and the receiver starts to receive packets, the developed test tool will record the location of both sender and receiver vehicles, which will then be saved in a log file stored on the Android device. After we record the location of the sender in the log file, our data analysis consists of calculating the packet delivery ratio along with the distance between sender and receiver. Specifically, by obtaining the packet delivery ratio for each intersection at different distances, we can draw conclusions on how intersection characteristics will impact message dissemination in vehicular scenarios. In addition, the different intersection types can be modeled, and further analysis can be done based on the obtained models.

3.2. GRCBox Overview. To enable V2V communications, we require a device that provides ad hoc network connectivity in the 5.9 GHz band. Since we use Android devices to launch applications, an option would be to enable ad hoc network connectivity in this device. However, in order to do that, a rooted Android phone is required, thus not being very practical for end users. In addition, the communication range achieved would be quite limited. We provide an alternative solution called GRCBox [23], a solution capable of providing ad hoc communications without having to root smartphones. GRCBox is a multi-interface low-cost connectivity device based on Raspberry Pi. Using the GRCBox, V2X communications are supported, and full integration with smartphones is achieved.

Table 1: Comparison of related works.

Related works	Frequency band used	Experiment type	Environment used	Types of blockages	Street details	Performance metrics
Böhm et al., 2010 [11]	5.9 GHz	Real world	Urban, highway, rural	Vegetation, buildings, parked vehicles	Not specified	Distance versus packet reception ratio
Meireles et al., 2010 [12]	5.85–5.925 GHz, 2.412 GHz	Real world	Urban and parking lot	Buildings, trees, vehicles (truck, van)	Various lanes street	Distance versus received signal strength indicator, distance versus packet delivery ratio
Sommer et al., 2011 [13]	5.89 GHz	Real world and simulation	Urban and rural	Residential and commercial buildings	Intersection	Distance versus received signal strength, length of intersection versus received signal strength, index versus received signal strength
Sommer et al., 2012 [14]	5.89 GHz	Real world and simulation	Urban and rural	Vehicles	One-lane and two-lane street	Received signal strength versus distance
Sommer et al., 2015 [15]	5.89 GHz	Simulation	Highway and suburban	Building and vehicles	Two-lane street	Empirical cumulative density function versus beacon interval, channel busy ratio, time after encounter versus beacon interval
Lin et al., 2012 [16]	5.9 GHz	Real world and field trial	Not specified	Cochannel interference	Not specified	Distance versus packet loss, distance versus latency
Gozalvez et al., 2012 [17]	5.895–5.905 GHz	Real world	Urban and highway	Buildings, trees, vehicles	Various lanes street	Distance versus packet delivery ratio
Schumacher et al., 2012 [18]	5.9 GHz	Real world	Urban	Buildings	Intersection	Distance versus signal power, distance versus packet delivery ratio
Tchouankem et al., 2013 [19]	5.9 GHz	Real world and simulation	Rural	Vegetations	Intersection	Distance versus signal power, distance versus packet delivery ratio
Tchouankem and Lorenzen, 2015 [20]	5.9 GHz	Real world	Urban and rural	Buildings and vehicle	Intersection	Distance versus signal power, distance versus packet delivery ratio

Table 1: Continued.

Related works	Frequency band used	Experiment type	Environment used	Types of blockages	Street details	Performance metrics
Barcelos et al., 2014 [21]	5.9 GHz	Real world	Urban/rural (campus environment)	Buildings	Two-lane street	Distance versus average packet loss, distance versus average latency, distance versus average delay, distance versus bitrate
Viriyasitavat et al., 2016 [22]	2.4 GHz	Real world and simulation	Urban (open environment)	Vehicle	One-lane street	Distance versus packet delivery ratio, time versus penetration distance, time versus reachability
Our work	5.8 GHz	Real world	Rural, urban, mixed	Buildings, vegetations	Intersection	Distance versus packet delivery ratio heat maps for packet delivery

A Raspberry Pi 2 device model B1 is the main hardware of our GRCBox, a single board computer that has the size of a credit-card and it costs only 35 USD. This device has enough CPU power to perform low-scale network routing. A Raspbian distribution based on Debian is installed in this device. This Raspbian distribution supports the current networking hardware while avoiding common problems of other embedded operating systems.

Each GRCBox is equipped with several network interfaces: one inner interface acting as an Access Point for the users, allowing them to connect to the GRCBox using smartphones supporting WiFi communications in the 2.4 GHz band. The outer interface offers vehicular communications, where it connects to a vehicular network in the 5.8 GHz band. In addition, one can add other network interfaces that connect to the Internet. For instance, one network interface can connect to a WiFi Access Point, and yet another can be used to connect to a 4G cellular base station. Figure 1 shows a descriptive diagram of our GRCBox connectivity features.

Several services are provided by the GRCBox. GRCBox's inner interface acts as a soft-AP (Access Point) for smartphones. Once these smartphones are connected to the GRCBox, they can access the services that run on the external networks. Since every connection is forwarded by the GRCBox, any application needing to use an available interface that differs from the default one (providing Internet connectivity) must notify the GRCBox. These steps require rules that are defined by rule type, interface name, protocol, source port, source address, destination port, and destination address.

In this work, we use the GRCBox at intersections to forward packets that are produced by the Android application at the user's side and placed on one of the vehicles, to the packet destination, which is the Android application placed

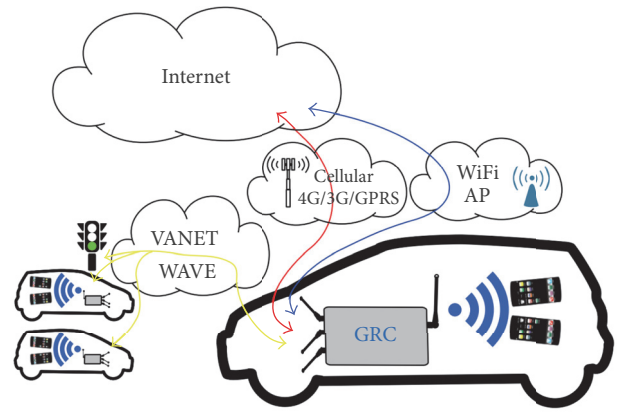

Figure 1: GRCBox Hardware module connected to a VANET with three different nodes [23].

at the receiver vehicle. Thus, both GRCBoxes act as the entry gate of packets traveling in the VANET and to be delivered to the GRCBox-aware application running on the smartphones. In our case, the packets are forwarded in a broadcast manner. Thus, appropriate rules are defined before transmission starts to match the target ports and interfaces.

Regarding the configuration of the GRCBox, thanks to our specific application, which will be explained in Section 3.3, the user does not need to set up the rules, as it will be done automatically once the application is launched. In terms of hardware, we need to configure the interfaces to indicate whether they are inner or outer interfaces. Since we only need the VANET communication, only two interfaces are needed. One interface (inner) acts as an Access Point (AP) for mobile devices. Another interface (outer) will

create a VANET with other GRCBoxes located within nearby vehicles. In this case, a device capable of transmitting in the 5.8 GHz band is needed for the outer interface.

3.3. Android Tool. We have built a specific tool for measuring the data delivery ratio in the target scenarios. The tool is actually an Android-based application that is GRCBox-aware. The Android application contains libraries and plugins able to connect to the GRCBox module so that, at the user side, one does not need to configure the connection to the GRCBox's outer interface. Hence, once the Android smartphone connects to the Access Point (AP) of the GRCBox (in this case GRCBox's inner interface), it would instantly be connected to the whole GRCBox environment and the VANET without further settings. Also, based on its functionality, we have different instances running at the sender and at the receiver ends.

At first, the application will check if it is connected to the GRCBox device on the sender's side. Also, the user can input the log file name, the packet transmission rate, and the size of the packet. In this case, we have chosen the sending parameters similar to those typical of CAM/DENM messages [34, 35], having a size of about 300 bytes, selecting a packet rate of 30 packets per second to allow quick gathering of large amounts of data. Also notice that since packets are being broadcasted, the transmission rate is limited to 6 Mbps. At the receiver's side, GRCBox connectivity is also tested, and the user can introduce the log file name and select when to start gathering data. The transmission of packets is started when, at the sender's end, the user presses the start button, triggering the transmission of a packet train at the defined rate and packet size and using the broadcast mode. Similarly, the transmission stops as the user stops the application. This will cause the application to automatically store the whole log file in a local file at both sender and receiver ends. In a nutshell, our Android-based application is used to define parameters such as data rate, packet size, and log file name. It starts the sending process upon receiving the corresponding user command; then, when the user stops the application, the log file is automatically stored.

3.4. Data Analysis. The data collected is saved in a log file located in the Android device's storage. This log file contains all the data required to analyze the packet delivery ratio at different distances. For this purpose, we are interested in comparing the geographic information of both endpoints, and so the log file contains the coordinates of the sender and the receiver in terms of latitude and longitude (flat terrain is assumed). Based on this geopositioning information, we then calculated the distance in meters between the vehicle localization and the center of the intersection, where the sending vehicle passes through as part of its designated trajectory.

The distance is calculated with the help of GeographicLib [36], a tool providing a straightforward calculation of distance based on latitudes and longitudes. From each endpoint, in this case, the sender and the receiver, we analyzed the log file that is stored on both sender and receiver sides.

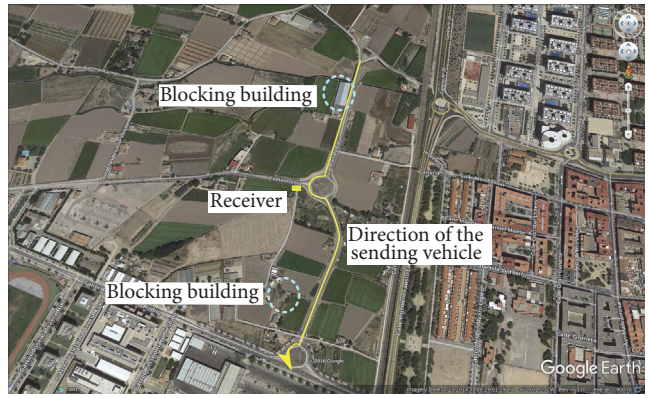

Figure 2: Location and the trajectory for Scenario 1 (open).

As for the delivery ratio, we need to compare the log files containing packets sent at the sender side and the log files containing packets received at the receiver side. This can also be calculated by referring to the geoposition information provided by both sides.

4. Selection of Target Intersections

For our experiments, we selected three different types of intersections, each one with different characteristics. In particular, the types of intersections were chosen to obtain different degrees of obstruction. The geographical location of each intersection is shown in Figures 2, 4, and 6. The yellow line with an arrow indicates the trajectory and the direction of the sending vehicle, while the yellow point indicates the location of the receiving vehicle (static). We now proceed to provide more details about each of them.

4.1. Intersection 1 (Open Scenario). The first intersection selected is an open space. It was taken in a low populated area in the outskirts of the city of Valencia (Latitude 39.483920, Longitude −0.333793). In this intersection, no relevant signal blockages are present. In fact, Figure 2 shows that the only blocking structures are two buildings, one south of the roundabout and the other one north. Thus, the line-of-sight is not blocked along the trajectories of the vehicle, meaning that the degree of obstruction is minimal. As shown in Figure 3(a), the receiving vehicle is located near the intersection, being surrounded by grass fields and facing no significant signal blockage.

4.2. Intersection 2 (Buildings Scenario). The second intersection selected is in a residential block, which is located in a crowded and dense area of the city (latitude 39.473695, longitude −0.332307). In this intersection, buildings are present as blockages to the line-of-sight, meaning that the degree of obstruction is nearly maximum. Based on the aerial view shown in Figure 4, we can see that the environment consists of a dense neighborhood, without additional urban elements separating them except streets themselves, meaning that an urban canyon is formed. In Figure 5(a) we can see that the chosen intersection is surrounded by at least two-floor buildings. So, from the perspective of the receiving vehicle,

(a) Outside View (b) Inside View

Figure 3: View of the vehicle parked at Intersection 1.

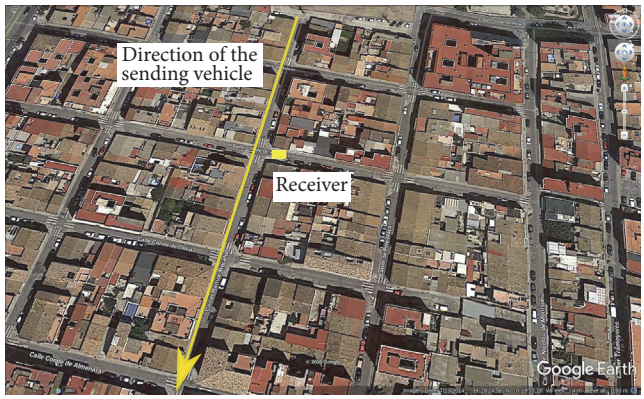

Figure 4: Location and the trajectory for Scenario 2 (buildings).

the line-of-sight is quite limited as the furthest view that one can glimpse from inside the mentioned vehicle is of, at most, 20 meters. By defining this type of intersection, we expect that the transmission of packets in this location would be the worst case scenario.

4.3. Intersection 3 (Trees Scenario). The third selected intersection is a mix of the previous two scenarios, as the line-of-sight is blocked by either buildings or trees. The intersection lies in a residential area near a university campus (latitude 39.473848, longitude −0.341330), and the degree of obstruction can be considered moderate. Figure 6 shows that this kind of intersection has some buildings in the surroundings, but also open space and vegetation along the trajectory. A mix between these characteristics causes communication in this kind of environment to produce interesting results as the line-of-sight characteristics are variable, being that sometimes it is blocked by a building or tree, while at other times no obstacle will block sight. Figure 7(a) presents the real view of the intersection. As shown, the receiving vehicle is surrounded by trees and, within meters, there is an open field. However, the street itself is located in a residential area plenty of tall buildings.

5. Experimental Results

We have done real experiments with vehicles to gather the location (coordinates) of the vehicles when packets are successfully delivered at each intersection. We also gathered data when the antennas are located either inside the vehicle on the dashboard or on the rooftop of the vehicles. The data was gathered from a set of five vehicle runs at each intersection, and the measured coordinates are then validated using real maps.

5.1. Results for Intersection 1. Figure 8(a) shows the percentage of messages received as a heat map for the first intersection, which has the lowest degree of obstruction, based on the locations of the sender associated with successful packet delivery. In this experiment, the two antennas involved were located in the vehicles' dashboard. As expected, the packets can be delivered successfully having as source nearly any position along the vehicle trajectory. The only gap detected occurs due to the blocking caused by the two available buildings. However, the delivery ratio is much higher when it is at the center of the intersection and gets lower as the vehicle moves away until the maximum tested distance (about 300 meters).

Figure 8(b) presents the results when the antenna is located on the rooftop instead. We can now observe that the point density is higher and that there are no gaps. In fact, the impact of physical obstructions is still relevant, but it is merely limited to a slight reduction of the packet delivery ratio.

5.2. Results for Intersection 2. This second intersection is quite narrow, having tall buildings on all sides that create an urban canyon. Figure 8(c) shows the locations associated with successful transmission of the packets when the antenna is located in the dashboard. We can see that successful transmissions are basically restricted to a range of just one block (about 50 meters), again experiencing a descending delivery ratio when moving away from the center of the intersection.

If instead the antenna is located on the rooftop, Figure 8(d) shows results similar to those in the previous figure, although now the overall delivery ratio increases, reaching up to two blocks away from the intersection (about 100 meters) while mostly maintaining an acceptable delivery ratio.

5.3. Results for Intersection 3. Since this third type of intersection presents a moderate degree of obstruction, the results in terms of radio range should be in between the results for the first and second types of intersections. Figure 8(e) shows that the locations associated with a successful transmission

(a) Outside View (b) Inside View

Figure 5: View of the vehicle parked at Intersection 2.

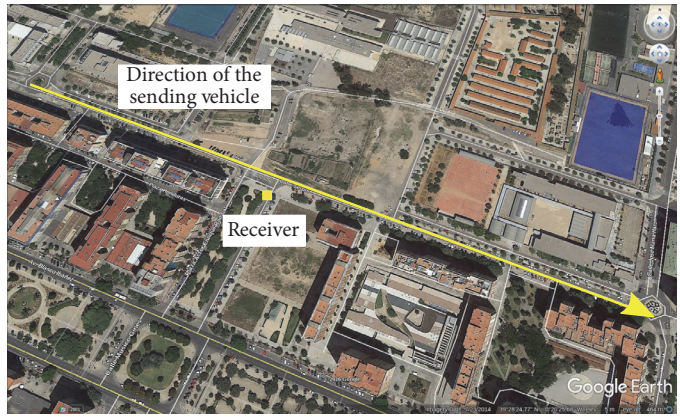

Figure 6: Location and the trajectory for Scenario 3 (trees).

indeed reach greater distances compared to the second type of intersection, having values resembling more the first intersection. This occurs since the obstacle closer to the vehicle in this situation is mainly vegetation, which does not negatively impact communications the same way as buildings; in addition, the streets are wider than in the second scenario.

When locating the antenna on the rooftop, results become much better. Now, although we cannot associate the entire vehicle path with good transmission conditions, the results of Figure 8(f) clearly show that high delivery ratios can be maintained up to about 100/150 meters. Again, the delivery ratio near the intersection is significantly high, experiencing a constant drop as we move away.

6. Intersection Modeling

Based on the results obtained in our experiments, we now proceed to detail how the different intersections were modeled. Our purpose is to obtain a generic model that allows integrating the different behaviors observed in simulation tools, as well as analytically studying the effectiveness of event-related message delivery at intersections.

6.1. Modeling Procedure. In order to model the different intersections, our procedure was the following: first, we obtained the number of packet transmissions and receptions for each position registered; second, we determined the packet delivery ratio value associated with each distance range; finally, we performed a curve fitting process to derive optimal parameters.

In detail, the results of the first step of the experiment consist of a list of coordinates (i.e., latitudes and longitudes) stored at the sender, with another similar list stored at the receiver's side. The sender coordinates are the sender's actual location when a packet is sent. Logically, the list at the sender side has more entries than the one at the receiver side as several packets get lost. So, we must compare the difference between these two lists of coordinates. A packet is successfully received if an entry (coordinate) at the sender's list is also present in the receiver's list. The coordinate is then translated into the distance by considering the coordinates relative to the center of the intersection using the *haversine* formula implemented in the GeographicLib library.

The outcome of the first step is then grouped into small intervals, with the interval width equal to 5 meters. The delivery ratio derived for the different intervals is then plotted using a bar chart, thereby resembling a histogram (although it is not so in a strict sense). By following the same procedure for the different antenna locations (rooftop versus dashboard), we can then obtain a comparative chart for the target intersection that allows checking packet delivery ratio in both cases.

Once these distributions are calculated for the three types of intersection and for both antenna locations, we proceeded to find the best fit for our data. The curve fitting was done using the nonlinear least-squares Marquardt-Levenberg algorithm (implemented in the GNUPLOT software) to derive a

(a) Outside View (b) Inside View

Figure 7: View of the vehicle parked at Intersection 3.

general model for the curve, determining which function is more adequate for our purposes, as well as the best parameter values for each distribution.

6.2. Fitting Results. For each curve, we tried to find a common model that would be suitable for both antenna positions (dashboard or rooftop) and the different type of intersections (open, building, and trees). Our intention was that only one parameter would vary from one scenario to another, allowing to seamlessly model different types of intersections having variable degrees of radio visibility. After evaluating several fitting functions (polynomial, power) for the different types of intersection and antenna locations, the best fitting was obtained using a Gaussian function:

$$f(x) = ae^{-(x-b)^2/2c^2}. \quad (1)$$

Notice that variables x, a, b, and c are generic variables, meaning that (1) will be adapted to our specific requirements. In particular, we set x as the distance from the intersection and fix the probability of reception to one exactly at the intersection (distance zero), so a is one and b is zero. Thus, the only parameter to fit is c, that is, the *standard deviation*. So, finally we have the following expression:

$$f(x) = e^{-x^2/2c^2}. \quad (2)$$

This exponential function computes the delivery ratio for a particular distance x. As the distance grows, this probability asymptotically becomes 0. The value of the constant c (or standard deviation σ) will depend on the scenario and the antenna position and reflects the variation or dispersion of the data values.

The resulting bar charts and fitting results are shown in Figures 9(a), 9(b), and 9(c). If we take a look at the experimental results for Intersection 1 (see Figure 9(a)), we can quickly notice that there is a significant difference between the delivery ratio for the *dashboard* and *rooftop* location cases. The curve fit for the *dashboard* antenna location shows that, for low distances, the delivery ratio is still comparable to the one from the *rooftop* fit. After a distance of about 20 meters from the intersection, the bars show a quick attenuation. Also, we observe that it loses contact after about 200 meters. We can observe how, when the distance is of about 120 meters, the delivery ratio suddenly drops, being followed by a moderate increase. This is an effect of the buildings present in the environment, as we can see in an aerial view of the street shown in Figure 2. Concerning the delivery ratio for the rooftop scenario, high delivery values are sustained for a distance up to 70 meters, after which they experience a 20% drop. In this same scenario for the *dashboard* case, the drop ratio is significantly higher (50%). Thus, we can conclude that antenna location has a very significant impact on packet delivery success.

Concerning the second intersection, the bar chart shown in Figure 9(b) clearly shows a significant difference compared to the previous one. In fact, the distance range is now quite reduced, with the fact that the packet delivery ratio drops to only 35% in about 40 meters (for the "dashboard" antenna position). Beyond 50 meters, the delivery ratio becomes near zero. If we focus now on the curve fit for the rooftop scenario, we find that differences towards the dashboard case are quite clear, similarly to what occurred for Intersection 1. However, with respect to that first intersection, we now see that, at a distance of 50 meters, the packet delivery ratio for the rooftop is nearly 0.8, while for the dashboard it is only 0.3, both values much lower than those measured in Intersection 1. This is why we can categorize this second intersection as an urban canyon, which is a worst case scenario associated with the maximum degree of obstruction.

Regarding the results for Intersection 3, Figure 9(c) shows that when the antenna is located in the dashboard, there is a loss of radio connectivity after about 70 meters. Instead, when the antenna is on the rooftop, contact is maintained beyond 250 meters, a much greater distance. Compared to the two previous intersections, the fittings in this scenario are indeed a situation in between intersections 1 and 2.

Overall, we consider that the obtained results are quite reasonable by considering that our experiments were made in scenarios where no interference is hindering our communications band, meaning that the channel only experiences the effect of additive white Gaussian noise. In such situation, the fitting corresponds to a standard AWGN channel model.

We now focus in detail on the outcome of fitting results and the corresponding fitting errors. Notice that (2) introduced parameter c, the standard deviation of the Gaussian function, which allows adapting the fitting curve to each type of intersection and antenna location. In Table 2, we now detail the values of this parameter for each case. It is interesting to observe that this parameter decreases for lower radio ranges at intersections, being directly related to the packet delivery ratio. In fact, the higher the parameter, the higher the packet delivery ratio for a certain distance towards the intersection.

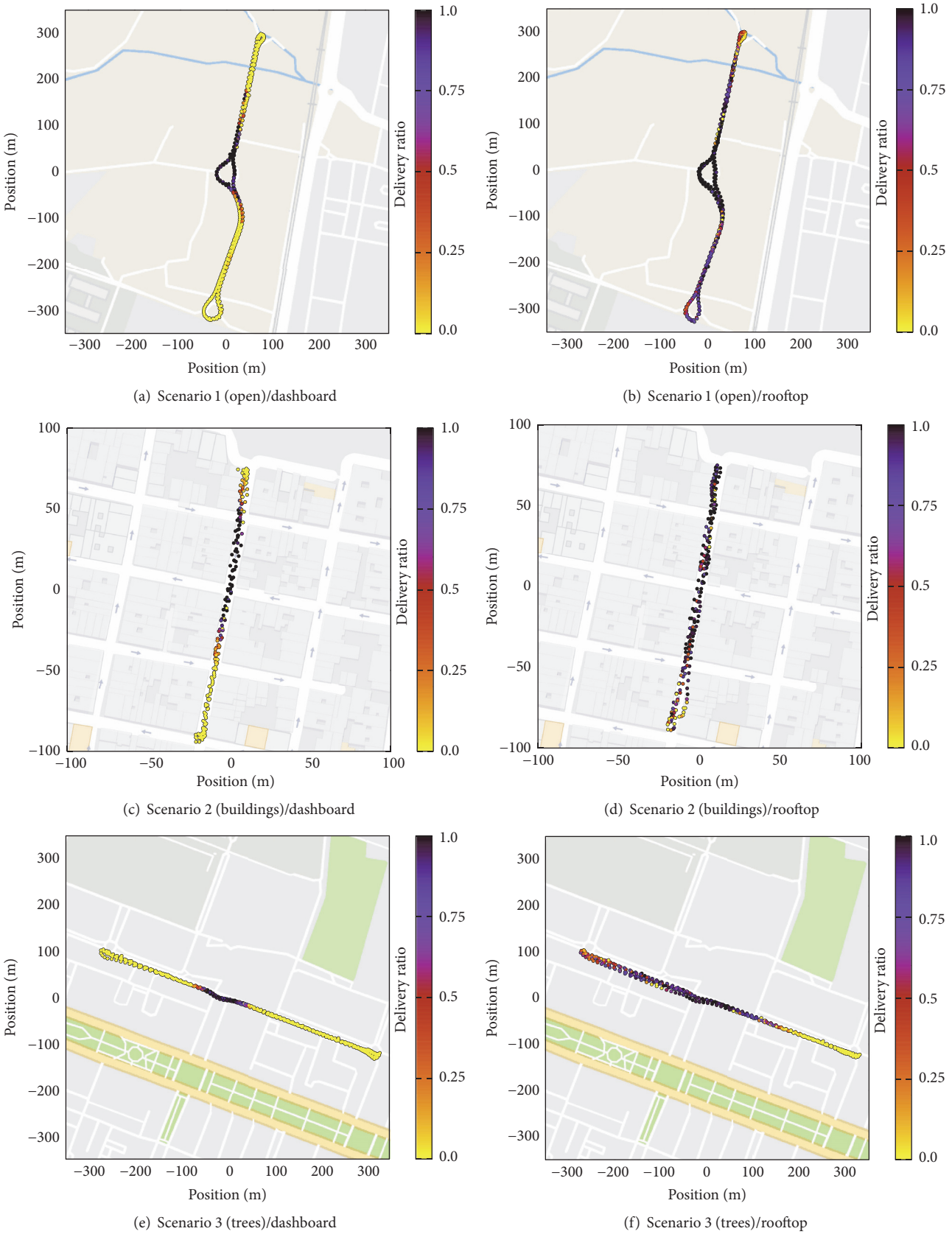

(a) Scenario 1 (open)/dashboard

(b) Scenario 1 (open)/rooftop

(c) Scenario 2 (buildings)/dashboard

(d) Scenario 2 (buildings)/rooftop

(e) Scenario 3 (trees)/dashboard

(f) Scenario 3 (trees)/rooftop

Figure 8: Heat maps of different scenarios. Each plot shows the packet delivery ratio depending on the sender position, scenario (open, building, and trees), and antenna location (dashboard, rooftop).

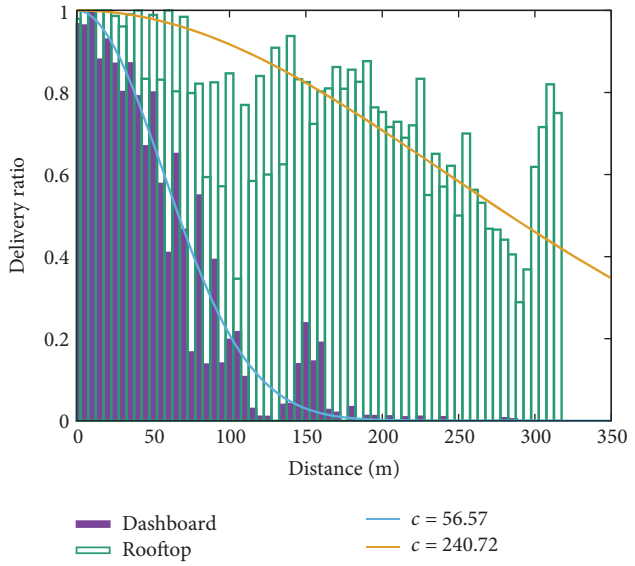

(a) Delivery ratio at Intersection 1 with the antenna put on the dashboard or rooftop

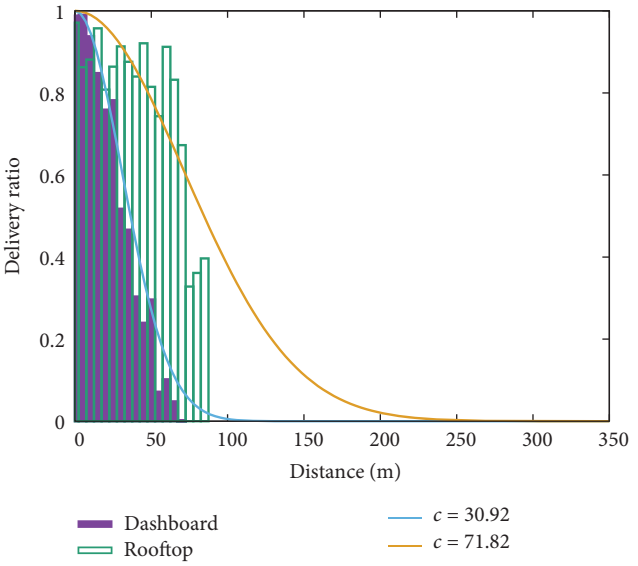

(b) Delivery ratio at Intersection 2 with the antenna put on the dashboard or rooftop

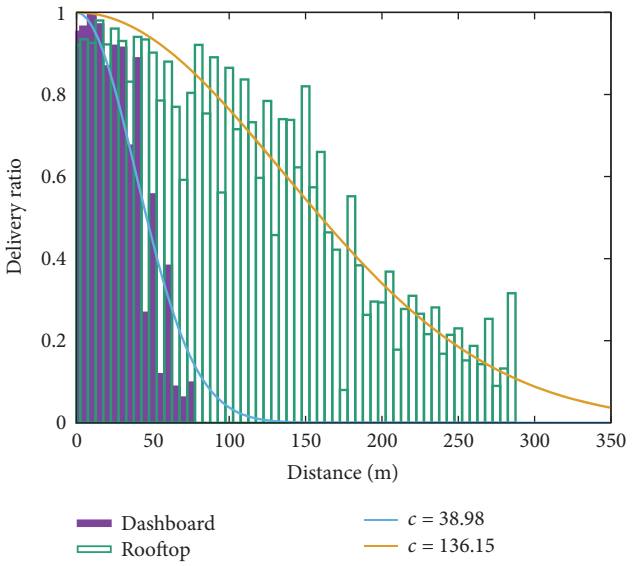

(c) Delivery ratio at Intersection 3 with the antenna put on the dashboard or rooftop

Figure 9: Curve fittings of delivery ratio versus distance.

Table 2: c parameter and χ^2 error values for each scenario and antenna position.

	Antenna on dashboard		Antenna on rooftop	
	c	χ^2	c	χ^2
Intersection 1	56.57	15.35	240.72	30.15
Intersection 2	30.92	12.84	71.82	21.67
Intersection 3	38.98	6.18	136.15	20.14

In detail, we can see that c values for the first intersection are the highest ones. On the other hand, for Intersection 2, the lowest values are obtained, with Intersection 3 characterized by intermediate c values. Also, regarding antenna locations, we find that c value for the rooftop results is always more than twice those obtained with the antenna in the dashboard. The largest relative difference is detected for Intersection 1, where c value for the rooftop case is more than four times greater than the one for the dashboard case. This occurs because, for this kind of intersection, packet losses are mostly related

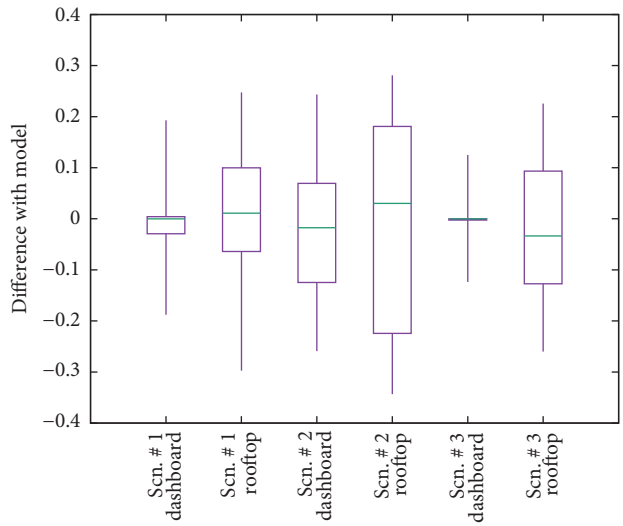

Figure 10: Differences among the fitted models and data.

to signal power dropping due to distance, and the rooftop antenna location thereby emerges as the optimal option to mitigate such power losses.

Table 2 also shows the fitting error expressed as χ^2, the sum of the squares of the differences between the model function and the actual delivery ratios obtained from the experiments. Additionally, Figure 10 shows a box and whisker plot of the difference distribution for each scenario and antenna position. The box shows the 2nd, 3rd, and 4th percentiles, and the whisker is the mean value plus/minus the standard deviation. The model fitting is clearly more accurate for the dashboard scenarios than when mounting the antenna on the rooftop. This occurs because, in the latter case, the range is not large enough to reach near-zero values.

7. Model Applicability to Simulation Environments

In general, a detailed channel characterization between two endpoints requires studying the signal to noise plus interference values at the receiver, which includes modeling in detail the signal propagation conditions in the target environment. In the specific case of vehicular networking environments, this includes the modeling of signal reflections and Doppler spread in the presence of various obstacles, including buildings, trees, and vehicles. However, such a detailed signal propagation analysis is extremely complex, and so it becomes computationally prohibitive to undertake such a detailed analysis when studying traffic communications in a large area, especially for vehicular networking studies where this area can grow up to the size of an entire city or even greater. To address such problem, empirical path loss models for urban environments have emerged (e.g., Nakagami [37] and Durgin et al. [38]). However, these models provide a generalization of the propagation behavior, meaning that they fail to provide a detailed characterization of very specific transmission conditions, such as the intersection propagation conditions addressed in this paper. Yet the problem of how to adapt our model to simulation environments remains, as it requires knowing in advance the actual characteristics of each specific intersection in order to adequately model it.

To achieve the intersection modeling requirements enabling the adoption of our models, we propose automating the intersection classification process by analyzing the street width and the presence of buildings in a preprocessing step before the actual simulation. This way we avoid having to manually tag each intersection manually and benefit from the models hereby derived with little additional complexity.

It is worth highlighting that widely used map providers such as OpenStreetMap [39] already include such street and building information for many relevant cities, which simplifies and makes feasible the adoption of our solution.

8. Event Notification Effectiveness on Intersections

To further validate our research work, we have also analyzed the probability of successful delivery of notifications associated with critical events. As explained earlier, such event notification dissemination typically relies on multihop broadcasting to make sure that the information arrives to all vehicles in a certain target area. However, since such dissemination procedure is prone to cause broadcast storm problems and since urban obstacles will typically hinder dissemination towards vehicles in nearby streets, different proposals consider it optimal to perform timely broadcasts when vehicles are located at intersections to maximize reachability. Such timely broadcasts for moving vehicles, though, rely on mapping GPS coordinates to map details, and the overall effectiveness will highly depend on the GPS error introduced at the time of broadcasting.

Taking the aforementioned issues into consideration, in this section, we will use the models derived in Section 6 for the different intersection types and antenna locations to study the probability of successfully delivering an event-related message at an intersection when considering different GPS error values. We are assuming that the vehicle intends to send a packet when located at the center of the intersection to maximize the packet delivery ratio. However, if we take the GPS error into account, we could expect that the error it introduces could impact the packet delivery ratio, especially in urban canyon scenarios. To this purpose, we define different maximum values for the GPS error (which typically ranges between 5 and 50 meters) and create normal distributions where 99.7% of the values are inside this maximum distance (3σ rule). Then, considering this probability distribution for the vehicle location when transmitting a packet, we combined it with the models derived in the previous section to gain awareness about the expected success ratio for the event message delivery.

In Figure 11, we evaluate the impact that the GPS error ranges will have on the delivery ratio for each scenario, with the antenna located either on the dashboard or on the rooftop. The three intersections that have different levels of obstruction are compared. In these plots the delivery ratio from the fitted model is shown for three significative points

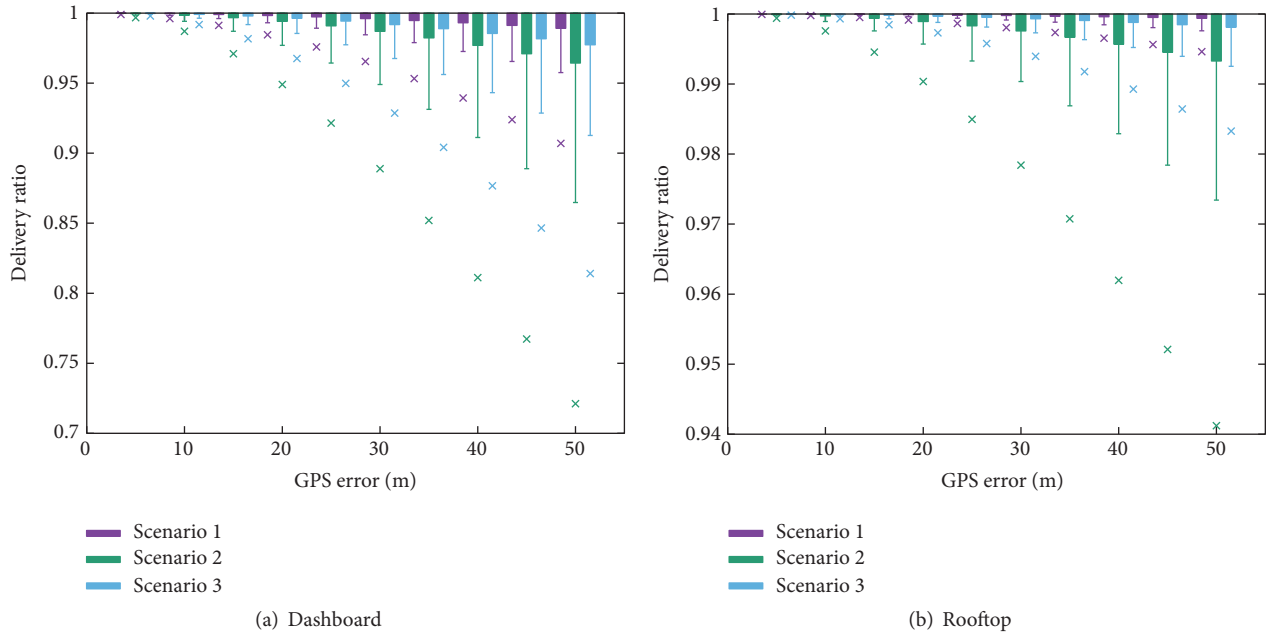

FIGURE 11: Delivery ratio at the three intersections for different GPS error ranges.

in the error distribution: the bar corresponds to the interval from 0 to σ (68% of values), the line corresponds to $[0, 2\sigma]$ (95%), and the cross is $[0, 3\sigma]$ (99.7%).

If we focus on the case where the antenna is located in the dashboard (see Figure 11(a)), a significant difference is detected when we have a GPS error of 50 meters. In the case of Intersection 1, a GPS error of up to 50 meters still shows acceptable packet delivery levels; on the contrary, for Intersection 2 (urban canyon), the delivery ratio is much worse than for the other two cases.

Figure 11(b) shows that when installing the antenna on the rooftop, the impact of GPS error is now reduced as the delivery ratio in these cases, when compared to the previous ones, is much better. This means that, in general, effective propagation of messages at intersections is possible, even in urban canyons and despite GPS errors, as long as rooftop antennas are used so that their extended radio range compensates for the poor radio visibility and positioning error.

In a nutshell, again we find that the different antenna positions and the characteristics of intersections clearly affect the probability of successful packet delivery even with the presence of GPS error. That being said, the most reliable sending process takes place when we put the antenna on the rooftop of the vehicle and the transmission occurs at an open space intersection (with minimum obstructions). The worst case occurs at the urban canyon intersection (maximum obstruction) when the antenna is located within the vehicle, in the dashboard, thereby matching our initial hypothesis.

9. Conclusions and Future Works

Recent efforts to minimize accidents in vehicular environments have led safety issues to represent one of the most important applications in the context of ITS. In this scope, intervehicular communication can play a very relevant role by allowing quickly notifying neighboring vehicles about dangerous events. However, these notifications should be delivered quickly and reliably, which can be a strict requirement in urban environments since buildings and other obstacles are prone to hinder signal propagation. Thus, timely message delivery at the center of intersections emerges as the main solution allowing avoiding urban obstacles in a simple and straightforward manner.

In this paper we have studied the packet delivery effectiveness achieved on different types of intersections (no obstacles, urban canyon, and partial obstruction) and when locating the antennas on either the dashboard or the rooftop. Extensive experimental results using broadcast traffic have shown that the impact of the intersection type is significant, as differences of up to 150 meters in transmission range were detected. Also, we find that having a rooftop antenna is also a critical factor, allowing extending the transmission range between 100 and 250 meters, which may represent more than a 100% increase in some cases.

Additionally, we have modeled all the obtained results by finding the best-fitting function and then applying regression. We find that a Gaussian function offers adequate fits for all cases by just varying one parameter. This way, our model allows seamlessly representing different types of intersections and bringing these results to simulation environments.

Based on our model, we then made an analytic study to determine the probability of a successful event dissemination process at intersections, for the different types of intersection and antenna locations tested, when varying the maximum GPS error. We find that, in general, dissemination is highly effective, even in urban canyons and for high GPS error conditions, as long as rooftop antennas are used, with the more restrictive dashboard solutions being not recommended. This way, using the previous models and assisted by real-time

geolocation and maps, we can first determine the type of scenario to use and then, knowing the GPS error, determine the expected delivery ratio.

As future work, we will translate our results to a simulation platform in order to achieve a more realistic simulation model able to better resemble real-life experiments. Also, since we used the standard GPS device embedded in the smartphone for localization purposes, it would be interesting to test with more precise outdoor geolocation devices. Another consideration to be kept in mind is to evaluate the feasibility of V2V communications through the use of LTE-based intervehicle communications.

Conflicts of Interest

The authors declare that there are no conflicts of interest regarding the publication of this paper.

Acknowledgments

This work was partially supported by the "Ministerio de Economía y Competividad, Programa Estatal de Investigación, Desarollo e Innovación Orientada a los Retos de la Sociedad, Proyectos I+D+I 2014," Spain, under Grants TEC2014-52690-R and BES-2015-075988.

References

[1] J. M. Hernández-Mũnoz, J. B. Vercher, L. Mũnoz et al., "Smart cities at the forefront of the future internet," in *The Future Internet Assembly*, pp. 447–462, Springer, 2011.

[2] Z. Xiong, H. Sheng, W. Rong, and D. E. Cooper, "Intelligent transportation systems for smart cities: a progress review," *Science China Information Sciences*, vol. 55, no. 12, pp. 2908–2914, 2012.

[3] C. T. Barba, M. Á. Mateos, P. R. Soto, A. M. Mezher, and M. A. Igartua, "Smart city for VANETs using warning messages, traffic statistics and intelligent traffic lights," in *Proceedings of the IEEE Intelligent Vehicles Symposium (IV '12)*, pp. 902–907, June 2012.

[4] P. Papadimitratos, A. La Fortelle, K. Evenssen, R. Brignolo, and S. Cosenza, "Vehicular communication systems: enabling technologies, applications, and future outlook on intelligent transportation," *IEEE Communications Magazine*, vol. 47, no. 11, pp. 84–95, 2009.

[5] S. Grant-Muller and M. Usher, "Intelligent transport systems: the propensity for environmental and economic benefits," *Technological Forecasting and Social Change*, vol. 82, no. 1, pp. 149–166, 2014.

[6] M. Sepulcre and J. Gozalvez, "Experimental evaluation of cooperative active safety applications based on V2V communications," in *Proceedings of the 9th ACM International Workshop on Vehicular Inter-NETworking, Systems, and Applications (VANET '12)*, pp. 13–20, ACM, June 2012.

[7] X. Ma, X. Chen, and H. H. Refai, "Performance and reliability of DSRC vehicular safety communication: a formal analysis," *EURASIP Journal on Wireless Communications and Networking*, vol. 2009, Article ID 969164, 13 pages, 2009.

[8] F. J. Martinez, C.-K. Toh, J.-C. Cano, C. T. Calafate, and P. Manzoni, "A Street Broadcast Reduction scheme (SBR) to mitigate the broadcast storm problem in VANETs," *Wireless Personal Communications*, vol. 56, no. 3, pp. 559–572, 2011.

[9] M. Fogue, P. Garrido, F. J. Martinez, J.-C. Cano, C. T. Calafate, and P. Manzoni, "PAWDS: a roadmap profile-driven adaptive system for alert dissemination in VANETS," in *Proceedings of the 10th IEEE International Symposium on Network Computing and Applications (NCA '11)*, pp. 1–8, Cambridge, Mass, USA, August 2011.

[10] J. A. Sanguesa, M. Fogue, P. Garrido, F. J. Martinez, J.-C. Cano, and C. T. Calafate, "A survey and comparative study of broadcast warning message dissemination schemes for VANETs," *Mobile Information Systems*, vol. 2016, Article ID 8714142, 2016.

[11] A. Böhm, K. Lidström, M. Jonsson, and T. Larsson, "Evaluating CALM M5-based vehicle-to-vehicle communication in various road settings through field trials," in *Proceedings of the 35th Annual IEEE Conference on Local Computer Networks (LCN '10)*, pp. 613–620, October 2010.

[12] R. Meireles, M. Boban, P. Steenkiste, O. Tonguz, and J. Barros, "Experimental study on the impact of vehicular obstructions in VANETs," in *Proceedings of the IEEE Vehicular Networking Conference (VNC '10)*, pp. 338–345, December 2010.

[13] C. Sommer, D. Eckhoff, R. German, and F. Dressler, "A computationally inexpensive empirical model of IEEE 802.11p radio shadowing in urban environments," in *Proceedings of the 8th International Conference on Wireless On-Demand Network Systems and Services (WONS '11)*, pp. 84–90, January 2011.

[14] C. Sommer, S. Joerer, and F. Dressler, "On the applicability of Two-Ray path loss models for vehicular network simulation," in *Proceedings of the IEEE Vehicular Networking Conference (VNC '12)*, pp. 64–69, Seoul, Korea, November 2012.

[15] C. Sommer, S. Joerer, M. Segata, O. K. Tonguz, R. L. Cigno, and F. Dressler, "How shadowing hurts vehicular communications and how dynamic beaconing can help," *IEEE Transactions on Mobile Computing*, vol. 14, no. 7, pp. 1411–1421, 2015.

[16] J.-C. Lin, C.-S. Lin, C.-N. Liang, and B.-C. Chen, "Wireless communication performance based on IEEE 802.11p R2V field trials," *IEEE Communications Magazine*, vol. 50, no. 5, pp. 184–191, 2012.

[17] J. Gozalvez, M. Sepulcre, and R. Bauza, "IEEE 802.11p vehicle to infrastructure communications in urban environments," *IEEE Communications Magazine*, vol. 50, no. 5, pp. 176–183, 2012.

[18] H. Schumacher, H. Tchouankem, J. Nuckelt et al., "Vehicle-to-Vehicle IEEE 802.11p performance measurements at urban intersections," in *Proceedings of the IEEE International Conference on Communications (ICC '12)*, pp. 7131–7135, June 2012.

[19] H. Tchouankem, T. Zinchenko, H. Schumacher, and L. Wolf, "Effects of vegetation on vehicle-to-vehicle communication performance at intersections," in *Proceedings of the IEEE 78th Vehicular Technology Conference (VTC Fall '13)*, pp. 1–6, September 2013.

[20] H. Tchouankem and T. Lorenzen, "Measurement-based evaluation of interference in Vehicular Ad-Hoc Networks at urban intersections," in *Proceedings of the IEEE International Conference on Communication Workshop (ICCW '15)*, pp. 2381–2386, IEEE, London ,UK, June 2015.

[21] V. P. Barcelos, T. C. Amarante, C. D. Drury, and L. H. A. Correia, "Vehicle monitoring system using IEEE 802.11p device and Android application," in *Proceedings of the 19th IEEE Symposium on Computers and Communications (ISCC '14)*, pp. 1–7, Madeira, Portugal, June 2014.

[22] W. Viriyasitavat, S. Midtrapanon, T. Rittirat, and S. Thanumaiweerakun, "Performance analysis of android-based real-time message dissemination in VANETs," in *Proceedings of the International Conference on Computing, Networking and Communications (ICNC '16)*, pp. 1–5, IEEE, February 2016.

[23] S. M. Tornell, S. Patra, C. T. Calafate, J.-C. Cano, and P. Manzoni, "GRCBox: extending smartphone connectivity in vehicular networks," *International Journal of Distributed Sensor Networks*, vol. 2015, Article ID 478064, 13 pages, 2015.

[24] A. Buchenscheit, F. Schaub, F. Kargl, and M. Weber, "A VANET-based emergency vehicle warning system," in *Proceedings of the IEEE Vehicular Networking Conference (VNC '09)*, pp. 1–8, October 2009.

[25] J. Yang, J. Wang, and B. Liu, "An intersection collision warning system using Wi-Fi smartphones in VANET," in *Proceedings of the 54th Annual IEEE Global Telecommunications Conference: "Energizing Global Communications" (GLOBECOM '11)*, pp. 1–5, December 2011.

[26] S. Patra, S. Tornell, C. Calafate, J. Cano, and P. Manzoni, "Messiah: an its drive safety application," in *XXV Jornadas Sarteco*, Valladolid, Spain, 2014.

[27] L.-D. Chou, J.-Y. Yang, Y.-C. Hsieh, D.-C. Chang, and C.-F. Tung, "Intersection-based routing protocol for VANETs," *Wireless Personal Communications*, vol. 60, no. 1, pp. 105–124, 2011.

[28] H. Saleet, R. Langar, K. Naik, R. Boutaba, A. Nayak, and N. Goel, "Intersection-based geographical routing protocol for VANETs: a proposal and analysis," *IEEE Transactions on Vehicular Technology*, vol. 60, no. 9, pp. 4560–4574, 2011.

[29] T. Acarman, C. Yaman, Y. Peksen, and A. U. Peker, "Intersection based routing in urban VANETs," in *Proceedings of the 18th IEEE International Conference on Intelligent Transportation Systems (ITSC '15)*, pp. 1087–1092, IEEE, Las Palmas, Spain, September 2015.

[30] X. Guan, Y. Huang, Z. Cai, and T. Ohtsuki, "Intersection-based forwarding protocol for vehicular ad hoc networks," *Telecommunication Systems*, vol. 62, no. 1, pp. 67–76, 2016.

[31] W. Vandenberghe, I. Moerman, and P. Demeester, "On the feasibility of utilizing smartphones for vehicular ad hoc networking," in *Proceedings of the 11th International Conference on ITS Telecommunications (ITST '11)*, pp. 246–251, IEEE, Saint Petersburg, Russia, August 2011.

[32] S. M. Tornell, C. T. Calafate, J.-C. Cano, P. Manzoni, M. Fogue, and F. J. Martinez, "Evaluating the feasibility of using smartphones for ITS safety applications," in *Proceedings of the IEEE 77th Vehicular Technology Conference (VTC Spring '13)*, pp. 1–5, Dresden, Germany, June 2013.

[33] R. Frank, W. Bronzi, G. Castignani, and T. Engel, "Bluetooth low energy: an alternative technology for VANET applications," in *Proceedings of the 11th Annual Conference on Wireless On-Demand Network Systems and Services (WONS '14)*, pp. 104–107, IEEE, Obergurgl, Austria, April 2014.

[34] ETSI, "Intelligent Transport Systems (ITS); vehicular communications; basic set of applications; part 3: specification of decentralized environmental notification basic service," TS 102 637-3, 2010.

[35] ETSI and Intelligent Transport Systems (ITS), "Vehicular communications; basic set of applications; part 3: specification of decentralized environmental notification basic service," TS 102 637-2, 2010.

[36] C. F. F. Karney, "Transverse Mercator with an accuracy of a few nanometers," *Journal of Geodesy*, vol. 85, no. 8, pp. 475–485, 2011.

[37] M. Nakagami, "The m-distribution—a general formula of intensity distribution of rapid fading," in *Statistical Methods in Radio Wave Propagation*, Pergamon Press, 1960.

[38] G. Durgin, T. S. Rappaport, and H. Xu, "Measurements and models for radio path loss and penetration loss in and around homes and trees at 5.85 GHz," *IEEE Transactions on Communications*, vol. 46, no. 11, pp. 1484–1496, 1998.

[39] M. Haklay and P. Weber, "OpenStreet map: user-generated street maps," *IEEE Pervasive Computing*, vol. 7, no. 4, pp. 12–18, 2008.

Hindawi
Mobile Information Systems
Volume 2017, Article ID 8149348, 13 pages
https://doi.org/10.1155/2017/8149348

Research Article

High-Accuracy Tracking Using Ultrawideband Signals for Enhanced Safety of Cyclists

Davide Dardari,[1] Nicoló Decarli,[1] Anna Guerra,[1] Ashraf Al-Rimawi,[1] Víctor Marín Puchades,[2] Gabriele Prati,[2] Marco De Angelis,[2] Federico Fraboni,[2] and Luca Pietrantoni[2]

[1]*Department of Electrical, Electronic and Information Engineering "Guglielmo Marconi", The University of Bologna, Bologna, Italy*
[2]*Department of Psychology, The University of Bologna, Bologna, Italy*

Correspondence should be addressed to Davide Dardari; davide.dardari@unibo.it

Received 18 November 2016; Revised 30 January 2017; Accepted 9 February 2017; Published 15 March 2017

Academic Editor: Cristiano Silva

In this paper, an ultrawideband localization system to improve the cyclists' safety is presented. The architectural solutions proposed consist of tags placed on bikes, whose positions have to be estimated, and anchors, acting as reference nodes, located at intersections and/or on vehicles. The peculiarities of the localization system in terms of accuracy and cost enable its adoption with enhanced risk assessment units situated on the infrastructure/vehicle, depending on the architecture chosen, as well as real-time warning to the road users. Experimental results reveal that the localization error, in both static and dynamic conditions, is below 50 cm in most of the cases.

1. Introduction

In recent years, vulnerable road users (VRUs) injuries and mortality have rapidly grown due to the increased road traffic: around 2000 people riding bicycle are killed every year in traffic accidents in EU countries [1] and about 30% of cyclist fatalities take place at junctions [1, 2]. In this scenario, it becomes urgent to develop solutions in order to both encourage people to cycle and make cycling safer at the same time. As regards the last point, increasing road users' awareness of cyclists' presence in the surrounding becomes an essential issue along with the possibility of warning cyclists during dangerous maneuvers of cars and heavy goods vehicles (HGVs).

Today several technologies are available and could be exploited to detect dangerous situations for cyclists. In order to choose the proper one, we propose a multidisciplinary approach based on a deep analysis of the most dangerous scenarios and situations. In this context, the starting point is a behavioral investigation which takes a central role in establishing the users' acceptance, to enhance the cyclists' comfort together with their safety and to put the final user at the center of all the investigation and the ultimate aim of the technologies that will be developed. For these reasons, the technological requirements for such application must account for several and heterogeneous aspects in order to make it effective, reliable, and user-friendly and with low-cost.

To this end, in this paper we first provide an analysis of accidents statistics involving cyclists. Second, a survey of existing technologies, with a particular emphasis on their pros and cons, is undertaken. Starting from the previous outcomes, we propose a new detection architecture providing high-accuracy localization and tracking of road users based on the ultrawideband (UWB) technology [3]. UWB, in its IEEE802.15.4a standard implementation [4], has already proved to be the best candidate in achieving high localization accuracy at low cost, thanks to its high temporal resolution and the ability to resolve multipath and to coexist with other wireless technologies [5–7]. We experimentally characterized the performance of the implemented UWB-based tracking system by means of indoor and outdoor measurements campaigns, as detailed in the numerical results.

The availability of accurate real-time tracking of road users opens the door to the introduction of advanced risk

assessment (RA) units, both on vehicles and on the infrastructure (on-site), capable of predicting critical situations and providing a suitable feedback to the road user through ad hoc human machine interfaces (HMIs). Moreover, it also enables the possibility of offering additional services to cyclists, such as enhancing the functionality of green waves by accounting for the amount of people approaching the traffic light. These applications are currently being investigated in the Europe-funded project XCycle (http://www.xcycle-h2020.eu).

The rest of the paper is organized as follows: Section 2 presents an analysis of accident statistics involving cyclists; Section 3 reports a summary of the available technologies for detection of cyclists; Section 4 presents the considered architecture for enhanced safety of cyclists; Section 5 describes the localization method considered exploiting UWB signals; Section 6 shows some experimental results characterizing the system performance; finally, Section 7 concludes the paper.

2. Analysis of Accident Statistics Involving Cyclists

2.1. Analysis of Accidents Reports. In 2012, 2143 bicyclists died in road accidents in Europe [1]. Although the number of cycling fatalities did not increase from 2004 to 2013, the proportion of cyclist fatalities with reference to overall road fatalities has a growing trend [1]. The majority (52%) of cyclist deaths on the European roads between 2011 and 2013 had passenger cars as opponent vehicles, whereas the 24% involved goods vehicles or buses/coaches [8]. Cyclist accidents involving HGVs have shown to be more fatal given that HGVs are involved in 12% of cyclist accidents (data from 2005 to 2010) [2]. According to the data provided by the Italian National Institute of Statistics [9], 575.093 road accidents occurred in the period ranging from 2011 to 2013, on the Italian road network. Of these, 49.621 road accidents involved at least one injured or killed cyclist. The number of bicycle fatalities during this period was 823 (1.7% of roads accidents involving at least one injured or killed cyclist). Previous research identified intersections as more dangerous for bicyclists in comparison with other types of infrastructure [10–13]. Within the countries that report accidents location to the Community database on Accidents on the Roads in Europe (CARE) [2], 29% of the cyclists' fatal accidents between 2005 and 2010 took place at junctions. From those, 83% took place at crossroads. Among the accidents ending in serious injury, 41% occurred at junctions, which represents a higher percentage than that of injuries occurring outside of junctions (31%). In Italy, the 44.9% of the accidents involving a cyclist injury or death in 2011–2013 (22.294) took place at crossroads [9]. From these accidents, the majority (78.5%) involved a passenger car and a 7.1% involved a truck. Moreover, accidents with cars and trucks represented the 32.2% of the overall cyclist fatalities, which highlights the importance of the study and prevention on these scenarios.

The present study focuses on road conflicts between cyclists and passenger cars or goods vehicles at intersections. Among the most investigated types of maneuvers or violations associated with bicycle to motorized vehicles crashes at intersections, most of them are related to the type of accident labeled "looked-but-failed-to-see" [14, 15]. Some studies revealed that failure to see a cyclist may be due to driver inadequate scanning strategy, visual search strategies, and misplaced expectations of cyclist behavior [16–18].

Moreover, previous cycling safety research has found that left- and right-turning vehicles had an effect on bicyclist injury occurrence and were frequent in bicycle accidents taking place at intersections [16, 19–21]. These two scenarios are the so-called left turn and right turn scenarios. We will proceed to explain them with more detail below.

2.2. Left Turn Scenario. This scenario involves a vehicle turning left at an intersection and the driver failing to yield to a cyclist that approaches the intersection from the opposite direction, or getting in the trajectory of a cyclist approaching on the same direction. In both situations, the cyclist and the driver start their maneuvers on opposite sides of the road. Figure 1 displays the maneuver with a cyclist approaching on the opposite direction.

In the case of bicyclists coming in the same direction of the vehicle, blind spots or objects obstructing the view of the motorist could be a contributing factor to the failure to detect them.

2.3. Right Turn Scenario. The right turn scenario involves a vehicle failing to yield a bicyclist that rides straightforward in the same direction. It most commonly takes place when a vehicle and a bicycle arrive at the same time at an intersection with at least three branches [21]. Figure 2 shows the driver's and cyclist's maneuvers involved in the scenario.

Among truck drivers, one of the main contributing factors of this scenario could be that of failing to look/see the bicyclist going straight forward while turning [22]. Blind spots may be the cause, or the contributing factor, of this type of human error.

Cooperative systems, also exploiting infrastructure-based sensors, could be useful to improve detection of cyclists and may assist drivers in minimizing blind spots and "looked-but-failed-to-see" errors. New technological solutions aimed at detecting bicyclists and conveying this information to the driver may play an important role in the prevention of these detection failures and, consequently, of the potential collisions.

3. Bicyclists Detection Technologies

The previous analysis has revealed how accidents occur due to a lack of visibility between the road users, especially at junctions and in the presence of large vehicles. This section aims at describing the main technologies capable of improving the *visibility* and then increasing the safety of road users. Specifically, we will distinguish between *on-site* and *on-vehicle* solutions depending on the sensors' location. For each solution the advantages and disadvantages will be illustrated.

Table 1 reports some examples on the panorama of technological solutions for detection of bikes. Sensors, for example, cameras or radars, can be placed on the infrastructure (i.e., on-site) or on vehicles. Most of the detection approaches do not require technology on-bike (e.g., radar, cameras, or

Table 1: Summary of available technologies.

Technology	Pros	Cons
Cameras	Accurate detection and users' discrimination	Difficult operation in bad weather conditions, false alarms
Thermal cameras	Accurate detection and users' discrimination	Cost, false alarms
Ultrasonic sensors	Reliable detection in every weather condition	Poor users' discrimination
Inductive loops	Average users discrimination	Undersurface. Large infrastructure. Very low range
LIDAR	Accurate detection and users' discrimination	Very high cost, complex deployment and complex data processing
Radar (on-air)	Reliable detection. Good angular resolution	Poor users' discrimination
Radar (under surface)	Average users' discrimination	Undersurface. Very low range
RFID	Accurate detection and perfect users' discrimination	Tags needed. Poor angular and ranging resolution
GPS	Localization of different users	GPS receivers needed. Medium localization accuracy, latency

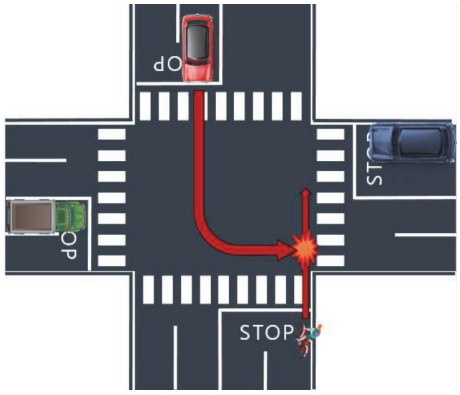

Figure 1: Left turn scenario.

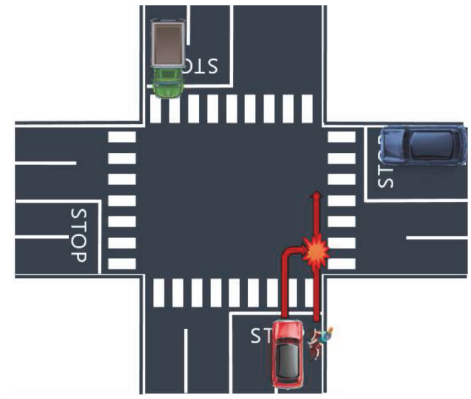

Figure 2: Right turn scenario.

sonar) while others do (e.g., global positioning system (GPS) receivers or radio-frequency identification (RFID) tags).

For what concerns the characteristics of the different technologies, narrow-beam radars or sonar-based systems are efficient for detecting the presence of a user in a bicycle-path and providing an alert sign. However, they are not effective in enabling potential collision prediction or multitarget discrimination at junctions. On the other hand, cameras and especially thermocameras perform well in large road junctions and can be used for trajectory (collision) prediction. Some weather conditions make detection with normal cameras difficult (e.g., darkness or rain can decrease the capability of identifying cyclists). Thermocameras may solve, in part, this problem, but they are currently still quite expensive and might fail during the summer because the high temperature of the asphalt might hide the presence of persons. Inductive loops and undersurface radars are effective but have limited range, infrastructural problems and poorer target discrimination.

A common shortcoming of all these passive technologies is that there is always a nonnegligible probability of false alarms that may discourage users to trust the system. On the other side, the main advantage is that they do not require dedicated hardware on bike.

Other solutions, such as GPS and RFID, that require bikes equipped with dedicated technology, respectively, a GPS receiver and a RFID tag, eliminate the presence of false alarms but do not provide sufficient localization accuracy. Moreover, GPS is expensive and battery hungry and is characterized by a large response delay that prevents its use in RA.

As regards the on-vehicle technologies, they are often based on proximity sensors, camera, or radar and they usually provide warnings to other road users, such as cyclists, by means of visible alerts. Communication operations between vehicles, infrastructure, and cyclists/pedestrians are not provided by such systems as the majority of them rely on LEDs to prevent a possible collision with other road users. Moreover, the few on-vehicle solutions sometimes lack reliability in terms of misdetections and false alarms.

To conclude, the main disadvantages of the today's solutions also represent incentives for future improvements. Specifically we envisage the following desired capabilities:

(i) Submeter localization and tracking with extreme low-latency (<500 ms)

(ii) Possibility of detecting and discerning different road users (reducing or eliminating false alarms)

(iii) Possibility of predicting the road users' trajectories

(iv) Possibility of communicating with other road users (e.g., cyclists or pedestrians) and warning them in a specific way

Based on the above considerations, the need of a low-cost, low-latency detection and submeter localization, and communication technology clearly emerges to support new generation RA systems capable of predicting the situation of collision and provide a suitable feedback to the vehicle and to the cyclist via ad hoc HMIs.

In the following section we propose on-site and on-vehicle architectures using the UWB technology.

4. Proposed System Architectures and Technologies

Inspired by the shortcomings that emerged in the current available technologies, in this section we will describe a localization system capable of improving the cyclists' visibility and achieve submeter accuracy, thus guaranteeing an increased safety for the road users.

The proposed architecture is based on active, small, and low-cost tags mounted on the bikes. Contrary to their passive counterparts, active tags are equipped with a transmitting section and are able to send and/or receive interrogation signals, thus also enabling the possibility of communicating with the vehicle and/or the infrastructure and including HMI. In the future, if energy efficiency wants to be pushed at most, semipassive tags could be considered at bike side, thus minimizing the energy necessary for detection and localization and using most of the battery power just in the case of HMI activation [23, 24].

Tag detection and tracking are performed by analyzing the data exchanged by the tag and a set of reference nodes, called *anchors*, placed in known positions in the space, forming the so-called real-time locating systems (RTLS). In the following two architectures will be presented. The main difference of the proposed architectures lies on where anchors are deployed.

More specifically, we consider an *infrastructure-based* architecture with anchors placed in the correspondence of the crossing's infrastructure (e.g., at traffic lights) and a *vehicle-based* architecture with anchors mounted on vehicles (e.g., cars and trucks). In both solutions several anchors interact with tags by performing different kinds of measurements, as it will be clarified in Section 4.1; then a central unit gathers the information from all the anchors and fuses it to estimate the position of each tag (i.e., each bike). According to this scheme, in the first architecture the central unit is placed on the infrastructure, while in the second it is mounted on the vehicle.

In the following, we will introduce the underlying UWB technology and communication protocol, and then both architectures will be detailed.

4.1. UWB Technology and Communication Protocol. While the IEEE802.11p standard is emerging as the key technology for vehicular communications, a similar counterpart for high-accuracy positioning and tracking for intelligent transportation systems has not been presented yet. Our proposal is to consider UWB signals to achieve the target submeter positioning accuracy. In accordance with the FCC definition,

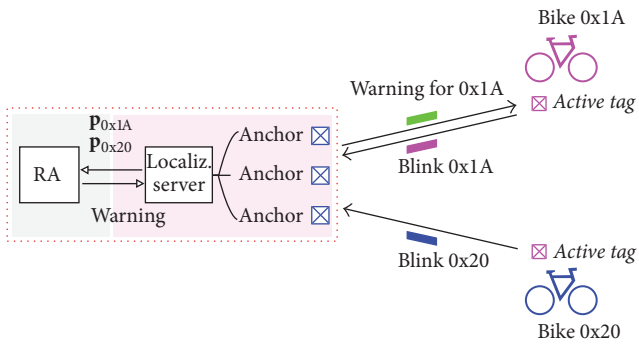

Figure 3: Proposed system using active UWB tags.

UWB signals are characterized by a bandwidth larger than 500 MHz. The classical and simplest method to obtain UWB signals is by means of impulse radio UWB (IR-UWB) [3]. In an IR-UWB system, a sequence of short pulses (typically with duration around 1 ns) is transmitted per information bit in order to collect more energy and allow multiuser access [25]. The short duration of the pulses guarantees a fine resolution in signal time-of-arrival (TOA) measurement and multipath discrimination so that time-based localization algorithms can benefit in obtaining accurate localization estimates [6]. The UWB technology is currently utilized as baseline in high-performance short-range RTLS using active tags according to the IEEE 802.15.4a and IEEE 802.15.4f standards as well as proprietary schemes [4, 26].

In Figure 3, the conceptual architecture is shown. As it is possible to see, the different road users periodically transmit a blink packet following the ISO/IEC 24730-62:2013 [27] standard containing their unique 64-bit identifier (ID) to the on-site and/or on-vehicle anchors using the UWB link. In our implementation, once a tag enters the monitored area, it is detected by the anchors and the localization server assigns it a temporary 16-bit ID *(tag index)*. Such a tag index is used to address the tag until it exits the area and it allows drastically reducing the size of the exchanged packets during the tracking process, thus reducing the risk of packets collision. The anchors receive these blink packets and, thanks to ad hoc processing schemes, determine the road users' positions and other tracking parameters *(localization engine)*. Then, if the RA unit predicts a potential dangerous situation, a warning is sent to a specific bike in order to activate the on-bike HMI.

In the following the two architectures proposed will be analyzed in order to better put in evidence their main peculiarities.

4.2. Infrastructure-Based Architecture. The infrastructure-based architecture is schematically depicted in Figure 4(a). As previously mentioned, in this solution, anchors are placed on the infrastructure, for example, at the corners of the junction in correspondence of the traffic light towers, while active tags are on bikes. Note that vehicles can be equipped with active tags as well, and, thus, they can be tracked by the system. This allows drawing a virtual map of all the road users.

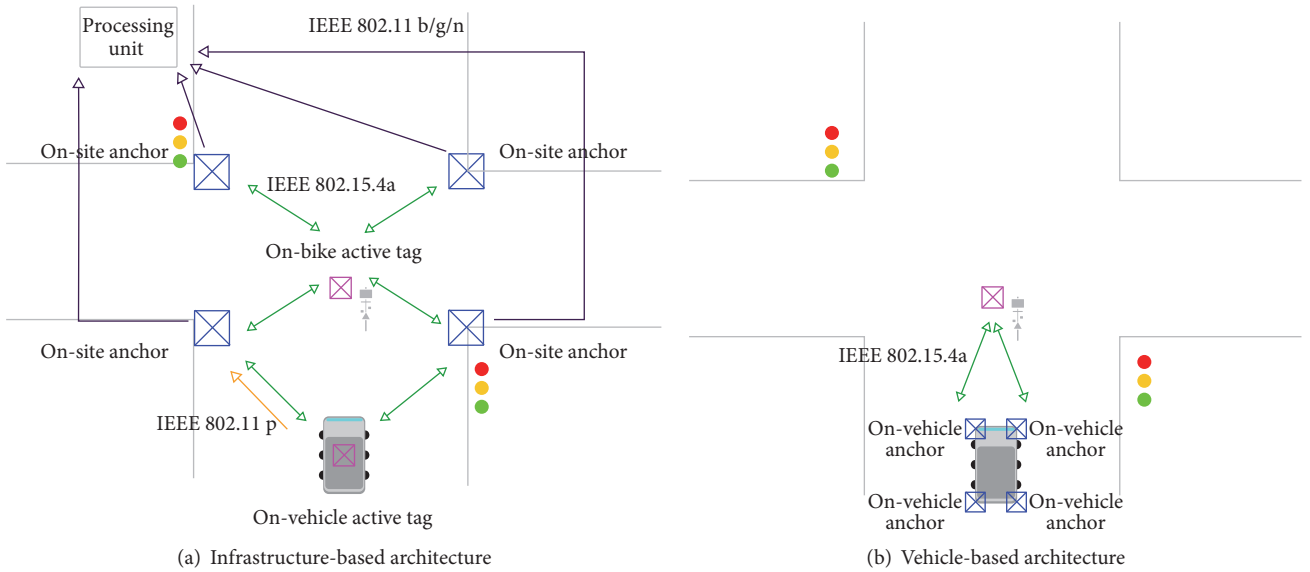

(a) Infrastructure-based architecture

(b) Vehicle-based architecture

FIGURE 4: Localization architectures with anchors (blue) placed on the infrastructure (a) or on the vehicle (b) and tags (pink) placed on bikes and vehicles.

Given their active nature, tags periodically send interrogation signals compliant with the IEEE 802.15.4a standard to the anchors. The exchanged messages contain the ID thanks to which each road user can be discriminated. The communication between vehicles and the infrastructure can be ensured by IEEE 802.11p links, whereas infrastructure-to-bike communication is enabled by the UWB IEEE 802.15.4a link.

Each anchor node receives the UWB signals from bikes and vehicles while keeping the synchronization with the other anchors. Starting from the sensed data, the processing unit performs both localization and RA process, as reported in Figure 3. The former consists in estimating the position, relative speed, and acceleration of each active tag. These data are then communicated to the RA unit whose main task is to establish the probability of collisions or more generally the presence of some risky situation. For instance, vehicles can inform the infrastructure whether they intend to start a dangerous maneuver, for example, the right and left turn, via a IEEE 802.11p link (an alternative option could be that of using the UWB technology). Based on this information and on the estimated position of all road users present in the junction, the RA unit could detect a dangerous situation and send back a warning message to the involved vehicle and to the cyclist. The on-bike device is able to activate its HMI (e.g., a visible or audible alert) to proper inform the bicyclist of the potential dangerous situation.

The main advantage of this solution is the good localization coverage that can be achieved thanks to deployment of anchors at the corners of the area to be monitored. On the other hand, this architecture is suitable in situations in which the time needed to prevent a bicycle running into a possible dangerous situation could be relaxed, as for example, in the left turn scenario, because of the potentially nonnegligible latency introduced by the vehicle-infrastructure-bike interaction.

4.3. Vehicle-Based Architecture. Figure 4(b) reports the vehicle-based architecture. Contrary to the previous described scenario, here vehicles are equipped with anchors. This means that the processing unit, consisting of the localization and RA engines represented in Figure 3, is mounted on vehicles.

The on-vehicle anchors receive the interrogation signals from the on-bike active tags in accordance with the UWB IEEE 802.15.4a standard. Thanks to these interrogations, the location engine running on-vehicle is able to determine the position and other navigation parameters (e.g., speed, acceleration) of the bikes with respect to the vehicle. Then, based on the relative coordinates of vehicle and bicycle, the RA module, still working on-vehicle, can determine whenever a dangerous situation is present or not and take proper countermeasures. As before, exploiting the same IEEE 802.15.4a links adopted for bicycle localization, the vehicle can send warnings to the on-bike tag regarding the risk and properly activate the on-bike HMI.

The main novelty of this solution is that anchors are closer to each other in comparison with the infrastructure-based approach. Therefore, the tags are always located outside the perimeter described by the anchors. As known in localization theory, this is not the optimal configuration for a localization system, since geometric dilution of precision (GDOP) issues can degrade the localization accuracy [28]. For this reason, in Section 5.3, the investigation of the impact of the geometry will be carried out, in order to understand the scale of performance degradation. On the other hand, the main advantage of such a configuration is that bicycle localization can be performed without the need of a specific infrastructure placed at the intersection and no false alarms occur. Moreover, this architecture is more promising when the decision about a possible risky situation and the relative warning message have to be rapidly conveyed to the vehicle

driver and to the on-bike module thanks to the direct interaction between the two road users. For example, it is well suited in the right turn scenario where a stringent latency requirement has to be met.

4.4. Enhanced Services. The localization system described in the previous sections could also enable new services, as, for example, those related to green-wave scenarios. Specifically, different green-wave approaches could be implemented: one could be aimed at informing cyclists about how to adjust their speed in order to get the green light at the next junction, while another possibility is that of synchronizing traffic lights based on the number and speeds of cyclists estimated to arrive at next intersections. For this kind of application, the infrastructure-based architecture is the most promising one. Indeed, the anchor nodes placed on the crossing area can monitor the number, direction, speed, and acceleration of cyclists at the exit of the considered intersection. Based on these parameters, a dedicated processing unit can estimate the number of bikes and the time needed to arrive at the next junction and thus the traffic lights can be programmed accordingly to allow a safer transit of cyclists. The mechanism through which the cyclists are localized and tracked is the same as described in Section 4.2.

5. The UWB Tracking Subsystem

In this section, the RTLS proposed and implemented for this application is described. As already introduced, the localization process is based on the capability of extrapolating positioning information starting from the UWB signals exchanged between nodes. Specifically, anchors receive the interrogation signals compliant with the IEEE 802.15.4a standard sent by active tags powered by an on-board battery and including a radio transceiver with transmitting/receiving capability.

5.1. On-Bike Module. The on-bike module implemented, shown in Figure 5, is mainly composed of an IEEE 802.15.4a transceiver connected to a UWB antenna. The transceiver communicates via Serial Peripheral Interface (SPI) with a MCU. The microcontroller unit (MCU) determines the sensor module behavior and implements all the functionalities needed for enabling localization and communication with vehicle and/or infrastructure. Output ports of the microcontroller unit (MCU) are then adopted for activating the on-bike HMI. As reported in the figure, the on-bike module is also equipped with additional 3D sensors (i.e., 3-axis accelerometer, 3-axis gyroscope, 3-axis magnetometer, and pressure sensor) whose output can be processed by the RA unit. All the sensors are periodically interrogated by the microcontroller unit (MCU). After the interrogation cycle, the sensor outputs are sent via the UWB link as payload of the blink packets to the anchors and thus made available for the location process running on vehicle or on infrastructure. The outputs of the localization estimation process consist of the bicycle ID, position coordinates, velocity, acceleration, absolute orientation, and the expected positioning accuracy.

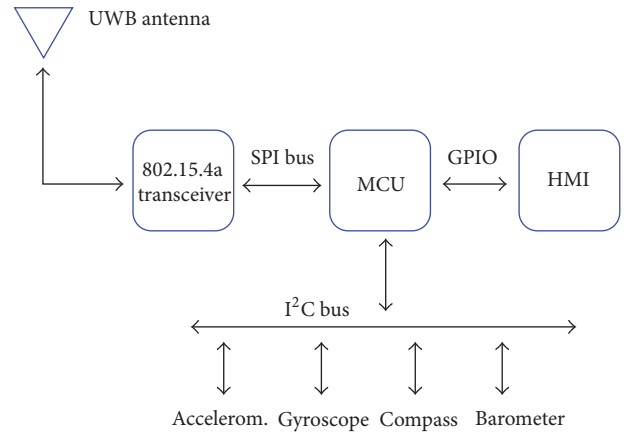

Figure 5: On-bike tag module.

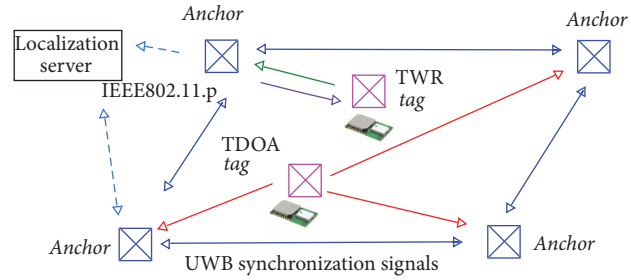

Figure 6: Localization scheme using TDOA and TWR tags.

The on-bike module also contains an HMI to proper inform the bicyclist of a potential danger predicted by the RA unit (either considering bicycle-vehicle interaction or bicycle-infrastructure interaction or simple detection by on-vehicle or infrastructure anchors). The bicycle HMI should be designed such that it requires minimal attention and does not distract the cyclist. Examples of HMIs are a flashing light display, an auditory alert, or a combination of both. The implementation of these should take into account the lighting conditions and background noise when cycling next to a truck. Other possibilities are, for example, HMIs based on helmet or handlebar vibrations.

5.2. Localization and Tracking Methods. The considered UWB RTLS is capable of providing submeter localization accuracy without resorting to costly and less accurate technologies such as GPS. The system deployment mainly consists on the installation of a sufficient number of anchors placed in known positions. The number of anchors depends on the area to be covered: the larger the space where tags can be placed is, the greater the number of anchor nodes should be to guarantee an acceptable level of tracking accuracy.

The main approaches to infer tag's position resort to TOA measurements as done in two-way ranging (TWR) and time difference-of-arrival (TDOA), as shown in Figure 6 and more schematically in Figure 7 [28]. TWR is based on packet exchanges between a couple of nodes (e.g., with reference to Figure 7(a), the tag, node B, and one of the anchors, node

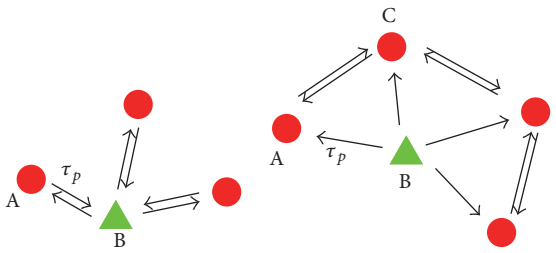

Figure 7: TWR and TDOA localization techniques.

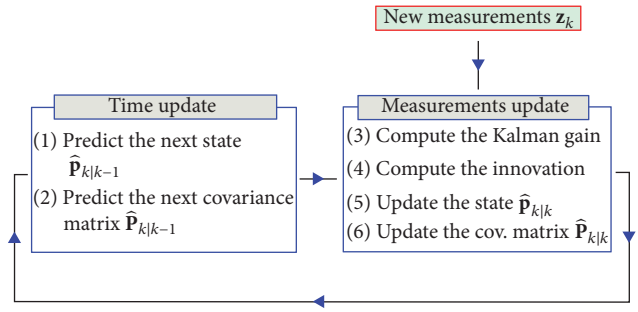

Figure 8: Bayesian filtering iterations.

A). The round-trip time of this *ping-pong*, $\tau_{RT} = 2\tau_p + \tau_d$, is measured with τ_p being the time of flight and τ_d the response delay, so that distance is estimated *(ranging)* [29]. This process must be repeated for any anchor and tag couple. Considering at least three anchors performing the TOA measure, it is possible to estimate the position of the device resolving a triangulation problem.

Differently, the TDOA principle lies on the idea of estimating the position of the transmitting tag by using the difference in time at which the signal arrives at multiple anchors. Therefore, the tag is expected to be placed on a hyperbole where the anchors are in the foci of the curve and where the distance between them is a priori known [30]. Note that, in this case, anchors exchange the collected time-based measurements, as reported in Figure 7(b). Having at least three anchors (i.e., two TDOA measurements) it is possible to estimate the position of the tag. This requires a very accurate synchronization among nodes that has to be guaranteed by distributing a common clock via cable or wirelessly.

If from one side, TWR provides a higher positioning accuracy thanks to the possibility of better counteract oscillators clock drifts, from the other side TDOA permits a drastic reduction in packet exchanges between tags and anchors, thus allowing a significant improvement in terms of refresh rate and multiple tags management. In fact, in TDOA each tag sends a very short blink packet which is received by the network of anchors. Due to the short duration of the blink packet emitted, a large number of tags can be managed at the same time, with both random channel access (e.g., aloha-based solutions) or time-scheduled transmissions (e.g., time division multiple access (TDMA)). In this manner, differently from the TWR scheme, a single uplink tag-anchor is sufficient for positioning (the downlink channel is then used only for infrastructure-to-bike or vehicle-to-bike communication). This solution allows building an extremely simple architecture for the tag, since all the heavy processing for localization is demanded to the central unit placed on infrastructure or vehicle. Moreover, the short blink packets contribute in maintaining the power consumption at tag side low, thus enabling battery-powered, low-cost solutions.

We implemented both the TDOA (with wireless synchronization) and TWR to make some comparisons in terms of performance, as it will be presented in the numerical results. At central unit side, based on the collected measurements, the tag position calculation is performed through state-of-the-art Bayesian filters. Specifically, we implemented a Bayesian filter using the particle filter approach employing measurements fusion mechanisms and clock drift compensation techniques to enable TDOA. The overall latency is less than 500 ms.

Figure 8 shows the classical two steps constituting the Bayesian filtering iterations. As it can be seen, the main objective is to infer an estimate of the state (e.g., tag's position coordinates, absolute orientation, and velocity) and its covariance matrix (i.e., a measure of the estimation uncertainty). More specifically, the first step consists in performing a prediction based on the history of the collected measurements *(time update)*. Once new measurements become available *(measurement update)*, an estimation correction phase can be undertaken based on the computed Kalman gain which is an indicator of the measurements and prior predictions reliability. In our approach, the observation is modeled as a unimodal Gaussian distribution centered in the difference between the estimated TDOA and the true TDOA and with a TOA error standard deviation of 0.2 m characterized from measurements. Regarding the mobility model, we assumed two different solutions depending on the availability of the speed information. In the speed-unawareness case, the density function describing the mobility model corresponds to a Gaussian distribution centered in the previous estimated position, whereas in the second case a speed learning approach is adopted where the speed is evaluated from earlier estimated positions with a sliding window. For further details, the reader is invited to refer to [31]. Note that, if tags broadcast their sensor data, inertial measurements fusion techniques can be adopted for improved localization accuracy [31].

5.3. Impact of Architecture on the Localization Accuracy: Performance Limits. As anticipated in Section 4, a discussion about the anchor nodes placement is necessary. In fact, it is well known from the localization literature how the geometrical configuration of anchors impacts the localization accuracy. Such effect, known as GDOP, arises when combining different measurements and can worsen or improve the performance in given position of the space where the tag could be present.

In order to access the potential localization accuracy, in particular in the vehicle-based infrastructure which is known unfavorable from the GDOP point of view, a theoretical analysis based on the position error bound (PEB) [32] is

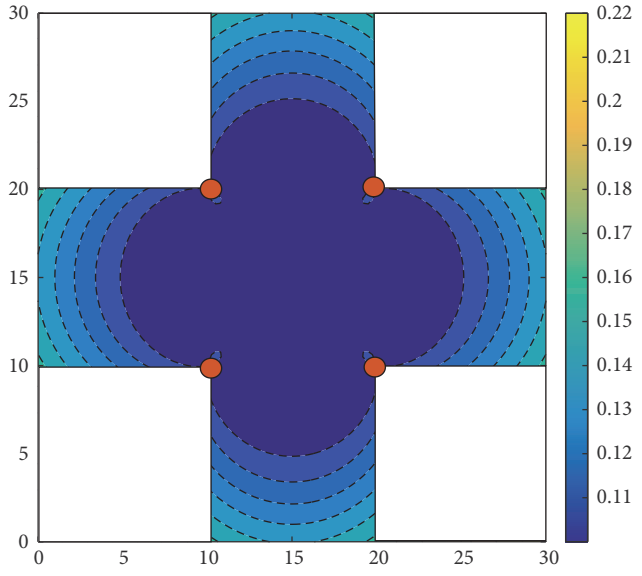

Figure 9: PEB [m] for infrastructure-based positioning.

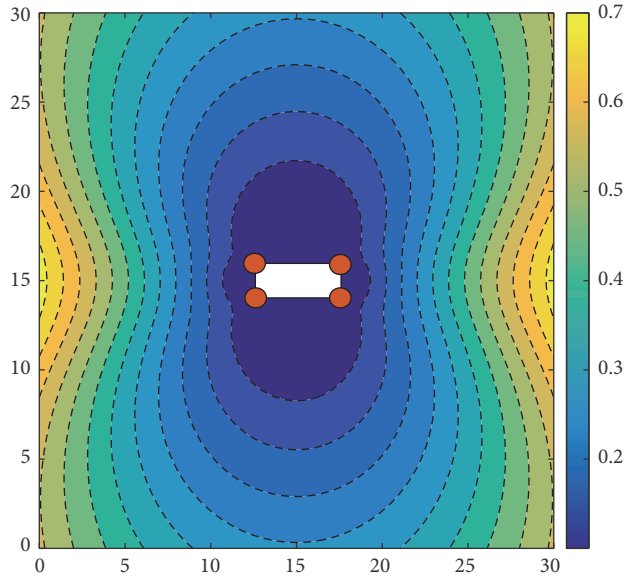

Figure 10: PEB [m] for vehicle-based positioning (small truck).

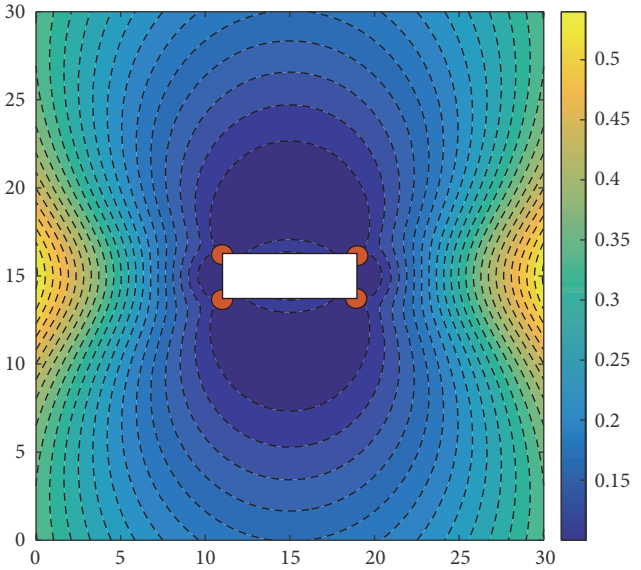

Figure 11: PEB [m] for vehicle-based positioning (large truck).

here carried out. PEB is a tool for determining what is the theoretical best positioning accuracy that an algorithm can provide starting from a certain setting in terms of measurements and geometrical configuration of anchors and tag. Specifically, it is defined as

$$\mathrm{PEB}(\mathbf{p}) = \sqrt{\mathrm{tr}\left(\mathbf{J}^{-1}(\mathbf{p})\right)}, \tag{1}$$

where $\mathbf{p}$ is the tag position, $\mathrm{tr}(\cdot)$ is the trace operator, and $\mathbf{J}(\mathbf{p})$ is the positioning Fisher information matrix (FIM). Following [32], it is possible to obtain

$$\mathbf{J}(\mathbf{p}) = \Gamma \sum_{i=1}^{N} \mathbf{G}(\boldsymbol{\Theta}_i), \tag{2}$$

where N is the number of independent measurements (i.e., the number of anchor nodes), $\Gamma = f(\sigma^2)$ with σ^2 being the variance of the ranging observation noise, then carrying information on the measurements quality, and $\mathbf{G}(\cdot)$ is the geometric matrix related to the GDOP with $\boldsymbol{\Theta}_i$ representing the ith anchor direction, then carrying information about the anchors' placement. Note that, given the FIM in (2), it is possible to optimize the anchors deployment in order to maximize the informative content of the measurements and thus the localization accuracy. Therefore, an accurate analysis of the best anchors' deployment is strictly related to the optimization of the GDOP function. Moreover, as previously mentioned, from (1) to (2), it is possible to understand how the number of anchors (i.e., N) impacts the localization performance.

In Figure 9 the PEB for the infrastructure-based architecture is shown. Specifically, a standard deviation of 20 cm for ranging is considered, and the presence of 4 anchors placed in the correspondence of the traffic lights in a $30 \times 30\,\mathrm{m}^2$ junction. Anchors are depicted with brown circles and are placed in coordinates (20, 10), (20, 20), (10, 20), and (10, 10). From the figure, it is possible to see how the localization error is equalized in the entire scenario, always between 10 and 20 cm. On the other hand, Figures 10 and 11 show the PEB for the vehicle-based architecture. Again, a ranging standard deviation of 20 cm is considered with the presence of 4 anchors placed at the corners of (i) a vehicle (small truck) of size $2 \times 5\,\mathrm{m}^2$ and (ii) vehicle (medium-sized truck) of size $2.5 \times 8\,\mathrm{m}^2$. In both cases the truck is assumed in the middle of the scenario. From the figures, it is possible to notice the GDOP effects, which are more pronounced in the direction of the vehicle. In fact, the localization error increases moving away from the vehicle, and such performance degradation is less severe in the orthogonal direction. This is mainly due to the geometrical placement of the anchors along the long vehicle. When adopting vehicle-based architectures, it is then fundamental to consider location estimates only in a certain area of some meters around the vehicle, where the location process is effective.

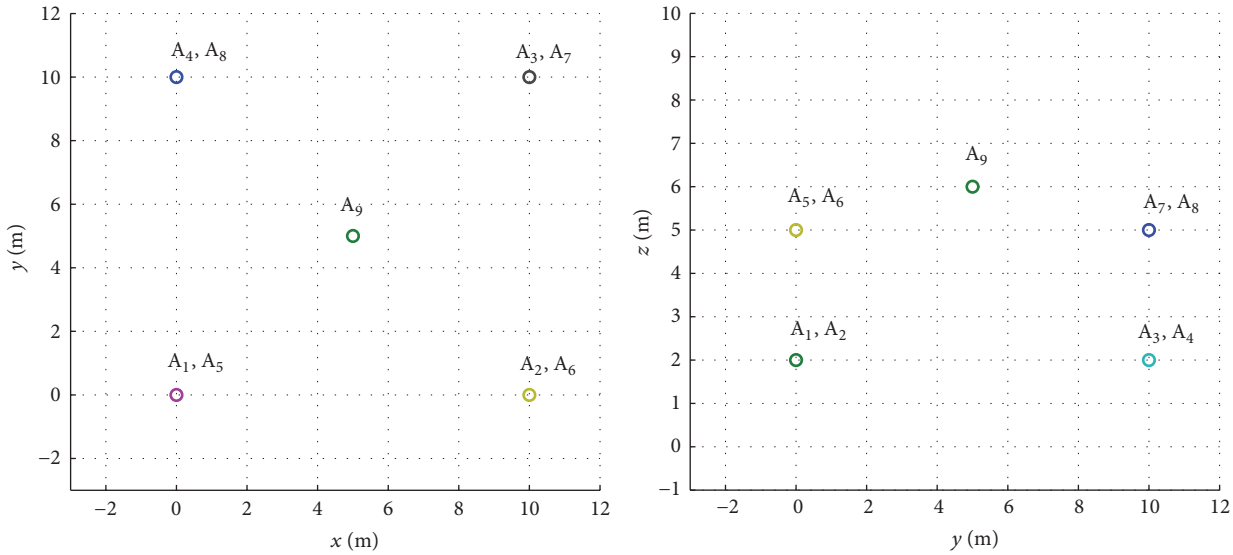

Figure 12: Anchors deployment: x-y plane on the left and y-z plane on the right.

It is important to notice that the final localization accuracy is also impacted by propagation conditions, in particular by the presence of non-line-of-sight (NLOS) channels between tags and anchors [33–35]. In fact, due to the time-based localization technique proposed, an obstacle can interact in several manners with the radio signal used, for example, for ranging. One typical effect is the obstruction of the direct path so that TOA estimation is wrongly performed on a reflected path, then relating to a larger distance with respect to the *optical* ray. In other cases, also if the direct path is not completely blocked, the propagation inside a different medium slows down the electromagnetic wave. In both cases, NLOS channel conditions cause an overestimation of the distance and consequently lead to a decreased positioning accuracy [28].

In our scenario, such conditions could occur for several reasons. In an infrastructure-based solution, NLOS condition could be caused by the presence in the crossing area of large trucks blocking the tag-to-anchor signal. Due to the particular characteristic of such a scenario, where the obstruction of other vehicles change rapidly with time (differently from traditional NLOS conditions caused, for example, by walls or furniture), the investigation of the impact of such effects requires ad hoc measurements in real dynamic conditions. Such an investigation is part of our future experimental activity even though redundancy appears the most viable solution in rapidly changing scenarios. Differently, in the vehicle-based solution, the NLOS channel could arise due to the intrinsic shape of the vehicle, which obstructs some of the anchors placed on it. When NLOS channel conditions are present, the localization accuracy decreases and ambiguities in the position can arise due to an insufficient number of measurements. However, thanks to the considered tracking scheme, where a location engine continuously tracks a given tag starting from new measurements and the prior location estimation, ambiguities can be strongly mitigated. Moreover, NLOS conditions can be reduced by deploying a larger number of anchors nodes and by fusing inertial data. Notice that, thanks to the considered TDOA scheme, this translates only on an increased complexity at the processing unit side, with no modifications required at tag side and no additional complexity.

6. Experimental Results

In this section preliminary experimental results using the implemented localization system are described in order to assess the localization accuracy in static and dynamic scenarios. The purpose is also to analyze the performance degradation when considering TDOA with wireless synchronization instead of TWR. The measurement campaigns have taken place in the CASY (Center of Complex Automated Systems) indoor flight arena at the University of Bologna premises and in a controlled junction in Cesena, Italy.

6.1. Indoor Measurements and Results. The measurements have taken place in an area of $11 \times 11 \times 6\,\text{m}^3$ where tags can move on the x-y plane with a z coordinate that ranges from 1 to 2 m. A set of 22 infrared cameras (VICON Bonita 10), installed in the monitored area, have been adopted to infer the exact tags' positions as they can achieve a millimeter localization accuracy. 9 anchor nodes are considered, according to the deployment represented in Figure 12. Specifically, we have considered the following deployments:

(i) All anchors: when all the reference nodes (A_i $i = 1, 2, \ldots, 9$) are active

(ii) Lower circle: only A_i $i = 1, 2, \ldots, 4$

(iii) Upper circle: only A_i $i = 5, 6, \ldots, 8$

(iv) Mixed: mixed combination between lower and upper circle: for example, A_1, A_3, A_6, A_8

As mentioned before, the number of active anchor nodes is one of the parameters that determine the localization

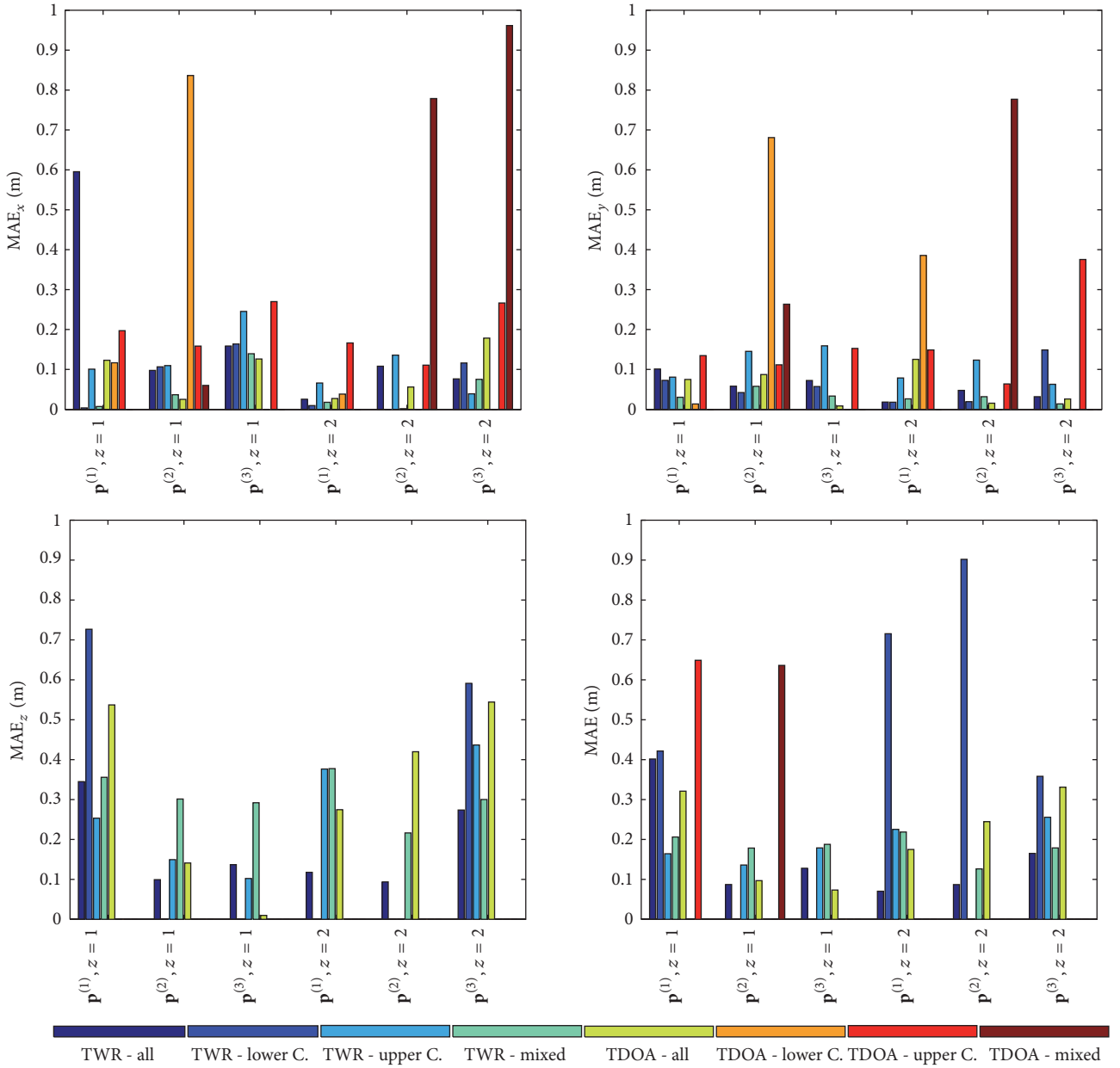

Figure 13: Localization error considering static tags.

accuracy of the system. For this reason, a preliminary study concerned the localization performance as a function of the number of anchors in static conditions, that is, with the tag placed in a set of fixed positions. For each test position in space, 500 estimates have been collected using a personal computer running the localization algorithm based on Bayesian filtering.

6.1.1. Results. The performance metric adopted for assessing the localization performance is the mean absolute error (MAE) defined as

$$\text{MAE} = \frac{1}{N}\sum_{i=1}^{N} \left\| \mathbf{p} - \widehat{\mathbf{p}}_i \right\|, \tag{3}$$

where $\mathbf{p}$ represents the true tag position as derived by the VICON system while $\widehat{\mathbf{p}}_i$ is the estimated position. N represents the number of estimates for each set of measurements.

In static conditions, the tag is placed in different fixed unknown positions inside the area. In the following, we will indicate with $\mathbf{p}^{(j)}$ with $j = 1, 2, 3$ the three testing positions in the x-y plane while as regards to the z coordinate, two different heights, that is, $z = 1\,\text{m}$ and $z = 2\,\text{m}$, have been taken into account. For each tag's position, we aim at analyzing the localization performance as a function of the number of anchors and of the chosen localization technique.

Figure 13 reports the MAE for each tag's position and coordinate as function of different anchors' deployments and

Table 2: Localization error (RMS) averaged over different tag positions.

Loc. technique	Anchors config.	x error [m]	y error [m]	z error [m]	Global error [m]
TWR	All anchors	0.26	0.06	0.20	0.15
TWR	Lower circle	0.44	0.07	1.15	0.83
TWR	Upper circle	0.13	0.11	2.55	0.74
TWR	Mixed	0.06	0.03	0.31	0.18
TDOA	All anchors	0.10	0.07	0.37	0.20
TDOA	Lower circle	1.41	1.22	7.49	4.34
TDOA	Upper circle	0.20	0.19	6.23	3.13
TDOA	Mixed	1.97	2.23	5.44	3.18

localization approaches. Only anchors geometric configurations resulting in a submeter localization error are reported. As one can observe, the TWR technique is more accurate in estimating the x and y coordinates and then TDOA, and this is particularly verified for anchors at the same height. Such degradation of the localization performance in TDOA is also due to anchors synchronization mismatches but it can be counteracted using an increased number of anchors. When considering a proper anchors deployment TDOA results are satisfactory for the application under consideration.

Table 2 reports the mean square error averaged over the tag positions and shows how the UWB localization system is able to infer the tag positions with centimeter localization accuracy also in indoor environments, especially when operating in TWR fashion and with a high number of anchors. We expect that in outdoor conditions the performance could improve because of the absence of strong multipath caused by signal reflections on the walls as indoor.

In dynamic conditions, the tag was free to move in the flight arena. During this test the tag did not follow only a longitudinal path but also performed rotational movements and modified its height. The average speed of the tag is 4.5 km/h and the distance covered is approximately 100 m.

Figure 14 reports the true and estimated tag trajectories. It is possible to observe that the estimated trajectory, marked with red circles, diverges from the true one, indicated with a dashed blue curve, especially in correspondence of rapid changes of direction. Nevertheless, this inconvenience could be solved by refining the mobility model in the Bayesian tracking algorithm which is one of the future tasks.

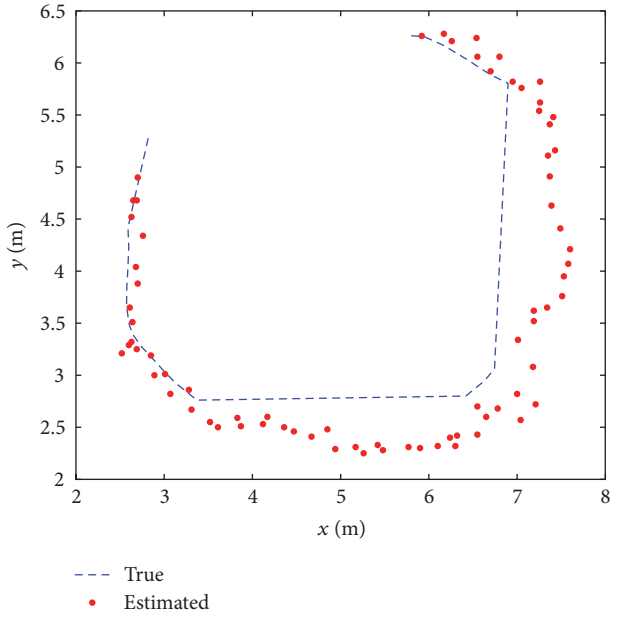

Figure 14: Localization error example for a dynamic tag.

6.2. Outdoor Measurements and Results. The measurements have taken place in an area of approximately $40 \times 70\,m^2$. 5 anchors nodes have been located on a junction as illustrated in Figure 15, left by blue-squared markers, at a height of ≈2.90 m. A bike has been equipped with an active tag. The aim of the outdoor measurements campaign has been to qualitatively assess the performance of the UWB tracking system and to analyze the impact of the HMI on the cyclist behavior considering the infrastructure-based scenario. In fact, either the left turn or right turn scenario has been emulated twice: the first time the HMI, consisting of a buzzer and a led, was not activated while the second time, it was remotely enabled in order to warn the cyclists of the approaching vehicle. In both situations, the position and the velocity of the cyclists have been recorded over time. About 20 candidates participated in the experiments and undergo a survey to test their opinions and acceptance on the adopted technology.

Figure 15 reports an example of results for one candidate. On the top-left, the cyan-colored markers indicate the cyclist's trajectory while on the bottom-left, the latter are interleaved with red markers indicating the spatial points relative to the activation of the user's HMI. As expected, the HMI is enabled in the correspondence of the junction, that is, where a dangerous situation for the cyclists could happen. On the right, the recorded speeds of the two situations are displayed. As it is evident, the cyclists behavior (in this case, its speed) sharply changed after the activation of the HMI enhancing its safety in approaching the intersection. The next activity foresees the assessment of the performance of the vehicle-based architecture and the integration of a RA unit which can infer the risk based on previous positions estimates in order to automatically activate the HMI.

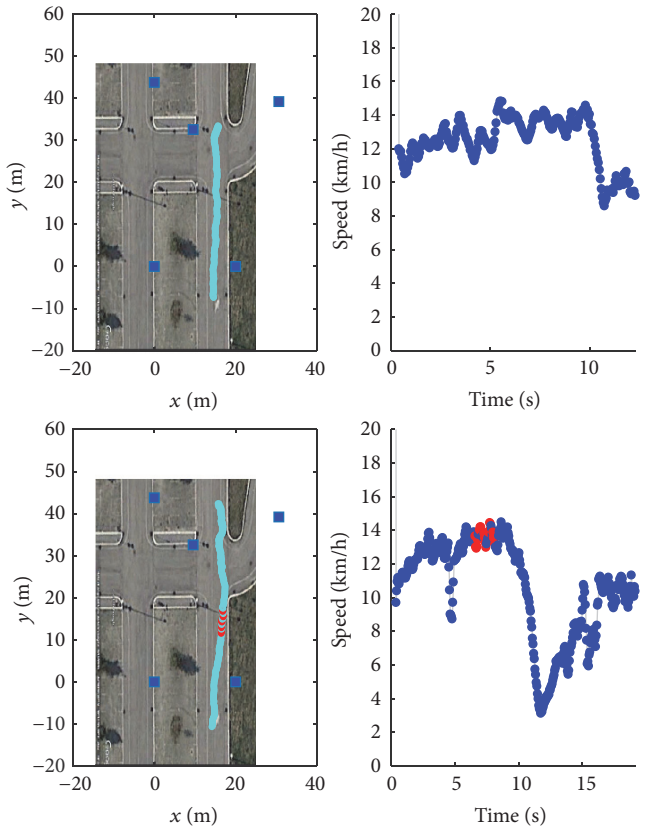

FIGURE 15: Example of outdoor measurements result.

7. Conclusions and Future Perspectives

Starting from a deep analysis of road users' behavior and of typical dangerous situations, in this paper two architectures performing RA and providing a feedback to the road users and, in particular, to cyclists, on potentially dangerous situations have been presented. To enable such architectures, we proposed a localization system based on the UWB technology capable of guaranteeing high-accuracy localization and tracking, in which bikes are equipped with low-cost and low-complexity active tags and with HMI. Reference nodes can be placed both at the junctions *(infrastructure-based architecture)* or on vehicle *(vehicle-based architecture)*. Preliminary experimental activities have been conducted to assess the feasibility of the proposed solutions in static and dynamic conditions. Results show the possibility of achieving submeter localization accuracy and good tracking capabilities, even in harsh propagation environments.

In the future, the behavioral investigation will take a central role in evaluating different HMI solutions, to alert cyclists of dangerous situations in order to enhance their comfort and safety, without being source of distractions or annoying the final users, thus establishing the technology acceptance.

Competing Interests

The authors declare that there is no conflict of interests regarding the publication of this paper.

Acknowledgments

The authors would like to thank Federica Zonzini, Nicola Mimmo, Jurgis Aleksandravičius, Beatrice Borghetti, and Ahmed Elzanaty for the cooperation in the experimental characterization of the performance and Lorenzo Marconi for the concession of the DEI-CASY flight arena and the VICON facility. This work has received funding from the EU Horizon 2020 Research and Innovation Programme under the project XCycle (Grant no. 635975).

References

[1] ERSO, "Traffic safety basic facts 2015: cyclists," Tech. Rep., European Road Safety Observatory, 2015.

[2] European Commission, "CARE database," http://ec.europa.eu/transport/road_safety/specialist/index_en.htm.

[3] M. Z. Win, D. Dardari, A. F. Molisch, W. Wiesbeck, and J. Zhang, "History and applications of UWB," *Proceedings of the IEEE*, vol. 97, no. 2, pp. 198–204, 2009.

[4] "IEEE standard for information technology—telecommunications and information exchange between systems - local and metropolitan area networks - specific requirement part 15.4: Wireless medium access control (MAC) and physical layer (PHY) specifications for low-rate wireless personal area networks (WPANs)," IEEE Std 802.15.4a-2007 (Amendment to IEEE Std 802.15.4-2006), pp. 1–203, 2007.

[5] H. Soganci, S. Gezici, and H. V. Poor, "Accurate positioning in ultra-wideband systems," *IEEE Wireless Communications*, vol. 18, no. 2, pp. 19–27, 2011.

[6] D. Dardari, A. Conti, U. Ferner, A. Giorgetti, and M. Z. Win, "Ranging with ultrawide bandwidth signals in multipath environments," *Proceedings of the IEEE*, vol. 97, no. 2, pp. 404–425, 2009.

[7] Y. Shen and M. Z. Win, "Fundamental limits of wideband localization—Part I: a general framework," *IEEE Transactions on Information Theory*, vol. 56, no. 10, pp. 4956–4980, 2010.

[8] E. T. S. Council, "Making walking and cycling on europes roads safer," Tech. Rep. (PIN Flash 29), 2015.

[9] ISTAT, "Survey on road accidents resulting in death or injury," http://www.istat.it/en/archive/87804.

[10] S. Kaplan and C. Giacomo Prato, "A spatial analysis of land use and network effects on frequency and severity of cyclist-motorist crashes in the copenhagen region," *Traffic Injury Prevention*, vol. 16, no. 7, pp. 724–731, 2015.

[11] N. T. R. Romanow, A. B. Couperthwaite, G. R. McCormack, A. Nettel-Aguirre, B. H. Rowe, and B. E. Hagel, "Environmental determinants of bicycling injuries in Alberta, Canada," *Journal of Environmental and Public Health*, vol. 2012, Article ID 487681, 12 pages, 2012.

[12] M. Stone and J. Broughton, "Getting off your bike: cycling accidents in Great Britain in 1990–1999," *Accident Analysis & Prevention*, vol. 35, no. 4, pp. 549–556, 2003.

[13] F. Wei and G. Lovegrove, "An empirical tool to evaluate the safety of cyclists: community based, macro-level collision prediction models using negative binomial regression," *Accident Analysis and Prevention*, vol. 61, pp. 129–137, 2013.

[14] M.-B. Herslund and N. O. Jørgensen, "Looked-but-failed-to-see-errors in traffic," *Accident Analysis and Prevention*, vol. 35, no. 6, pp. 885–891, 2003.

[15] A. Koustanaï, E. Boloix, P. Van Elslande, and C. Bastien, "Statistical analysis of 'looked-but-failed-to-see' accidents: highlighting the involvement of two distinct mechanisms," *Accident Analysis and Prevention*, vol. 40, no. 2, pp. 461–469, 2008.

[16] M. Räsänen and H. Summala, "Attention and expectation problems in bicycle-car collisions: an in-depth study," *Accident Analysis and Prevention*, vol. 30, no. 5, pp. 657–666, 1998.

[17] M. Räsänen, H. Summala, and E. Pasanen, "The safety effect of sight obstacles and road-markings at bicycle crossings," *Traffic Engineering & Control*, vol. 39, no. 2, pp. 98–102, 1998.

[18] H. Summala, E. Pasanen, M. Räsänen, and J. Sievänen, "Bicycle accidents and drivers' visual search at left and right turns," *Accident Analysis & Prevention*, vol. 28, no. 2, pp. 147–153, 1996.

[19] R. Aldred and S. Crosweller, "Investigating the rates and impacts of near misses and related incidents among UK cyclists," *Journal of Transport and Health*, vol. 2, no. 3, pp. 379–393, 2015.

[20] L. F. Miranda-Moreno, J. Strauss, and P. Morency, "Disaggregate exposure measures and injury frequency models of cyclist safety at signalized intersections," *Transportation Research Record*, no. 2236, pp. 74–82, 2011.

[21] W. Niewoehner and F. A. Berg, "Endangerment of pedestrians and bicyclists at intersections by right turning trucks," Statistics, National Highway Traffic Safety Administratio, 2005.

[22] HVU, "accidents between trucks turning right and bicycles going straight ahead," Tech. Rep., Danish Road Traffic Accident Investigation Board, Copenhagen, Denmark, 2006.

[23] N. Decarli, F. Guidi, and D. Dardari, "Passive UWB RFID for tag localization: architectures and design," *IEEE Sensors Journal*, vol. 16, no. 5, pp. 1385–1397, 2016.

[24] D. Dardari, N. Decarli, A. Guerra, and F. Guidi, "The future of ultra-wideband localization in RFID," in *Proceedings of the IEEE International Conference on RFID (RFID '16)*, pp. 1–7, Orlando, Fla, USA, May 2016.

[25] M. Z. Win and R. A. Scholtz, "Impulse radio: how it works," *IEEE Communications Letters*, vol. 2, no. 2, pp. 36–38, 1998.

[26] Z. A. Lu, S. Gezici, and G. Ismail, *Ultra-Wideband Positioning Systems: Theoretical Limits, Ranging Algorithms, and Protocols*, Cambridge University Press, 2008.

[27] "ISO/IEC 24730-62:2013 standard," 2013.

[28] D. Dardari, E. Falletti, and M. Luise, *Satellite and Terrestrial Radio Positioning Techniques: A Signal Processing Perspective*, Academic Press, Cambridge, Mass, USA, 2011.

[29] Z. Sahinoglu, S. Gezici, and I. Guvenc, *Ultra-Wideband Positioning Systems*, Cambridge University Press, New York, NY, USA, 2008.

[30] B. T. Fang, "Simple solutions for hyperbolic and related position fixes," *IEEE Transactions on Aerospace and Electronic Systems*, vol. 26, no. 5, pp. 748–753, 1990.

[31] D. Dardari, P. Closas, and P. M. Djuric, "Indoor tracking: theory, methods, and technologies," *IEEE Transactions on Vehicular Technology*, vol. 64, no. 4, pp. 1263–1278, 2015.

[32] D. B. Jourdan, D. Dardari, and M. Z. Win, "Position error bound for UWB localization in dense cluttered environments," *IEEE Transactions on Aerospace and Electronic Systems*, vol. 44, no. 2, pp. 613–628, 2008.

[33] L. Mucchi, A. Sorrentino, A. Carpini, M. Migliaccio, and G. Ferrara, "Physically-based indicator for identifying ultrawideband indoor channel condition," *IET Microwaves, Antennas and Propagation*, vol. 8, no. 1, pp. 16–21, 2014.

[34] N. Decarli, D. Dardari, S. Gezici, and A. A. D'Amico, "LOS/NLOS detection for UWB signals: a comparative study using experimental data," in *Proceedings of the IEEE 5th International Symposium on Wireless Pervasive Computing 2010 (ISWPC '10)*, pp. 169–173, IEEE, Modena, Italy, May 2010.

[35] S. Maranò, W. M. Gifford, H. Wymeersch, and M. Z. Win, "NLOS identification and mitigation for localization based on UWB experimental data," *IEEE Journal on Selected Areas in Communications*, vol. 28, no. 7, pp. 1026–1035, 2010.

Hindawi
Mobile Information Systems
Volume 2017, Article ID 8923782, 18 pages
https://doi.org/10.1155/2017/8923782

Research Article

LTE Network Enhancement for Vehicular Safety Communication

Wooseong Kim[1] and Eun-Kyu Lee[2]

[1]*Department of Computer Engineering, Gachon University, 1342 SeongNam-ro, Gyeonggi, Republic of Korea*
[2]*Department of Information and Telecommunication Engineering, National University, 119 Academy-ro, Yeonsu-gu, Incheon, Republic of Korea*

Correspondence should be addressed to Wooseong Kim; wooseong@gachon.ac.kr and Eun-Kyu Lee; eklee@inu.ac.kr

Received 13 October 2016; Revised 8 January 2017; Accepted 15 January 2017; Published 19 February 2017

Academic Editor: Barbara M. Masini

Direct vehicle-to-vehicle (V2V) and vehicle-to-infrastructure (V2I) communications have been popularly considered for safe driving of manned or unmanned vehicles. The V2I communication is better than the V2V communication for propagating safety messages at critical regions like intersections where the safety messages must be delivered to surround vehicles with low latency and loss, since transmitters as infrastructure can have line of sight to the receiver vehicles and control wireless medium access in a centralized manner unlike V2V. Long-Term Evolution (LTE) cellular networks are rapidly deployed in the world with explosively increasing mobile traffic. As many automobile manufacturers choose LTE on-board devices for telematics, the LTE system can be utilized also for safety purposes instead of 802.11p/WAVE based roadside units (RSUs). Previous literatures have studied mostly current LTE system analysis in aspect of theoretical network capacity and end-to-end delay to investigate feasibility of V2I communication. In this paper, we propose new enhancement of a current LTE system specified by 3rd-Generation Partnership Project (3GPP) LTE standards while addressing major delay challenges. From simulation, we confirm that our three key solutions can reduce end-to-end delay effectively in the LTE system to satisfy requirements of safety message delivery.

1. Introduction

In the past, attempts have been made to introduce vehicular communication for Intelligent Transport Systems (ITS) using the 5.9 GHz dedicate frequency spectrum, based on Dedicated Short-Range Communications (DSRC) and the IEEE 802.11p/Wireless Access for Vehicular Environments (WAVE) standards [1, 2]. For example, the International Organization for Standardization (ISO) and European Telecommunications Standards Institute (ETSI) Cooperative Intelligent Transport Systems (C-ITS) standards elaborated several use cases regarding traffic control and road safety, not only for vehicle-to-vehicle (V2V) direct communication between vehicles, but also for vehicle-to-infrastructure (V2I) indirect communication using roadside units (RSUs) along the road [3]. The United States Department of Transportation (USDOT) has issued an Advance Notice of Proposed Rule Making (NPRM) mandating the use of this technology for cars in the near future. Manufacturer-implemented standard hardware for the V2V direct communication inside cars is coming soon, but dedicated RSUs using the 802.11p/WAVE standards are difficult to expect, due to the large investment.

Recently, the pace of Long-Term Evolution (LTE) deployment has accelerated over the world for increasing data-hungry smart devices. Widely deployed LTE networks, instead of dedicated ITS infrastructure, can provide traffic-control and road-safety services. 3rd-Generation Partnership Project (3GPP) system architecture (SA) WG 1 which defines service requirements for LTE system also completed requirements for vehicular communication in LTE networks [4]. Furthermore, the automotive industry is now embedding LTE clients in vehicles to realize "connected car" with a constant Internet connection for various telematics services, which can be used for safety purposes.

Two types of safety messages are defined in the standard: a Cooperative Awareness Message (CAM) and a Decentralized

Environmental Notification Message (DENM) [5, 6]. CAMs are periodically broadcasted (in the range of 1–10 Hz) to neighboring vehicles to advise them of the senders' direction, speed, and geolocation. DENMs are triggered by emergencies and specific purposes. Vehicles broadcast those safety messages in V2V direct communication with a Decentralized Congestion Control (DCC) function to avoid congestion in the designated radio frequency, which is also required in the regulation.

RSU infrastructure using LTE towers has the advantages of preventing transmission collisions by centralized transmission control and covering a large road area with line of sight; contrarily, V2V direct communication can suffer from shadowing by big trucks in the roads. However, CAMs are more of a challenge for LTE RSUs (i.e., LTE base station/eNB) because an LTE eNB has limited capacity to serve periodic CAMs from all vehicles within a cell. A DENM that is less frequently invoked, for an emergency stop or an intersection collision warning, is considered as a major use case for the LTE networks [6]. However, dual-radios of 802.11p/WAVE for CAMs and LTE for DENMs are costly and inefficient.

Standards and literatures clarified that the CAM and DENM should be delivered with the expected service requirement of 100 ms end-to-end latency [5, 6]. However, relaying CAMs or DENMs from one vehicle to another is still a challenge for current LTE networks, in terms of limited channel capacity and network architecture. Fortunately, LTE system has several useful features which apply to road safety and traffic control, such as Group Communication System Enablers (GCSE) and Evolved Multimedia Broadcast Multicast Service (eMBMS). Previous studies about vehicular safety communication using LTE networks have investigated scalability and delay problems according to the large number of vehicles or the scheduling mechanisms in eNBs [7–9]. However, a detailed analysis based on the 3GPP LTE standard in order to investigate the feasibility of LTE RSUs has not yet been conducted.

In this paper, we first introduce the useful features of the 3GPP LTE standards for vehicular communications. Then, we investigate their feasibility for CAM and DENM delivery in terms of network overhead and end-to-end delay and finally propose three key ideas to reduce the overhead and delay to satisfy safety requirements. The rest of this paper is organized as follows. In Section 2, we introduce previous works on the LTE system for vehicular communications. In Sections 3 and 4, we overview eMBMS and GCSE as representative LTE features for vehicular communication. We propose an enhanced LTE network model for vehicular safety applications in Section 5 and discuss implementation issue of our idea in Section 6. We evaluate performance of conventional and proposed approaches in Section 7. We discuss remain challenges and conclude in Sections 8 and 9.

2. Related Works

Several researches have been conducted on the applicability of LTE cellular technology to vehicular safety communication. Vinel [10] compared the IEEE 802.11p/WAVE and LTE system in terms of delay and scalability for vehicular safety applications. Mathematical models of the IEEE 802.11p/Carrier Sense Multiple Access (CSMA) and Time-Division Long-Term Evolution (TD-LTE) were developed to compare their system capacity. According to the analysis results, the LTE system was inadequate to support beaconing messages, such as CAMs, because of its limited capacity. Other existing literatures [8, 9] also mentioned that downlink and uplink channel capacities are limited for CAMs. In detail, downlink channels suffer from congestion more in unicast mode than broadcast mode, and the expiration of the CAM deadline (i.e., 100 ms) increases exponentially as the number of vehicles exceeds 100. In addition, the CAM delivery success ratio is dependent on the uplink capacity. TD-LTE, with an up to downlink ratio of 1 : 9, shows only 60% delivery success because of the limited uplink capability. Accordingly, scalability should be enhanced in both up and downlink, for example, by broadcast or multicast instead of unicast and access control for uplink.

Kihl et al. [11] proposed eMBMS (i.e., multicast in downlink) based vehicular communication in the LTE network. The authors assumed a DENM scenario rather than the CAM for V2I communication, since DENM is infrequently generated. Simulation results show that among several scheduling methods, delay-based weight scheduling can satisfy a target delay, 100 ms of safety applications with at least 50 vehicles. Unfortunately, no results are available regarding situations with more than 50 vehicles, which could be a practical assumption considering the normal macrocell range. Furthermore, a detailed analysis of the latency is missing.

Mangel et al. [12] showed a numerical delay analysis of the Universal Mobile Telecommunications System (UMTS) and the LTE system based on 3GPP standard specifications. They argued that the LTE system could meet the safety message deadline better than UMTS, at least in the random access delay for the uplink transmission if the LTE system deals with 1,500 CAMs per second using the eMBMS in downlink transmission. Although this study opens the possibility of LTE for CAM delivery, it does not show a detailed procedure for vehicular communication in the LTE network. [13, 14] propose the eMBMS based adaptive CAM rate control that can invoke congestion in safety channels, which disturbs emergency messages dissemination in time. In [15], authors derive uplink capacity for CAM dissemination at intersection for varying number of vehicles, where the vehicle broadcasts the CAM through designated radio resource blocks using GPS information. However, detail implementation is not described. [16] describes a detailed architecture of LTE eMBMS for CAM and DEMN dissemination and shows the eMBMS can improve network efficiency and latency when number of vehicles is high enough.

A survey paper [7] introduced existing issues in the LTE system and network deployment for vehicular communications. For the downlink transmission, the authors pointed out that eMBMS causes additional delay due to its session establishment procedures even though it uses fewer radio resources than unicast. In the matter of vehicular network deployment, a back-end server for road safety can reduce the workload of vehicles and eNBs. For example, the server only

disseminates CAMs or DENMs to geolocationally relevant vehicles since the safety communication range of the vehicles is not likely coincident with the LTE cell area. In addition, an eNB or the server can ignore duplicate messages triggered by the same event or aggregate consecutive messages that are destined for the same vehicle to reduce number of transmissions, which has been explored in ETSI C-ITS under GeoNetworking [17]. Another survey [18] introduces many studies about Heterogeneous Vehicular Network (HetVNET) that integrates cellular networks with Dedicated Short-Range Communications (DSRC). This survey provides comprehension of recent wireless networks techniques for HetVNETs that is still at beginning phase.

For machine type communication (MTC), 3GPP has explored several techniques to support coexistence of the MTC traffic with legacy UE in terms of random access overload [19]. [20, 21] also introduce QoS based access barring approach for different classes of MTC devices in 3GPP LTE-A networks. Here RACHs are preallocated or barred dynamically for different MTC classes with different backoff procedures. In [22], authors propose scheduling schemes for uplink channel of LTE for MTC considering QoS such as throughput and allowed delay of each device. [23] proposes load-aware association at overlapped cell area for MTC devices. In [24], device to device (D2D) communication of 3GPP Rel-12 is adopted for dedicated broadcast/multicast vehicular safety communications with eMBMS based D2D resource allocation. In [25], authors review various approaches of the D2D communication for vehicular safety communications. They classify those approaches by operator assistance, discovery candidate, QoS, and so forth and compare their performance qualitatively. Recently, [26] enhances the V2V communication for scalability and robustness using LTE D2D and full duplex technologies which improve LTE spectrum reusability and beacon transmission rate for neighbor vehicle awareness compared to previous half-duplex D2D.

3. Evolved Multimedia Broadcast Multicast Service

The Evolved Multimedia Broadcast Multicast Service (eMBMS) [27, 28] was developed for delivering multimedia broadcast/multicast content to mobile clients, that is, user equipment (UE) in LTE system, which is an effective way to save radio resources for delivering broadcast contents compared to using multiple unicasts. The eMBMS requires several networks' equipment such as Broadcast/Multicast Service Centers (BM-SC), MBMS gateways, Multicell Coordination Entities (MCE), and eNBs, as illustrated in Figure 1(a). The BM-SC is a Broadcast/Multicast Service Center that manages multimedia data along with related information such as the broadcast/multicast area, content, and time and sends them to the MBMS gateways and the MCE. The MCE provides eNBs with control information to schedule their radio resources for the broadcast/multicast data transmission within the eMBMS area. Here the broadcast/multicast radio channel resources are synchronized among multiple cells (Cells 1–4) that participate in concurrent broadcast/multicast transmissions using a single frequency in order to form a large service area as shown in Figure 1(a).

As can be seen in the detailed eMBMS procedures in Figure 1(b), UE first receives System Information Block (SIB) 13 to obtain multicast notifications and the Multicast Control Channel (MCCH) configuration of the corresponding Multimedia Broadcast Single Frequency Network (MBSFN) area [29]. Next, the UE can receive *MBSFN Area Configuration* through the MCCH once the UE receives a notification, indicated by an M-RNTI (Multicast Radio Network Temporary Identifier) via the Physical Downlink Control Channel (PDCCH). The *MBSFN Area Configuration* includes information that identifies which subframes the UE should monitor to obtain the eMBMS data and physical channel characteristics (e.g., Modulation and Coding Scheme (MCS), logical channel Identifier (ID)). With this information, the UE receives broadcast data from the eMBMS channel and decodes them.

Basically, since all broadcast data are delivered through the eMBMS channel, the UE has to know scheduling information of the Multicast Traffic Channel (MTCH) of interest. Such scheduling information can be acquired from the MCH Scheduling Information (MSI) with a logical channel ID of the MTCH. Then, the UE keeps receiving the MTCH of the logical channel that the UE is interested in. The logical ID is mapped with a Temporary Mobile Group Identity (TMGI) as a session ID in an application layer. Thus, the UE manages both the logical channel ID and the TMGI together after the UE selects a broadcast/multicast session with the TMGI in the application layer.

The above complicated eMBMS procedure is designed for multimedia broadcast/multicast purposes not for real-time bidirectional communications, and it causes a long end-to-end delay. The total delay can be more than 100 ms, which consists of at least 80 ms for SIB 13, 40 ms for MSI acquisition, and several more subframes until receiving the actual data, depending on MTCH scheduling. This is far more than the vehicular communication safety requirements, that is, less than 100 ms. In connected mode, an UE could receive data within 100 ms, assuming the UE already knows the *MBSFN Area Configuration* and the MSI. However, it could be challenge to acquire the configuration information at real time when UE move and they need a new configuration of a changed eMBMS area. To avoid this service interruption, the configuration can be made before the vehicle enters a new area otherwise. If the single eMBMS area covers all roads in wide area, that is, several km, irrelevant safety information (DENM is only required to propagate within 300 m [5, 6].) will be broadcasted over the entire eMBMS area, which wastes radio resources significantly and causes scalability problem.

4. Group Communication System Enablers (GCSE)

A Group Communication System Enabler (GCSE) was standardized for group communication such as a mission-critical push to talk (MC-PTT) using unicasts or multicasts in LTE

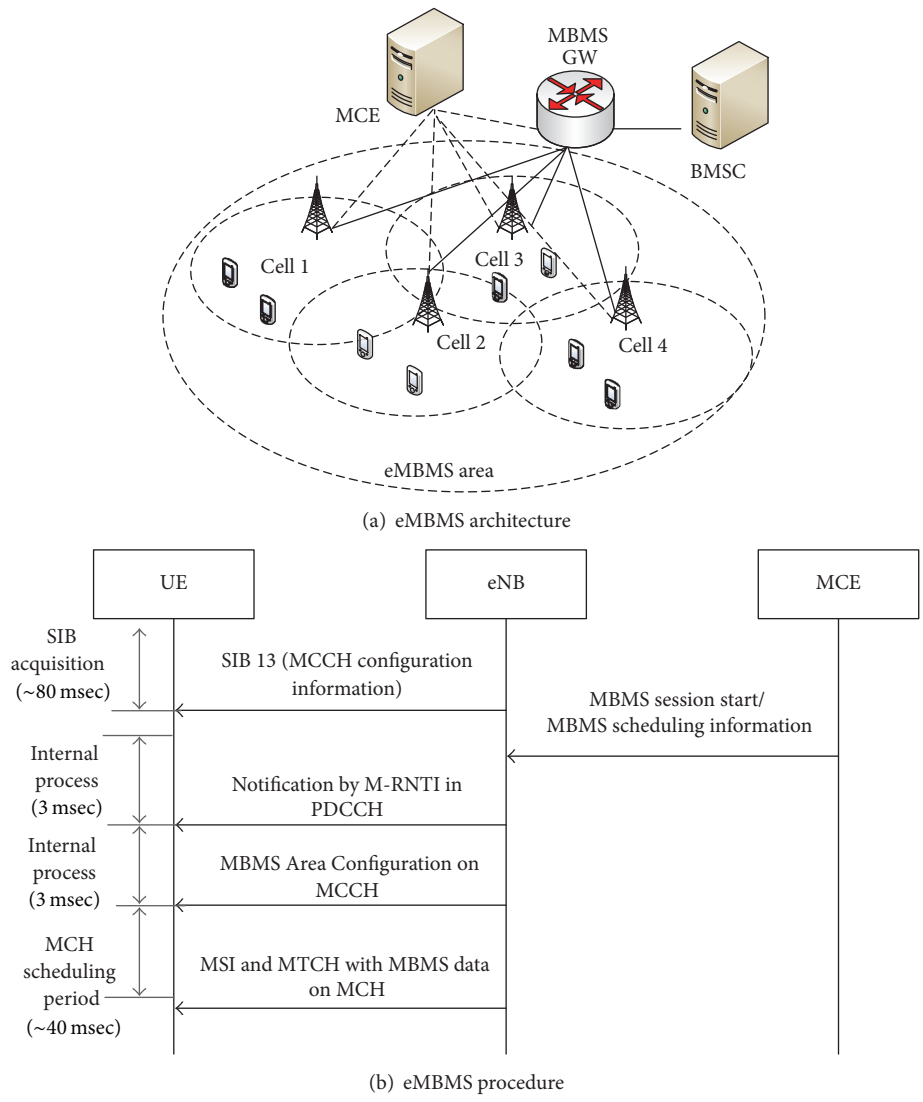

Figure 1: eMBMS architecture and multicast data reception procedure.

networks [30]. The GCSE can be applied to vehicular group communication. Figure 2 depicts the GCSE architecture that consists of a GCS application server (AS), the BM-SC, and the MBMS gateway, in addition to an Evolved Packet Core (EPC) network (i.e., eNBs and PDN-GW (P-GW)). The GCS AS manages group members and relays data from one to the others using multiple unicasts or a single multicast. For instance, suppose that UE 1–6 belong to the same group and UE 1 tries to send data to others, UE 2 receives the data by unicast and others receive it by multicast as shown in Figure 2.

For the multicast, the GCS AS requests a Temporary Mobile Group Identity (TMGI) to the BM-SC that manages multicast streaming to multiple eNBs through the MBMS-GW and then sends the TMGI to group members using application protocols. The GCS AS has unicast connections to the member UE before changing the unicast connections into a multicast connection. The GCS AS determines an optimal time to switch from multiple unicasts to single multicast and vice versa. The eMBMS for the multicast can consume more radio resources than the multiple unicasts according to number of member UE since the multicast requires designated radio resources periodically regardless of traffic presence. Once the multicast group is established, the GCS AS can activate or deactivate the multicast bearer with Quality of Service (QoS), session start time, MBMS area information, and so forth.

According to [31], a high priority QoS Class Indicator (QCI), even for MC-PTT, has very relaxed requirements: GBR voice (75–100 ms), non-GBR signalling (60 ms), and data (200 ms) for one-way delay from a gateway to UE. Thus, the round-trip time based on these requirements cannot satisfy the maximum delay for vehicular safety defined in the ITS standardization organization and governments [5, 6], since interaction between humans is typically more tolerant than communication between machines.

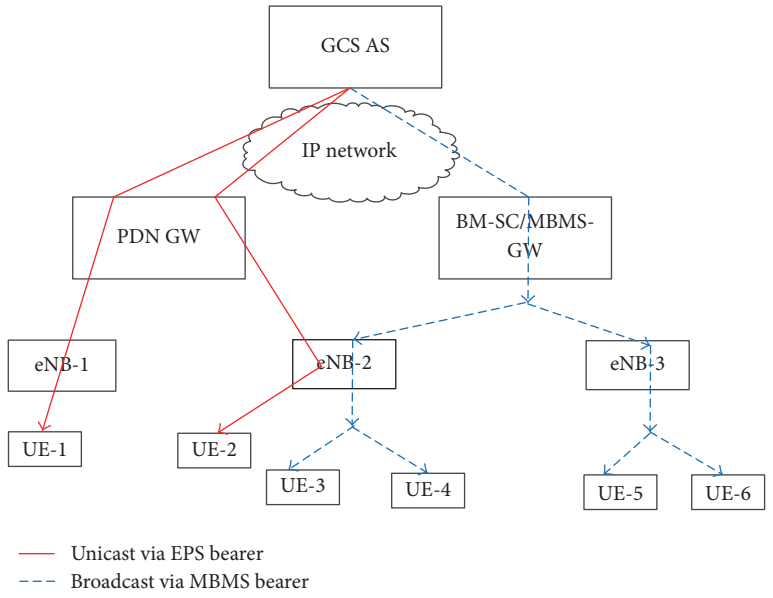

Figure 2: GCSE service architecture.

5. LTE Enhancement for Vehicular Communication

In previous sections, we overviewed useful features of LTE system for vehicular safety communications. Basically, those features allow vehicle UE to exchange CAMs or DENMs without modification of the current LTE system. However, end-to-end delay requirement for safety messages delivery is guaranteed in the current system.

Three major delay factors in the current LTE communication for vehicular group communications are defined as follows:

(i) Random access (UE-eNB): delay from uplink access and data transmission by idle or connected UE

(ii) Group management (UE-GCS AS): delay from joining or leaving the group with long RTT from eNB to GCS AS since the GCS AS is located outside the EPC

(iii) Downlink configuration (UE-BM-SC): delay from eMBMS configuration information acquisition

In this section, we propose new enhancements for the LTE system to enable delay-critical communication for road safety, which lead to solving above three delay problems. Solutions for each delay term are summarized as below and details of each solution are introduced in following sections:

(i) A persistent uplink channel based on geolocation: to reduce the access delay and resource waste

(ii) A Mobile Edge Cloud (MEC): to reduce the RTT between UE and GCS AS

(iii) A cell-based multicast with geolocation: to reduce configuration delay for multicast stream reception

5.1. Geolocation-Based Persistent Uplink Channel. For the initial uplink transmission, UE should first perform a random access in order to maintain orthogonality among uplink transmissions from many UE. An eNB synchronizes the arrival times of the uplink signals from the UE by shifting the transmission time according to the UE's locations.

As shown in the detailed random access procedure in Figure 3, UE first sends a randomly chosen preamble to eNB through a random access channel (RACH) and waits for a random access response (RAR). The RAR contains the preamble index, uplink timing adjustment, and uplink resource assignment information for the UE. The UE sends a connection request using the assigned resource with the UE identity (ID) if the received preamble index is the same as the sent preamble. The UE ID is used for contention resolution, in case more than two UE setups coincidentally send the same preamble. The eNB returns the ID to the UE with a new Cell Radio Network Temporary Identifier (C-RNTI) as a radio connection ID in the connection setup message. Next, the UE sends the C-RNTI and a Buffer Status Report (BSR) message in the connection-complete message and receives an uplink grant with the C-RNTI for actual data.

The random access procedure takes a total of 67 ms on average, as calculated in Table 1 and Figure 3. However, the initial access latency increases exponentially as attempts fail. If eNB uses backoff indication to control the access attempts of many UE setups, it can take more than several seconds because the maximum backoff time is 960 ms, and up to 200 random access retries are allowed in the standard. Only two retries with several ms backoffs could defeat our latency goal, even without considering additional hybrid automatic-repeat request (HARQ) delays from retransmissions.

In [7], authors argue that vehicle clients can always be connected to reduce the initial access delays. The connected UE instead need a scheduling request (SR) procedure for the uplink grant, as shown in Figure 4. For the SR, a periodic Physical Uplink Control Channel (PUCCH) is assigned for

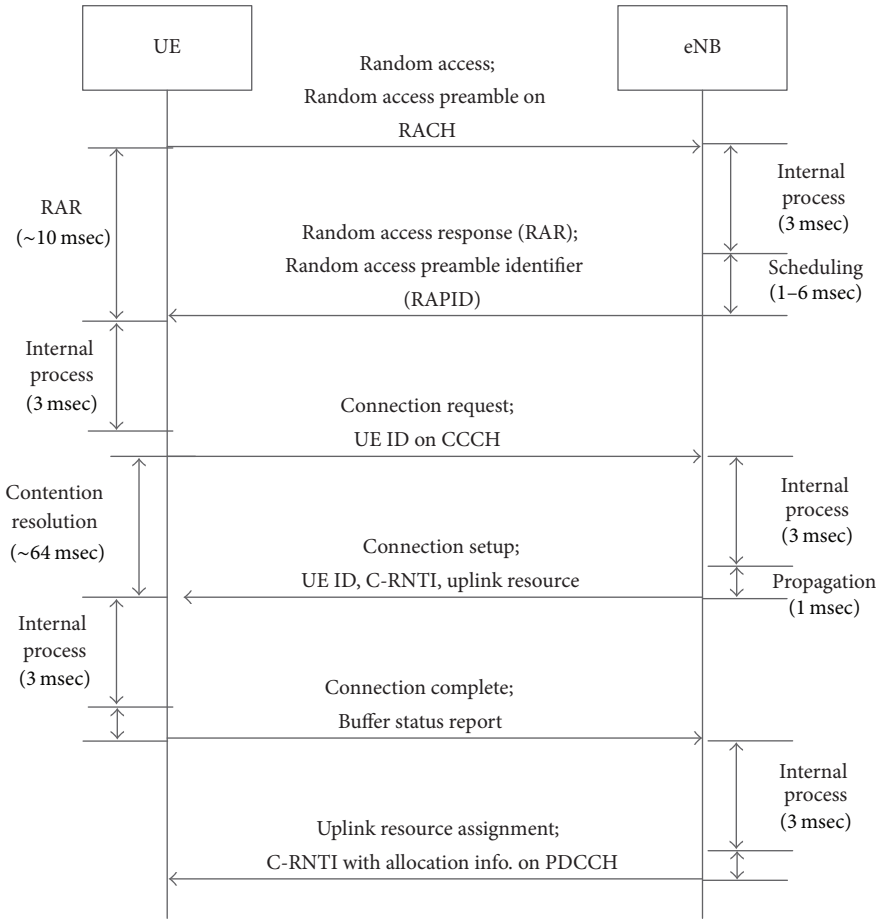

Figure 3: Random access procedure and delay of each step.

Table 1: Random access delay analysis.

Procedure	Detail	Total average delay
Random access (RA)	RACH subframe [1, 20 ms] RAR window [1, 10 ms] RAR process [4 ms]	19 ms
Contention resolution (CR)	Connection request [4 ms] Connection setup [1, 64 ms] Connection setup process [4 ms]	40 ms
Uplink resource allocation (UL)	Buffer status report [4 ms] Uplink grant process [4 ms]	8 ms

each UE; otherwise, the UE must perform a random access procedure. The SR period depends on the network load; the period tends to be longer if eNB has many connected UE to schedule on the limited PUCCH for the SR.

As a detail of the SR procedure, the UE sends the SR via the PUCCH, and the eNB assigns an uplink grant for the BSR. The UE reports the current buffer status using the BSR and receives an uplink grant for data. The two request/response procedures for BSR and data take 8 ms each. On average, a total of 21 to 26 ms is spent transmitting safety messages, assuming the SR period is around 10 ms. It takes longer if the BSR or data transmission fails (e.g., 8 additional ms for each retransmission). For instance, if two retransmissions occur, a total of 42 ms is necessary.

The delay of the connected UE allows safety messages to be delivered within the deadline. However, connecting all UE with periodic PUCCH resources for the SR is inefficient in terms of scalability and resource wastes; the delay will increase according to the number of connected UE setups. Supposing that the PUCCH is allocated around 5% of the 5 MHz uplink resources, 17 UE setups can have the SR every Transmission Time Interval (TTI); each radio block (RB) is normally multiplexed by 17 UE setups for PUCCH format 1 of the SR. Thus, a total of 170 connected UE setups are supported

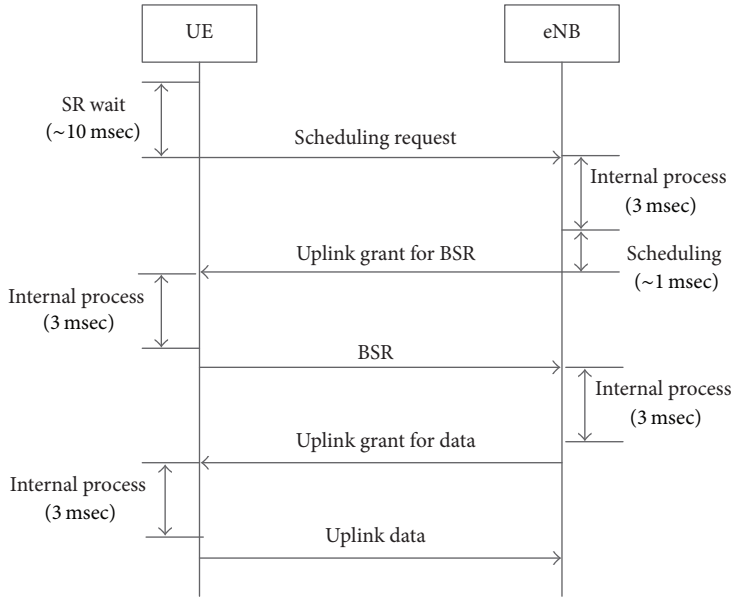

Figure 4: Scheduling request procedure and delay of each step.

with a 10 ms SR period. However, the eNB may need to extend the SR period or increase the PUCCH resources, since the 3GPP LTE standard requires a minimum of 300 UE setups without Discontinuous Reception (DRX), according to [32], and the conventional UEs such as handheld devices may coexist. For example, 600 connected UEs (e.g., 300 vehicles and 300 legacy UEs) lead to an increase in the SR period of about 50 ms, which is still valid, but can be a challenging value if transmission failure occurs. Furthermore, the periodic SR resource of PUCCH for each UE is wasted if there is no data to send. Considering limited resource of the PUCCH, an alternative method to simultaneously reduce the delay and overhead should be considered. Always connected vehicles also cause significant overhead to eNB due to frequent handover procedures.

We propose a geolocation-based common persistent channel for idle or connected vehicles in LTE networks as described in Figure 5. The eNB assigns uplink resources periodically for common persistent channels in which many vehicles send safety messages directly to the eNB by competition. This common uplink (CUL) channels allow skipping the SR and BSR procedures and reduce uplink resource waste by sharing the uplink resource with others.

Within the common channel, there is unfortunately no mechanism to avoid collision completely, like Wi-Fis listen-before-talk. In order to reduce collisions and resource waste, therefore the persistent common channels can be assigned according to geographical location, that is, a road segments 1–4, as can be seen in Figure 5. The eNB can schedule uplink channel resources dynamically based on the vehicle density per segment. In the figure, number of vehicles is different to the road segments. Accordingly, the eNB can assign more common channels to segment 1 rather than others. In practice, the eNB can configure the common channel patterns using period and offset values based on the road density.

Above approach has twofold critical problems; first, random access procedure is still necessary for idle UE. Secondly, CUL channels are also can be wasted. Thus, additional geolocation-based random access is conducted for idle state UE and collision avoidance before CUL channels. Figure 6 shows a detailed procedure of our proposed scheme. UE selects a preamble and sends it through a random access channel (RACH) (noted as R1–R4 in Figure 5) that the eNB assigns periodically for each road segment. Only UE which receives the RAR from the eNB can send prepared packets of safety messages through the persistent channel of the road segment (noted as C1–C4 in Figure 5). The RAR PDU includes multiple RARs for UE which is limited by a transmission block (TB) size. Currently, only a few UE setups, for example, less than 5 UE setups, are addressed in the same RAR PDU. However, vehicular communication can generate more simultaneous RA procedures. For our approach, the eNB has to assign enough resources for the RAR PDU before the CUL channel. For example, suppose maximum TB size for 5 MHz (25 PRBs) is 1096 bits with MCS = 2 and 2 PDCCH symbols, then about 19 RARs can be delivered in each subframe (each RAR is 7 bytes including a header). Thus, the eNB can send more than 50 RARs using 3 subframes before the CUL channel subframe. However, UE may not receive the RAR due to RAR overhead in RA explosion. In such situation, a current LTE system defers RA attempts for a while using backoff or blocks RA from UE in a certain category using system information. Similarly, our approach also defers to perform RA until only several consecutive RACH opportunities due to delay-sensitive vehicular communication.

Finally, our approach would take around 10–15 ms from the initial access to sending a safety message, depending on persistent channel schedule, and is also able to apply to idle UE. Furthermore, the eNB can reassign uplink resources

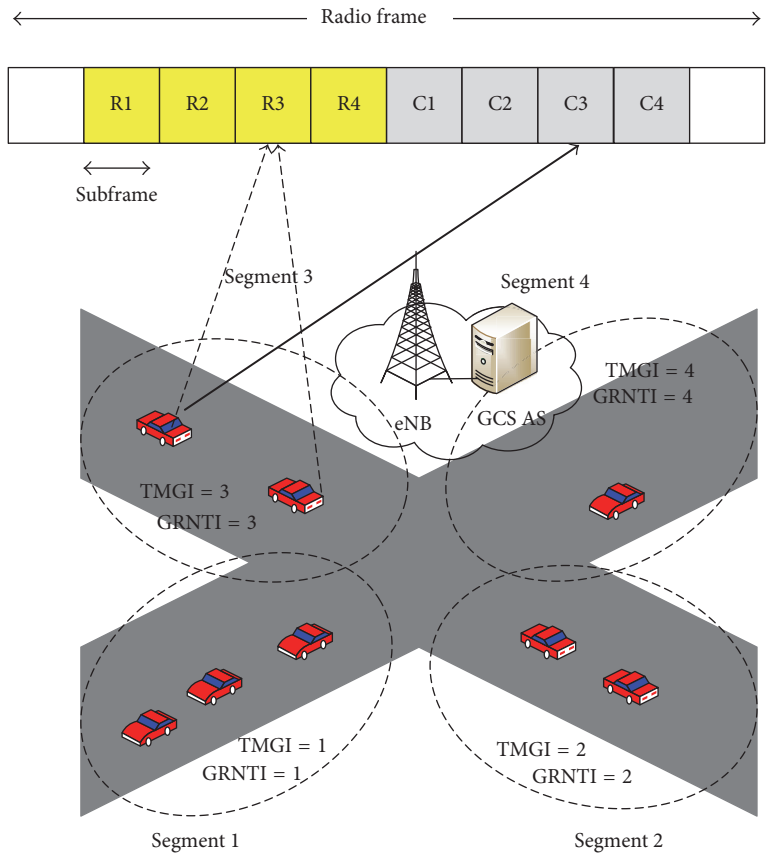

Figure 5: Geolocation-based uplink and downlink channel assignment model.

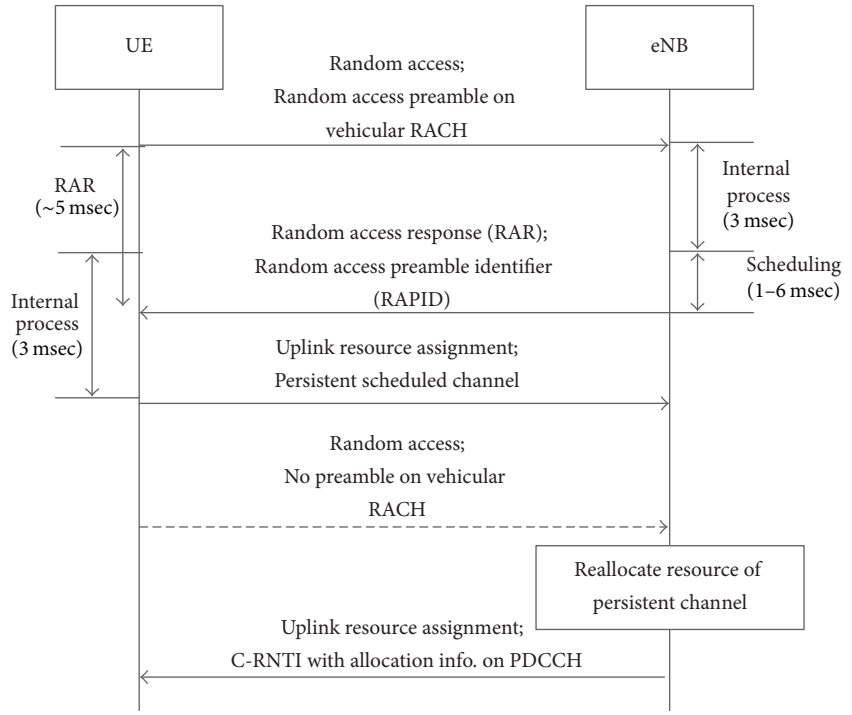

Figure 6: Our proposed approach for safety message uplink transmissions.

reserved for the persistent uplink channel to other uplink channels if no preamble appears in the corresponding RACH, which can prevent uplink resource waste. For instance, if there is no preamble detected in R2 in the figure, the common channel C2 can be reused for uplink transmissions for other UE setups.

Our approach requires precise geolocation information to allocate radio resources for fine road segments, which is assumed to get basically a precise GPS receiver, but many state-of-the-art localization techniques such as crowdsourced V2V and dead reckoning can be considered additionally. Further enhanced localization techniques can improve flexibility in resource scheduling.

5.2. Group Communication Application Server on Mobile Edge Computing. When a vehicle sends a DENM message to the GCS AS out of the EPC network, the message must travel through the EPC network and external networks like the Internet to reach the GCS AS. Further, the message should return to the LTE network to be distributed to member vehicles using a multicast. We can shorten the long safety message route by locating the GCS AS close to the UE, as shown in Figure 5. We can remove the entire backhaul delay, more than 20–30 ms, if we place the GCS AS inside eNB. Recently, Mobile Edge Computing (MEC), the ETSI standard working group, has defined programmable APIs for computing platforms to be located inside the eNB or near the cell site. The MEC is applicable to vehicular communication since it occurs within a specific traffic area (e.g., 300 m for the DENM) that is usually smaller than LTE cell area (e.g., 500 m–1 km). However, the safety messages from the cell-edge area may need to be relayed to neighboring eNBs if every eNB has an individual GCS AS inside. A hierarchical GCS AS architecture can be considered for such cases.

In current LTE networks, all bearers have always to be terminated at the gateway. Thus, the gateway controls the route of the group communication bearer to the GCS AS, based on policies given by a policy server once the application of vehicular group communication creates a group, using protocols like SIP, HTTP, and so forth.

However, in the proposed architecture, eNBs should deal with traffic steering and QoS guarantees for vehicular safety communication. For this, LTE specification has to be changed to terminate UE bearers at the eNB instead of the gateway for the MEC-based applications/services like GCS AS. Alternatively, software define networking (SDN) technology can be applied on top of the legacy LTE network [33], where the MEC provides northbound APIs for the traffic steering to establish directly an end-to-end path for a bearer on top of legacy LTE nodes using switch control protocols like OpenFlow [34–36]. Accordingly, radio bearers are routed to application servers in the MEC by IP-based routing rather than GTP-based tunneling. Recently, many researches about 5G explore the traffic steering techniques using the SDN to support handover and edge cloud computing in a flat architecture of wireless access and core networks.

5.3. Cell-Based Multicast with Geodata. The eMBMS is effective for improving downlink scalability but inappropriate for delay-critical machine-to-machine (M2M) group communication, such as vehicular safety communication. In human group communication, the group-call setup delay for mission-critical purposes requires less than 300 ms. Vehicular communication is more dynamic than human group communication in terms of joining or leaving the group. Thus, multicast session acquisition for group communication for vehicles should be performed faster than in the current approach. Thus, the eMBMS configuration and TMGI acquisition delay should be reduced.

Simple mapping of the TMGI to a road segment, as in Figure 5, can remove the current lengthy group establishment procedure that allocates the TMGI to a certain group in the eMBMS system. Vehicles can derive the group TMGI of the corresponding road segment based on geolocation information (i.e., GPS and map data). So our approach does not need the group join and leave procedures caused by mobility. The mapping information is given by an eNB using radio resource control (RRC) messages that are faster than SIB, when the vehicles enter the LTE cell area initially or by handover. Although the group establishment delay can be ignored, there is still a delay from acquiring the eMBMS configuration information. Using eMBMS for vehicular communications can be costly according to amount of safety data. Switching between multiple unicasts and multicasts using the eMBMS based on the data also causes signalling overhead in EPC networks.

Multicast using a Physical Downlink Shared Channel (PDSCH) (i.e., cell-based multicast) can be a more flexible and efficient alternative for vehicular group communication than the eMBMS because vehicular group communication area is not wide unlike conventional eMBMS service area; a single LTE eNB can cover the communication area. 3GPP studied recently this single-cell point-to-multipoint transmission [37]. The eNB assigns dynamically multicast downlink resources only when necessary, instead of the fixed downlink resources for the eMBMS. The eNB sends multicast data via normal PDSCH with a group RNTI (G-RNTI), a new RNTI for the group communication. Once the UEs receive the PDCCH, they first descramble the PDCCH area with the C-RNTI as a blind search in order to find the downlink channel assignment (i.e., time/frequency resources) and the MCS in the PDSCH for unicast. After that, they repeat the procedure with the G-RNTI to look for a multicast channel assignment. After then, UE decode PDSCH with those channel assignment information to obtain unicast and multicast packets. Consequently, this cell-based multicast can save downlink resources and remove the prerequisite procedures to receive group data, such as the eMBMS configuration and MCH Scheduling Information reception.

The G-RNTI can be assigned to each road segment along with the TMGI as shown in Figure 5. A safety message broadcast area might not be exactly the same as the road segment. For instance, highway road segments are continuous compared to those in the Manhattan grid. The broadcast area can be parts of two segments in such situations. In addition,

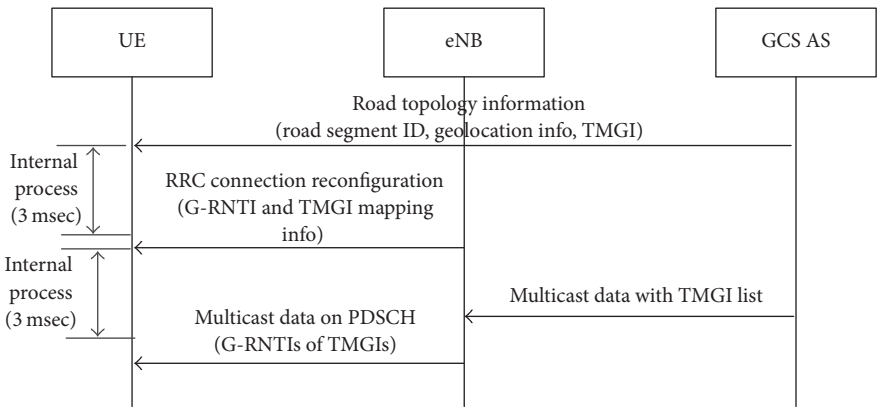

Figure 7: Geolocation-based G-RNTI allocation and multicast procedure.

```
SystemInformationBlockType21-r14 ::=              SEQUENCE {
      roadInfo-r14                                SEQUENCE {
         roadId                                   INTEGER (0···549755813887),
         LAT                                      SEQUENCE {
              begin                               BIT STRING (SIZE (64))          -- Need OR
              end                                 BIT STRING (SIZE (64))             OPTIONAL,     --
         }
         ALT                                      SEQUENCE {
              begin                               BIT STRING (SIZE (64))          -- Need OR
              end                                 BIT STRING (SIZE (64))             OPTIONAL,     --
         }
   lateNonCriticalExtension                 OCTET STRING                     OPTIONAL,
     ···
}
```

Figure 8: System Information Block for road segment identification and GPS information.

vehicles on the edge of a road segment, even in Manhattan, must listen to safety messages from a next segment. eNB can multicast safety messages using all neighboring G-RNTIs in a greedy manner, but it would cause overhead. Therefore, the GCS AS manages the road topology within the cell area and allocates group IDs to each road segment. Then, the GCS AS determines the broadcast area with the group IDs, as described in Figure 7. Actually, the G-RNTI is only known to the eNB because of it is radio-link layer information and is changeable by the eNB. Thus, the eNB gives the G-RNTI and TMGI mapping information to the UE using RRC message as shown in Figure 7. Whenever the GCS AS receives CAM or DENM from a vehicle, it decides on the broadcast area and sends the safety messages to the eNB with the corresponding TMGIs. The eNB multicasts the safety messages using G-RNTIs matched with the TMGIs. The UE must know which TMGIs/G-RNTIs are used to receive the safety messages based on their location and road topology information given by the GCS AS. The proposed procedure needs an initial delay to acquire the road topology and mapping information, only about 3–6 ms in a connected mode while UE can receive configuration information of the eMBMS in idle mode. In order to avoid frequently connecting UE to receive those information, group communication area can be configured wider with multiple eNBs, where the TMGI/G-RNTI mapping information should be handled in the GCS AS.

6. Implementation

For implementation of the road based RACH and preamble assignment, vehicles have to acquire road topology information from a network. Figure 8 shows system block information that is broadcasted periodically from a cell, which includes LTE system information to communicate with eNB for UE. We propose to add road topology information that consists of GPS and road segment identification in the SIB. Thus, vehicles recognize road segment IDs once they receive the SIB messages from eNB.

Another information element shown in Figure 9 has resource assignment of CUL and RACH according to the road segment IDs. With these two SIBs, each vehicle knows which channel it has to use for sending safety messages.

In security aspect, user bearer in a legacy system is encrypted by shared private keys between UE and network, which are stored in user subscription server and several encryption or integrity keys are derived for different purposes and protocol layers such as radio link and network layers from the private key [38]. Vehicular communication requires the security association with the network to guarantee reliability in safety message dissemination. Our approach considers mainly radio-link security in terms of UE authentication and message integrity rather than a core network because the UE bearer is relayed within eNB. Connected vehicles can update a key for the radio access during handover. Idle vehicles have to

```
SystemInformationBlockType21-r14 ::=              SEQUENCE {
      roadInfo-r14                                SEQUENCE {
        roadId                                    INTEGER (0···549755813887),
        lowLatencyUL                              SEQUENCE {
        commonULsubframe                          SEQUENCE {
            cycle                                 INTEGER (0···549755813887), -- Need OR
            offset                                INTEGER (0···549755813887), -- Need OR
        }
        commonULRach                              RACH-ConfigDedicated
    }
    lateNonCriticalExtension              OCTET STRING                        OPTIONAL,
    ···
}
```

Figure 9: System Information Block for common uplink and RACH resource information.

(a) Manhattan (b) Tiger map

Figure 10: Manhattan grid covered by a single macrocell.

derive the key using a network key in a mobility management entity (MME), which causes network traffic between the eNB and MME and key acquisition latency. To avoid this issue, long DRX that has been discussed for MTC can be applied to keep the UE awake [39]. Also, the eNB can keep the context of idle UE to reduce trials to query the security key. Security still has more challenges especially for the idle mode vehicles. We will revisit this issue in future work.

7. Evaluation

In this section, we investigate LTE assisted DENM and CAM vehicular communications with simulation and numerical analysis and discuss their feasibility.

First, we evaluate one of DENM applications, Intersection Collision Risk Warning (ICRW) in a single LTE cell under realistic vehicular traffic. The DENM occurs rarely according to traffic situation compared to the CAM. To estimate number of vehicles near intersection for the ICRW, we first conduct preliminary experiment using traffic simulator, Simulation of Urban Mobility (SUMO) [40]. We captured realistic road environment at Manhattan, New York, using OpenStreetMap [41] as shown in Figure 10(a). Figure 10(b) shows a tiger map of the Manhattan area covered by a single macro eNB with 500 m radius. There are almost 180 road segments with different number of lanes and 100 intersections. Here we count the number of candidate vehicles for the ICRW with varying multiple random trips where multiple vehicle flows (i.e., car follower model) move from one to another road segment in the map.

Figure 11(a) shows average number of vehicles within 5 m from an intersection (alarm zone) with varying traffic generation durations. According to the duration of traffic generation, the number of vehicles number in the zone is slightly different but comparable. For example, total 24 vehicles are shown in 500 s while 15 vehicles are detected in 100 s.

In contrast, arrival rate (denoted by r) of the vehicle flows affects vehicle density notably compared to the generation duration and number of entering vehicle flows (denoted by variable e), 15 vehicles in $r = 1$, but more than 50 vehicles in $r = 0.3$ as shown in Figure 11(b) where each vehicle arrives every 1 or 0.3 s and average 5 vehicle flows are generated, simultaneously. Additionally, the vehicle density highly depends on the size of alarm zone as shown in Figure 11(c); the zone size increases the density more aggressively especially in higher arrival rate (80 vehicles at 10 m to 140 vehicles at 30 m with $r = 0.3$).

As a consequence, vehicle density is related to arrival rate of vehicle flows and vehicle speed. Considering average vehicle speed in the Manhattan (about 9 m/s (32 km/h)), the arrival rate might be about $r = 0.3$ with either $e = 5$ or $e = 10$ as shown in Figure 12. Suppose that alarm zone is set as 20 m (a second distance by maximum speed 60 km/h), about 120

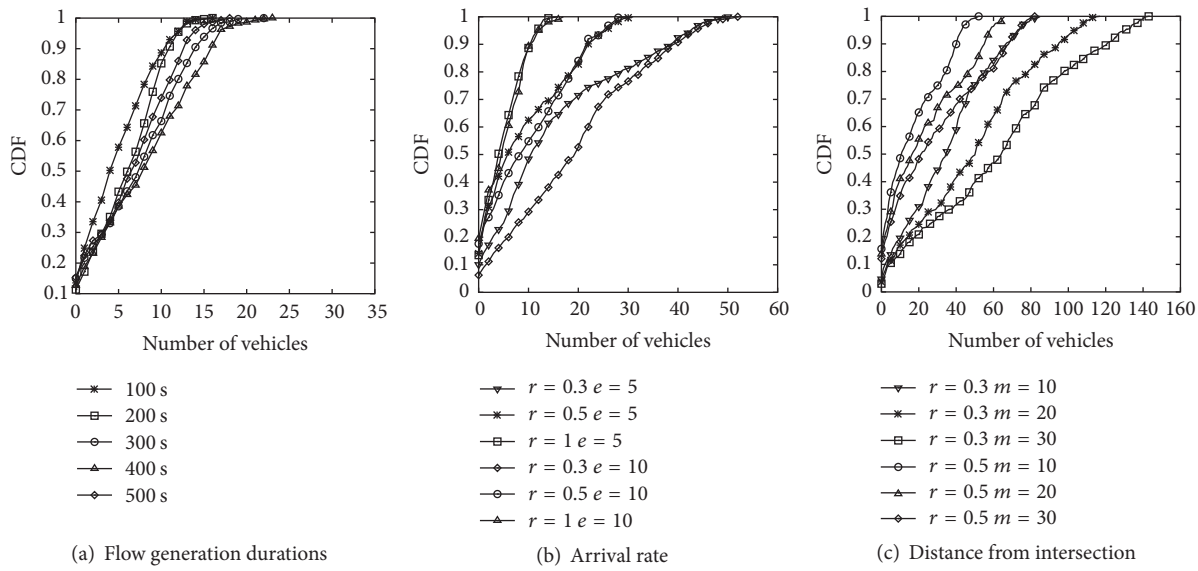

Figure 11: CDF of vehicle density near intersection area.

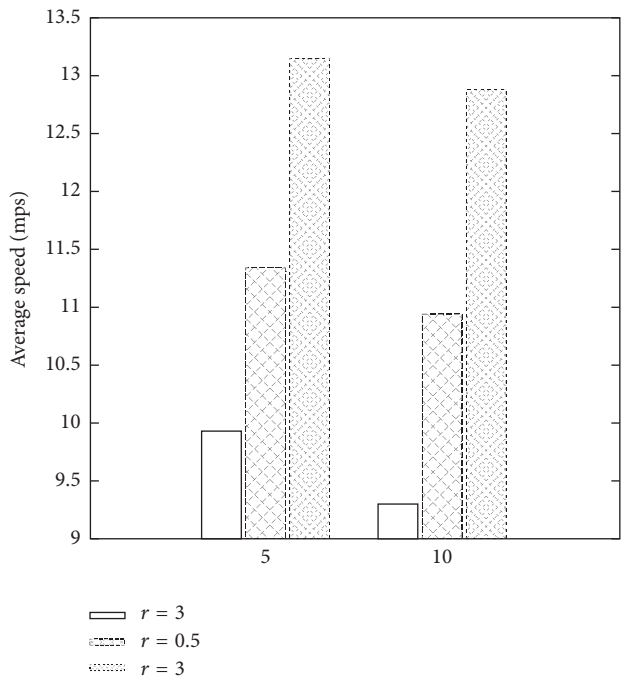

Figure 12: Average speed of vehicles in road segment.

DENMs might be necessary for average Manhattan vehicle flow (cf. 140 DENMs for 30 m).

In the above example, the eNB should provide 120 RACH opportunities for intersection alarm every second, which does not cause significant overhead in the LTE system since only a couple of RACH opportunities are needed in a single radio frame. In other words, ICRW messages can be delivered probably without collision if the macro eNB assigns only one or two designated RACH or uplink RBs every radio frame for each road segment. Although more RACHs are necessary for more intersections to avoid collision completely, the DENM can be supported normally due to its low overhead.

Unlike an event-triggered message such as the ICRW, CAMs or periodic DENMs dissemination is typically more challenging due to frequency of periodic broadcast and number of vehicles sending messages. For numerical analysis of the CAMs, we establish a simple model that copes with access in RACH or CUL channels with varying arrival rate of the safety messages. If vehicle i does not have queued messages with arrival rate of periodic safety messages, CAMs, λ, where the message arrivals are exponentially distributed, it can have a new message to send at time t with a probability, $p_{t,0}$, which is actually a probability of a packet arrival within a unit duration time window (i.e., λ is average number of CAMs per LTE subframe).

$$p_{t,0} = 1 - e^{-\lambda}. \tag{1}$$

Some vehicles have safety messages in the queue for retransmission if they fail last time. Backoff window, ω for random access can be configured to avoid collisions from concurrent transmission because safety messages can be generated simultaneously by multiple vehicles. In this situation, all vehicles with the backlog will send messages at the time t, with transmission probability of $p_{t,1}$.

$$p_{t,1} = \frac{2}{\omega + 1}. \tag{2}$$

At the common uplink data channel, collision probability of vehicle i can be

$$p_{c,i} = 1 - \prod_{i \neq j} \left(1 - p_{t,1|0,j}\right), \tag{3}$$

where $p_{t,1|0,j}$ is a conditional probability of the $p_{t,1}$ under $p_{t,0}$, which indicates a transmission probability of node j which has queued packets.

Even though simultaneous preamble transmissions occur, orthogonal random preambles can be decodable in eNB. Available preambles are different to eNB status; there might be fewer preambles remained for the initial access if the eNB reserves many preambles for designated uplink transmissions. If r preambles are available for the initial random access for vehicles, n, which information is broadcasted in SIB2 message, a probability to select duplicate preambles, p_r, is

$$p_r = \begin{cases} \dfrac{r!\,(r-1)!}{(r-n)!\,(r+n-1)!} & \text{if } r \geq n \\ 1 & \text{if } r < n. \end{cases} \quad (4)$$

Thus, successful access probability in RACHs p_s is derived by failure case in which same preamble is chosen by multiple UE setups which are willing to send the preamble in next RACH subframe.

$$p_s = 1 - p_{c,i} p_r. \quad (5)$$

To figure out feasibility of our approach, several different approaches to reduce delay from uplink data transmission are compared. Expected delay of each approach is different as below. Delay values T_d of each step for an uplink transmission are shown in Table 1. Actual data transmission delay through the uplink data channel is ignored assuming requested grant is fully accepted by eNB. Additionally, T_{UL_p} is considered to investigate delay impact on transmission in a CUL data channel.

(1) Legacy uplink access delay,

$$T_d = T_{\mathrm{RA}} + T_{\mathrm{CR}} + T_{\mathrm{UL}}. \quad (6)$$

If UE fails to acquire uplink grant due to collisions, it has to spend more time of $T_{\mathrm{RA}}+T_{\mathrm{CR}}$ by repeating these procedures. For simplicity, CR failure is not handled in this analysis.

(2) Data transmission in a CUL data channel in this approach, UE send data without initial RA procedure because they are supposed to have connections to eNBs. Thus, transmission failure occurs only by the collision probability.

$$T_d = T_{\mathrm{UL}_p}. \quad (7)$$

This scheme can reduce delay by skipping procedures of $T_{\mathrm{RA}} + T_{\mathrm{CR}}$ for a data transmission, and a part of T_{UL} can be also omitted because CUL channels are periodically scheduled by eNB. Instead, T_{UL_p} is added since T_d depends on eNB scheduling for the CUL.

(3) Random access with a CUL, this approach is also based on the CUL like previous one, but it needs initial RA procedure in advance in order to reduce transmission collisions in the CUL and is applicable to idle UE.

$$T_d = T_{\mathrm{RA}} + T_{\mathrm{UL}_p}. \quad (8)$$

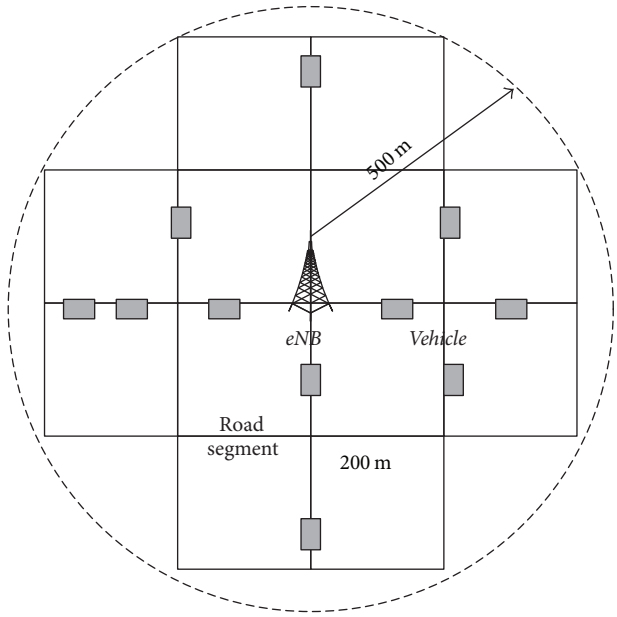

Figure 13: LTE network and road topology for evaluation.

(4) Geolocational road based random access (GeoRA) for a CUL, this is our proposed approach that extends previous CUL to RA using geolocation road information. Expected delay is same as the previous RA with the CUL approach in each road segment. However, T_{RA} is longer than previous one by times of number of road segments because vehicles as UE are distributed over multiple RACHs according to road segments. In other words, the RACH period of our scheme is longer than the previous approach.

$$T_d = T_{\mathrm{RA}} + T_{\mathrm{UL}_p}. \quad (9)$$

Using (1)–(5) and expected delay of each approach, we simulate uplink transmissions for safety messages in a simple one-cell LTE network with varying number of UE and RACH resources. Figure 13 shows a simulation road topology that consists of 30 road segments of 200 m within the urban LTE cell that covers 500 m radius range and total 300 vehicles that are distributed uniformly over the road segments and sending safety messages to each other. Herein we assume 16 dedicated preambles are assigned for vehicular communication.

Figure 14(e) shows expected delay to send a single safety message to the eNB with varying number of vehicles. Here we assume that a RACH and a persistent common uplink channel are assigned, respectively, every 10 ms, that is, one subframe per a radio frame. According to the arrival rate of the safety messages, average delay exponentially increases in most of approaches, Figures 16(a)–16(d). In the figure, $\lambda = 0.01$ means that 10 CAMs are sent per second, and $\lambda = 0.001$ is a 1 CAM per second. For the CAM delivery, $\lambda = 0.01$, all of approaches do not satisfy deadline, 100 ms for near 300 UE setups. But lower arrival rate of safety messages (i.e., less than 0.001) like DENMs can be dealt with by most of approaches except GeoRA. In the GeoRA, a period of a dedicated RACH

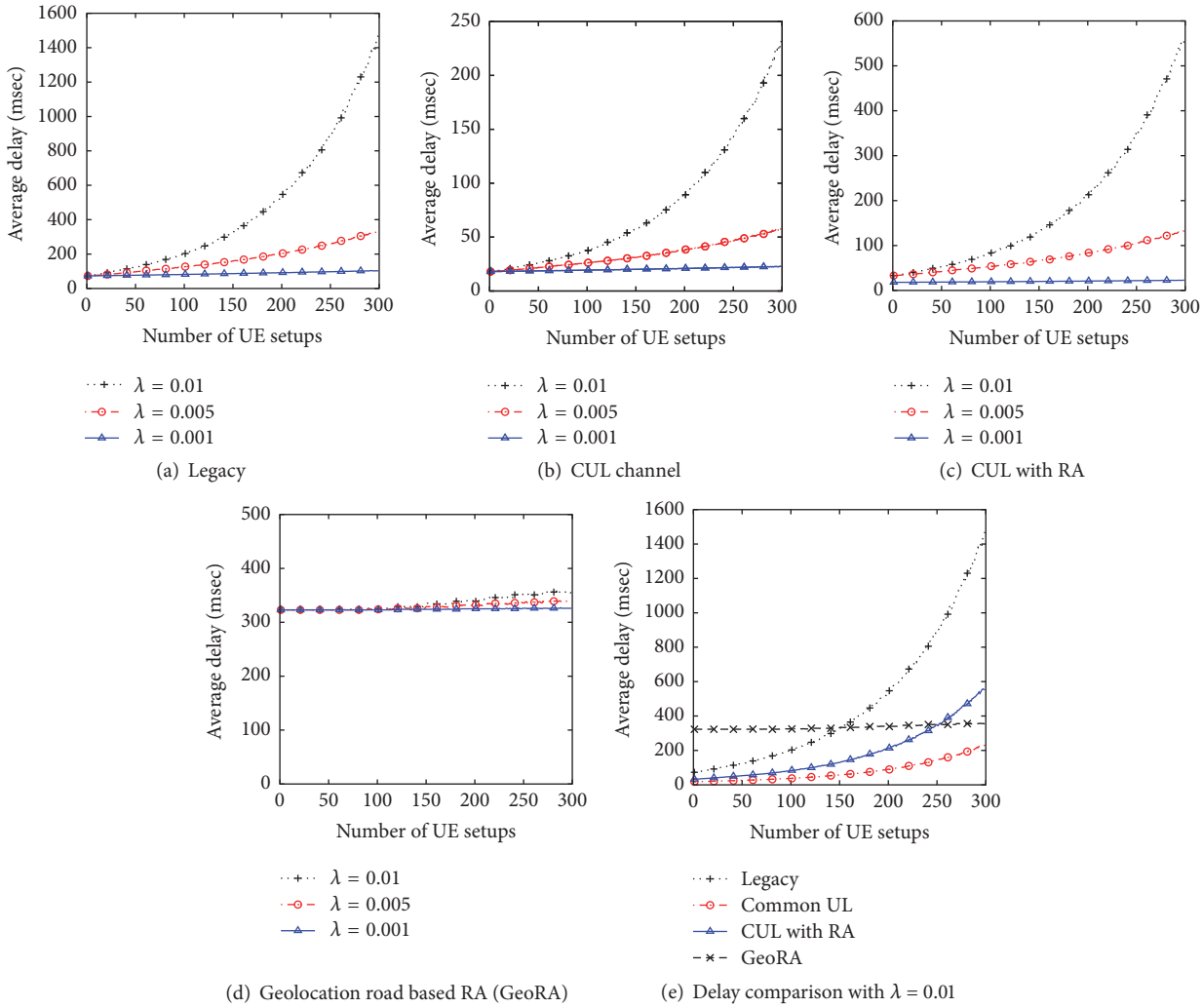

FIGURE 14: Average delay with varying arrival rate of safety messages.

assigned to each road can be 10 ms × 30 since the RACH period is multiplied by number of road segments. Figure 14(e) shows comparison of the four approaches with $\lambda = 0.01$. CUL channel for data transmission achieves better than others since delay expense from collisions is less than others.

Figure 15 illustrates delay performance of the CUL with different CUL periods (i.e., 10, 5 and 1 ms). Frequency of CUL allocation affects average delay as shown in Figure 15(a); average delay increases as the CUL period increases. For the CAM, however, every subframe should have the CUL for more than 300 UE setups. In 5 MHz bandwidth (i.e., 25 physical resource blocks (PRB)), overhead can be near 25% since 6 PRB is enough for the safety messages with lowest modulation, BPSK (2 kbit message size according to [42, 43]). Additionally, almost 20 times CUL waste could occur for a single safety message transmission in case of the 300 UE setups as shown in Figure 15(b). Random access can reduce such wastes of uplink resources by selecting a transmitter and rescheduling an unused CUL resources to other UE setups. Delay from the random access can be reduced by increasing number of RACHs as follows.

Figure 16 depicts average delay with varying RACH opportunities for the safety transmission with $\lambda = 0.01$. In LTE standard, RACH can be assigned once every radio frame (RACH = 10 ms), a half of a radio frame (RACH = 5 ms), even or odd subframe (RACH = 2 ms), and so forth. Most of cases except the CUL shows that delay decreases with more RACH opportunities; the CUL approach does not use RACHs. However, deadline requirement of safety purpose cannot be satisfied except the GeoRA with RACHs in every the other subframe. In Figure 16(e), delay comparison with RACH = 2 notes that the CUL and the CUL with RA outperform than GeoRA until around 150 UE setups because a longer RACH period of the GeoRA takes probably a large part of total delay in lower collision situation. In consequence, GeoRA can adjust RACH opportunities to improve performance by allocating more RACHs on dense road segments or simply grouping road segments dynamically according to the total number of vehicles.

Figure 17 depicts average delay with varying group size of road segments with every 5 ms RACH. The group size is a number of road segments which are assigned for each RACH.

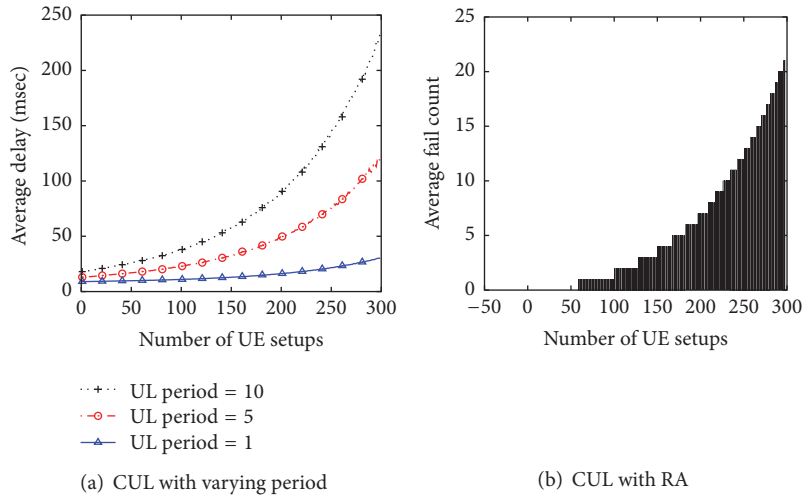

(a) CUL with varying period (b) CUL with RA

Figure 15: Common uplink data channel access performance.

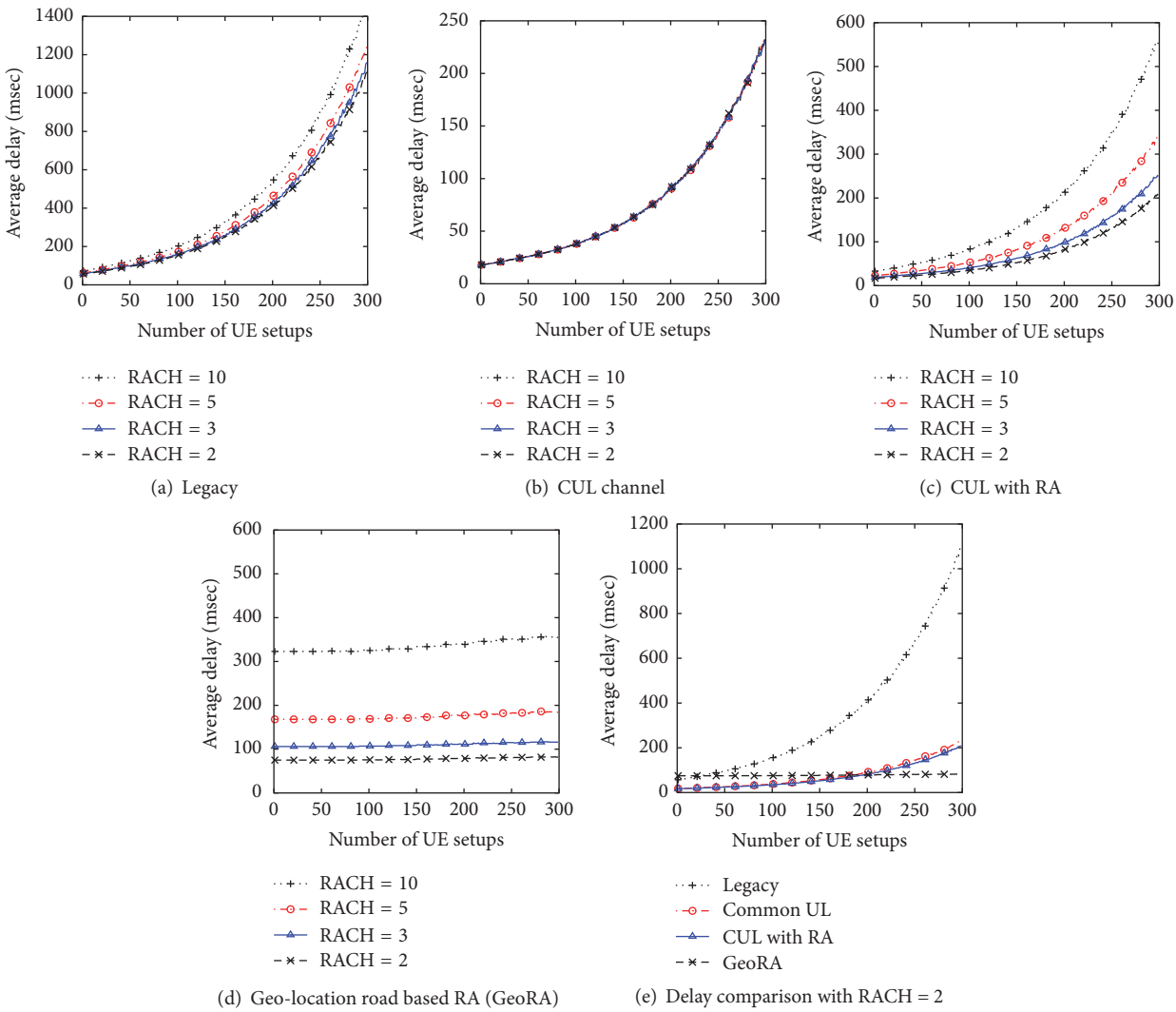

(a) Legacy (b) CUL channel (c) CUL with RA

(d) Geo-location road based RA (GeoRA) (e) Delay comparison with RACH = 2

Figure 16: Average delay with varying period of RACH.

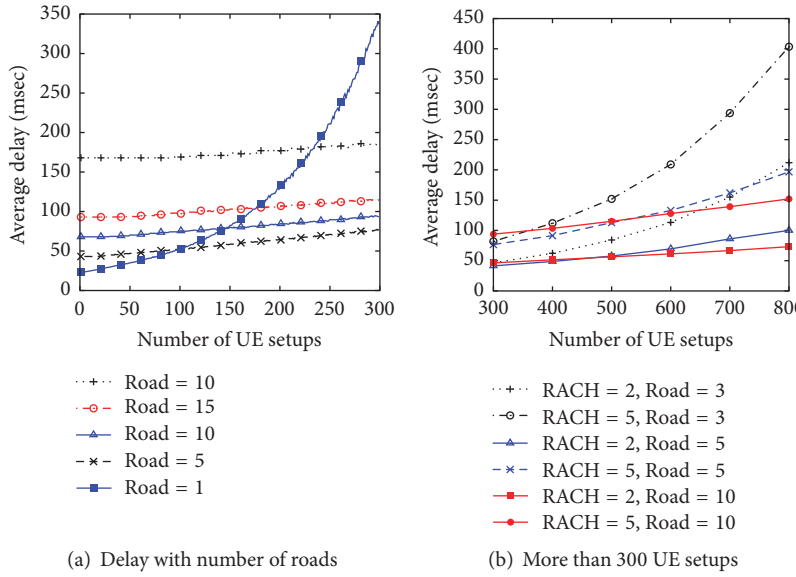

(a) Delay with number of roads (b) More than 300 UE setups

Figure 17: Geolocation road based RA performance.

Consequently, the road segment group with size = 5 achieves minimum delay, about 70 ms compared to other group sizes less than 300 UE setups. Large road segment groups that probably suffer collisions in the RACH have longer delay even though they have more frequent RACH opportunities. Since cell-based multicast and GCS AS delay are no more than 10 ms, vehicular safety communication can be supported in LTE networks. However, more UE increase the delay in such large size group as can be seen in Figure 17(b). For example, the Road = 5 shows longer delay than Road = 10 with same RACH frequency = 5, 150 and 200 ms in 800 UE setups, respectively. To say, the RACH frequency is more critical than transmission collision among UE setups with large number of UE setups. Also, delay gap between different RACHs, 2 and 5 in same group size, supports that argument.

8. Discussion

Our approach still has many challenges to discuss in future works. Uplink transmission failure causes additional delay, which may require more RACHs. Otherwise, an additional mechanism can be considered to prioritize a random access for a retransmission by vehicles. For example, dedicated RACHs or preambles for retransmissions can be assigned.

Another issue is that the RACHs should be shared by normal human devices like smart phones and tablets and vehicles at the same time. It is burden to eNB that vehicles use RACH at every other subframe. Also, it leads to decrease RA performance of normal users. Thus, the eNB has to control a group size of road segments according to number of UE setups instead of increasing use of RACHs.

9. Conclusion

ITS is an attractive application for globally deployed LTE networks; however, the LTE system has not been fully investigated in terms of feasibility for safety purposes. Although several LTE system features are currently used for mission-critical group communications, they are inadequate for vehicular safety communication according to our analysis. We identified three major delay factors in LTE-based group communication and proposed corresponding solutions: a geolocation road based random access with a persistent uplink channel, a GCS AS on a mobile edge cloud, and a geolocation road based cell multicast.

From our simulation and analysis, we conclude that the total delay can be less than 80 ms with reasonable overhead of RACHs and persistent uplink channels; the uplink access takes 70 ms, the cell multicast takes about 5 ms, and the GCS AS may require an additional 5 ms processing delay. As a consequence, LTE networks using our enhanced features can support vehicular safety communications. Future works will include the investigation of efficient uplink channel scheduling for dynamically updated road topology and multiple cell-based broadcasts for fast-moving vehicles.

Competing Interests

The authors declare that there is no conflict of interests regarding the publication of this paper.

Acknowledgments

This research was supported by the National Research Foundation of Korea (NRF) funded by the Ministry of Science, ICT & Future Planning (2016R1C1B1016084).

References

[1] D. Jiang and L. Delgrossi, "IEEE 802.11 p: towards an international standard for wireless access in vehicular environments,"

in *Proceedings of the IEEE Vehicular Technology Conference (VTC Spring '08)*, pp. 2036–2040, 2008.

[2] S. U. Eichler, "Performance evaluation of the IEEE 802.11 p wave communication standard," in *Proceedings of the IEEE 66th Vehicular Technology Conference (VTC-Fall '07)*, pp. 2199–2203, 2007.

[3] ISO, "Intelligent transport systems ł cooperative ITS ł using V2I and I2V communications for applications related to signalized intersections," ISO/PDTS Std 19091, 2015.

[4] TR 22.885 v14.0.0, Study on LTE support for V2X services(Rel.14), 3GPP Std, 2015.

[5] ETSI, "Intelligent Transport Systems (ITS); Vehicular communications; Basic set of applications; Part 2: specification of cooperative awareness basic service," ETSI Std TS 102 637-3, 2010.

[6] ETSI, "TR 102 962 intelligent transport systems (its); Framework for public mobile network," Tech. Rep., ETSI, 2012.

[7] G. Araniti, C. Campolo, M. Condoluci, A. Iera, and A. Molinaro, "LTE for vehicular networking: a survey," *IEEE Communications Magazine*, vol. 51, no. 5, pp. 148–157, 2013.

[8] M.-A. Phan, R. Rembarz, and S. Sories, "A capacity analysis for the transmission of event and cooperative awareness messages in LTE networks," in *Proceedings of the 18th ITS World Congress*, Orlando, Fla, USA, October 2011.

[9] K. Trichias, J. van den, G. Berg, J. de Jongh, and R. Litjens, "Modeling and evaluation of LTE in intelligent transportation systems," in *Proceedings of the Joint ERCIM eMobility and MobiSense Workshop*, D. Dimitrova, M. Brogle, T. Braun, G. Heijenk, and N. Meratnia, Eds., pp. 48–59, University of Bern, Bern, Switzerland, June 2012.

[10] A. Vinel, "3GPP LTE versus IEEE 802.11p/WAVE: which technology is able to support cooperative vehicular safety applications?" *IEEE Wireless Communications Letters*, vol. 1, no. 2, pp. 125–128, 2012.

[11] M. Kihl, K. Bur, P. Mahanta, and E. Coelingh, "3GPP LTE downlink scheduling strategies in vehicle-to-infrastructure communications for traffic safety applications," in *Proceedings of the 17th IEEE Symposium on Computers and Communication (ISCC '12)*, pp. 000448–000453, Cappadocia, Turkey, July 2012.

[12] T. Mangel, T. Kosch, and H. Hartenstein, "A comparison of UMTS and LTE for vehicular safety communication at intersections," in *Proceedings of the IEEE Vehicular Networking Conference (VNC '10)*, pp. 293–300, IEEE, Jersey City, NJ, USA, December 2010.

[13] Y. Yang, P. Wang, C. Wang, and F. Liu, "An eMBMS based congestion control scheme in cellular-VANET heterogeneous networks," in *Proceedings of the 17th IEEE International Conference on Intelligent Transportation Systems (ITSC '14)*, pp. 1–5, IEEE, Qingdao, China, October 2014.

[14] W. Wu, P. Wang, C. Wang, and F. Liu, "A beacon rate control scheme based on embms in cellular-vanets heterogeneous networks," in *Internet of Vehicles-Safe and Intelligent Mobility*, pp. 324–335, Springer, Berlin, Germany, 2015.

[15] L.-C. Tung and M. Gerla, "LTE resource scheduling for vehicular safety applications," in *Proceedings of the 10th Annual Conference on Wireless On-Demand Network Systems and Services (WONS '13)*, pp. 116–118, Banff, Canada, March 2013.

[16] J. Calabuig, J. F. Monserrat, D. Gozálvez, and O. Klemp, "Safety on the roads: LTE alternatives for sending ITS messages," *IEEE Vehicular Technology Magazine*, vol. 9, no. 4, pp. 61–70, 2014.

[17] ETSI, "Intelligent Transport Systems (ITS); Vehicular Communications; GeoNetworking; Part 3: network architecture," ETSI EN 302 636-3 V1.1.2, ETSI Std, 2014.

[18] K. Zheng, Q. Zheng, P. Chatzimisios, W. Xiang, and Y. Zhou, "Heterogeneous vehicular networking: a survey on architecture, challenges, and solutions," *IEEE Communications Surveys & Tutorials*, vol. 17, no. 4, pp. 2377–2396, 2015.

[19] TS 37.868 RAN Improvements for Machine-type Communications, 3GPP Std.

[20] J.-P. Cheng, C.-H. Lee, and T.-M. Lin, "Prioritized random access with dynamic access barring for ran overload in 3gpp lte-a networks," in *Proceedings of the IEEE GLOBECOM Workshops (GC Wkshps '11)*, pp. 368–372, IEEE, Houston, Tex, USA, December 2011.

[21] T.-M. Lin, C.-H. Lee, J.-P. Cheng, and W.-T. Chen, "PRADA: prioritized random access with dynamic access barring for MTC in 3GPP LTE-A networks," *IEEE Transactions on Vehicular Technology*, vol. 63, no. 5, pp. 2467–2472, 2014.

[22] A. S. Lioumpas and A. Alexiou, "Uplink scheduling for machine-to-machine communications in LTE-based cellular systems," in *Proceedings of the IEEE GLOBECOM Workshops (GC Wkshps '11)*, pp. 353–357, IEEE, Houston, Tex, USA, December 2011.

[23] M. Hasan, E. Hossain, and D. Niyato, "Random access for machine-to-machine communication in LTE-advanced networks: issues and approaches," *IEEE Communications Magazine*, vol. 51, no. 6, pp. 86–93, 2013.

[24] L. Gallo and J. Harri, "Short paper: A LTE-direct broadcast mechanism for periodic vehicular safety communications," in *Proceedings of the IEEE Vehicular Networking Conference (VNC '13)*, pp. 166–169, Boston, Mass, USA, December 2013.

[25] A. Khelil and D. Soldani, "On the suitability of device-to-device communications for road traffic safety," in *Proceedings of the IEEE World Forum on Internet of Things (WF-IoT '14)*, pp. 224–229, IEEE, Seoul, South Korea, March 2014.

[26] A. Bazzi, B. M. Masini, and A. Zanella, "Performance analysis of V2v beaconing using LTE in direct mode with full duplex radios," *IEEE Wireless Communications Letters*, vol. 4, no. 6, pp. 685–688, 2015.

[27] TS 23.246 Multimedia Broadcast/Multicast Service (MBMS); Architecture and functional description, 3GPP Std, http://www.3gpp.org.

[28] J. Huschke and M.-A. Phan, "An overview of the cellular broadcasting technology embms in lte," in *Next Generation Mobile Broadcasting*, p. 223, 2013.

[29] "TS 36.331 Evolved Universal Terrestrial Radio Access (E-UTRA)," Radio Resource Control (RRC); Protocol specification, 3GPP Std.

[30] TS 22.468 Group Communication System Enablers for LTE (GCSE LTE), 3GPP Std, http://www.3gpp.org.

[31] TS 23.203 Policy and charging control architecture, 3GPP Std, http://www.3gpp.org/.

[32] TR 36.913 Requirements for further advancements for Evolved Universal Terrestrial Radio Access (E-UTRA), 3GPP Std, http://www.3gpp.org/.

[33] B. Lantz, B. Heller, and N. McKeown, "A network in a laptop: rapid prototyping for software-defined networks," in *Proceedings of the 9th ACM SIGCOMM Workshop on Hot Topics in Networks*, p. 19, Monterey, Calif, USA, October 2010.

[34] N. McKeown, T. Anderson, H. Balakrishnan et al., "OpenFlow: enabling innovation in campus networks," *ACM SIGCOMM*

Computer Communication Review, vol. 38, no. 2, pp. 69–74, 2008.

[35] R. Bifulco, M. Brunner, R. Canonico, P. Hasselmeyer, and F. Mir, "Scalability of a mobile cloud management system," in *Proceedings of the 1st ACM Mobile Cloud Computing Workshop (MCC '12)*, pp. 17–22, August 2012.

[36] L. E. Li, Z. M. Mao, and J. Rexford, "Toward software-defined cellular networks," in *Proceedings of the 1st European Workshop on Software Defined Networks (EWSDN '12)*, pp. 7–12, IEEE, Darmstadt, Germany, October 2012.

[37] "Study on Support of single-cell point-to-multipoint transmission in LTE," TR 36.890 v13.0.0, 3GPP Std, 2015.

[38] 3GPP, "TS 36.300 Evolved Universal Terrestrial Radio Access (E-UTRA) and Evolved Universal Terrestrial Radio Access Network (E-UTRAN); Overall description; Stage 2," 3GPP Std, 2015.

[39] S. Kim, K. Jung, J. Choi, and Y. Kwak, "Improving LTE/LTE-A UE power efficiency with extended DRX cycle," in *Proceedings of the 80th IEEE Vehicular Technology Conference (VTC '14)*, pp. 1–5, IEEE, Vancouver, Canada, September 2014.

[40] M. Behrisch, L. Bieker, J. Erdmann, and D. Krajzewicz, "Sumo-simulation of urban mobility," in *Proceedings of the 3rd International Conference on Advances in System Simulation (SIMUL '11)*, Barcelona, Spain, 2011.

[41] https://www.openstreetmap.org/.

[42] D. Eckhoff, N. Sofra, and R. German, "A performance study of cooperative awareness in ETSI ITS G5 and IEEE WAVE," in *Proceedings of the 10th Annual Conference on Wireless On-Demand Network Systems and Services (WONS '13)*, pp. 196–200, Banff, Canada, March 2013.

[43] Q. Xu, T. Mak, J. Ko, and R. Sengupta, "Medium access control protocol design for vehicle-vehicle safety messages," *IEEE Transactions on Vehicular Technology*, vol. 56, no. 2, pp. 499–518, 2007.